THE UNIVERSITY
of EDINBURGH

Explosive Spalling of Concrete in Fire:

Novel Experiments under Controlled Thermal and Mechanical Conditions

Ieuan Jack Clowes Rickard

Doctor of Philosophy

The University *of* Edinburgh

2020

Explosive Spalling of Concrete in Fire:

Novel Experiments under Controlled Thermal and Mechanical Conditions

by

Ieuan Jack Clowes Rickard

The thesis was been supervised by:

Professor Luke Bisby

Professor Tim Stratford

[Horror Vacui]

Abstract

Modern concretes are increasingly susceptible to a failure mechanism known as heat-induced explosive concrete spalling. This involves the sudden loss of material during severe thermal exposures such as might be experienced during a fire. This typically occurs violently, and could result in; severe loss of cross-section, direct thermal exposure of the internal steel reinforcement or prestressing, and – in some cases – structural collapse. As such, heat-induced explosive concrete spalling in fire poses a credible risk to reinforced and prestressed concrete structures and has received considerable research attention in recent decades. Certain types of structures such as tunnels have historically been more susceptible to spalling due to the concrete used, the particular mechanical conditions, and the potential fire loads and dynamics involved. However, with advancements in concrete technology being driven by sustainability and optimisation, spalling is becoming more prominent in conventional concrete structures such as buildings and bridges.

Due to the complex nature of heat-induced explosive spalling there is currently no validated guidance to enable the design of concrete mixes to prevent spalling, nor any established, widely verified, repeatable test methods to confidently quantify or demonstrate spalling resistance for a particular mix in a given end-use application. As a result of this lack of validated testing and the complexity of the phenomenon, no theoretical or computational models yet exist that can predict spalling with sufficient confidence to be used in design.

The aim of this thesis was to advance experimental spalling research through the development of an experimental apparatus which addresses deficiencies of others, most notably repeatability and control of thermal and mechanical boundary conditions under a range of relevant heating scenarios. Following this, the aim was to carry out carefully controlled, repeatable experiments with a precision and scale which has not been achieved before, in order to understand variability in spalling phenomena and improve knowledge of some of the main parameters that are known to influence spalling.

In this thesis the key variables known to influence concrete's spalling propensity are identified, initially based on the available research literature. Following this, an experimental method and framework to allow repeatable testing of concrete mixes, with careful control of these key variables, is developed, presented, and applied. This experimental method is based on the use of a radiant panel array impose an incident

heat flux on samples. This approach to heating was developed previously at The University of Edinburgh, and has been referred to as H-TRIS within the spalling community. This name will be used throughout the thesis but it should be noted that since this work other authors have made use of the same apparatus and chosen not to use this name to describe the movable radiant panels.

The experiments and development of the method are split into three stages within this thesis. Initially, four heavily instrumented furnace tests were carried out within the Prometheus testing facility at CERIB, France, on a total of thirty six concrete samples with a range of mix (i.e. polypropylene fibre content) and geometric parameters (i.e. plan dimensions and thickness). Importantly, this also allowed the thermal exposure received by the samples when tested under exposure to standard cellulosic, and French modified hydrocarbon temperature versus time curves to be monitored and characterised, as well as giving insight into the influences of different key sample parameters.

Second, thirty-three samples, all of which were cast in parallel with the samples used in the CERIB furnace tests, were transported to Edinburgh and tested using the H-TRIS experimental method and apparatus. This involved upgrading the existing H-TRIS apparatus with more powerful radiant panels to allow replication of the more severe thermal exposures used to assess concretes for use in tunnels. This test series allowed validation of the thermal exposures being used and a comparison of the differences between the two test methods, as well as further investigation of key parameters thought to influence spalling.

For the final test series, a 3 Meganewton uniaxial loading frame was designed and constructed within the H-TRIS apparatus to allow application of simultaneous uniaxial external loading coincident with heating. Understanding the influence of mechanical loading and restraint on spalling performance is critical, since concrete is typically loaded in real end-use applications. The loading method and magnitudes were chosen so as to maintain relevance to concrete tunnelling construction within this thesis – however the versatility of the experimental method ensures the relevance of the resulting data to a range of possible structural concrete applications. Forty-five samples were tested in this test series, allowing the influence of loading and restraint to be carefully investigated, as well as permitting comparison of the effects of various other parameters believed to influence spalling.

Taken together, the 114 concrete samples tested under various conditions for this thesis have provided a range of insights into the influence of different parameters on heat-induced explosive concrete spalling. These include – for the first time ever – careful quantification of the variability of spalling and specific knowledge of the parameters which may play the most important causal roles with respect to spalling in practice. Through the testing, a test apparatus able to accurately and repeatably control the necessary thermal and mechanical parameters was developed, and a guidance for carrying out spalling experiments has been developed and presented, making it available for future research studies and possibly also for compliance testing in practice. It has been shown existing experimental approaches have deficiencies and that this kind of carefully considered approach to experimental spalling research is required.

Lay Summary

The use of concrete in construction is widespread. Heat-induced explosive spalling of concrete is a failure mechanism in which the surface of the concrete breaks off violently during fire or severe thermal exposure. This is thought to be a result of the rapid heating that results in a build-up of thermal stresses and moisture pressure within the concrete.

Despite over a century of research into the spalling phenomena, it remains poorly understood and there is still very limited guidance as to when spalling might pose a risk or how to mitigate against it. Spalling is recognised to be of particular concern in concrete tunnels due to both the concretes used and the potential fire conditions. However, the materials used in building construction are continually being developed and modern concretes have been observed to be more susceptible to this spalling failure mechanism than was previously the case.

This thesis describes an extensive experimental campaign comprising of over 100 tests on concrete samples of varying scales. The samples were tested both in standard fire-resistance furnaces and using the novel apparatus which was developed. The experimental programme was designed in order to develop the novel experimental method that allows precise control of both the thermal and mechanical boundary conditions during testing with a focus on suitable testing for tunnel linings. The apparatus developed allows repeatable and comparable experiments to be carried out. The experimental work whilst successfully facilitating the development of the experimental apparatus was also designed to allow insight into the influence of key parameters thought to influence spalling. As many repeats were carried out, the variability of spalling could also be demonstrated. Finally, recommendations are made for future experimental research and engineers working in a design capacity.

Acknowledgements

First and foremost, I would like to thank my primary supervisor Professor Luke Bisby, without whose guidance and support, this project would not have been successful. After initially inspiring me to undertake this research project, he remained a source of inspiration and guidance throughout, despite his many commitments. I would also like to thank my second supervisor Professor Tim Stratford who was supportive throughout.

I would like to acknowledge Dr Cristian Maluk for his seminal intellectual contributions with the development of the initial H-TRIS testing method and apparatus and his guidance and assistance during the early days of the project. His work provided the foundation for the work described in this thesis.

The research described in this thesis would not have been possible without the generous financial support of EPSRC, the financial support and collaboration of Ove Arup and Partners Ltd, and the support in kind of CERIB.

In particular I would like to thank Dr Susan Deeny at Ove Arup and Partners Ltd. who provided support and guidance throughout the project and facilitated many meetings with engineers working internationally in industry. I would also like to thank the many staff members at Arup, both in the Fire and the Tunnels teams, who engaged with my project and shared their knowledge and experience.

At CERIB, whilst I am grateful to all who were involved, I would particularly like to thank Fabienne Robert for facilitating the four furnace tests and Baptiste Hainault who helped immensely with the practicalities of casting and testing at their facilities.

The years spent carrying out experimental work would have been much less productive without Michal Krajčovič, who continues to be an irreplaceable member of staff in the fire group and helped with all the practical issues I encountered in my experimental work. Thanks also go to Mark Partington whose ability to fabricate precise and creative solutions made the development of the loading frame possible.

I would also like to thank Nikolai Gerasimov for his considerable assistance with running tests and repairing of H-TRIS, Juan Hidalgo Medina and Felix Wiesner for their contributions to the software for the fire lab, Jamie Maclean for his help with testing and Zaid Al-Azzawi for his assistance with the modelling of the loading frame. In addition, everyone who was there to bounce ideas off, help out casting and moving

samples around, and most of all make my research at The University of Edinburgh an enjoyable experience. You all know who you are. This includes Ben, Chris, Emma, Eric, Fabio, Felix, Jamie, Juan, Martyn, Mohammed, Nikolai, Simon, Zaid, Zafiris and everyone else in John Muir.

Finally yet importantly, I would like to thank my family who have supported me throughout my many years at university and Kate, Pixel and Leela who supported me in the final write up stages. This document would not have happened without you.

Contents

List of figures

List of tables

1 Introduction

1.1 Background and research significance

Heat-induced explosive concrete spalling is a phenomenon wherein the surface of a concrete element breaks away violently when subjected to a steep in-depth thermal gradient, as is the case during a fire. This may result in damage to the concrete element varying from loss of a few millimetres of concrete cover to, in some cases and particularly for the high strength mixes used in modern concrete construction, progressive (and eventually total) loss of concrete section. Whilst such spalling is unlikely to pose an immediate risk to life safety in most cases, the cost and downtime needed for repairs to reinstate a structure are likely to be considerable. In the most severe cases spalling could cause partial collapse, or flooding, of submerged tunnels. Researchers and designers have been aware of the potential problems associated with heat-induced explosive spalling of concrete for more than a century, and there are many examples of explosive spalling occurring during fires. The direct economic impacts of spalling damage can be enormous; for example given that the Channel Tunnel facilitates £91.4bn of trade annually, downtime as a result of fire would equate to approximately £250m per day, not accounting for indirect losses (Ernst and Young LLP, 2016). For this reason (and others), concretes used in tunnels are typically required to demonstrate suitable performance as regards explosive spalling when tested under credible worst-case fire scenarios.

Despite the awareness of the problems associated with spalling, no standardised, systematic method to predict or test for the spalling resistance of a particular concrete mix currently exists. This is particularly problematic for the tunnelling industry in needing to gain necessary approvals for particular mix designs for precast concrete tunnel lining segments. Currently, jurisdiction-specific and largely ad hoc approvals and testing programmes are applied on a case-by-case basis. A wide range of poorly comparable spalling test methods at various scales is currently used within the research community. The result being that it is difficult to compare results from different laboratories and researchers, or to develop mix design guidance for use in industry.

The current project sets out to develop and validate a novel test method to study explosive spalling of concrete with a focus on tunnel linings. This was done through three experimental phases. While developing the test method and experimental apparatus a total of 114 samples were tested across four furnace tests and 78

experiments. This carefully controlled experimental campaign represents a large contribution to the available experimental data on heat-induced spalling and the apparatus developed offers a new approach to spalling research and allows accurate control of the thermal and mechanical boundary conditions during experiments.

1.2 Research objectives

The aim of this project is to improve upon experimental spalling research, and through well controlled (thermally and mechanically) repeatable experiments, improve upon the current understanding of spalling. This is done through the extension and development of an experimental apparatus and method that is capable of performing experiments to investigate spalling with a focus on concrete used for precast segmental tunnel linings, but has applicability to all relevant applications of structural concrete. This apparatus development is carried out to allow careful control of both thermal exposure and externally applied mechanical load. Through the development of the apparatus, experiments are carried out which enable assessment of the influence of some of the known key variables that influence heat-induced spalling. The primary objectives of the project presented in this thesis are to:

- evaluate the thermal exposures experienced by samples tested in standard fire-resistance testing using the temperature versus time curves used for the testing of tunnel lining segments;
- develop an apparatus capable of recreating these thermal exposures in a repeatable manner and demonstrate that the thermal exposures are comparable;
- develop a loading frame to allow simultaneous sustained loading and heating of samples during experiments;
- develop a wealth of comparable data on some of the main factors that are known to influence spalling through extensive experimental work with many repeat experiments;
- through carefully controlled experiments, and multiple repeats, gain an insight into the potential randomness or variability of spalling; and
- make recommendations as to the appropriate experiments to use for spalling research - this will be based on an experimentally established understanding of the true influence of each of the key parameters thought to influence spalling, and include the influence of sample size, sample thickness, thermal exposure and loading/ restraint conditions.

1.3 Scope of work

It was hypothesised that extensive, carefully controlled experimental work – such as have never previously been performed and documented within the research literature - would provide valuable insights into the spalling phenomenon, and explanations as to the current apparent lack of understanding of, and ability to predictively model, spalling. It was thought that spalling may be inherently variable or random, and that carefully controlled experiments could allow this to assessed, along with the development of a better understanding of the influencing parameters.

In order to investigate the hypothesis and meet the aims of the project, three phases of experimental work have been conducted. This includes the testing of 114 carefully designed samples of varying scales, 36 of which were tested in four furnace tests at CERIB in France, and the remaining in 78 experiments at The University of Edinburgh.

Carrying out furnace tests allows the thermal exposure experienced by samples when tested to both the ISO 834 (International Organisation for Standardization, 1999) and French Modified Hydrocarbon (Ministère de l'Equipement, 2000) temperature versus time curves to be assessed. These thermal exposures were then recreated using the experimental apparatus at The University of Edinburgh. The first two phases of the experimental work were concerned primarily with establishing a suitable thermal exposure. This was done through comparison with the thermal exposure experienced by samples in furnace tests, this being the accepted thermal exposure in design. The third experimental phase developed a 3 MN uniaxial loading frame and investigated the influence of externally applied mechanical load on spalling when tested to the thermal exposures defined in Phase 1 and Phase 2 of the experimental work.

The comparison of the 114 results from three phases of experimental work allows the importance of influencing parameters to be assessed and recommendations for future experimental work to be established. Based on the experimental apparatus developed, and the knowledge of the research field, proposals are made as to the future applicability of this experimental approach.

1.4 Outline

The contents of each chapter are outlined below.

Chapter 2

A review of the testing and experimental methods currently used to research or assess concrete spalling is provided. This literature review gives context to the methods used today by looking back to their origins and explores the variety of experimental approaches in use.

Chapter 3

The experimental apparatus developed during this project is described in detail. This includes the two versions of the H-TRIS testing apparatus, a 3 MN uniaxial loading frame and equipment used for calibration. The process of developing the apparatus is described including solutions to issues encountered to aid future research. This chapter will aid future researchers in overcoming experimental challenges and designing experiments for spalling research.

Chapter 4

This chapter describes Phase 1 of the experimental work. The results of four furnace tests on 36 samples varying in size from “small scale” to “full scale” are presented. The tests were carried out to the ISO 834 and French modified Hydrocarbon standard temperature versus time curves. Thorough instrumentation of the samples allowed the thermal exposure experienced by the samples to be assessed. The testing allowed comparison of the influence on spalling of thermal exposure, sample size, sample thickness, curing conditions and the addition of polypropylene fibres.

Chapter 5

This chapter describes Phase 2 of the experimental work. In this chapter, the results of 33 experiments carried out using the H-TRIS apparatus are presented. These experiments were carried out on samples cast with the samples used in Phase 1. The thermal exposures experienced by samples in the standard furnace tests of Phase 1 were successfully recreated using the H-TRIS apparatus at The University of Edinburgh. While allowing validation of the thermal exposures used the results of the experiments also allowed further comparison of the influence of the parameters investigated in Phase 1 of the experimental work.

Chapter 6

This chapter describes Phase 3 of the experimental work. In this chapter, 45 experiments carried using the latest H-TRIS apparatus complete with uniaxial loading frame are described. The experiments made use of the thermal exposures defined in Phase 1 and Phase 2 of the experimental work. The experiments allowed insight into the influence of uniaxial compression, sample thickness, thermal exposure and heated area on spalling. As many repeat experiments were carried out, including nine repeats of one experiment, it was possible to assess the variability of spalling behaviour.

Chapter 7

This chapter provides discussion and analysis relating to the positioning of thermocouples in large concrete casts and uncertainties in temperature measurements. These issues were present across all three experimental phases. Assessment of the influence of assumed parameters in heat transfer assessments is also provided.

Chapter 8

This chapter provides discussion and conclusions relating to the development of the experimental apparatus including reflection on the approach taken in the work described in this thesis. The potential future application of the H-TRIS experimental apparatus is also discussed.

Chapter 9

This chapter provides discussion and conclusions relating to the experimental results. In addition, recommendations for future experimental work are provided.

Chapter 10

This chapter provides recommendations to structural and/or fire safety engineers, including advice on interpreting experimental results and specifying testing.

2 Review of literature

2.1 Summary

Heat-induced explosive spalling of concrete poses a credible risk to concrete structures that could potentially be exposed to fire. The spalling phenomenon has received considerable attention in recent decades and despite research efforts, there is still no validated guidance to enable the design of concrete mixes to prevent spalling. There are also no established, widely verified, repeatable test methods to confidently quantify or demonstrate spalling resistance for a particular mix in a given application. As a result of the status of the experimental research, and the limited understanding of spalling, there are also still no models that can predict spalling with sufficient confidence to be used in design.

Much work has been carried out over the past 100 years in which spalling was either directly considered or encountered. The author believes that the variety, and in some cases quality, of experimental approaches adopted, and the difficulty faced comparing results, is partly responsible for the continued lack of understanding of the spalling phenomena.

Spalling research and the elevated temperature performance of concrete is a broad subject. This literature review is focused on experimental approaches to spalling research; from the first fire-resistance tests to the experimental approaches being used today. The intent of this literature review is to convey the variety of experimental research being carried out and discuss the issues encountered in the experimental research community, which will have contributed to the lack of progress in the field.

Where other aspects of spalling research are touched on, a high-level summary is provided and the reader is referred to reviews by others, which have been written with a different focus.

The aim of the literature review is to set the scene for a concerted effort to improve upon approaches taken to experimental work, specifically with regard to the apparatus and method, and to aid the development of a repeatable experimental approach.

2.2 Introduction

2.2.1 What is spalling?

Heat-induced spalling refers to the breaking away of pieces from the surface of concrete when exposed to a severe thermal exposure like that which may be experienced in a fire (Bailey and Khoury, 2011; Bisby, Mostafaei and Pimienta, 2014).Spalling can take several different forms. The most violent of which being heat-induced explosive spalling of concrete, which is the focus of this project. Some images of spalled samples from experimental work carried out by the author are shown in Figure 2.1 and Figure 2.2. The spalling shown in Figure 2.1 is the more usual level of spalling that might be observed in a furnace test. The cover to the reinforcement has spalled away, which results in loss of strength of the reinforcement bars as they quickly reach elevated temperatures. Figure 2.2 is an example of severe explosive spalling of a thin, high strength concrete mix that was used to demonstrate spalling.

Figure 2.1: Spalled surface of a large-scale sample tested in a furnace test - the internal reinforcement has been exposed by spalling of the concrete cover

Figure 2.2: An example of total loss of section of a high-performance prototype concrete mix due to explosive spalling

As shown, this loss of surface material can lead to reductions in cross section, changes in load distribution, loss of insulation to internal reinforcement and, in some extreme cases, loss of the whole cross section. The violent and often progressive nature of explosive spalling means it is likely to be the most serious of the different spalling types for a structure. Spalling is an extremely complex phenomenon and is not well understood. It involves time and temperature dependent mechanical stresses, temperature gradients, differential thermal stresses, moisture movement, and microstructural and chemical changes with increasing temperature (Deeny *et al.*, 2014).

Concrete structures have historically performed very well in building fires (Bailey and Khoury, 2011; Bisby, Mostafaei and Pimienta, 2014) as concrete is non-combustible and has a relatively low thermal conductivity and diffusivity. The concrete core and reinforcement bars of reinforced concrete elements are protected in fire by the concrete cover and, if the cover remains in place, heat flow to the reinforcement and the inner concrete core occurs slowly. This slow heat transfer provides the necessary fire-resistance. The traditional approach to design for fire-resistance of a concrete structural element is to specify the minimum overall element dimensions and cover depths to reinforcement. The available evidence from real fires suggests that these simple, prescriptive approaches have historically yielded an acceptable level of fire performance in concrete buildings (Bisby, Gales and Maluk, 2013; Bisby, Mostafaei and Pimienta, 2014) and that heat-induced concrete spalling, while it has been observed in some cases, has not caused enough concern to directly impact design of reinforced concrete buildings.

While not currently considered directly in building design, spalling is considered in the design of concrete tunnel linings. The desire to improve understanding of spalling in concrete tunnel linings was one of the initial motivations for this project. Spalling is typically of greater concern in tunnels than in buildings. The fire loads, fire dynamics and construction of tunnels result in a more severe thermal exposure than would be typical of a building fire (Beard and Carvel, 2012). There is also a tendency to use higher performance concretes than in conventional building construction. The combination of these two factors leads to an increased likelihood of spalling occurring. That is not to say that spalling should not be considered in the design of buildings. The use of some contemporary concrete mixes in buildings could introduce a greater spalling risk. The contemporary concretes particularly those with higher strength and/or reduced permeability, appear more prone to heat-induced spalling (Kodur, 2000). The difference in behaviour of modern concrete mixes under severe thermal exposures has been shown by both experiences from real fires and recent research on heat-induced spalling (Maluk *et al.*, 2015; Hulin *et al.*, 2016). Based on these observations it is thought that heat-induced spalling of concrete may become a more prominent issue in future, further increasing the need to understand the spalling failure mechanism and influencing parameters. Figure 2.3 shows a comparison of the performance of normal strength and high strength concrete when full scale columns were subjected to a loaded fire-resistance test at the NRCC (Kodur, 2000).

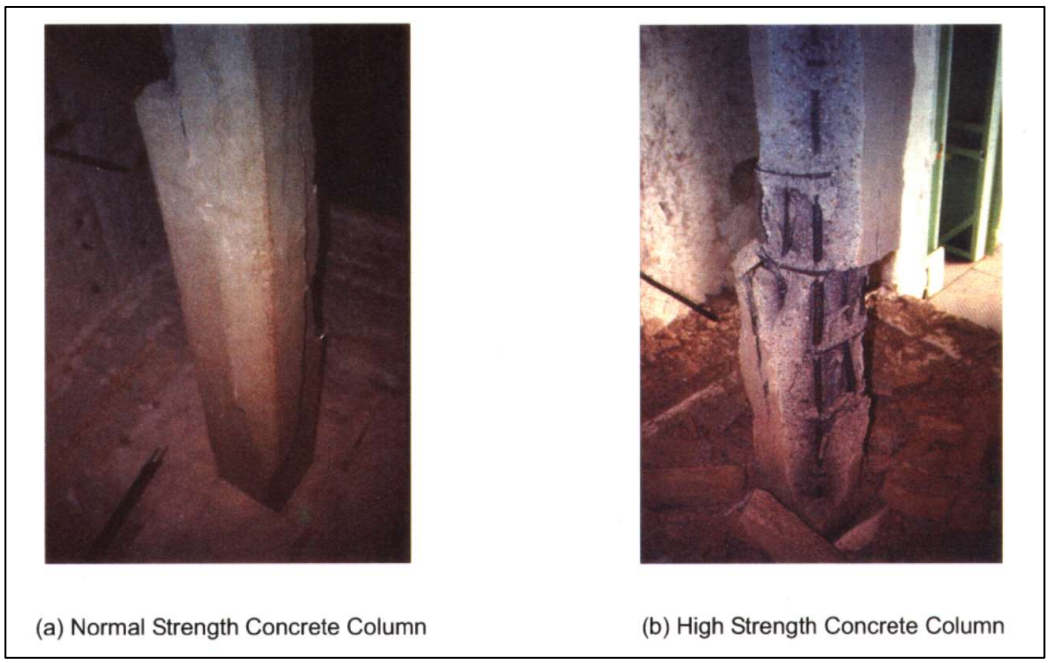

Figure 2.3: Visual comparison of the performance of normal and high strength concrete columns after furnace testing. Reproduced from work at the National Research Council of Canada (Kodur, 2000)

2.2.1.1 Terminology

Authors in the spalling research community have used different terminology over the years to describe spalling. For clarity the intended meaning of spalling specific terms in this thesis are set out below.

- **Spalling/Explosive spalling**
  These terms are used interchangeably. As set out above, the focus of this research project is on explosive spalling of concrete tunnel linings where fragments of the concrete surface are ejected violently. Unless otherwise specified, spalling should be taken to mean explosive spalling.
- **Sloughing off**
  This term is used within the spalling community to refer to the loss of heat damaged concrete. This is a gentle falling off of concrete which has been severely damaged and often occurs after testing as the dry heated concrete rehydrates naturally due to ambient humidity.
- **Aggregate spalling**
  This term refers to very small flecks of aggregate or cement paste which are ejected from the surface of a heated sample - typically less than 10mm diameter and with a depth of 1-2 mm. These small spalls are often attributed to failure of an individual piece of aggregate. Typically, only one or two of these “aggregate spalls” were observed and it would be very early in an experiment. The phenomenon was not prolonged.
- **Popcorn spalling**
  This is a term coined by the author to explain an unusual spalling phenomenon observed during some of the experiments carried out in this thesis. Popcorn spalling consists of many rapid small spalling incidents. Similar to aggregate spalling but fast and prolonged with a rate of around one small spall per second.

2.2.2 Importance of mitigating against spalling

The importance of preventing, or properly accounting for, explosive spalling during design of concrete structures is related to at least three design considerations:

1. **Life safety** – Explosive spalling reduces structural capacity, and hence 'fire-resistance', and could result in life-threatening structural collapses, exacerbated fire spread, or loss of water-tightness (particularly important in submerged tunnels).
2. **Asset protection and financial losses** – Explosive spalling causes damage to concrete elements, raising concerns for both direct and indirect economic losses, increased post-fire downtime and repair, asset protection, business continuity, and so on.
3. **Project risk** – The predominant approach to actually assess spalling risk for concrete mixes used in real projects (at least in tunnelling projects where spalling mitigation can influence concrete mix design) is by full-scale furnace testing of representative structural elements. This approach presents serious technical challenges and generates project risk as a concrete may fail at a late stage of design. It is generally not feasible to run multiple tests, and in tunnel design and construction, testing is often performed late in the design stage after the concrete mix and tunnel lining thickness have been fixed. Test failure would result in redesign and project delays, thus reducing design confidence in the early stages. Reliance on small sets of tests also places restrictions on the Contractor, limiting their ability to change concrete mix designs in response to supply, constructability, or economic factors occurring after testing (Deeny *et al.*, 2014). Project risk due to heat-induced spalling of concrete is usually less critical in other areas of construction, where spalling is rarely explicitly considered and 'fire-resistance' is assured by relying on historical evidence for furnace tests and real building fires. Whether structural engineers ought to be more reflexive as regards the potential consequences of concrete spalling in modern building projects is open to debate.

Addressing the above design issues for modern concrete mixes requires the ability to quantitatively *predict* explosive spalling – such that the depth of spalling to be expected during a credible design fire can be approximated and accounted for during the structural design process – or *prevent* spalling – such that design can performed confidently neglecting its influence. Whilst considerable progress has been made on

both fronts in recent decades, both remain difficult challenges and are the focus of a great deal of research internationally (Dehn, 2015).

2.2.2.1 The cost of spalling

The potential costs of spalling in buildings are hard to quantify. However, in tunnels the costs associated with repairs and loss of revenue during rehabilitation are likely to be considerable. For example, the direct repair costs following the 2008 Eurotunnel fire were estimated at £46 million, and given that the tunnel facilitates £91.4bn of trade annually, downtime as a result of fire could be as high as £250m per day, not accounting for indirect losses (Ernst and Young LLP, 2016). There are no obvious documented cases of large-scale structural failures or collapses that can be attributed directly to explosive spalling, and the consequences of spalling for structural performance of concrete structures remains a topic of on-going research (Kelly and Purkiss, 2008).

2.2.3 Current knowledge of spalling

The available research on heat-induced spalling suggests that it exhibits a stochastic nature, and experimental results are sometimes contradictory. Whether this is due to genuine randomness or to insufficiently controlled or instrumented testing environments is a matter of debate (Bisby, Mostafaei and Pimienta, 2014). The uncertainty even on a fundamental level of how one experimental parameter influences the spalling behaviour hinders design and often results in conservative and/or semi-arbitrary mitigation measures being used. Despite uncertainty and variation in results, general trends as to the factors that increase the risk of spalling can be identified. With some exceptions, spalling propensity generally increases with increasing compressive strength, rate of heating, moisture content, mechanical restraint, and imposed compressive load (Bailey and Khoury, 2011; Jansson, 2013; Bisby, Mostafaei and Pimienta, 2014). The variables thought to influence spalling will be discussed in more detail in Section 2.4. This knowledge has come from the research and observations of spalling from the past century. While concrete technology has advanced, the observations and experiences of early occurrences of spalling are worth noting and give context to the more recent research and developments. Some historical observations and research is given in Section 2.3 before the factors influencing spalling and more recent testing and experimental work are discussed in Section 2.4 and Section 2.6 respectively. The current guidance available to designers is discussed in Section 2.9.

2.3 Historical context

2.3.1 Development of reinforced concrete

Reinforced concrete as we know it today was first realised in 1877 as part of an attempt at fireproof construction (Hyatt, 1877). Thaddeus Hyatt carried out research to improve on the iron beam floors, which were previously classed as “fireproof” due to their incombustibility. Structural failures in fire led to the realisation that whilst these iron beams were incombustible they were not “fireproof”. This was a well-known problem and Hyatt reports that it became a standing rule amongst fire fighters to beware of “fireproof” structures considering them more unpredictable in fire than timber construction.

Hyatt recognised that in order for a floor comprised of iron beams to be “fire proof” the iron must be protected from heat. He proposed encasing the iron beams within an insulating layer of concrete. In his research, he demonstrated that concrete made from “New Portland Cement”, a cement that he had invented, was able to resist fire exposure and remain intact after rehydration on cooling. He also measured the thermal expansion of both the concrete and wrought iron and demonstrated that they were similar enough that he believed they could be considered the same, meaning no problems would arise during heating.

Through extensive ambient temperature testing of this new construction method Hyatt discovered that the concrete could act structurally with the iron. The result was that a much more efficient structural system of embedded strips of iron within concrete slabs was proposed. After developing the system, Hyatt carried out loaded furnace tests to demonstrate its fire-resistance. In these furnace tests, the samples of reinforced concrete were placed 12 inches above a 6-inch-thick bed of fuel and heated for 10 hours. At this date, there were no standardised fire curves to follow and researchers tended to aim for the most severe conditions they were able to create. After testing, the concrete slabs were sprayed with water and shown to resist both the furnace test and rapid cooling well. Hyatt was aware of the implications of his breakthrough discovery and the many potential uses of this economical structural system. No spalling was observed in these tests and based on the results of his research this new construction system appeared to provide a real “fireproof” solution.

2.3.2 Early reinforced concrete construction

In the years following on from the work of Hyatt, and other pioneers, a number of reinforced concrete “fireproof” structures were built. One of which being the reinforced concrete warehouse constructed in 1909 in Far Rockaway, Long Island. This warehouse was advertised as “fire proof” and the developers were so confident of this that the claim was written proudly on the external walls. The building is shown in Figure 2.4.

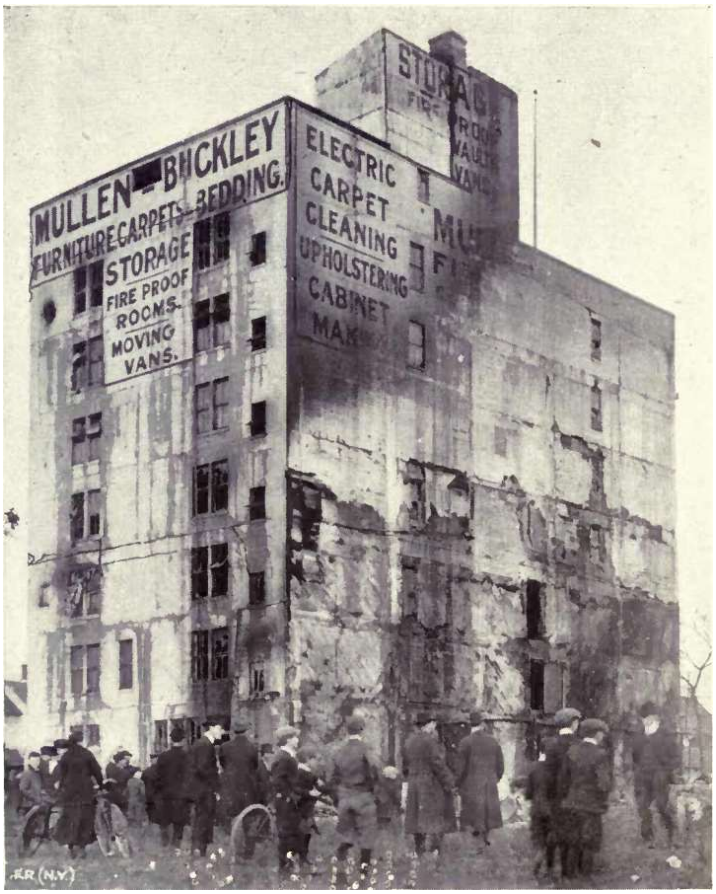

Figure 2.4: Far Rockaway Warehouse reproduced from report on the 1916 fire. (Woolson, 1918)

In 1916, a fire occurred in the warehouse and the structure proved not be as “fire proof” as thought. Severe spalling occurred in the fire and it is an early, well documented, example of the occurrence of concrete spalling in fire. Ira Woolson reported on the fire for the national board of underwriters and this report was later incorporated into Red Book No. 214 of the British Fire Prevention committee (Woolson, 1918). The reinforced concrete warehouse constructed in 1909 was branded as fireproof yet it experienced extensive spalling and structural failure when a fire broke out. In the report, Woolson describes loss of the full cover to reinforcing

bars and collapse of one area of the building. It appears from the report that the prominent theory at the time was that the spalling was a result of the differential thermal expansion of aggregates. The fire performance of quartz gravel concrete as used in the construction of the warehouse was considered to be poor. In his report, Woolson thought the fire to be small and the extent of the damage to be greater than expected, he stated that;

> *"A logical explanation of the phenomena is therefore necessary for future guidance."*

The use of round columns was suggested to prevent corner spalling and the focus of theories to explain the phenomena seemed to be on aggregate types and concrete element geometry. There was no mention of moisture content or pore pressure contributing to spalling in this early report. It is clear though that the need for understanding of the spalling phenomena had been identified.

Figure 2.5: Far Rockaway warehouse damage on fourth floor reproduced from report on the 1916 fire (Woolson, 1918)

In his note on the report, included within Red book No. 214, Ellis Marsland of the British Fire Prevention Committee, acknowledges the serious nature of spalling with his statement about the use of unsuitable aggregates, believed to be the cause of spalling, he states that:

"*Unless some more suitable fire-resisting aggregates are adopted, or a protective covering devised where unsuitable ones are used, reinforced concrete may be discredited.*"

This statement made over 100 years ago shows the importance of understanding spalling, something that we are still struggling with today, was recognised. While the use of reinforced concrete in construction was never discredited, spalling does still pose a risk and it is though that these risk levels could change with evolutions in the concrete mixes being used.

2.3.3 Origins of modern fire-resistance testing

In order to give context to the work which is being carried out today it important to understand the origins of fire-resistance testing. The approach of classification based on an ability to resist exposure to a defined elevated temperature for a period of time has its roots in the work being carried out in the early 1900s. This was the period when the requirement for a standardised test was recognised. In 1903 Edwin Sachs (Sachs, 1903) in his position as chairman of the British Fire Prevention Committee proposed that the term "fire proof" which was being used to describe buildings was removed. Instead he proposed buildings be described as "fire resisting" with a clear classification system to enable some level of quantification and comparison of the fire-resistance of a building. The classification system suggested was very basic and consisted of three different classifications each with two sub categories, A and B. The categories were temporary protection, partial protection, and full protection. Temporary protection was classified as the building material or system being able to resist temperature exceeding 1500°F for at least 45 minutes for class A and 60 minutes in the case of class B. Partial and Full protection classes required that a minimum temperature of 1800°F was resisted for specified periods of time between 90 and 240 minutes. For different element types, minimum areas to be tested and times for application of water under pressure were also included. For the testing of floors and ceilings, a load level for testing was also defined. Sachs stated that guidance given was not just his own work but also the work of the British Fire Prevention Committee and that they desired that the approach be adopted internationally to strengthen testing operations and "*systematize the various methods of testing and the principles of testing*".

In the US, the National Fire Protection Association, NFPA worked to develop the fire-resistance testing standards (NFPA, 1917, 1918). They involved organisations who

were performing the existing tests including Underwriters Laboratories, the National Bureau of Standards, and the National Board of Fire Underwriters. This work eventually resulted in the production of guidance and a fire curve for use when carrying out fire-resistance testing. The guidance and fire curve were reported in the 1917 and 1918 annual meetings of the national fire protection association and eventually adopted in ASTM C19 which then became ASTM E119 (ASTM International, 2018).

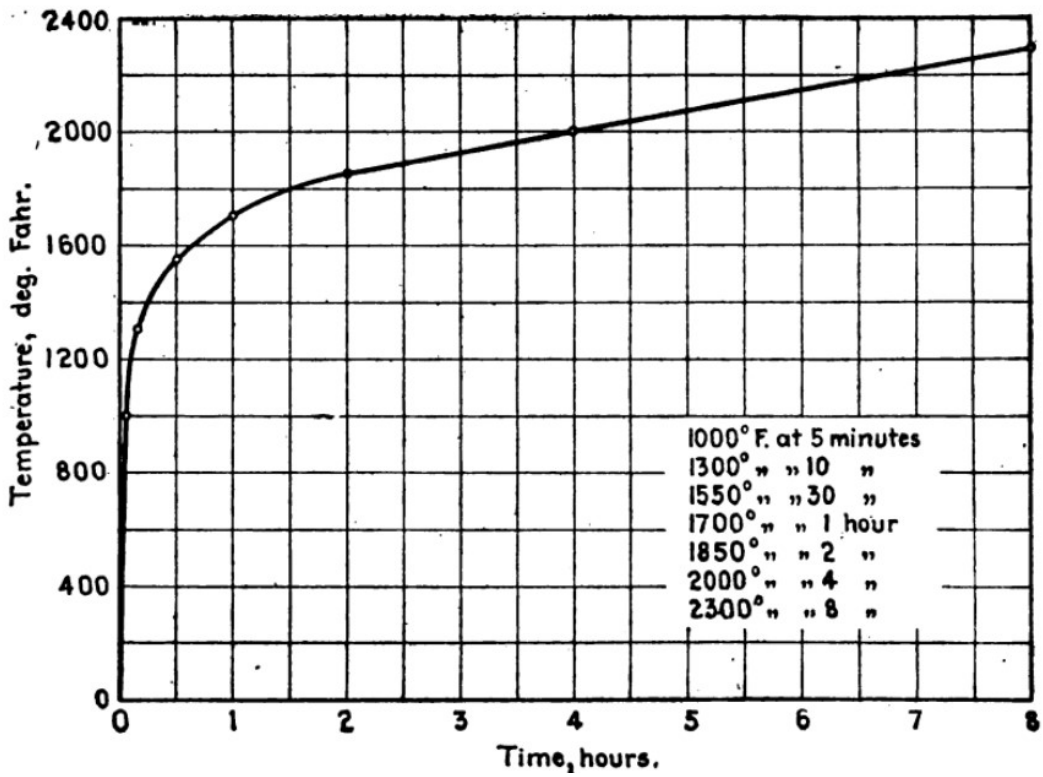

Figure 2.6: Temperature time curve for fire-resistance testing reproduced from (NFPA, 1918)

The guidance for adoption from 1918 (NFPA, 1918) stated that the furnace should be controlled to the temperature time curve shown in Figure 2.6 based on the average of not less than three thermocouples recorded at a maximum interval of five minutes.

The temperature time curve given in the current version of ASTM E119 is reproduced in Figure 2.7. While some of the guidance, including that on the measurement and control of the furnace temperature has changed. It can be seen that in the 100 years since its initial proposal the temperature versus time curve itself has not changed.

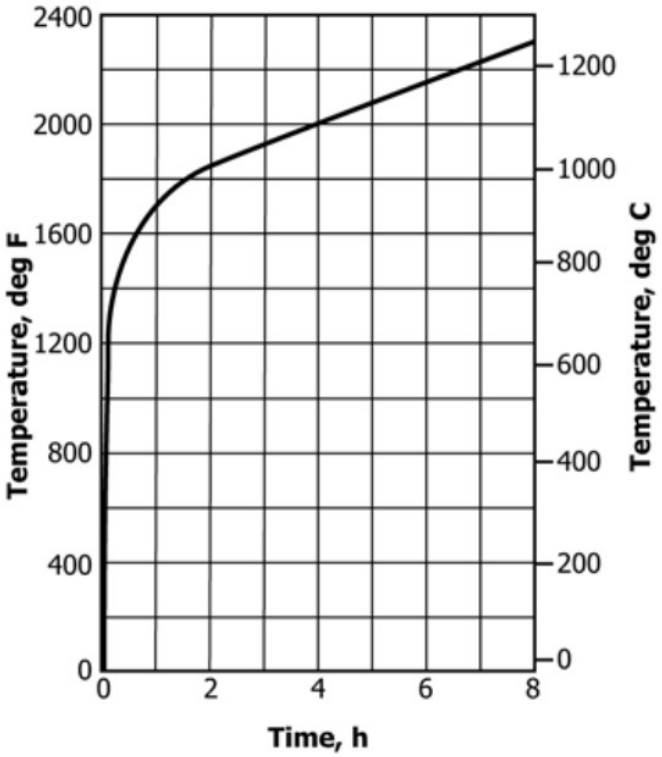

Figure 2.7: Temperature versus time curve reproduced from ATM E119 (ASTM International, 2018)

The original basis for the fire curve is unclear but it appears from the comments by Woolson in the proceedings (NFPA, 1918) that is has no real scientific basis and was not intended to remain unchanged. Woolson states:

> *"That curve which was presented last year purely as an arbitrary curve, has had a years service by the Underwriters' Laboratories and by the Bureau of Standards at its laboratories in Pittsburgh. The unanimous judgement of those who have used it is that it should not be changed, at least at the present time. There is nothing to suggest the curve is not approximately right for the work the Laboratories are doing."*

In the 1917 (NFPA, 1917) report which presented tentative proposals for the fire-resistance testing guidance Woolson stated

> *"We want to get it as nearly right as possible before it is finally adopted, because, after it is adopted by these various associations, it will be pretty hard to change it."*

These comments on the two reports indicate that Woolson was aware that the guidance, and the temperature versus time curve proposed, were not perfect. He was

also aware that once adopted, changing this curve would be difficult. It is surprising that this original temperature versus time curve and approach to testing has remained unchanged in a century of research, as it has not been without criticism. Researchers have made efforts to improve on the testing. In some cases, modification of the original fire testing standards was achieved by creating additional temperature versus time curves for testing. The ISO 834 (International Organisation for Standardization, 1999) curve is very similar to that specified by ASTM E119 and was developed in parallel. Some comparison of the ASTM and ISO curves was carried out when bringing the ASTM testing guidance more in line with ISO 834 was discussed (Wolfenden *et al.*, 1987). Other curves, which have been created since these original ones, include amongst others, the hydrocarbon curve (BSI, 1999), slow heating curve (BSI, 1999) French modified hydrocarbon curve designed for tunnels (Ministère de l'Equipement, 2000), RABT tunnel curves (Haack, 1998), and the RWS tunnel curve (Breunese, Both and Wolsink, 2008). The RABT tunnel curves were based on tests carried out in an abandoned tunnel in Norway in the early 1990s and the RWS curve is based on the results of testing carried out by TNO in the Netherlands in 1979.

Some of the key criticism of the standardised furnace tests carried out to temperature time curves came from Harmathy and Lie in their paper which explores the issues arising from ASTM E118 testing and gives a view for the future of fire-resistance testing (Harmathy and Lie, 1970). They discuss how the ASTM fire testing guidance was based on testing practices in 1917 rather than having any scientific basis. They are very critical of the test not representing a real fire. Despite research carried out soon after the standard's publication in understanding the thermal exposures associated with real fires, it took too long to challenge the standard. By which time

> "*a great deal of money had been spent by the industry on standard fire endurance tests, so that it became next to impossible to under-take a major overhauling of the test standard."*

This same issue would be faced today, perhaps to an even greater extent, if the fire-resistance testing standards were to be rewritten and the test procedures changed significantly.

Harmathy and Lie also discussed issues with the early test thermal exposure, a parameter thought to be a critical for spalling which has been found to usually occur in the first 30 minutes of a test (Malhotra, 1984). They stated that:

"During a fire test heat is transferred to the specimen partly by convection from the turbulent gases and partly by radiation from the gases and the furnace walls. The thicker the gas layer between the specimen and the furnace walls and the lower the thermal conductivity and diffusivity of the furnace lining materials, the larger the coefficient of radiant heat transfer… It must be pointed out, however, that for reasonably well-designed furnaces differences in the type of fuel, furnace lining materials, etc. are not expected to affect the heat transfer to the specimen for more than about 30 min from the beginning of the fire test."

As highlighted by Harmathy and Lee in 1970, even if the temperature versus time curve is followed perfectly, there are other issues with early-test heat transfer that can arise due to the design of furnaces. Aside from there still being variations between furnaces, current standards permit the furnace gas temperature to deviate from the target temperature time curve during the initial stages of the test (International Organisation for Standardization, 1999). This allowable variation is presumed to be due to the difficulties in controlling the initial increase in temperature in a furnace and the need for it to be realistically possible for the standards to be met. The author is not aware of any scientific justification for the lack of precision, particularly as this has been identified as a critical period of a test for spalling. The current temperature deviations permitted are covered in more detail in Section 2.6.1.

Work to improve the control of furnaces with the use of plate thermometers (Wickström, 1994) has been carried out since this paper but furnace dimensions and design, particularly of the furnaces often used for research, can vary greatly. It is challenging that the critical time period for the occurrence of spalling coincides with the period of least certain control of the thermal boundary conditions in furnaces.

Harmathy and Lie envisioned a potential change in testing to use realistic temperature versus time curves; improvement has been made here in recent years. They also envisioned controlling the thermal exposure as a heat flux versus time removing issues that arise as a result of controlling gas temperature in a furnace. Their paper concludes by highlighting the importance of understanding the behaviour of materials stating that

"Even the most sophisticated treatise on the behaviour of buildings or building elements in fire remains mere speculation if it is not based on a thorough knowledge of the behaviour of the component materials. This is why the authors

believe that any progress over the next 10 or 20 years will be measured by progress in understanding the behaviour of materials."

Understanding spalling as a material behaviour of concrete falls into this observed area of research need. Harmathy and Lie's critical evaluation of standardised fire-resistance testing and the use of furnaces should have sparked positive change and development in the field but seems to have gone largely unrecognised for the past 50 years.

2.3.4 Early observations of spalling in research

Early mentions of spalling of concrete in research do not typically come from research carried out specifically to investigate spalling. Usually tests were fire-resistance tests that may have been designed in an attempt to limit spalling or in which spalling may have been observed. It is possible to gain insight into the development of spalling theories from studying this early research.

One early project in which spalling was considered and attempts were made to mitigate against it was the research on the fire resistive properties of columns carried out by Walter Hull (Hull, 1918, 1919, 1920). In his 1919 report on the heat insulating properties of materials used in fire resisting construction (Hull, 1919) he shows an awareness of the influence of heating rate on spalling when he states

"it was decided to use a rather slow temperature rise in order that none of the specimens should spall or break up".

This comment is not justified in the report which was part of a larger project investigating the fire-resistance of reinforced concrete columns with a focus on the influence of aggregate type on fire-resistance (Hull, 1920). In the 1920 paper Hull reports on some results of 78 column tests with seven different aggregates and three column cross sections. Different reinforcement configurations were also investigated. The column tests were carried out in a gas fired furnace with baffles to prevent direct flame impingement on the samples and the furnace temperature followed the standard temperature time curve from the 1917 report of committee on fireproofing (NFPA, 1917) which later became the curve used in ASTM E119. The samples tested were circular and square columns with a height of 8'9" and either 18" or 12" diameters or 16" square cross section. These samples were loaded and heated simultaneously using a hydraulic jack and hand pump. The working load of the column was maintained throughout heating and then either the load was increased to failure at the

end of the fire test or if it withstood the maximum load of the jack, it was cooled and tested to failure residually. The testing showed that three of the aggregates had a much poorer performance in fire than the other four. The aggregates that performed poorly all contained quartz and two also contained either sandstone, or granite and gneiss. The columns made from limestone and dolomite aggregates did not spall and performed the best residually. It was concluded that columns which did not spall and had 1 ½" of cover to reinforcement would be capable in almost all cases of resisting a severe fire for 4 hours. For construction 2" of cover were recommended, Hull deemed this cover thickness to be insufficient when the concrete is susceptible to spalling. Efforts were made to mitigate against spalling and Hull demonstrated that the use of a light reinforcement layer in the outer concrete could effectively increase the fire-resistance of the columns by holding cracked concrete in place. The addition of a plaster layer with light reinforcement was suggested for existing concrete columns that may be susceptible to spalling. This work appears to be some of the first working directly targeting the prevention or reduction of spalling.

2.3.5 Early theories as to the spalling failure mechanism

A number of theories as to the mechanism of spalling emerged over the early years of spalling research. As mentioned previously, researchers first encountering spalling appeared to be focused on the properties of the aggregates being used.

Theories associated with the moisture content of the concrete and resulting pore pressure on heating also began to emerge. Harmathy (Harmathy, 1965) proposed that the failure mechanism could be the result of a moisture clog with water vapour condensing in the cold areas of the concrete effectively blocking the pores and resulting in an increased pore pressure. Other theories included the theory proposed by Saito (Saito, 1965) that the explosive spalling was a result of non-linear temperature distribution resulting in a failure of the surface concrete in compression and not associated with moisture. He stated confidently that

> *"explosive spalling is not caused by the steam pressure of the heated water within concrete voids but caused by thermal stress of concrete near the surface".*

Saito proposed that the spalling failure mechanism is a compression failure and that when the thermal stresses near the surface exceed the compress strength of the

concrete spalling occurs. His proposed solution to spalling is to use aggregates with low coefficients of thermal expansion.

The moisture clog theory developed by Harmathy remains one of the most favoured explanations of spalling and much research has been carried out in an attempt to investigate it further. It is noteworthy that the pore pressures typically measured in concrete are not sufficient to cause failure of the concrete. Section 2.5 provides further information on spalling theories.

2.3.6 Early attempts to use additives to mitigate against spalling

Polypropylene, PP, fibres are often used as a measure to mitigate against spalling and are recommended in codes and guidance, for example Eurocode 2 (British Standards Institution, 2005). It is unclear where the idea of using PP fibres to mitigate against spalling originated. This section discusses some of the early attempts to use additives to reduce spalling.

2.3.6.1 Polypropylene fibres

The book Fibre Cements and Fibre Concretes by Hannant (Hannant, 1978) describes the addition of different fibres to cements and concretes. Hannant writes,

> *"the incorporation of fibres into brittle things has been an elementary technology for millennia."*

His book goes on to describe the state-of-the-art use of fibres in cements and concretes and investigates the scientific principles of how fibres improve brittle materials. There is no mention of spalling in this book, but some fire testing of fibre reinforced concrete is briefly mentioned. Hannant mentions some concrete with Kevlar fibres that was tested by Walton (Walton and Majumdar, 1978) and another test that was carried out at the fire research station on a 50mm thick, 0.9m square, concrete slab containing 1.25% by volume of PP fibres. This is perhaps the first fire test on concrete containing PP fibres, fibres that are now a commonly used additive to help reduce spalling. Hannant reports that the PP fibres made no difference to the concrete and it was able to achieve a 30 min fire-resistance rating, failing due to the back-face temperature exceeding the maximum permissible temperature of 160°C. What is interesting is that Hannant writes that the PP fibres melted in the test *"leaving fine channels and an additional porosity in the panel"*. It is clear that the test was not carried out to investigate spalling nor were the fibres added to help mitigate against spalling. However, this observation could have later lead to the use of PP fibres to

mitigate against spalling with researchers trying to allow moisture escape. It is also possible that the realisation that PP fibres can help reduce spalling came from another source.

2.3.6.2 Polymer dispersion

Perhaps one of the first well documented uses of additives specifically to reduce spalling risk would be the 1980 research by Chandra, Berntsson, and Anderberg (Chandra, Berntsson and Anderberg, 1980). They experimented with the addition of a polymer to concrete in an attempt to improve its spalling performance. A polymer addition called Cemos described as an *"acrylate-styrene copolymer dispersion modified with asphalt*" was used. They were trying to address issues with moisture transport and vapour pressure and the additive was used to increase the porosity of the concrete. They believed that explosive spalling was greatly influenced by vapour pressure build up inside the concrete and thermal gradients and that these were both linked to the porosity of the concrete. The authors state,

> "*The steam pressure and thermal gradient depend mainly on the pore system of the concrete. The more open the structure, the less will be the steam pressure as well as the thermal gradient."*

Tests were carried out on 2.5 cm thick plates of normal concrete and lightweight aggregate concrete in a small gasoil-fired furnace following the standard temperature time curve. Ten different specimens were tested. None of the lightweight concrete specimens spalled. However, it was found that samples of normal strength concrete heated on two sides with this polymer did not spall, whereas samples without the added polymer did spall. The focus of the authors was on the contribution of moisture and pore pressure build up. The influence of load/restraint is not mentioned and was not investigated. Despite the effectiveness of this polymer being demonstrated, it was not widely adopted and is not a standard method for reducing spalling risk.

2.3.7 Summary of historical testing

Through the discussion of the development of standardised furnace tests and the early observations from research and real fires of the performance of reinforced concrete a number of key points can be highlighted. These are given in bullet points below.

- The furnace test, while commonplace, has non-scientific origins and is not representative of real fires.
- Issues surrounding harmonisation of furnaces and heat transfer to samples in the early stages of a furnace test can arise. Attempts have been made to reduce this effect.
- Early testing was predominately fire-resistance testing in which spalling was observed rather than testing to investigate spalling.
- The earliest theories as to the cause of spalling appear to be focused on the aggregate type being used, with more complex theories beginning to develop over time.

2.4 Factors influencing spalling

The factors thought to influence spalling have generally been acknowledged for many years, with different researchers favouring certain theories about the failure mechanism and attaching importance to the control of variables associated with those theories. Historical papers demonstrate that even early researchers appreciated the influence of many of the variables.

2.4.1 Dougill 1971

In the conclusions of his PhD research Dougill (1971) identified the factors identified as having an influence on spalling. These can be summarised as:

- Member size and geometry
- Loading and restraint conditions with high axial load or restraint promoting spalling
- Aggregate type
- Moisture content (through concern over steam pressure)

This list of factors identified in 1971 are still considered to be influencing factors to this date. Dougill was not particularly focused on the thermal exposure to the concrete during testing and this is a parameter that has received more interest in recent years.

2.4.2 CIRIA report on spalling of concrete in fires

In 1984 CIRIA published a technical note on the spalling of concrete in fires (Malhotra, 1984). The need for clearer guidance and a consolidation of spalling knowledge was recognised and the report is primarily a literature review identifying gaps in spalling knowledge and making suggestions for further research.

It is noteworthy how much was known about the variables influencing spalling at the time of writing. Researchers are still working to understand the influence of these parameters now, over 30 years later. The CIRIA report provides a review of the state-of-the-art-knowledge at the time and gives recommendations for how the research should progress. The document discusses historical experimental investigations into the spalling behaviour of concrete. The conflicting theories as to the cause of spalling are identified with the theories of Saito (Saito, 1965) and Harmathy (Harmathy, 1965). These were discussed previously in Section 2.3.5

There was an effort to establish the consensus at the time as to the factors influencing spalling. As part of the CIRIA report, a survey similar to one that had been carried out previously was sent around research laboratories. The outcomes of the survey were very much in line with the original 1970 survey and there appeared to be no significant change in the views or experience of spalling in the time since. As part of the original survey, 13 labs responded to questions about the spalling phenomena. Based on the survey the factors that were identified by the labs as having an influence on spalling were; aggregate type, concrete density, age, moisture content, restraint to expansion, aggregate size. With:

> "*the nature of the aggregate, free moisture and restraint to expansion … considered to be important in that order.*"

Present day views on the factors influencing spalling would include these factors.

After reviewing some of the available experimental results the document concludes that spalling can be eliminated or reduced by reducing moisture content, reducing compressive stress, using lightweight concrete, using supplementary reinforcement meshes and providing additional protection. Importantly the report also acknowledges that:

> *"the knowledge on the causes of spalling, particularly of different section shapes and concrete types, is limited."*

2.5 Stresses within heated concrete

While the phenomenon of heat-induced spalling remains poorly understood it is clear that spalling must be the result of stresses or pressures which occur in concrete during heating. Concrete has an inherently random structure of different aggregate particles and cement paste in addition to both free moisture in pores and chemically bound moisture within the cement paste (Callister and Rethwisch, 2010).

A thermal exposure to the concrete surface results in a thermal gradient through the sample, inducing thermal stresses and causing the evaporation and movement of free moisture as well as the release of chemically bound water from the cement paste. The Encyclopedia of Thermal Stresses provides a discussion of these stresses (Schrefler, Pesavento and Gawin, 2014). Figure 2.8 reproduced from this encyclopedia shows these stresses. Note that these stresses are, to an extent, theoretical as it is not possible to measure such stresses within concrete and the magnitude and relative contribution of each stress to spalling remains unknown. The stresses are discussed in the following sections and theories relating to the cause of spalling typically centre around these stresses. These theories will be touched on in Section 2.5.3 and through the literature review.

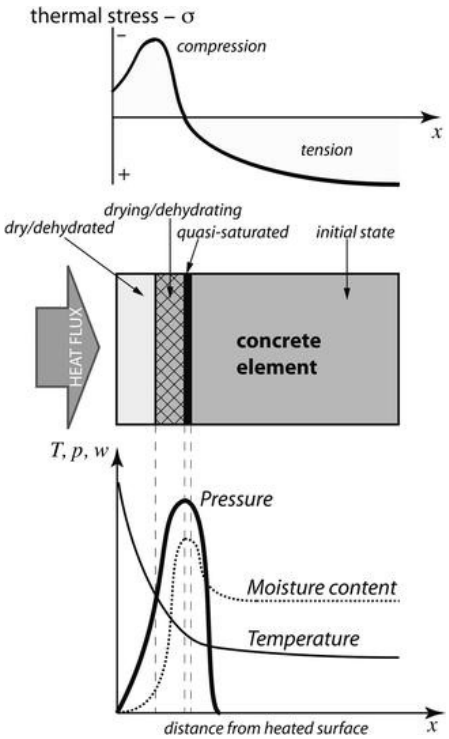

Figure 2.8: Diagram of theoretical stresses within heated concrete (Schrefler, Pesavento and Gawin, 2014)

2.5.1 Thermal stress

Concrete, along with most solids, expands when heated and contracts when cooled. Rapid heating of concrete, as would occur in a fire, results in a steep thermal gradient. The unheated side of an element, or the internal concrete of a specimen heated on all sides, can remain relatively cool while the surface temperature increases significantly, see Figure 2.8. The presence of this thermal gradient results in the expansion of the hot surface being restrained by the cooler concrete within the sample. This leads to a compressive stress in the surface, and tensile stresses in the cool concrete as a result of the hotter concrete pulling the cool concrete.

In addition to these global thermal stresses, there are likely to be local stresses because concrete is a random matrix of different aggregate particles, additives, and cement paste. The different aggregate types, sizes, and shapes are likely to have different coefficients of thermal expansion and differences here can initiate the same type of stresses on a macro scale. The performance of different aggregates at elevated temperature has been explored by researchers over the years (Johnson and Parsons, 1944; Robert and Colina, 2009; Kirnbauer and Schneider, 2011; Xing *et al.*, 2011). The influence of different aggregate types are not investigated in this thesis. However, the thermal expansion of different aggregates are shown in Figure 2.9 and Figure 2.10 for information.

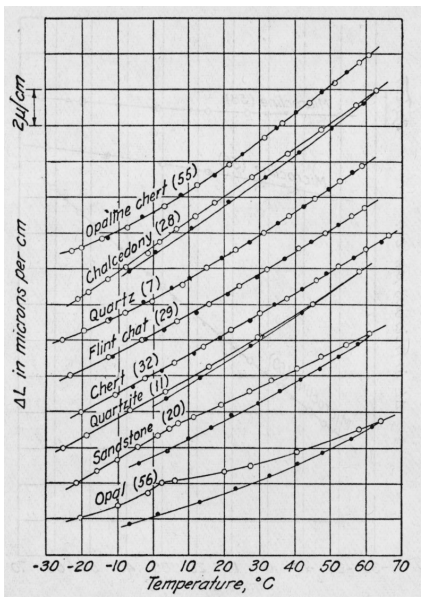

Figure 2.9: Thermal expansion curves of various siliceous rocks. Reproduced from (Johnson and Parsons, 1944).

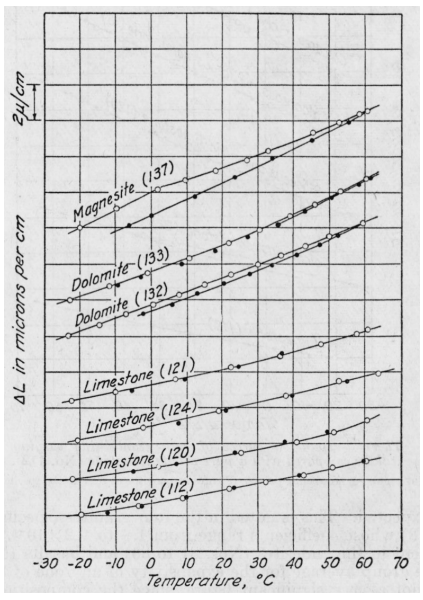

Figure 2.10: Thermal expansion curves of various siliceous rocks. Reproduced from (Johnson and Parsons, 1944).

It is thought that the thermal stresses in concrete which is heated on one face may be relieved by heat-induced bowing of a sample. A thicker sample could better resist this bowing, and the resultant thermal stresses would be greater than in a thin sample that was able to bow slightly. Similarly, if the heated concrete is under compression from an external source this could be expected to reduce the tension within the concrete but also prevent the release of the thermal stresses.

2.5.2 Pore pressure and moisture migration

As mentioned previously, concrete contains both free and chemically bound moisture (Khoury, 2000). When heated, this moisture evaporates and expands resulting in a pressure increase. The water vapour migrates through the pores of the concrete until it either escapes or condenses upon reaching cooler concrete. The pressures within the concrete as a result of this water vapour are dependent on a number of factors including the heating rate, moisture content, porosity, and permeability of the concrete. A popular theory, shown in Figure 2.8, is that as the moisture migrates from the hot concrete to the cool concrete it condenses within the pores resulting in a saturated layer, which restricts the movement of further water vapour and could result in an area of increased pore pressure. This saturated layer is often referred to as a moisture clog in the spalling community and is associated with theories that spalling is a result of pore pressure (Harmathy, 1965). When considering spalling as a result of pore pressure the pressure within the concrete would need to exceed the concretes tensile strength in order to cause the concrete surface to be detached violently.

2.5.3 Current position and theories

A large number of factors have been observed to influence heat-induced spalling of concrete and it is likely that, with the development of concrete mixes to meet environmental or structural performance requirements, there will be additions to this list. Some of the parameters currently thought to be important, and their generally accepted influence on spalling, are:

- **Thermal exposure** – Increasing the severity of thermal exposure is thought to lead to increased spalling propensity although this is not always evident (Jansson and Boström, 2013).
- **Moisture content** – Higher moisture content is thought to lead to increased spalling propensity (Harmathy, 1965; Copier, 1983; Ko, Ryu and Noguchi, 2011; Toropovs *et al.*, 2015).
- **Compressive strength** – Higher strength concretes are thought to be more susceptible to spalling (Phan, 1996; Anderberg, 1997), although this is disputed by some (Ali, 2002).
- **Permeability** – Lower permeability is thought to increase spalling propensity (Bosnjak, 2014).
- **Porosity** – Increased porosity is thought to result in a decreased spalling propensity (Matesová and Keršner, 2006; Rossino *et al.*, 2013; Yermak *et al.*, 2017)
- **Sample geometry** – Geometry has been observed to influence spalling (Guerrieri and Fragomeni, 2016; Lucio-Martin, Puentes and Alonso, 2019).
- **Sample size and thickness** – Larger and thicker samples are thought to be more prone to spalling (Jansson and Boström, 2013)
- **Reinforcement** – Reinforcement is thought to influence spalling but the influence is unclear. Reinforcement can allow moisture transport, increase stresses, and hold samples together (Copier, 1983; Rahim *et al.*, 2013).
- **Age of concrete** – Age influences concrete properties, and has been considered an influencing parameter for spalling (Boström and Jansson, 2011; Lenglet, 2011).
- **Aggregate Type** (Robert and Colina, 2009; Xing *et al.*, 2011)
- **Mix additives** (e.g. Silica fume) – These alter concrete properties and are believed to influence spalling (Rahim *et al.*, 2013)
- **Presence of polymer or steel fibres** – Fibres such as polypropylene are believed to reduce spalling propensity. Other fibres have also been observed to influence spalling (Heo *et al.*, 2011; Ozawa and Morimoto, 2014; Sanchayan and Foster, 2016).
- **Loading conditions** – Compression is believed to increase spalling propensity (Jansson, 2013; Rahim *et al.*, 2013; Miah *et al.*, 2016)
- **Restraint conditions** – Restraint is believed to increase spalling propensity (Hertz and Sørensen, 2005).

The above wide range of parameters have been identified by the spalling research community as having potential influence on heat-induced spalling (Koenders and Dehn, 2011; Pimienta and Meftah, 2013; Dehn, 2015; Jansson McNamee and Boström, 2017; Huang and Burgess, 2019).

The two key mechanisms which are currently acknowledged by this research community as contributing to explosive spalling are associated with the different stresses present in concrete upon heating. See previous sections. The inability of theories to explain the contribution of all influencing parameters has prevented widespread acceptance, and the challenges faced validating these theories add further complications. As a result, none have been widely accepted.

A summary of the dominant theories and issues with them is provided by Khoury (Khoury, 2000). He notes that for pore pressure spalling, the theoretical pressures predicted are substantially less than the tensile strength of concrete meaning that surface spalling would not be possible.

Harmathy (Harmathy, 1965) originally hypothesized that the pore pressure in heated concrete is increased due to the formation of a liquid water 'moisture clog' that results from moisture transport and condensation in the cooler zones within the concrete core. In recent research, the peak pore pressures have been measured by some as 0.7 MPa (Jansson and Boström, 2010). Other authors have similarly found experimentally that the maximum pore pressure is significantly lower than the elevated temperature tensile strength of the concrete (Felicetti, Lo Monte and Pimienta, 2017) and that spalling can occur when pore pressures measured within the test specimens are low (Mindeguia *et al.*, 2015).

With respect to spalling theories relating to thermal stress, Khoury noted that: *"very few concrete structures are loaded to levels where the necessary failure stress state is reached. This makes thermal stress spalling, by itself, a relatively rare (but not impossible) occurrence."* (Khoury, 2000).

Some authors favour the theory that spalling relates to differential thermal stresses in the concrete induced by thermal gradients, differential thermal expansion, and induced restrained deformations that develop during heating (Zhang and Davie, 2013). These thermal stress based theories often explain spalling as a compressive failure of the surface concrete (Dougill, 1972).

Modern variations on these core theories on the spalling failure mechanism are summarised by Robert Jansson in his PhD thesis (Jansson, 2013), and further theories and discussions of the failure mechanism have been presented more recently (Mindeguia *et al.*, 2015; Liu, Tan and Yao, 2018). It is generally accepted that the spalling failure mechanism is likely a result of the combination of thermal stresses and pore pressures, but a lack of understanding remains.

The continuing development of new variations on theories demonstrates that, to date, it has not been possible to develop a sufficient understanding of the spalling mechanism. While researchers have proposed theories, none of these have been proven despite the confident conclusions that can often be found in research papers on the subject. The current status of spalling knowledge and experimental research has not allowed a validated model to be produced, and there is currently no model that can predict spalling with confidence.

Rather than expanding further upon un-validated theories, this review focuses on issues associated with experimental research and the reasons why, after over 100 years, authors are still hypothesising as to what the spalling failure mechanism could be. It is the author's view that this is largely due to the inconsistency and lack of control in experiments, a selection of which have been detailed in this review to demonstrate the variety. In many cases, researchers appear to set out to investigate a specific theory and this will shape their experimental approach. Care has been taken to ensure that the experimental approach developed in this thesis is not prejudiced in this way.

The following sections discuss the modern experimental research being carried out to investigate spalling and the attempts to understand the potential failure mechanisms.

2.6 Modern experimental work and testing to investigate spalling

Due to the volume of experimental work that has been carried out on concrete in fire, and at elevated temperatures, this section will focus on work carried out specifically to investigate spalling. The parameters influencing spalling have been identified over the past 100 years and these were summarised in Section 2.4. Different researchers still maintain theories as to the importance of each variable and this tends to shape the recent testing that has been carried out. Spalling theories were mentioned in Section 2.3.5 and 2.5.3.

The aim of this section is to demonstrate the variety of experimental methods in use and discuss some of the key outcomes and the issues arising. The amount of spalling specific research being carried out has increased greatly in recent years and there is now an International Workshop on Concrete Spalling held every two years. The proceedings from the fifth conference contained 35 papers from around 100 authors (Jansson McNamee and Boström, 2017). Three of these papers described work carried out by the author. These covered testing as part of an international attempt to compare test methods (Jansson McNamee *et al.*, 2017), a collaborative project testing recycled tyre fibres (Figueiredo *et al.*, 2017) and description of some of the tests carried out as part of this PhD project (Rickard *et al.*, 2017).

The increase in interest in the field of spalling research should help to advance knowledge on the topic. However, there does seem to be a general lack of direction in the experimental work with researchers often focusing on their own interests. This has been improved with the creation of the RILEM technical committee for spalling which the author is a member of (RILEM TC SPF). The committee has a number of goals, one of which is to provide guidance for spalling testing including which measurements should be taken and which test parameters should be controlled and how. This guidance, when finalised, should serve to aid the comparison of outcomes from different research projects. One of the obstacles faced when trying to compare testing or experimental work is that whilst the test methods are extremely varied there can also be a lack of appreciation for the need to control and document testing parameters with care, particularly thermal exposure. This issue is discussed in more detail in Section 2.6.1 and throughout the discussion of experimental approaches.

2.6.1 Control of thermal exposure

The control of experimental boundary conditions is critical if meaningful results are to be obtained. One area where modern spalling research seems to suffer is in the consistency of thermal exposures in terms of control, application, and severity. Since the standard fire curves have become commonplace in compliance testing they have also been adopted in many cases for research. This is justifiable if aiming to develop a concrete mix optimised to pass this approvals test but in order to understand the spalling phenomena and enable performance-based design to real fire exposures the standard fire curves are limiting. The historical criticisms of Harmathy and Lie (Harmathy and Lie, 1970) were discussed in Section 2.3.3.

It is appreciated that following a standard gas temperature-time curve is not the same as directly controlling the thermal exposure to which a sample is subjected (Harmathy and Lie, 1970; Connolly, 1995; Maluk *et al.*, 2016; Maluk, 2017; Torero, Law and Maluk, 2017). Improved control and understanding of the thermal boundary conditions can be achieved if the thermal exposure is controlled directly. This approach is common practice in fire science research. Test apparatus such as the cone calorimeter (British Standards Institution, 2015) and FPA (ASTM, 2013) both control the heat flux applied to samples.

Attempts have been made to harmonise furnace testing with the use of plate thermometers. However, in fire-resistance testing large deviations from the desired temperature versus time curve are permissible during the early stages of testing. This period is known to be critical for spalling. The permissible variation depends on the temperature time curve being used but there is typically an initial period where there is limited or no requirement for temperature accuracy followed by permitted variation. For the ISO 834 temperature versus time curve there is no limit on individual furnace gas temperatures within the first 10 minutes then after ten minutes the temperatures of furnace control thermocouples must be within 100°C of the target temperature. The average gas temperatures within a furnace are limited from a time of 5 minutes through comparison of the area under the target and achieved temperature versus time curves. Further information is provided in Section 4.8 where the validity of the furnace tests carried out as part of this research project is assessed.

In experiments carried out using non-standard test methods, the thermal exposure often aims to recreate that of a standard fire-resistance furnace test through another heating method. Even if the temperature time curve can be followed, the thermal

exposure is unlikely to be directly comparable to that of a furnace due to the different thermal properties of the heating environment and the control methods used. For example, thermal exposure at the beginning of a furnace test is dominated by direct radiation from the burner flames with furnace thermocouples measuring gas temperature. A small electric oven would be expected to be predominantly convective heating, with no initial spike in radiative heat transfer. Works referenced above explain this in detail.

Test methods that do not follow one of the standard fire curves often try to recreate a standard temperature time curve but are limited by the capabilities of apparatus being used. Others make use of constant thermal exposure usually defined as a temperature or severe exposure such as direct flame impingement from a blowtorch. These experiments can all give some qualitative indication as to the spalling propensity but are difficult to compare. The knowledge that can be obtained from running a small test series with a thermal exposure that is not comparable to that of other researchers is limited.

In many cases it can be said that little emphasis has been placed on the heat transfer to the samples and that focus of the testing has been elsewhere, be that on mix design or novel instrumentation. The standard temperature time curves are often used as a fix, allowing the complexities of this aspect of the testing to be ignored. Simplifying the testing in this manner for many years has failed to yield any real quantifiable progress and conflicting results and theories are still abundant. Emphasis must be placed equally on all parameters thought to influence spalling to minimise the uncertainty in test results and maximise the knowledge gain. Concrete is already inherently variable and variations in results can be seen at ambient temperatures in simple compression tests of cubes and cylinders (Halstead, 1969), when further complexity is added to a test, great care must be taken if understanding is to be gained.

2.6.2 Modern fire-resistance furnace testing

As mentioned in Section 2.3.3 the 'fire-resistance' of structural elements (of all material types) is assessed in practice using large-scale 'fire-resistance' tests. These tests subject loaded, representative, and typically full-scale (or as close to full-scale as possible) structural elements to a standard gas temperature versus time curve within a fire testing furnace. Explosive spalling has been directly observed for a large number concrete elements tested in this manner, for more than a century (Hull, 1920), however this spalling has historically been mild and not thought to be of critical importance for the overall fire-resistance of concrete structures. In recent decades, however, with the advent of engineered high-strength, high-performance, and self-consolidating concrete mixes with increased propensity for explosive spalling, spalling has become a more common failure mode for concrete elements tested in furnaces (Maluk, Bisby and Terrasi, 2017).

Since explosive spalling depends not only on material parameters but also on structural parameters, it is necessary to repeatably and accurately reproduce realistic conditions (e.g. geometry, boundary conditions, applied mechanical and thermal loads, etc.) when experimentally studying spalling of different concrete mixes. Such control over testing parameters is challenging when testing in furnaces, particularly during the early stages of heating which are critical for influencing explosive spalling.

2.6.2.1 Approvals testing for tunnel applications

In relation to heat-induced spalling, furnace testing is typically used as an approvals test for tunnels. These kinds of tests are carried out to demonstrate the performance of concrete for tunnel linings but the use of certain concrete mixes falling outside of available guidance could result in approvals testing being carried out for a building. The approvals testing is used to support design assumptions of: (1) no spalling under a 'standard fire' heating scenario (i.e. where none is observed in furnace testing); or (2) a certain depth of spalling (sometimes assumed as the final spalling depth observed during standard furnace testing). However, given the known variability of spalling for a single mix under slightly different thermal and mechanical conditions (Maluk *et al.*, 2015), neither assumption can usually be confidently defended based on the available experimental evidence. It is unlikely that the conditions experienced by the test specimen in the furnace will be representative of reality.

The reliance on full scale furnace testing is particularly problematic for assessing the spalling risk of concrete tunnels or tunnel lining segments. A number of furnace test

procedures have been applied to assess spalling of concrete for tunnelling applications; however there has been little harmonization of these from either a thermal or a mechanical perspective. The majority of these test large-scale tunnel structure or lining samples exposed to a 'tunnel fire' heating regime (Haack, 1998; Ministère de l'Equipement, 2000) based on data from tunnel fire tests that are assumed to adequately represent the thermal environment during a severe fire within a tunnel.

Furnace testing of structural elements other than tunnel segments is also challenging as it is usually only possible to test single elements, and real loading/restraint cases may be hard to replicate. Demonstration by testing that a concrete mix will perform adequately is not as commonplace elsewhere in structural engineering as in tunnel engineering, but may be advisable where modern, high-strength concrete mixes are being used or where spalling could be a critical to meet functional performance objectives. This is the case, for example when applying slender ultra-high performance concrete slabs, pre-stressed with carbon fibre reinforced polymers, in building applications (Maluk *et al.*, 2015).

2.6.3 Different approaches to spalling experiments

The lack of solutions from more conventional testing has lead researchers to develop their own test methods. The adoption of a new or unusual test method may have occurred for a number of reasons. It could have been driven by the desire to investigate a specific parameter such as pore pressure build up or it may be a result of the cost and difficulty of testing using methods closer to the standardised furnace test methods. Great care must be taken when designing an experiment with the goal of investigating one specific parameter. As Thomas Kuhn stated, in reference to scientific research, in his 1962 book The Structure of Scientific revolutions: "*The answers you get depend upon the questions you ask*." (Kuhn and Hacking, 2012)

This section focuses on some of the different experimental methods that have been used in recent years. The intent of this section is to convey the variety of experimental approaches being used and some of the key issues with them. The, often questionable, results of individual experimental programmes will not be covered in depth.

Different experiment types have been selected in an attempt to show the breadth of approaches taken. Due to the sheer number of experiments carried out globally,

where either spalling was the research focus, or became the focus after it occurred, an exhaustive list here is not appropriate. There are many variations on these experimental approaches, coupled with experimental setups designed to investigate other parameters, which reported on spalling when spalling influenced the success of the designed experiment. It is worth noting the factors that have been identified as having an influence on spalling are often not accounted for adequately in the experiments described in this section. It is also worth noting that while the understanding of spalling is limited it is desirable to ensure that the outcome of experiments can be compared with research being carried out elsewhere.

2.6.3.1 Testing of loaded samples

The importance of loading and restraint for concrete spalling have been understood since the early days of spalling research with researchers being particularly concerned about compressive stress. Due to the lack of understanding of spalling it is desirable to test samples under loads representative of actual in-service load conditions. Many researchers have been carrying out tests without the application of any external load to samples. This is likely to be a result of the complexity and cost of developing loading frames that are able to work alongside different heating methods. As an example, the work carried out by Zeiml et al. (Zeiml, Lackner and Mang, 2008) investigating the behaviour of concrete tunnel linings would have been improved by carrying out loaded tests. Tunnel linings will be under load when in situ and it is believed by many researchers that this load is critical to spalling.

A number of approaches to application of load have been taken. These vary from applying a restraint, discussed in Section 2.6.3.2, to active biaxial loading of samples.

Boström et al. (Boström, Wickström and Adl-Zarrabi, 2007) made use of prestressing tendons to apply loading when they carried out a test programme on loaded cylinders and slabs of various sizes. They noted difficulties with the loss of compression due to the heating of the prestressing bars. In tests where the compression was lost, the spalling was reduced and so the theory of increased load increasing spalling propensity was demonstrated. They concluded that the application of compressive load influences both the probability of spalling occurring and the extent of spalling that will occur. Other research projects have also made use of this style of loading system (Boström and Larsen, 2006; Jansson, 2013; Jansson and Boström, 2013).

The application of realistic load to curved concrete tunnel segments can be challenging. The use of post stressing tendons is recommended by Efectis R0695

(Breunese, Both and Wolsink, 2008) as the preferred method for simulating tunnel loading but, as discussed, issues can arise with loss of tension.

The loading of tunnel segments is often achieved by loading the segment in bending. This method of loading a tunnel segment for a furnace test is show in Figure 2.11 which is reproduced from a paper describing repairs to a tunnel after fire (Høj, Tait and Macdonald, 1999). It is interesting to note that for this project they thought the realistic compressive stress in the tunnel segments to be approximately 5 MPa and the load levels applied during furnace tests were 2 MPa and 5 MPa. Their choice of loading for their tunnel tests can be used to inform decisions as to the appropriate load levels to be used. The concrete used for their tunnel segments was a C50/60 specification concrete that *"had been achieving average cylinder strength of 76 MPa in production"*. This deviation from the specification if not beneficial in terms of spalling performance.

A similar test setup used for testing carried out at CERIB (Robert, Collignon and Scalliet, 2013) is reproduced in Figure 2.12. In these tests it appears that a compressive stress of 2.11 MPa was used (specified as an axial force of 1408 kN over the cross section).

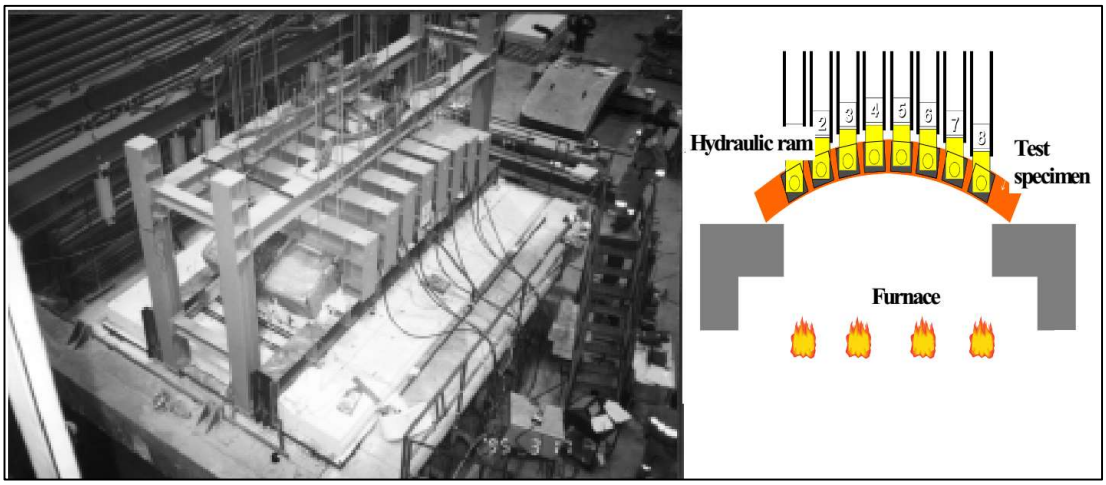

Figure 2.11: Loading configuration for a tunnel segment reproduced from (Høj, Tait and Macdonald, 1999)

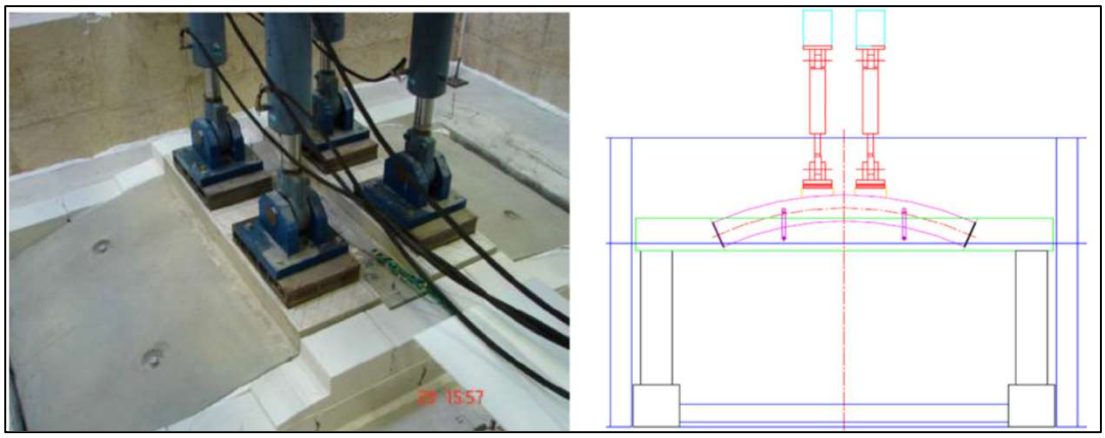

Figure 2.12: Test setup used for tunnel linings at CERIB reproduced from (Robert, Collignon and Scalliet, 2013)

Many methods of load application are capable of creating representative experimental conditions. If possible, the use of actively controlled external loading systems is preferred as they facilitate precise control of the load applied to the sample throughout the duration of the test/experiment. This approach was appreciated historically (Connolly, 1995) and in recent years has received more attention. A small uniaxial frame was used by Maluk (Maluk, 2014) during his PhD testing and a large uniaxial loading frame was developed as part of this research project (Rickard *et al.*, 2016). Researchers in Italy have also developed a sophisticated biaxial loading frame (Lo Monte and Felicetti, 2017). These loading frames, amongst others, allow the load levels to be maintained and monitored throughout the duration of experiments. The apparatus developed by the author also allows for modification to include loading ramps rather than just constant load.

2.6.3.2 Testing of restrained samples

A number of researchers have used steel restraint as a simple method of applying load to a sample during a spalling test. The use of restraint can allow simulation of more realistic in-service conditions than would be simulated with an unrestrained sample. Concrete is not usually free to expand in all directions when used structurally and is restrained to some degree although the correct level of restraint to apply to simulate a specific scenario would require assessment of the stiffness of the surrounding structure.

The application of restraint by the use of metal confinement results in the actual level of confinement experienced by samples during experiments being difficult to quantify. The restraint level is influenced by thermal expansion of both the concrete and the

restraint ring/frame as well as the stiffness of the restraint and the interface between the restraint and the concrete; in some cases, a pad is used. Perhaps one of the first instances of using this testing approach being used would be the “pilot test” carried out by Dougill (Dougill, 1971) on 300mm diameter mortar samples cast within a brass ring. The tests were intended to show the benefits of cracking. The samples are shown in Figure 2.13 which is reproduced from his PhD thesis. The samples were heated with oxy-acetylene flames and the temperature in the hot spot “exceeded 1250°C”. In the experiments one sample was heated locally and one more evenly over the surface. The formation of cracks around the heated area of the sample that experienced localised heating was noted as being beneficial for the prevention of spalling. For the sample that was heated more evenly, the brass ring confined the sample and prevented the formation of the cracks seen in the other sample. A violent failure was observed in this case. No attempt was made to quantify the restraint provided by the brass rings and it is not clear how comparable the thermal exposures were between experiments

Figure 2.13: Samples 300 mm in diameter restrained with a brass ring and heated with oxy-acetylene flames (Dougill, 1971)

Similar tests have been carried out since by other researchers including by Connolly as part of his PhD in 1995 (Connolly, 1995). Connolly carried out early pilot tests to investigate the importance of different parameters and, when he did not observe any spalling in tests carried out without mechanical restraint, he opted to cast concrete into a 150mm internal diameter 6mm thick mild steel tube. Spalling was observed when these restrained samples were tested with direct flame impingement from a

blowtorch. Unrestrained samples heated in the same way did not spall, so the importance of restraint was highlighted. The uncertainty in the level of restraint provided by the cool edge concrete and steel hoop was recognised. Connolly stated that

> *"further work would require that both heating and restraining forces be applied in a strictly controlled and quantifiable manner*"

As such, after these initial tests, Connolly went on to develop an alternative test method with great consideration of the control of the necessary parameters. Firstly, a loading apparatus was developed which enabled quantifiable load to be applied to concrete cylinders. The apparatus developed to apply the restraint is shown in Figure 2.14.

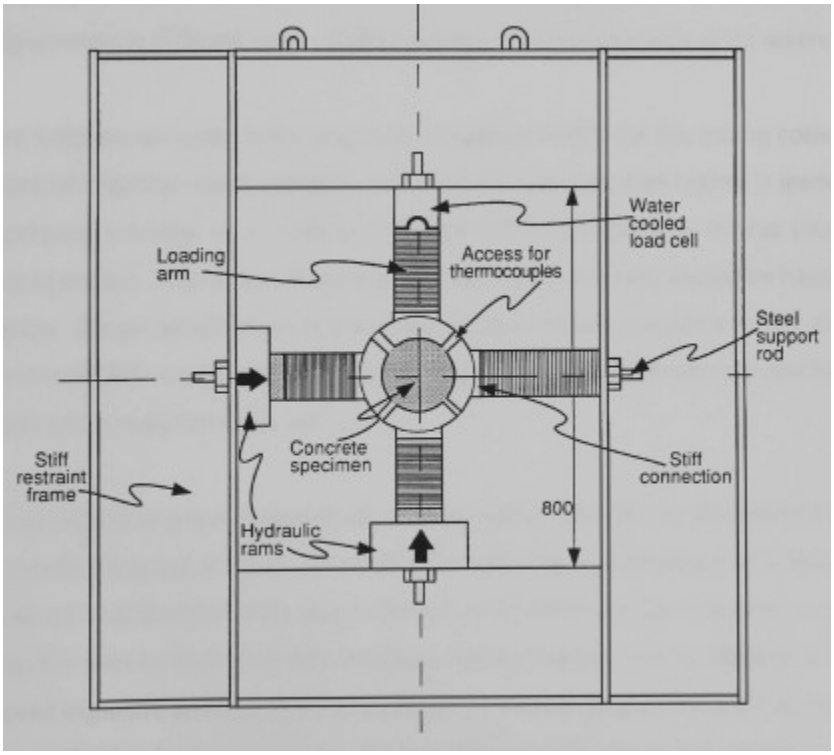

Figure 2.14: Improved test apparatus developed by Connolly to allow controlled restraint whilst heating reproduced from (Connolly, 1995)

Connolly then made efforts to properly control the thermal exposure to the sample by way of controlling the heat flux rather than the temperature. He states

> *"It has long been recognised within the fire testing community that the specification of a heating regime simply in terms of a time temperature regime is inadequate. As the temperature response of a concrete specimen will be*

governed by the net total heat flux incident to its surface, proper specification of the heating environment should be based on a heat flux criterion"

Constant heat flux levels for experiments were specified and an electrical heater was developed which was capable of achieving the desired heat fluxes. Connolly had considered altering the incident heat flux to the sample by changing the distance between the electric heater and the sample. This is the basis for heat flux variation used today in the H-TRIS testing methodology (Maluk *et al.*, 2016). Connolly did not pursue this approach, as he was unable to control the location of the heater with sufficient accuracy.

Despite the early researchers recognising that metal ring method of restraint does not allow for control or accurate quantification of the stress levels in concrete samples a number of researchers have continued to test using very similar methods. Conolly's recognition of the need to properly control the thermal exposure has also been neglected.

Hertz and Sorensen (Hertz and Sørensen, 2005) worked towards establishing a new small scale screening test. They set out to create the worst-case loading condition for spalling which they considered to be full restraint against thermal expansion. This work was informed by some earlier tests described briefly in the same paper in which localised heating of the centre of a concrete slab was carried out in order that the surrounding cool concrete would restrain the thermal expansion of the hot centre. In those tests, it was noted that spalling stopped when tension cracks formed in this outer cool restraining concrete. Based on this observation they concluded that the thermal stresses were critical for spalling and this same conclusion has been reached by other authors as previously discussed.

To better test samples with full restraint, standard sized cylinders usually used for compression tests were held within a 50mm thick steel mantle, see Figure 2.15. The philosophy was to create an easy, quick test method that, as a worst-case test, could indicate the real performance of a concrete. Heating was carried out using an oven that was heated to 1000°C before being opened to expose the front face of the sample to this temperature. This is a very crude and arbitrary way to control thermal exposure to the sample and is a step back when compared to the work of Connolly (Connolly, 1995). No attempt was made to try to understand the stress level in the sample as a result of the restrained thermal expansion. This, in combination with the unique heating conditions, makes comparison with results from other tests difficult. It is also

not possible to vary the amount of restraint provided by the mantle, and so properly understanding how restraint influences spalling is difficult. It was assumed that this is the worst-case restraint condition for spalling without having been able to test others. The crude approach to heating was described as the exposure that *"gives a temperature increase comparable to the increase from the hottest fires which do not melt the surface".*

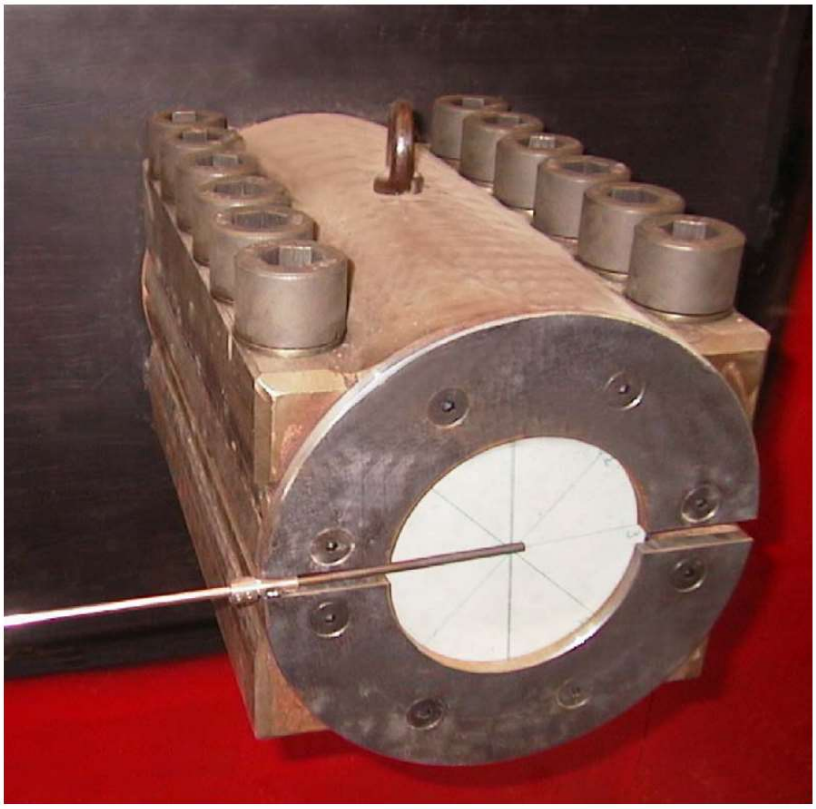

Figure 2.15: Test setup developed by Hertz and Sorensen reproduced from (Hertz and Sørensen, 2005)

In the years following these tests a number of researchers have experimented with samples restrained by metal hoops or frames with some efforts being made to understand the restraint provided (Zhao and Sanjayan, 2009; Tanibe *et al.*, 2011, 2013; Gulik *et al.*, 2016; Jansson McNamee *et al.*, 2017). The test method is typically approached as a simple to carry out screening method for different mixes with the goal often to be achieving worst-case conditions with respect to restraint.

The use of a metal hoop or frame is not the only way to create restrained conditions within a concrete sample. Other researchers (Werner and Rogge, 2014) have investigated localised heating of the centre of a concrete sample which results in the cool outer layer of the concrete restraining the central heated area. The restraint provided in this scenario is also very challenging to quantify.

2.6.3.3 Testing of Spherical samples

In an attempt simplify modelling (Debicki, Haniche and Delhomme, 2011, 2012) decided to attempt to create a symmetrical temperature gradient and thermal stress within a concrete sample by heating spheres of concrete suspended within an oven, see Figure 2.16. These spheres were fitted with a pressure gauge; pressure gauges are discussed in more detail in Section 2.6.3.7. The spherical geometry of the samples is not representative of any real scenario in which concrete may be used, but does allow some insight into the concrete behaviour to be gained. The inability to test under any load or restraint combined with the use of a sample geometry that is not representative of any end use application limits the usefulness of the test method. Since all the moisture is migrating towards the centre of the sphere the experiment has the potential to exaggerate the effects of moisture clog on vapour pressure build up. This effect will not be seen in any real application, as it is not usually possible for a concrete element to be heated on all surfaces. The results of these experiments are not considered particularly relevant due to the unrealistic test setup and will not be discussed further here.

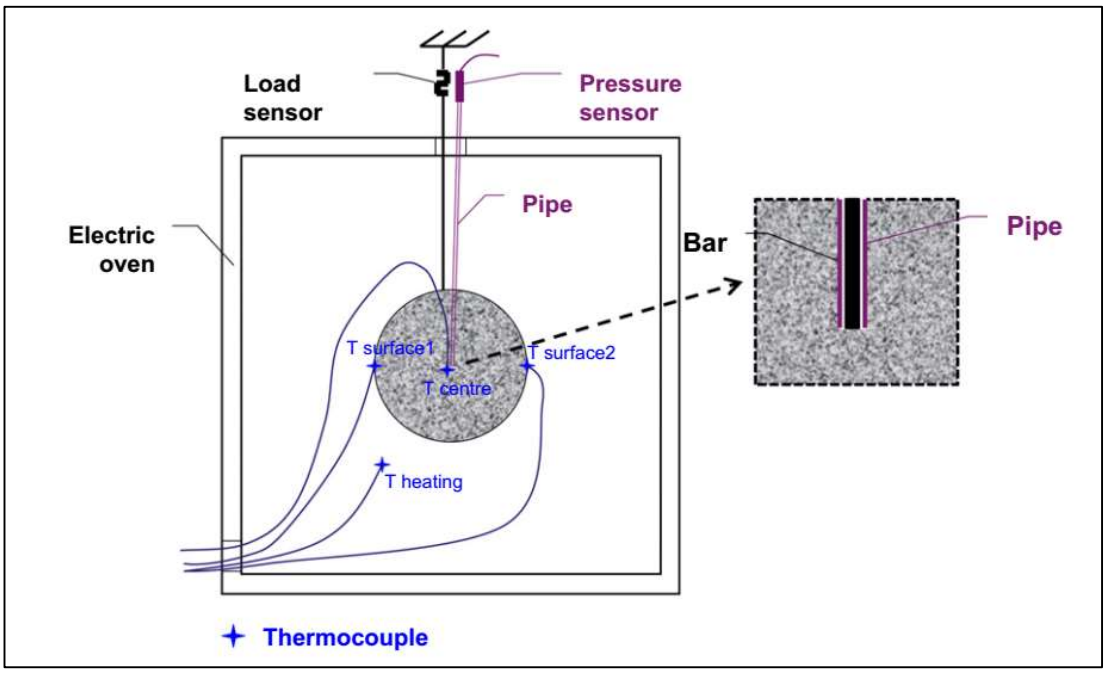

Figure 2.16: Test setup used for spherical tests reproduced from (Debicki, Haniche and Delhomme, 2012)

2.6.3.4 Testing cylinders or cubes in furnaces / ovens

The use of a concrete cylinder to assess compressive strength or indirect tensile strength is well established. Due to the small sample size, existence of moulds and

standardised nature of concrete cylinders many researchers appear to be drawn towards using them as samples for spalling experiments. Particularly as many samples can often be tested in one furnace test. While the results of these experiments may provide some qualitative comparison between different concrete mixes the sample size, geometry and loading conditions are not representative of any end use application. One experiment which took this approach is the work by Lee et al. carried out to assess the influences of mixed polypropylene and nylon fibres (Lee *et al.*, 2012). Figure 2.17 shows their test setups. They are very meticulous in their work documenting the concrete mix designs used the fibre properties and the influence of mix design on slump and compressive strength. Their lack of consideration of the suitability of their "fire test" is shown by their extremely brief description of the test. They do not say how the temperature was controlled, or how the furnace was fuelled, they simply say that

> *"The cylinders were placed in the furnace and heated according to the curve of ISO 834-1 … for 1 h".*

Figure 2.17: Concrete cylinders inside a furnace (Lee *et al.*, 2012)

They did not consider the impact of loading, restraint, sample size, or geometry. This work is worthwhile in that it demonstrated that for these test conditions the mixture of nylon and polypropylene fibres appeared more effective at mitigating spalling than simply using polypropylene fibres. It is important to note that it is not possible to assess, with any confidence, how this concrete might perform when tested to another test method. Care should be taken when interpreting the results as the furnace test is not well documented and it is unclear if any of the samples experienced direct flame impingement. The bias of the authors' views on the factors influencing spalling is also clear as they state,

> *"Because spalling damage occurs due to the high vapor pressure of moisture inside the concrete … adding fiber is a very efficient method of preventing spalling because it provides an escape path for the vapor pressure."*

Statements like this made with such certainty muddy the waters in the field of spalling research. Most researchers would agree that spalling is influenced by a combination of variables and there is still ongoing debate about the mechanism by which polypropylene fibres reduce the spalling risk.

Many other experimental programs have tested unrestrained cylinders or cubes (Hertz, 1984; Zhao and Sanjayan, 2009; Heo *et al.*, 2012; Huang *et al.*, 2015; Serrano *et al.*, 2016; Peng *et al.*, 2018) but their value is limited.

2.6.3.5 Testing samples exposed to direct flame

A common approach to applying a thermal exposure is to use a blowtorch or fire to heat concrete samples. While this is an attractive method due to the low cost and accessibility of blowtorches this method fails to adequately control the thermal boundary conditions. The extreme heating at localised points also introduces thermal stresses that would not be expected in any other form of heating for experimental work, and would be very unlikely in most real fire scenarios. The use of this type of method can provide a qualitative comparison of the performance of different mixes all tested in the same way, but is not representative of the conditions that concrete would be subjected to in a fire-resistance test or in a real fire. It is not possible to use data from these tests for design, and meaningful comparison with other experiments is not possible

Thermal imaging cameras or infrared thermometers are often used alongside this direct flame impingement method to determine the temperature at the surface of the

concrete. These have limited accuracy and measuring the concrete surface temperature behind the flame cannot be done with any confidence. The temperature measurements should be taken as estimates. The use of thermocouples within the samples would provide an indication as to the thermal exposure experienced but the majority of these test methods appear to be seeking to test with little investment of time or resources. As stated previously, these tests can provide a useful qualitative comparison between concrete mixes but great care should be taken when drawing conclusions about the behaviour of concrete based on this kind of testing. Some examples of the experimental setups are described below.

A barbeque style heating setup was used to investigate the influence of polypropylene and steel fibres on the residual properties of concrete exposed to fire (Serrano *et al.*, 2016). Concrete cylinders were heated over a fire of *"40kg of chopped wood, sprayed with gasoline".* The lack of understanding of the thermal exposure is demonstrated by the inconsistency of precision when analysing other parameters such as the residual cylinder strength of concrete. When the heating is so rough it is not appropriate to give the compressive strength of the concrete to three decimal places as its residual strength after "*direct exposure to the fire at 400°C maximum temperature*". Conclusions are also drawn by the authors about the thermal properties of the concrete mixes containing different fibres. This is not appropriate unless the thermal boundary conditions are accurately controlled. Some images of the test setup are reproduced in Figure 2.18, which show the samples being heated and temperature measurements being taken with a handheld infrared thermometer.

Figure 2.18 Concrete cylinders tested over burning wood reproduced from (Serrano *et al.*, 2016)

An example of the use of blowtorches for testing (Huang *et al.*, 2015) again shows a lack of understanding of the thermal boundary conditions. Tests were carried out on cubes and small slabs using blowtorches. This in itself can give some qualitative

comparison of the performance of a concrete mix as mentioned previously and has been used by many researchers as a quick test (Dougill, 1971; Jansson, 2013). This research then attempts to compare the thermal exposure to that of a hydrocarbon curve based on the surface temperatures measured using a thermal imaging camera. The heat transfer in these experiments using direct flame impingement should not be compared to that received by a sample when tested to a temperature time curve in a furnace as there are many differences in the experimental conditions. Figure 2.19 reproduced from (Huang *et al.*, 2015) shows the two experimental setups used.

Figure 2.19: Test setups for (a) cubes and (b) slabs reproduced from (Huang et al. 2015)

Other authors have carried out similar testing (Dougill, 1971; Connolly, 1995; Nuruddin, Azmee and Yung, 2014; Bodnarova, Valek and Novosad, 2015) and again it should be stated that while the thermal exposure is not well defined the results of testing like this can provide come indication as to the influence, if any, of changing the mix design. Care should be taken when interpreting results and meaningful comparison is not possible.

2.6.3.6 Testing samples using radiant heaters / radiant panels

The use of radiant heat sources has been explored by a number of researchers and allows the thermal boundary condition to be controlled in terms of a heat flux versus time history. As discussed in Section 2.6.1 this is the approach used elsewhere in fire science research. Early advocates of the use of radiant heat sources (Harmathy and Lie, 1970; Connolly, 1995) failed to influence the spalling research community and their approaches to testing were not continued. The approach to heating has had a

more recent revival with the work carried out at The University of Edinburgh (Maluk, 2014; Rickard *et al.*, 2015; Hulin *et al.*, 2016; Maluk *et al.*, 2016; Richards *et al.*, 2018) and this approach to testing will be discussed in more detail in Chapter 3.

Other researchers have used radiant sources to apply a thermal exposure but often did not quantify the thermal exposure in terms of heat flux preferring to discuss temperatures instead (Kalifa, Menneteau and Quenard, 2000; Felicetti and Lo Monte, 2013). It is a shame that the thermal exposures have not been quantified for these test methods. Quantification would allow simple comparison of the thermal exposure received by samples.

2.6.3.7 Testing of real tunnels with "mobile furnaces"

While not a testing approach aimed at spalling research, a number of "mobile furnaces" have been developed to expose in situ tunnels to a thermal exposure. These are typically used to assess the spalling risk in existing tunnels and consist of a system of burners supported close to the face of a tunnel. The thermal exposure is controlled in terms of temperature (Efectis Group, 2012; Pardon *et al.*, 2019).

Issues with direct flame impingement and appropriate control of thermal exposure remain. The influence of localised heating and choice of test location introduces further unknowns when attempting to assess the spalling risk for a whole tunnel. See Section 3.8.2 for a discussion of tunnel design considerations.

Figure 2.20: Efectis mobile furnace during a test on an existing tunnel (Efectis Group, 2012)

2.6.3.8 Instrumentation for pore pressure measurement

Many of theories discussed in Section 2.4 involve the migration of moisture with concrete and the build-up of pressure during thermal exposure. Much research has been carried out attempting to measure this pore pressure build up and assess the validity of the theories related to pore pressure and moisture clog. While this literature review is focused on the different test methods being used, it is worth commenting on some of the instrumentation being used. Pressure gauges have been developed in recent years in an attempt to record the pressure changes within the heated concrete. One such gauge was developed by researchers at CSTB in France (Kalifa, Menneteau and Quenard, 2000) the test setup used is shown in Figure 2.21. The gauge consists of thin tubes connected to pressure transducers by flexible tubes filled with silicon oil. These pressure gauges have allowed the theory that the spalling is a result of the pressure build up to be assessed. Alternative pressure probes have been used by other authors (Debicki, Haniche and Delhomme, 2012; Felicetti, Lo Monte and Pimienta, 2017).

It is worth noting that the pore pressure measured by researchers does not typically reach the tensile strength of the concrete even in experiments where spalling occurs. While there are uncertainties in what is being measured, the theory that spalling is purely a result of pore pressure appears to be incorrect.

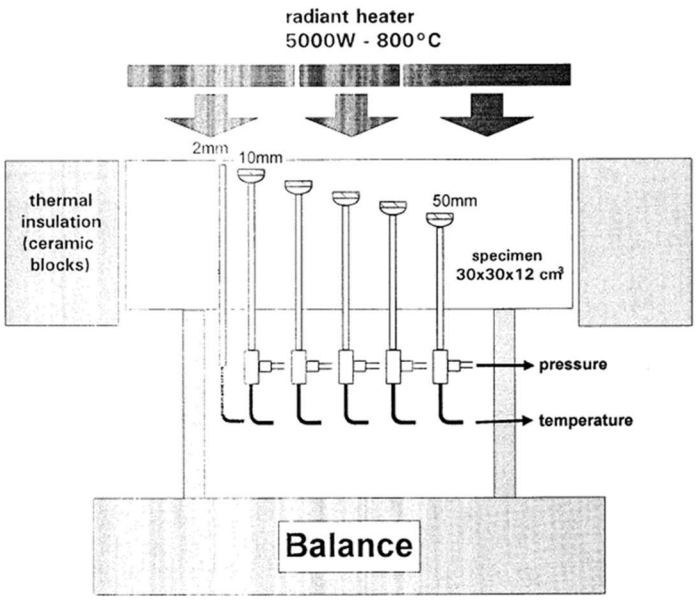

Figure 2.21: Sample containing pressure gauges heated with a radiant heater (Kalifa et al. 2000)

One concern with the use of probes to measure pore pressures within concrete is that the probes themselves will influence the pressure build up within the concrete. It has been observed in many tests that inclusion of thermocouples and lifting hooks can provide a route for the escape of moisture during testing. It seems likely that the same effects would be observed to some extent with pressure probes and this moisture escape would influence the pressure readings. The moisture escape itself has the potential to become an influencing parameter.

2.7 Recent Research community activity

Some of the many different experimental approaches to spalling research have been shown in the previous sections. In order to provide context as to the extent of research being carried out it is worth drawing attention to the conference series which focuses specifically on heat-induced spalling of concrete. This international conference is held every two years and was started in Leipzig in 2009. The conference is well attended with the 2017 conference held in Borås, Sweden featuring 35 papers, of which the author wrote or contributed to three papers. The 2019 edition of the conference was held in Sheffield, England and featured 30 papers. It is important to remember that the spalling community also contribute to other conferences and journals and so this represents just some of the work being carried out in this field.

Some of the work reviewed so far was carried out a number of years ago. In order to give the reader an appreciation for the state of the art experimental work being carried out, the work presented at The Sixth International Workshop on Concrete Spalling due to Fire Exposure, IWCS, will be reviewed here. The work presented at this conference has been selected to give an insight into the state of the art as it provides a snapshot across the field.

While some researchers may not have presented at this conference it was decided that reviewing the state of the art in this way removes bias towards any researcher or approach which could come from selecting certain publications. The papers presented at this conference are peer reviewed by a committee, which includes the author, and is predominantly made up of members of the RILEM technical committee for spalling. As such, it is known that the work is reviewed by researchers actively involved in spalling research themselves. It is important to note that some of the work which is presented at the conference represents “work in progress” and any issues highlighted in this review may be resolved.

The papers describing experimental work are detailed in Table 2.1 and the work presented in each paper is summarised. Following this, the experimental procedures adopted are assessed. The two research programmes which best addressed the challenges of designing appropriate experiments are reviewed in more detail in Sections 2.7.2 and 2.7.3.

Table 2.1: Summary of experimental papers from IWCS 2019

No.	Paper Title	Sample Details	Test apparatus	Comments
1	Mitigation of Fire-Induced Spalling of Concrete using Recycled Tyre Polymer Fibre (Li *et al.*, 2019)	Six samples. 500 x 500 mm 250 mm thick. One variable changed, three repeats of each experiment.	Electric radiant panel. Temperature controlled. Heat flux to sample not considered directly. Uniaxial loading applied using reaction frame.	Test methodology at Sheffield University was developed following the use of apparatus at The University of Edinburgh in a previous collaboration with the author. Sample size, thermocouple location, and loading are as recommended by the author based on the work described in this thesis. Experiments originally intended to use laboratory and apparatus in Edinburgh.
2	Experimental Study of the Spalling Behaviour of Ultra-High Performance Fibre Reinforced Concrete during fire (Schneider and Sajina, 2019)	Five plates of UHP concrete, 7990 x 790 x 130 mm. Notched edge to fit in frame.	Furnace test on unrestrained plates supported in side of furnace. ISO834 fire curve used.	Samples not representative of any real application. Acoustic emission monitoring used to estimate time of spalling. Thermocouples held on steel "U bars" for accurate placement. Thought that the Influence of these bars may be significant. Only one of each sample type tested reducing confidence in results.
3	Investigation of Size Effects in Concrete Spalling (Klimek, Hothan and Rogge, 2019)	Slabs of two sizes and different mix designs. No repeats.	Unrestrained and unloaded samples were suspended over a furnace. Experiments followied either RABTZT or ISO834 fire curves.	The researchers are interested in spalling of tunnel lining concretes. Flat slabs are suspended over the furnace with no load or restraint, which is not representative of in service conditions. Lack of repeat experiments make conclusions hard to defend.
4	Effect of geometry in concrete spalling risk subjected to high temperatures for thermal inertia studies (Lucio-Martin, Puentes and Alonso, 2019)	Small cylindrical, cubic, and prismatic samples used. With 150 x 150 x 400 mm prismatic samples being the largest.	Samples placed in a small furnace. Furnace specifications unclear. Heating cycles up to 550 °C. No loading or restraint provided.	Research is primarily concerned with concrete behaviour under heating cycles for energy storage. Only one of each sample geometry tested. The largest sample spalled violently when the furnace reached 400 °C after heating at a rate of 1°C/min. Spalling attributed to thermal gradient. Lack of repeats make conclusions hard to defend.

No.	Paper Title	Sample Details	Test apparatus	Comments
5	In situ concrete spalling risk assessment in tunnel by means of a mobile oil-fired furnace (Pardon *et al.*, 2019)	7 x 3 m slabs. Four tested in furnace with different heated areas and one in mobile furnace.	CSTB mobile furnace, CSTB Vulcain furnace	Experiments utilise a mobile furnace aiming to assess spalling risk in existing tunnels. This resolves the issue of recreating loading and restraint conditions. Issues with thermal boundary conditions were encountered. With spalling resulting in the loss of the hot concrete surface, the mobile furnace was not powerful enough to continue following the fire curve.
6	Investigation of the preventive effect on fire spalling of natural jute fibre in high performance concrete through ring-restrained specimen tests (Ozawa, Sukekawa and Akasaka, 2019)	Six samples cast in 8mm thick steel rings. Three mix designs and samples tested at two ages with no repeats. Overall sample dimensions 300 mm diameter and 100 mm thick.	Concrete restrained by steel ring. Heated on a gas-powered furnace with heating to the lower face of concrete to RABT 30 minute curve selected.	Hypothesised that the restraint and vapour pressure combined are the cause of spalling. Higher pore pressures and strains in the confinement ring were recorded in samples containing jute fibre yet no spalling occurred. Other samples spalled at lower recorded pressures and strains. No repeats of experiments. Results conflict with theories and hypothesis.
7	Fire-related spalling evaluation of ring-restrained polymer cement mortar and normal cement mortar (Sugino, Ozawa and Tanibe, 2019)	Four samples, two mortar types, same dimensions as in 6 above. No repeats.	Mortar restrained by steel ring. RABT 30 minute and ISO 834 curves used.	Samples not representative of any real application. No repeats. One of each sample type tested to each exposure. Not concrete that is being tested but mortar. As in the paper above, the authors found that samples which spalled didn't necessarily experience the greatest pore pressure or confinement stress.
8	Spalling behaviour of UHPC with modified microstructure due to fire load (Kirnbauer, 2019)	40 samples 250 x 300 x 40 mm. 20 tests with one set of repeats.	Unusual propane burner furnace was used. No loading or restraint applied to samples. Furnace burner appears close to samples meaning direct flame impingement is a possiblity.	Researchers attempted preheating/drying of samples to avoid spalling which showed some success. This is not likely to be feasible in real structures. Limited applicability of results due to sample geometry and loading not being representative of any real concrete use. Air entrainment agent and hollow glass beads that were added to concrete mixes were found not to prevent spalling.

No.	Paper Title	Sample Details	Test apparatus	Comments
9	Australian Large Scale Structural Fire Test Facility for Concrete Tunnel Linings (Guerrieri *et al.*, 2019)	12 in no. flat panels (1550 x 1550 x 300 mm) were used. Six sample types with one repeat for each. Also six curved segments (1700 x 3450 x 300 mm) tested with no repeats	Bespoke furnace and loading frame. Appears to be developed for a specific segment size. Segments loaded in compression to 6 MPa.	An impressive setup developed to carry out tests on tunnel segments. Furnace controlled with type K thermocouples, which is not common practice in Europe. Concluded that it's important to test loaded full-scale samples as they spall more than unloaded flat slabs. Loaded small slabs were not tested sp conclusions questionable. Importance of compressive load noted.
10	Prevent High Strength Concrete from Spalling Subject to ISO834 Fire (Du and Qi, 2019)	Cylinders heated in a furnace. Cylinder geometries were 100 mm diameter 200 mm long, and 300 mm diameter and 300 mm long	Samples heated in a furnace with no load or restraint.	No loading. Samples not representative of any end use application. No repeats of experiments. Researchers found that for their experiments a PP fibre dosage of 0.15% by volume was sufficient to prevent spalling. The certainty of conclusions is not appropriate given the lack of repeat experiments and limited applicability of experimental conditions.
11	Experimental Study on Mechanical Behaviours of Cementitious Grouts after Elevated Temperatures (Liu, Xiao and Liu, 2019)	Cuboids 40 x40 x160 mm and 70.7 mm cubes	Samples heated in a furnace. Details of which are not clear.	No spalling was observed in any of the samples therefore it is not possible to assess the influence of any of the parameters varied on spalling.

2.7.1 Considering the suitability of the experiments

Experiments on concrete at high temperature are challenging and expensive to carry out, and many laboratories are limited by the funding or facilities available. All experiments should be carefully designed, be they intended to investigate spalling or another topic. However, given that we have been researching spalling for over 100 years, it is vital that researchers consider how the results of any experiments will be useful.

In the event that experiments do not lead to complete understanding of the spalling phenomena the results must be compared to other work or further experiments carried out. Designing experiments to maximise potential for comparison with the results of other researchers is logical and involves careful control of boundary conditions and the use of similar, well-quantified, thermal exposures and/or mechanical load.

In order to ensure results are relevant, it is desirable for the experiments to be replicating, as closely as is possible, concrete in a real scenario. Confidence in the results can be gained by repeating experiments and this is common practice in all experimental work.

An effective experiment design will tick all of these boxes. The experimental programmes presented at the spalling conference and summarised in Table 2.1 can be assessed in consideration of these experimental goals. While difficult to define across the variety of experiments, and only based on the information presented in the papers, a qualitative assessment can be made. Table 2.2 allows a visual comparison of the 11 experimental programmes. A green tick indicates that the author believes the experiments achieve the goal; a tick and a cross indicates that the author believes the goals are partially achieved; a cross means the goal is not achieved.

Table 2.2: Evaluation of the experimental work presented

Paper number	1	2	3	4	5	6	7	8	9	10	11
Samples representative of a real application	✓	✗	✗	✗	✗	✗	✗	✗	✓ ✗	✗	✗
Repetition of experiments	✓	✗	✗	✗	✗	✗	✗	✓	✓ ✗	✗	✓
Comparable/recognised heating curve/ exposure attempted	✓	✓	✓	✗	✓	✓	✓	✗	✓	✓	✗
Sufficient control of thermal exposure throughout entire experiment	✓ ✗	✗	✗	✗	✓ ✗	✓ ✗	✓ ✗	✓ ✗	✓ ✗	✓ ✗	✓ ✗
Loading/restraint present	✓ ✗	✗	✗	✗	✗	✓	✓	✗	✓ ✗	✗	✗
Loading/restraint justified and quantified	✓ ✗	✗	✗	✗	✗	✓ ✗	✓ ✗	✗	✓ ✗	✗	✗

As shown in Table 2.2 none of these 11 experimental programs achieve all of the identified experimental goals. In addition, none of the experimental programmes use the same apparatus or procedure with the exception of the two experimental programmes carried out in Japan (Ozawa, Sukekawa and Akasaka, 2019; Sugino, Ozawa and Tanibe, 2019). These experiments used the ring restraint approach described in Section 2.6.3.2.

The experimental programmes which, in the opinion of the author, best met these criteria, were those described in Papers 1 and Paper 9 of Table 2.1. These experimental programmes will be discussed in more detail in the following sections.

2.7.2 Paper 1 – Sheffield University apparatus

The work described in this paper from The University of Sheffield (Li *et al.*, 2019) was heavily influenced by the work described in this thesis. The sample size and instrumentation cast within the samples is as recommended by the author of this thesis and the same as was used in the experiments described in Chapter 6. Originally, these samples were to be tested at The University of Edinburgh using the apparatus described in this thesis. Following six experiments carried out by the author on behalf of researchers at The University of Sheffield (Figueiredo et al., 2017) a similar apparatus to the one at The University of Edinburgh has been developed at The University of Sheffield. Figure 2.22 reproduced from the paper, shows their experimental setup.

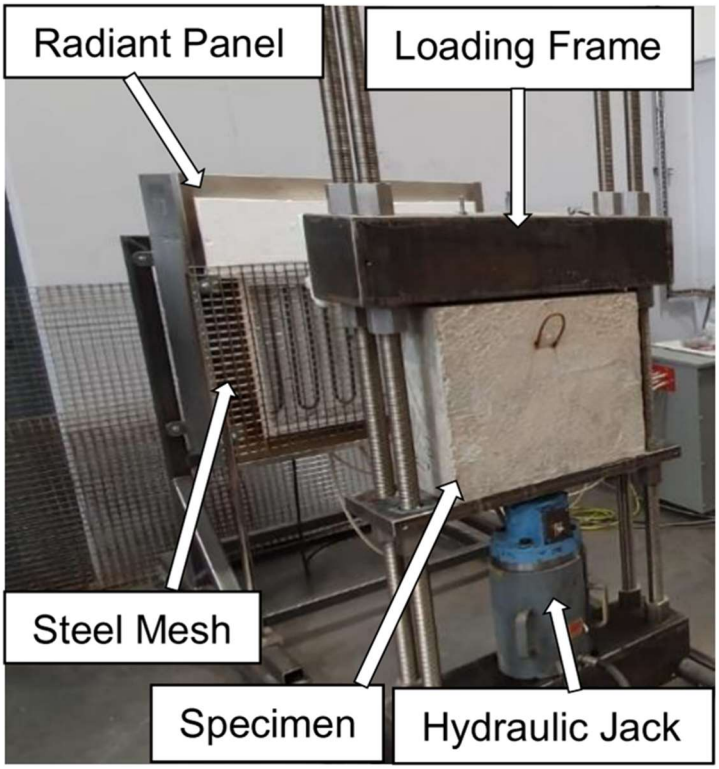

Figure 2.22: Apparatus for spalling experiments at The University of Sheffield

2.7.2.1 Heating

In these experiments an electric radiant panel is used to heat the samples, however, the heat flux is not quantified and the thermal exposure is approximated by temperature. It is understood that the power to the radiant panels is calibrated by heating a plate thermometer to follow, as closely as possible, the temperature time curve of the ISO 834 gas temperature time curve. The plate thermometer temperature

is approximated to be the same as the concrete surface temperature. It is also assumed that in a furnace test to the ISO 834 temperature time curve, the concrete temperature would be the same as the furnace gas temperature. These assumptions represent a significant simplification. As the plate thermometer was placed in front of a concrete sample the increase in separation to concrete surface would also reduce the incident heat flux experienced by the sample.

This experimental approach could be improved by attempting to quantify the thermal exposure from the electric radiant panels in terms of the incident heat flux, its uniformity, and the repeatability of the heating. There are many benefits to using a radiant panel and this apparatus is promising.

2.7.2.2 Loading/Restraint

Uniaxial loading of samples of this geometry was the experimental approach developed by the author of this thesis and the motivations for this are described further in Section 3.8. As such, the author agrees with this approach. Uniaxial loading is a common load condition for concrete and results could be considered relevant for a number of real applications.

With respect to the uniaxial loading frame itself, the cross heads of the uniaxial loading frame in Sheffield appear to be extremely thin. The author suspects that, due to deflection of the steel crosshead, the load from the hydraulic jack will not be uniformly applied across the sample. The compressive stress applied in these experiments was 10 MPa. For these samples, this equates to a centrally applied load on the lower steel crosshead of 1.25 MN. Potential for improvements to the loading frame should be should be considered in future work.

2.7.2.3 Summary of work presented in Paper 1

The work described in this paper focused not on understanding the spalling failure mechanism but on the potential for spalling reduction by addition of recycled tyre fibres. As in the experiments carried out by the author of this thesis (Figueiredo *et al.*, 2017) the recycled tyre fibres appear to reduce spalling. The motivation for this research appears to be demonstration of potential applications of recycled tyre fibres with a collaborating author being the managing director of TWINCON who manufacture these fibres.

This apparatus represents a significant improvement over that previously used at The University of Sheffield (Huang *et al.*, 2015). With further work, the results of experiments carried out using this apparatus should provide valuable, comparable data to advance the understanding of spalling. Similarities in the experimental approach mean that once the boundary conditions applied in experiments have been further quantified, comparison with the work presented in Chapter 6 of this thesis should be both simple and meaningful.

2.7.3 Paper 9 – Victoria University, Melbourne

The work described in the paper (Guerrieri *et al.*, 2019) is centred on standard testing to assess the spalling of concrete tunnel linings rather than experiments designed for research. It is understood that the apparatus development, and the testing of full-scale tunnel segments, has been driven by Australian regulators.

The apparatus is described as a “state-of-the-art full-scale structural testing furnace” and the first of its kind in Australia. The setup consists of a furnace and loading frame that has been designed to allow a uniaxial compression to be applied to a curved tunnel segment. This is shown in Figure 2.23, which is reproduced from the paper.

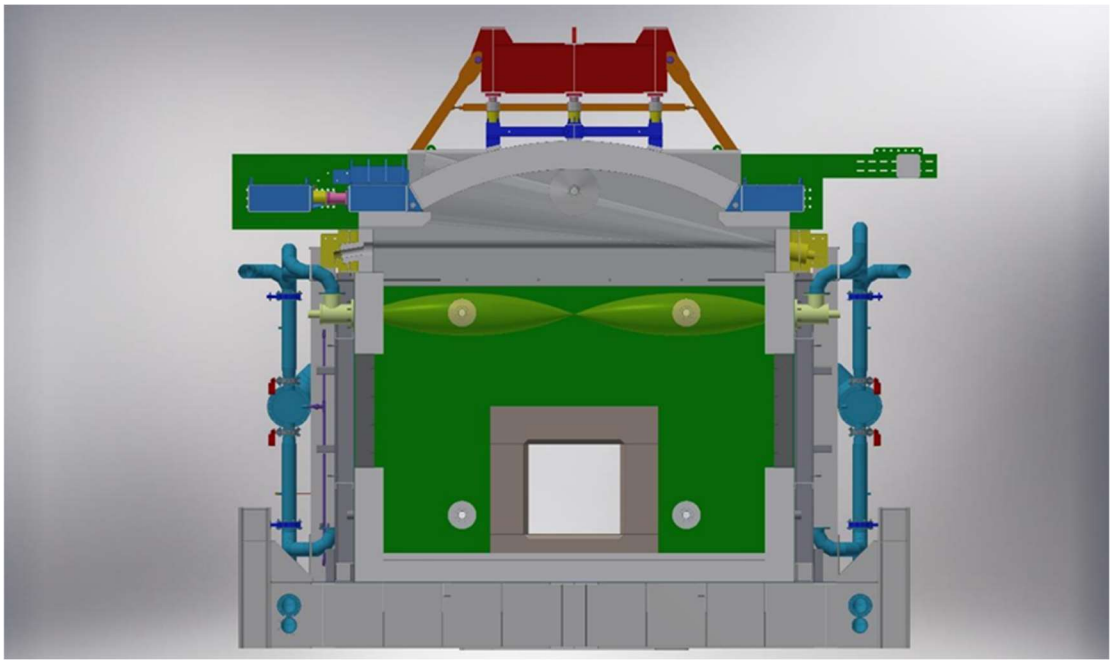

Figure 2.23:Apparatus used for spalling experiments at Victoria University

It is understood that the apparatus has been developed to carry out tests for a specific project. This being the $11 billion Metro tunnel project being carried out in Melbourne. It is unclear if the apparatus would be able to test tunnel segments of different geometries.

2.7.3.1 Heating

The furnace is controlled using eight K-type thermocouples; it is interesting that plate thermometers are the preferred instrumentation in Europe and K-Type thermocouples would not typically be used here. The author has not carried out any assessment as to the influence of furnace control instrumentation on the thermal exposure received by samples. The tests described in the paper are carried out to a RABT-ZTV (rail)

time temperature curve and the furnace struggled to follow this curve accurately, particularly in cooling. Figure 2.24, reproduced from the paper, shows the average gas temperatures in the furnace compared with the target temperature. These are the temperatures recorded in one experiment/test and the repeatability of the heating is not discussed.

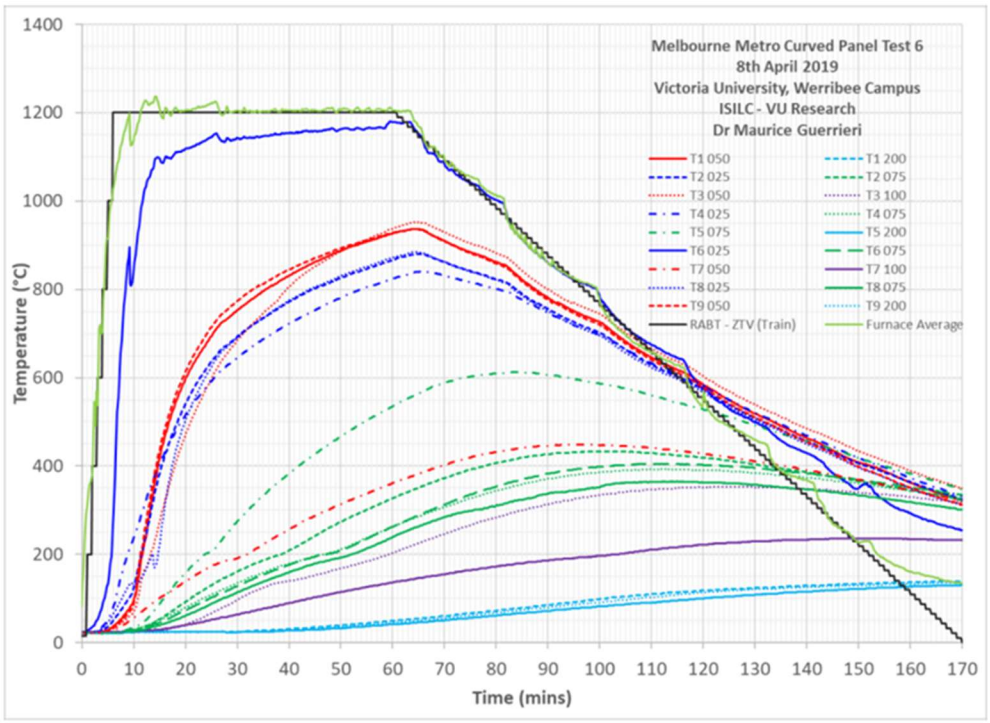

Figure 2.24: Temperatures recorded in one of the experiments carried out at Victoria University

2.7.3.2 Loading

It is understood that the bespoke loading frame applies compressive load at 13 different locations with the goal of achieving a uniform compressive stress in the segment of 6 MPa. The complexity of loading is a result of the curve of the sample. The load level selected specifically for the tunnel project for which the tests were being carried out.

If the goal is to achieve a hoop compression equivalent to a uniaxial compressive stress then the use of a curved segment and 13 point loading seems a complex approach. It is not clear how the appropriateness of the loading method was assessed or the consistency of the load condition on the sample verified.

Further discussion of loading in tunnels is provided in Section 3.8.

2.7.3.3 Summary of work presented in Paper 9

The work described in this paper reports the results of three tests carried out using the apparatus discussed above and compares the results to tests carried out on smaller unloaded flat samples. There are some questions around the control of thermal exposure and the suitability of using the furnace to investigate spalling. It is also unclear if the bespoke loading frame could be used for other tunnel geometries.

The conclusion drawn from the work presented that it is important to test full-scale samples is clearly unfounded as both the size and loading was varied between experiments. In addition, no repeat tests were carried out for the full-scale tunnel segments.

The experimental setup is impressive and would have been costly to build. Test rigs like this will be challenging for other laboratories to develop. In order to be able to maximise the comparable research being undertaken the author believes that investigating smaller scale, simpler experimental approaches (which allow control of boundary conditions) could prove more useful to the community. It should be noted that it is understood the apparatus development was driven by Australian regulators rather than the spalling research community.

2.7.4 Summary of the state of the art

As has been shown in this section, the status quo is that the spalling research community continues to use a variety of experimental approaches which, due to their design, fail to maximise applicability and usefulness of results. In many cases this may be due to the lack of resources or funding, and in some cases perhaps due to a lack of understanding. It is also apparent that there are few attempts to properly quantify the experimental boundary conditions.

The experimental work that was carried out by the author is described in the remainder of this thesis. The experimental apparatus and procedure was carefully considered to address the issues which, as has been shown, still exist to this day.

It is encouraging that, while there are some issues, the research being carried out by The University of Sheffield has adopted a similar approach for their ongoing work to that taken by the author in the experimental work described in this thesis.

It is the view of the author that the research community should define an approach to experiments to help improve the status quo. However, this has been met with resistance as researchers tend to favour their own approach and may have invested

significant time and money in the development of apparatus. Defining one apparatus may not be possible but some basic guidance could help harmonise the experimental work being carried out. It is hoped that this type of guidance will be produced by the Rilem technical committee.

2.8 Approaches to modelling of spalling

As has been discussed, there remains a fundamental lack of understanding as to exactly what causes spalling or what the failure mechanism is. A somewhat arbitrary failure criterion could be defined in order to develop a model that predicts spalling. Specification of a failure criterion fundamentally sets a bias based on the researchers' preferred theory. For example, the model could set failure based on pore pressure development, thermal stress or another defined parameter such as temperature. It is the view of the author that no such criterion is defensible in light of the extensive and contradictory data from different research programs (Koenders and Dehn, 2011; Pimienta and Meftah, 2013; Dehn, 2015; Jansson McNamee and Boström, 2017; Huang and Burgess, 2019).

Alternatively, a model could be created to fit a set of data. Adopting this approach is problematic due to the distinct lack of comparable data from spalling experiments. As covered previously, this is a result of the variety of experimental approaches, which at times can yield seemingly conflicting results.

It is the view of the author that the spalling community has not gained sufficient knowledge of spalling to enable modelling of the phenomena to be carried out, and so the work described in this thesis focuses on improving the experimental approaches and increasing the knowledge of the spalling phenomena. The development of a wealth of comparable data for spalling experiments with properly controlled and quantified boundary conditions could be seen as the responsibility of those with access to laboratory facilities who are working in the field. It is the view of the author that after over 100 years of research this approach remains necessary.

Despite the lack of understanding of spalling, researchers have attempted to develop spalling models. A number of related coupled thermo-hygro-chemo-mechanical codes of varying complexity are available in the literature; these generally attempt to predict spalling time and depth by simulating the stress state in heated concrete resulting from the relevant thermo-hygral and thermo-mechanical processes that take place during heating (Gawin, Pesavento and Schrefler, 2011; Zhang and Davie, 2013). However, even the most developed of these advanced models are, at present, unable to accurately predict spalling for a given concrete mix in a particular application and subjected to either standard or project-specific design fires.

A number of simplified spalling models (or spalling criteria) are also available in the literature – for instance assuming that only pore pressures are relevant (Dwaikat and Kodur, 2009) or that spalling will occur at a particular temperature in the concrete – however neither of these approaches is easily defended based on the available experimental evidence.

If the reader is interested in attempts at modelling spalling, details of models which have been developed can be found in the works of authors focused on modelling (Zeiml, 2008; Bosnjak, 2014). It is important to bear in mind the lack of understanding of spalling highlighted herein.

The development of models to compliment research is vital. Developed models that have been validated are able to compliment testing, resulting in a reduced number of experiments being carried out and ultimately allowing for design without demonstration of performance using testing. The current status of spalling knowledge and experimental research has not allowed a validated model to be produced and there is currently no model that can predict spalling with confidence.

The work presented in the rest of this thesis is purely experimental and as such a full and detailed review of modelling is considered outwith the scope of this project, and not included here.

2.9 Available design guidance

The need for a clear understanding of spalling and clear guidance to mitigate its effects were established over 100 years ago. While modern reinforced concrete construction is different from the early examples, spalling has not been resolved and remains a concern. In the absence of clear understanding of spalling, the guidance available is limited and vague. The guidance is often questionable, and its basis is unclear. For an area for which so little is really understood other than in a qualitative sense there are dangers associated with the implied certainty of specifying specifics associated with concrete design in guidance. The Eurocode guidance (British Standards Institution, 2004a, 2005) is applicable to concrete structure in general and can be seen to imply a much greater understanding of concrete spalling than is the reality.

The Eurocode guidance is aimed at concrete buildings assessed using the ISO 834 temperature time curve. There have also been attempts at creating guidance for the design of tunnels, an area where spalling is considered explicitly. NFPA 502 (NFPA, 2017) provides similarly vague guidance for the design of tunnel linings with respect to spalling and, when its evolution is studied, the iterations between the 4 versions which cover spalling demonstrate the lack of certainty associated with spalling design. These changes are discussed in Section 2.9.3. Other guidance has also been proposed for tunnels including in the EFNARC report although this has not been adopted. Members of the spalling research community appear to reject the report as it was developed by an organisation that represents producers and applicators of specialist building products for concrete (personal communications at meetings of RILEM TC SPF).

2.9.1 Eurocodes

Eurocode 2 (British Standards Institution, 2004a) gives guidance on the design of concrete structures. The inclusion of guidance for spalling into the Eurocodes poses an interesting problem. It is desirable that some sensible guidance is present and that extreme worst cases for spalling based on knowledge from previous testing are avoided. However, the level of understanding of spalling is arguably not sufficient that it is possible to make specific recommendations with such certainty as is implied in the Eurocodes. This section will give a discussion of the guidance given and the issues arising. In order to show how the Eurocode appears to deal with the different influencing parameters the points given in the guidance have been split into different

subheadings by parameter. This is not how they appear in the Eurocodes. They have been rearranged here for clarity.

2.9.1.1 General comments on spalling performance requirements

Spalling is first mentioned in in section 4.1 (2) of Eurocode 2 when discussing general design procedures. It is stated that spalling shall be avoided by appropriate measures or its influence considered. Appropriately considering the influence of spalling is challenging as it is not currently possible to have confidence in how much spalling is likely to occur for a mix that has not been tested. Without a well-controlled test and multiple repeats, knowledge is very limited. It would even be challenging to predict spalling performance for a mix that has been tested. The result is then that the desirable option for design is to use a concrete mix, which the designer can be confident will not spall.

Spalling is later touched on in the advanced calculation methods section where it states any potential failure mode not covered by the calculation method shall be *"excluded by appropriate means"*. If spalling as a failure mode in itself is to be excluded by appropriate means, it is clear that spalling should be avoided completely or there must be certainty that the spalling will be light enough that it will not cause any failure.

2.9.1.2 Moisture content

For normal strength concrete Eurocode 2 states that explosive spalling is unlikely to occur when the percentage moisture content is below a certain percentage, *k* by weight – this value is given in the national annex but recommended as 3 percent. In the UK the recommended value of 3 percent is used (British Standards Institution, 2004b). Eurocode 2 also states the moisture content of the concrete will be lower than this value of *k* for exposure classes X0 and XC1. These are defined in part one of Eurocode 2 (British Standards Institution, 2004a) as being concrete inside buildings with a low air humidity or concrete permanently submerged in water. This means Eurocode 2 considers that normal strength concrete members inside buildings with very low or low air humidity unlikely to spall and no further check is required.

The mention of the normal strength concrete in low humidity buildings being "unlikely" to spall is of particular concern as it implies that the risk of spalling has been evaluated and that although spalling may occur the frequency and/or severity of this spalling is low enough that it need not be considered even though it could cause failure. As discussed previously, we are not in a position to be able to say for certain that this is

the case, particularly when only judging a mix based on its strength (normal strength in this case), its moisture content as a percentage by weight and the furnace test exposure.

According to the Eurocode for beams, slabs and members with a moisture content over the value *k* the local loss of cover to one reinforcing bar or bundle of bars should be considered. Alternatively, the behaviour can be demonstrated to be acceptable by experiment either alone or with additional protection. In this case, it would not be desirable to carry out testing of the members due to the high costs associated and the potential that the member may not pass the approvals test. There are also no limits set on the moisture content, which could result in concrete that is very prone to spalling being code compliant. By specifying the damage to consider for design, it is implied that the potential consequence is understood.

2.9.1.3 Loading

In the advanced calculations section of Eurocode 2 part 2 (British Standards Institution, 2005) it is stated that the compressive zone of sections should be detailed with particular regard to spalling of concrete cover especially if directly exposed to fire. This means that for a beam in bending particular attention to detailing should be applied in the compression zones. This statement ties in with the theory that compression increases the spalling propensity of a concrete but does not state this explicitly nor give any additional guidance. It also implies that the areas of sections that are not in compression need not be detailed to the same standard. It seems unjustified to give this impression.

2.9.1.4 High strength concrete

High strength concrete has some additional guidance and requirements to be met with respect to spalling. This is in keeping with the current knowledge on spalling as high strength concrete has been observed to be more prone to spalling. The guidance given continues to be very specific yet also quite vague. The properties and recommendations are given for fire exposure corresponding to standard temperature-time curve only. The standard fire curve used by the Eurocode is the ISO 834 fire curve (International Organisation for Standardization, 1999). This means that guidance given does not apply when alternative fire curves are being used for design.

The spalling recommendations for high strength concrete state that for concrete grades C55/67 and C80/95 the rules given for normal strength concrete apply when the silica fume content of the concrete is less than 6% by weight of cement. This is a

very specific requirement which would be difficult to demonstrate is safe for all concrete mixes. This means that if the silica fume content is low that a concrete of these strength classes does not require particular attention unless it has a high moisture content. A concrete of strength class C 80/95 with a moisture content below 3% by mass requires no additional consideration of spalling in its design.

While it is desirable to be able to design without considering concrete mixes individually, it is important that boundaries defined in guidance are appropriate. Where there is uncertainty, it may be necessary to be less specific or include a factor of safety to ensure appropriately conservative design.

2.9.1.5 Methods to reduce spalling risk

For concrete strength classes of over C 80/95 and less than or equal to C 90/105 "methods" are given and it is stated that at least one method should be used. It is not clear if these methods are to prevent spalling or if they are to reduce the risk of spalling to an appropriate level considering the likely severity of spalling and the consequence for the structure. The methods given are reproduced and discussed below.

> *"Method A: A reinforcement mesh with a nominal cover of 15 mm. This mesh should have wires with a diameter ≥ 2 mm with a pitch ≤ 50 x 50 mm. The nominal cover to the main reinforcement should be ≥ 40 mm.*
>
> *Method B: A type of concrete for which it has been demonstrated (by local experience or by testing) that no spalling of concrete occurs under fire exposure.*
>
> *Method C: Protective layers for which it is demonstrated that no spalling of concrete occurs under fire exposure.*
>
> *Method D: Include in the concrete mix more than 2 kg/m^3 of monofilament polypropylene fibres."*

These methods to be used to prevent/ reduce the risk of spalling continue to be vague; Method B suggests that concrete, which has been demonstrated by local experience to not spall under fire exposure, can be used. There is no guidance as to what "local experience" would constitute appropriate demonstration that spalling does not occur. It is presumed that it is referring to furnace testing rather than real fires. It would be challenging for a concrete designer to have quantified, well reported results from real fire events using a specific concrete. The boundary conditions experienced in real fires are likely to be very different to those experienced by a concrete being tested in

a furnace test. Assuming that the probability of spalling occurrence and severity were defined and informed the development of the Eurocodes, establishing an equivalent level of safety by basing concrete mix choice on an observation of a real fire is unacceptable. Method C also gives the possibly to demonstrate performance of protective layers but does not specify how. It must be assumed that a suitable furnace test it desired.

The inclusion of 2 kg/m^3 of monofilament PP fibres recommended in Method D has been seen in some cases, whilst reducing spalling, to be insufficient to prevent spalling. It has also been observed that the fibre length and diameter are important parameters when specifying a fibre dosage. The variation in performance of different fibres could be sufficient to mean that the dosage recommended may not be effective, yet the fibre geometries are not mentioned.

In the UK national annex, it is stated that any of these methods A – D or a combination of those methods are accepted. It refers to these methods as "*methods to control spalling of high strength concrete"*. This is an ambiguous phrasing as it is not clear whether they are methods to prevent spalling or to reduce the probability of spalling or the severity of spalling.

2.9.1.6 Sub-section conclusions

Based on the points discussed above it is clear that the Eurocodes are ambiguous and perhaps outdated in the way they address the problem of heat-induced spalling of concrete. There is a need for the best guidance possible to be provided but care should be taken to qualify statements when the level of understanding of the phenomena is low, as is the current situation. Research has shown that the recommendations that are made in the Eurocodes are not necessarily sufficient to prevent spalling. An engineer unfamiliar with the current state of the art in spalling research could easily assume that the guidance given is based on a wealth of experimental testing, as is the case for example with concrete strength and safety factors in the Eurocodes. The reality is that whilst we have some understanding of the parameters which influence spalling we do not have a wealth of comparable data allowing us to make confident recommendations. This is due to the complexity of the phenomenon with many influencing parameters and the variety of approaches taken to research. It needs to be made clear that we are not yet capable of the probabilistic approach to concrete design with respect to spalling and that the recommendations are best practice to prevent spalling, and perhaps out of date.

Without this clarification, an engineer could test a concrete that is acceptable under the Eurocode guidance and find that it does spall. An equivalent level of safety to this could also then be proposed if it was believed that spalling is well understood and that the Eurocodes deemed those levels of spalling acceptable. Clearly, this is not the case.

2.9.2 Possible updates to the Eurocode guidance on spalling

There have been discussions in the spalling research community about the appropriateness of the guidance provided in the Eurocodes and recently papers have been published on the subject. The paper presented at the 2017 spalling conference (Robert *et al.*, 2017) is intended as a discussion piece to inform the update of the Eurocodes. The authors of the paper are the committee CEN TC 250/SC2/WG1/TG5 working on the updating of the Eurocodes. The paper discusses the current requirements of the Eurocodes briefly. The paper raises questions particularly that the Eurocode guidance only considers three parameters for spalling: strength, silica fume addition and moisture content. There are many parameters identified to have an influence on spalling and these may not be the most appropriate parameters to assess a concrete. The paper also highlights that the Eurocode guidance is currently only for the ISO 834 standard fire and that the spalling risk would be expected to be higher for the more severe fire curves. The authors state that there has been a lot of misuse of the Eurocode guidance in this respect. The report is not very critical of the Eurocode guidance and does not properly acknowledge the failings of the guidance. Since the publication of the Eurocodes researchers have found that the methods given in the guidance, for example the use of 2 kg of propylene fibres, have been insufficient to prevent spalling (Maluk, Bisby and Terrasi, 2014). While it is unclear exactly how the discussions will be incorporated into the Eurocodes it is noteworthy that updates are actively being discussed between the Euorcode committee and the spalling community.

2.9.3 NFPA 502

NFPA 502 (NFPA, 2008, 2011, 2017) gives guidance on road tunnels and bridges and includes guidance for the use of passive fire protection to protect the structure of a concrete road tunnel. As with the Eurocode guidance discussed in Section 2.9.1, there is a great deal of ambiguity in the guidance. The changes between versions are indicative of the lack of certainty surrounding heat-induced spalling. The 2008 edition of NFPA 502 introduced for the first time specific requirements for fire tests for tunnel

structural elements. The structural considerations for tunnels are described in chapter 7 of the code. The current 2017 version (NFPA, 2017) states that regardless of the length of the tunnel, it must be designed in such a way that progressive collapse of the primary structural elements is prevented. In addition, the fire curve to be used for testing should be the *"Rijkswaterstaat (RWS) time-temperature curve or other recognized standard time-temperature curve that is acceptable to the AHJ, following an engineering analysis…"*

The current criteria that must be met during 120 minutes of *"fire exposure"* are that there shall be no irreversible damage leading to progressive structural collapse and that: *"Tunnels with concrete structural elements shall be designed so that fire-induced spalling, which leads to progressive structural collapse, shall be prevented"*. This is an ambiguous statement and implies that spalling is permitted if it can be demonstrated that it will not lead to progressive collapse.

The failure criteria have changed through the editions of the standard, which demonstrates the lack of understanding of the phenomena of spalling and how to account for it. In the 2008 edition, tunnels that were cast in situ were to be protected with additional protection so that the concrete stayed below 380°C and tunnels with high strength precast elements were to be protected *"such that explosive spalling is prevented".* The requirement to insulate the tunnel lining to remain below a certain temperature is very conservative and likely to introduce huge costs to a project. The lack of certainty about the performance of high strength concrete is demonstrated by the avoidance of specifying a suitable temperature for a high strength tunnel lining to be kept below.

It is unclear why a critical temperature was specified for cast in situ tunnels but not for high strength concrete. This difference implies a lack of certainty about the behaviour of high strength concrete in fire as it is left to the designer to assess if spalling will occur. It is unclear why NFPA felt the critical temperature of 380°C not to be appropriate for high strength concrete.

In the 2011 edition, the requirement for additional protection to the concrete was removed and the failure criteria was that explosive spalling must be prevented. In 2014, this was relaxed further to progressive spalling being prevented, allowing for spalling to occur as long as it is not progressive through the testing. The distinction between precast and cast in situ construction methods did not continue beyond the 2008 version. If fire protection is used, the same temperature limits established in the

2008 edition are still used in the more recent editions. In the 2014 and 2017 editions, in addition to the temperature requirements when additional protection to the concrete is used, it is also stated that spalling must be prevented. This implies that these temperatures chosen to prevent spalling are not necessarily correct and that the concrete could spall below this temperature. It is not clear why this was added or if it was based on test results. In the annex providing additional information about testing the Efectis R0695 report (Breunese, Both and Wolsink, 2008) is recommended as an example of testing to assess spalling and thermal protection of concrete. This report will be discussed in Section 2.9.4.

It is not clear why the NFPA standard was so strict in the 2008 edition or what the justifications of the relaxation/alteration of the failure criteria are. The compulsory insulation to the concrete lining of the tunnel specified in the 2008 edition of NFPA 502 is a very conservative approach and very restricting introducing great costs in both materials and labour. Concrete can perform well in fire and it should be permissible to use unprotected concrete if it can be demonstrated to perform adequately. The definition of adequate performance may be that spalling does not occur or that spalling is not sufficient to cause collapse.

2.9.3.1 Case study – Port of Miami tunnel

A case study of the Port of Miami tunnel (Gulik *et al.*, 2016) gives an insight into a method of complying with NFPA 502 2008 edition (NFPA, 2008) for the design of passive fire protection systems. This tunnel was the first tunnel in The United States to include passive fire protection designed to NFPA 502. The existence of the paper shows that meeting the requirements of the code was thought to be challenging and the sharing the process followed was worthwhile. Interestingly the paper was published in 2016 after the standards had changed through a further two editions. The performance criteria for the passive fire protection, if used, did not change other than spalling not being permitted. Tunnels are no longer forced to include passive fire protection to the concrete so more conventional testing can be carried out. The primary authors of the paper are from Efectis Netherlands and the paper serves as an advert for the use of their MobiFire mobile furnace for use in industry, see Section 2.6.3.7.

During the design of the port of Miami tunnel, separate testing was carried out to investigate the spalling behaviour of the concrete being used and the insulation properties of the fire protection system. As the tunnel was precast, NFPA 502 stated

that explosive spalling had to be avoided. The designers made their own definition of spalling and decided to define explosive spalling as

> *"violently releasing concrete in layers with thicknesses more or less equal to the grain diameter of the course aggregate…deemed acceptable if falling off of pieces of concrete is limited to the cement skin (approx. 1 – 2 mm)."*

In the testing a series of *"generic"* temperature time curves were used in an attempt to simulate possible interface temperatures between a fire protection system and the concrete surface. Samples of the concrete were then tested to these curves using the Efectis mobile furnace and, once an interface temperature time curve was chosen, the fire protection system, which could deliver a similar interface temperature, was selected. This method of not testing the real system as it would be installed has a number of drawbacks, some of which are discussed in the paper. It is not clear if the chosen system was ever tested after the initial interface curve tests were carried out or if it was deemed acceptable based on manufacturers testing. A total of seven samples were tested and only one test was repeated it is also unclear what the age of the concrete at the time of testing was. Due to the lack of understanding of the spalling phenomena it is always desirable to test the selected real tunnel construction rather than specify based on unusual tests. This type of approach to testing could however reduce the number of fire-resistance tests required in the design stages of a tunnel, which uses a fire protection system to protect the concrete tunnel lining.

2.9.4 Efectis Report R0695

Efectis Report R0695 (Breunese, Both and Wolsink, 2008) is recommended by NFPA 502 2017 edition (NFPA, 2017) as a good example of testing practice of assessing spalling and thermal protection of concrete. This Efectis report gives some basic guidance on the test procedure for fire tests of concrete tunnel linings. The recommendations of this report are summarised in Table 2.3.

Table 2.3: Summary of Efectis R0695 test guidance

Test Parameter	Notes
Temperature-time curve	RWS temperature time curve specified others permitted. Deviation limits given based on areas under curve
Minimum sample size	Full scale for tunnel segments, 6-8 times thickness for cast in situ
Sample thickness	Can limit to 0.4 m for cast in-situ
Reinforcement	Must be similar to real tunnel application
Loading	Required - Internal post tensioning recommended, Should be equal to the compression in the real tunnel application
Instrumentation	Thermocouples not required in spalling test but recommended, required for assessment of insulating fire protection.
Concrete mix	Must be as used in practice including all additives
Casting	Cast in the same orientation as real tunnel segments and as close to actual manufacturing as possible
Curing	Concrete must be at least 90 days of age at time of testing, stored wrapped in plastic
Fire protection systems covered in guidance	Must be applied to the test sample as in real tunnel construction if it is to be used
Repeats required	At least two identical large scale test specimens

The guidance can be summarised as stating that the tests must be carried out on samples which resemble as closely as possible the true tunnel construction, and that the conditions, with the exception of the heating curve, need to be as close to in-service conditions as is possible. This was not the approach taken in the Port of Miami tunnel project. Had this document been recommended as a good example of testing in the 2008 edition of NFPA 502 the Port of Miami tunnel may have been designed differently. Due to the unknown nature of spalling, the requirement to test the tunnel construction as representatively as possible to how it will actually be constructed is justified. The approach taken in the Port of Miami tunnel, whilst offering an attractive method for choosing the insulation thickness, should also include tests of the final build in as close to real conditions as possible.

One issue that arises from the Efectis report is that post tensioning is recommended as a method for applying load to samples. There are issues with this approach both in terms of the load being representative of the true in-service load on a tunnel and

the presence of the tensioning rods within the concrete potentially having an influence on the test. The proposed experimental setup for testing a tunnel segment over a furnace is reproduced from R0695 in Figure 2.25

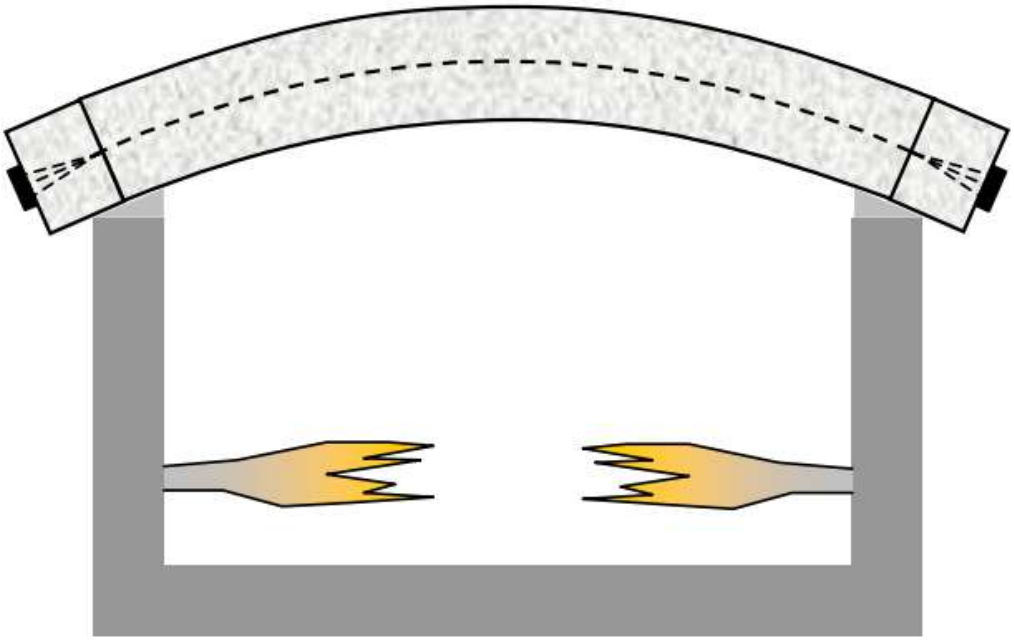

Figure 2.25: The use of post tensioning to apply load to tunnel segments during furnace testing. Reproduced from Efectis R0695 (Breunese, Both and Wolsink, 2008)

The methods of applying load during testing are discussed in more detail in Section 2.6.3.1.

2.10 Load Induced thermal strain

2.10.1 Overview

While not considered in the experimental work described in this thesis the phenomena of load induced thermal strain and its potential occurrence during the type of loaded experiments carried out for spalling research was discussed at length during the viva for this thesis. This section touches on the phenomena which is not currently considered in spalling research but which may prove to be an important factor.

Load induced thermal strain has been researched extensively and a review of the state of the art knowledge was produced recently by Torelli et al (Torelli *et al.*, 2016).

As defined by Torelli et al. load induced thermal strain or LITS is the strain component which accounts for the final strain condition when a concrete is subjected to both load and heating. This strain occurs only during the first heating of a concrete to a given temperature and is significantly influenced by the moisture flux.

The final strain condition in a concrete which has been both heated and loaded cannot be explained purely by the combination of thermal expansion, which would occur when the concrete sample is unrestrained and heated, and the compressive strain as a result of the externally applied load. Figure 2.26 has been reproduced from the review by Torelli et al to demonstrate this theory.

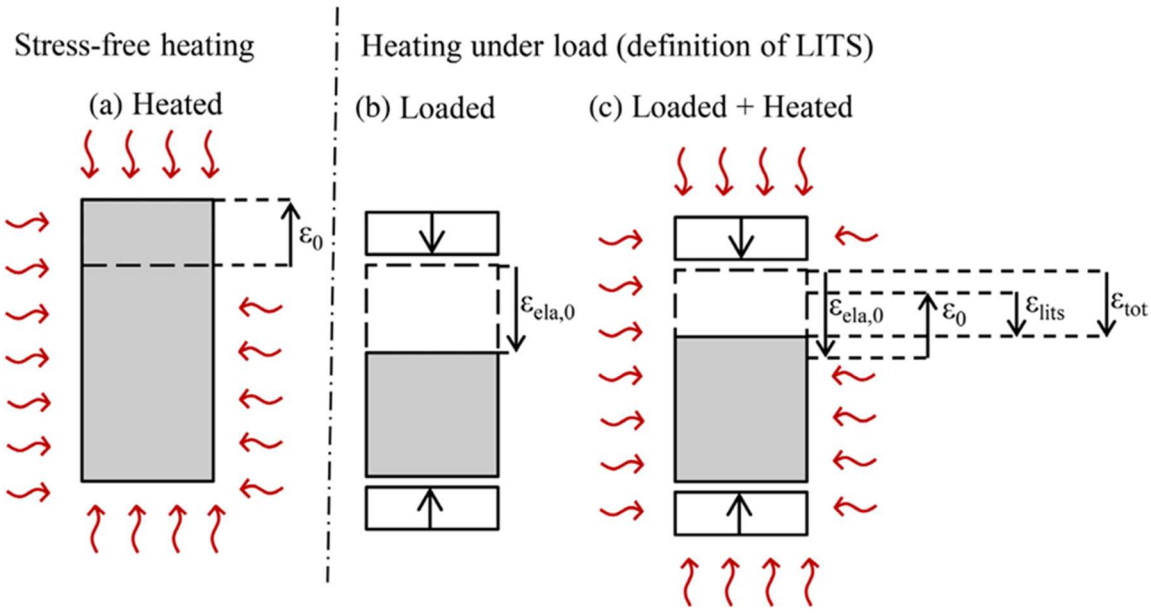

Figure 2.26: Schematic showing LITS reproduced from (Torelli *et al.*, 2016)

The free thermal expansion, ε_0, combined with the unheated compressive strain $\varepsilon_{ela,0}$, does not account for the resultant total strain , ε_{tot}. LITS, ε_{lits}, is the difference in strain. This can be expressed as:

$$\varepsilon_{tot} = \varepsilon_0 + \varepsilon_{ela,0} + \varepsilon_{lits}$$

2.10.2 Relevance to spalling research

Research into LITS is often carried out by first loading and then heating samples. This is the same sequence of loading which would occur in a real fire and is the usual approach taken when carrying out experiments to research heat-induced spalling of concrete under load.

As LITS develops in the loaded direction the additional stress due to restrained thermal expansion is mitigated. The stress state within a concrete sample when heated is believed to influence spalling and increased understanding of this could provide further clarity.

Currently both spalling and LITS are areas of concrete research that require further work. Al Hamd. et al (Al Hamd *et al.*, 2018) state: *"LITS is a complex and not fully understood the [sic] phenomenon that presents difficulties for numerical models."* The same could be said for the spalling phenomenon.

As the understanding of LITS improves, this knowledge may provide additional clarity and understanding of the spalling phenomenon. To date, LITS is not usually considered directly in spalling research and has not been the focus of the work described in this thesis.

As understanding of both phenomena improves, future work to combine knowledge of the two research fields could be beneficial to the holistic understanding of behaviour of concrete at elevated temperatures. A particular area of interest is understanding the stress state within heated concrete and how this may be influenced by moisture content and aggregate. Both LITS and spalling are influenced by moisture content and the phenomena could be linked directly.

2.11 Chapter conclusions

This literature review has demonstrated the current, limited, level of understanding of spalling and the limited improvements since the early 1900s. The current situation can be summarised that, despite a century of significant research efforts internationally, there is still no validated guidance to enable the design of concrete mixes to prevent spalling. Nor are there any established, widely verified, repeatable test methods that can confidently quantify or demonstrate spalling resistance for a particular mix in a given application. There is also currently no accepted and validated theory as to the mechanism of spalling. As a result, no models yet exist that can predict spalling with sufficient confidence to be used in design.

The huge variety of experimental setups in use and some of the issues encountered have been shown. Many issues arise from the lack of harmonisation of the experimental approaches and there seems to be a lack of emphasis on controlling all the necessary boundary conditions. The need for this kind of control was identified by early researchers but seems to have been forgotten.

There is a requirement for a focused effort in the community with respect to setting a standard for experimental approaches to spalling research. Improvement in this area may be one of the outcomes of the RILEM TC SPF of which the author is a member, which is focused on spalling research. The author is not of the view that any one test method should be favoured over another but that test methods used should be required to properly quantify the experimental conditions. In Section 2.7 issues with the current state of the art experimental approaches presented at The Sixth International Workshop on concrete spalling due to fire exposure (Huang and Burgess, 2019) were discussed and none of the approaches were deemed to provide satisfactory control of all the necessary parameters.

There have been many experimental programs carried out, typically using different apparatus, to investigate spalling, none of which were successful in “solving” spalling. Had all of these experimental programmes been carefully considered and harmonised there would be a wealth of properly comparable knowledge on spalling which, even without solving spalling, could be used to develop probabilistic tools and inform design guidance.

The different experimental approaches to understanding spalling were discussed by Dougill in his 1971 PhD thesis. He says

"One approach to the problem of general spalling would be to test a variety of slabs, with different degrees of restraint and thermal exposure, to determine the conditions, under which spalling occurs, in terms of particular combinations and values of the listed influential variables. … The principal advantage, of this approach, is that no knowledge is required of the mechanism of spalling or the manner in which heat is transferred within the slab and affects the properties of the materials involved. The main disadvantage is that many different combinations of variables have to be explored and, each combination requires a separate test. Clearly, the method is only viable if sufficient resources can be brought to bear and thus, this approach has little appeal until other alternatives have been tried"

Dougill identified that the approach of carrying out exhaustive testing varying all the necessary parameters is undesirable when compared with targeted testing to understand the spalling phenomena. With no solution to the problem of spalling after 100 years of research it could be said that these alternative methods have now been tried and that it is time to focus experimental efforts in a way that allows this exhaustive, properly comparable data to be developed.

In the work described in this thesis a test method was developed that allows repeatable testing to be carried out with all the relevant parameters controlled. Particular attention has been paid to quantifying the application of the thermal exposure to sample.

3 The H-TRIS experimental apparatus

3.1 Summary

This chapter describes the experimental apparatus used. The thermal exposure is applied to the samples using a moving radiant panel array. This heating method has been referred to in the spalling community as 'H-TRIS' and will be referred to throughout this thesis by that name. Other authors who have used the radiant panel array since have chosen not to use this name. The use of radiant panels to apply a controlled heat flux in this way for spalling research has been explored in the past (Connolly, 1995), but current approaches neglect heat flux and focus on controlling gas temperatures. This was covered in Chapter 2.

The two H-TRIS heating setups used throughout this thesis are described in this chapter. The background and philosophy behind the H-TRIS experimental method and apparatus is discussed in Sections 3.2 and 3.4. The two specific versions of H-TRIS heating system used within this thesis are then discussed in Section 3.5 and Section 3.6, including discussion of their limitations and various issues (i.e. growing pains) with the experimental setups. Mapping of the incident heat fluxes produced by the radiant panels at various standoff distances is described in Section 3.7, and the bespoke loading frame which was developed within the work of this thesis as part of the experimental setup is described in Section 3.8.

3.2 Introduction

In the literature review in the previous chapter some of the test methods being used to research fire performance of concrete and specifically heat-induced spalling of concrete are discussed. It is the author's belief that, due to the complexities of the spalling phenomena and the general lack of quantified understanding of the influence of different test parameters, great care must be taken in any experiments to understand spalling to properly control the experimental loading and thermal boundary conditions. In the absence of a quantified understanding of the influence of sample size, the samples tested must be of representative size, and without a better understanding of the influence of external loading, loads that are representative of the in situ loads which will be experienced by concrete in a real-world application should be applied where possible.

The experimental work carried out in this thesis project makes use of and further develops and builds upon a novel experimental apparatus known as H-TRIS Mark I.

This heating apparatus was initially developed by Dr. Cristian Maluk during his 2014 PhD at The University of Edinburgh, with a focus of achieving accurate and repeatable severe, one-sided thermal exposures on samples of concrete. During the project described in this thesis a new and enhanced H-TRIS apparatus (Mark 2) was developed with various significant improvements to allow application of more severe thermal exposures, with a peak incident heat flux of 300 kW/m^2 rather than around 100kW/m^2, which had previously been possible.

As discussed in Chapter 2, the load conditions to which a concrete sample is exposed are thought to be an important variable when assessing a concrete's spalling propensity. As such, a bespoke loading frame was also designed and constructed to enhance the H-TRIS testing method's ability to test for spalling, by allowing externally applied uniaxial compression during experiments carried out using the enhanced heating apparatus developed during the course of this thesis.

3.3 Acknowledgements

The work to develop the experimental apparatus was not carried out by the author in isolation. The development of the moving radiant panel array aspect of H-TRIS required the expertise of others, both technical staff and fellow members of the fire research group. Their expertise was called upon on many occasions throughout the author's years in the laboratory. Please see the thesis acknowledgements for the names of those who helped source products, troubleshoot, develop control software, and who shared their extensive knowledge of experimental work. The willingness of the fire group to share knowledge and help each other is unparalleled.

Particular thanks are due to Cristian Maluk who shared his knowledge while the author assisted him with his experiments on the original H-TRIS and then helped realise the improved heating aspect of H-TRIS that was used for the experiments detailed in this thesis. Further thanks are also due to Zaid Al-Azzawi for sharing his modelling expertise and sense checking the authors loading frame design. There would have been no experimental apparatus without you.

Funding for the experimental apparatus was obtained from a variety of sources including CERIB, EPSRC, Arup, and others not focused on spalling who saw the potential use of the apparatus researching their products. The author is not aware of the full finances but thanks must be given to those who contributed, Professor Luke Bisby for raising the funds, and to those who helped with the many rounds of research consultancy and collaborations that we carried out to raise money for the apparatus and fire lab.

The heating apparatus and loading frame remain in the laboratory for future researchers to utilise, adapt, and improve.

3.4 H-TRIS concept

The H-TRIS testing method and apparatus differs from other test methods typically used for concrete and assessment of structural elements since it relies on directly controlling the thermal exposure to the sample in the form of the applied incident heat flux. A similar experimental approach of controlling the thermal exposure directly (incident heat flux) is taken in experiments carried out using e.g. a fire propagation apparatus (FPA) (ASTM, 2013) or cone calorimeter (British Standards Institution, 2015). In all three of these experimental methods, the control of thermal exposure is achieved by controlling the incident radiant heat flux applied to the surface of the sample. Four electric lamps make up the heat source in an FPA, while an electric cone resistance heater is the heat source in a cone calorimeter. The heat sources used in the versions of H-TRIS to date (i.e. Mark 1 and Mark 2) consist of arrays of propane fuelled radiant panels that are configured to burn at a constant and uniform temperature.

The incident heat flux applied to a sample surface using the H-TRIS method is controlled by varying the distance between the sample and the radiant panels – in the case of the H-TRIS apparatus used in the current thesis, by moving the radiant panels relative to the sample surface. The incident heat flux could also be varied by moving the sample relative to stationary radiant panels. However, as H-TRIS was originally designed for experiments on concrete, steel, and other heavy or awkward construction materials, moving the radiant panel array remains the most practical solution. The distance between the samples and the radiant panels is varied by mounting the array of radiant panels onto a linear motion system. The limitations on the application of thermal exposure come from the type of radiant panels being used (i.e. their surface temperature) and the speed, accuracy, and total length of the linear motion system. The speed at which the linear motion system is able to move limits the possible rate of change of heat flux and potential incident heat flux versus time curves that can be recreated.

The length of the linear motion system, the total size of the radiant panel array, and the burning temperature of the radiant panels limits the maximum and minimum incident heat fluxes that can be achieved. The size of the array of radiant panels influences the uniformity of heating over the sample surface and the shape of the calibration curve, the theoretical peak heat flux would still be the same with different panel array sizes as this occurs when the view factor is close to 1. The use of a larger

array could allow this to occur further from the sample surface but would not change the theoretical peak heat flux (although it would improve the uniformity of heat flux over the target area, as discussed later in this chapter).

The incident heat flux at different standoff distances from the radiant panel array can be approximately measured using a Schmidt-Boelter heat flux gauge. Regular calibration of the heat flux versus distance from sample, coupled with precise control of the linear motion system, allows for highly repeatable (if partly uncertain – due to convective heat transfer at the samples' surface) application of the desired thermal exposures during experiments. An overview of the H-TRIS Mark 2 experimental setup is shown in Figure 3.1.

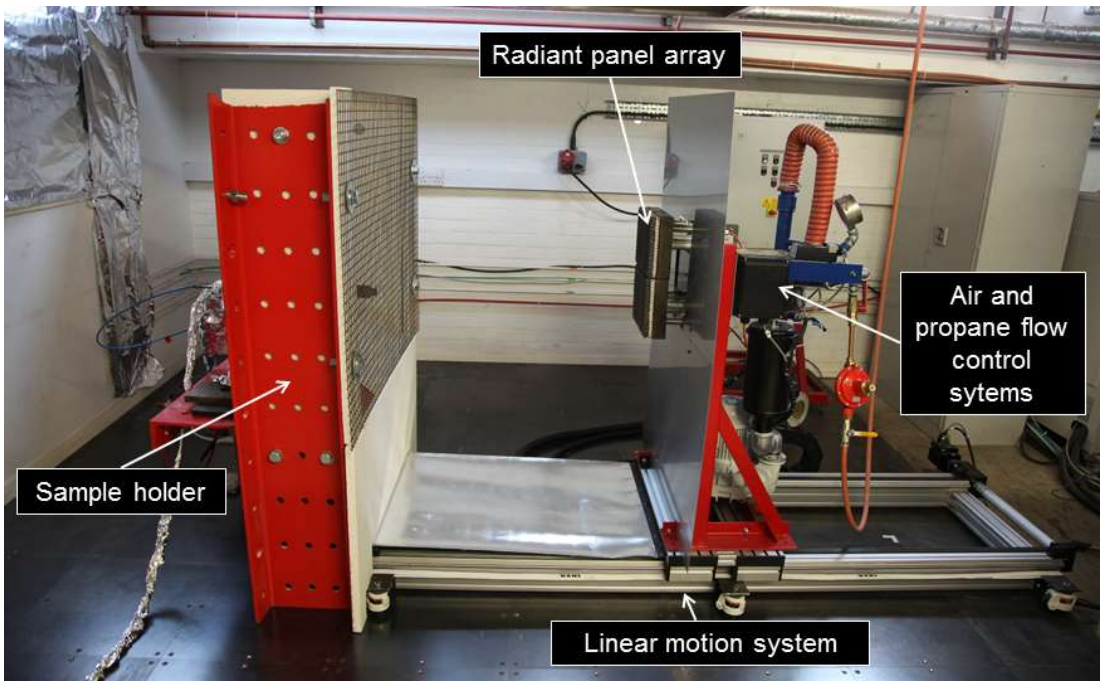

Figure 3.1:Overview of H-TRIS Mark 2 apparatus

3.4.1 Thermal exposure advantages

As previously mentioned the thermal exposure which can be imposed on a sample using the H-TRIS experimental apparatus is limited primarily by the radiant panels being used and the speed and range of the linear motion system. Within these limitations it is possible to impose any complex thermal exposure accurately by simply inputting the desired incident heat flux time curve into the bespoke H-TRIS software. Currently the peak incident heat flux which is achievable is about 300kW/m^2 and the maximum velocity of the panels is approximately 3 m/s which does not easily translate into a meaningful rate of change of heat flux as the heat flux versus distance calibration curve is nonlinear (as discussed in Section 3.7 of this thesis).

The thermal exposure in H-TRIS experiments is applied directly as an incident radiant heat flux with the testing specimen immersed (for most heat fluxes) in ambient conditions, rather than by heating in a closed oven or furnace and following a target gas temperature versus time curve (as in a standard fire-resistance test). Heating in this way introduces the possibility of accurately following cooling as well as heating curves, since there is no hot chamber around the sample. Accurate cooling of a hot furnace presents a challenge during testing because of re-radiation from the furnace walls, and most temperature versus time curves used for structural fire-resistance assessment therefore do not include a cooling phase.

The combination of the flexibility of heating curve and the ability to accurately control a decreasing thermal exposure or “cooling phase” makes the H-TRIS experimental apparatus a powerful tool for assessing and understanding the performance of materials and structural assemblies. There is potential for testing at constant heat fluxes and for running experiments to a selection of linear heat flux versus time ramps to assess the impact of the rate of change of heat flux. It is also possible to take the output of a fire model such as FDS (McGrattan *et al.*, 2013) as a semi-direct input to H-TRIS and run experiments to the realistic calculated thermal exposure for a specific design. Testing to a range of defined thermal exposures could, in future, allow for things such as performance based design of concrete where a suitable concrete can confidently be selected for the project specific use based on a thorough understanding of its behaviour under severe thermal exposures and at realistic thermal exposures used for design.

3.4.2 Observational advantages

Since samples which are tested using the H-TRIS experimental method and apparatus are tested “in the open”, rather than in a closed chamber, it is possible to make clear visual (and other) assessments of material/sample behaviour during H-TRIS experiments, on both the exposed and unexposed faces. The openness of the experimental setup also allows for extensive instrumentation and the use of multiple video cameras (including thermal imaging) throughout testing.

Using the H-TRIS method it is possible to test using essentially any internal instrumentation, such as pressure gauges (Kalifa, Menneteau and Quenard, 2000; Jansson and Boström, 2010; Mindeguia *et al.*, 2010; Felicetti, Lo Monte and Pimienta, 2017) and thermocouples. It is also possible to use other instrumentation which does not require access to the heated face. During some of the experiments conducted as part of Phase 3 of the experimental work of this project (see Chapter 6) a ground penetrating radar (GPR) technique was used to assess if it is possible to track moisture migration within the concrete during heating. This work is being carried out by other researchers. The setup and ease of measurement is shown in Figure 3.2. The work has not yet been completed but it has been demonstrated that it is practically possible to take these kind of measurements.

As there is no heated chamber in H-TRIS testing, it is also possible to use conventional photography and video equipment to record sample behaviour during experiments. Use of digital image correlation is also possible. Recent work on another PhD project (Gerasimov, 2020), which the author was involved in but which does not form part of the PhD project reported in this thesis, makes use of an image analysis system to monitor the expansion of intumescent paints in real time. The standoff distance between the radiant panels and the paint surface can be adjusted live thus maintaining control of the incident heat flux applied to the surface of the sample (which expands towards the radiant panels in the case of an intumescent coating). This type of sample monitoring and control of incident heat flux would be extremely challenging in an enclosed experimental environment (i.e. a furnace or an oven).

Figure 3.2: Ground-penetrating radar being used to attempt to assess moisture migration during an experiment (see Chapter 6 for additional details of this parallel project)

The two versions of H-TRIS that were used during the PhD project reported in this thesis are described in the following sections, including details of some of the issues and challenges faced during the experiments undertaken for this thesis. These descriptions of the performance and limitations of the experimental setups are provided based on the author's experience from extensive testing of a variety of different materials during the course of his PhD including: concrete, metals, engineered timber, plasterboard, and intumescent paints. This other work was carried out as part of confidential consultancies or collaborations with other researchers. As such it does not form part of this thesis. The author's understanding of the apparatus was however increased from this extensive experience.

3.5 H-TRIS Mark 1

H-TRIS Mark 1 is the most advanced version of the original H-TRIS apparatus developed by Dr Cristian Maluk during his PhD at The University of Edinburgh (Maluk, 2014). This H-TRIS Mark 1 setup has been improved upon over time, and the current version is different in several important respects to the version used for the testing carried out for Phase 2 of the current project (see Chapter 5). The version of H-TRIS Mark 1 used in the experiments described in this thesis is the same as the final version used by Maluk. It is referred to in the past tense as it has been updated and no longer exists in this configuration.

When the testing described in Phase 2 (Chapter 5) was carried out the linear motion system moving the radiant panels was a simple threaded rod linear motion system powered by a stepper motor. The radiant panels used as the heat source were FibreTech Metal Fibre radiant panels with the SFF1-35 sintered matting as the porous media (FibreTech, 2018). In the configuration used, these were capable of delivering a peak incident heat flux of around 100 kW/m^2. The combustion in these radiant panels occurs within the porous media, with the back of the panels serving as a mixing chamber for the propane and air. These FibreTech panels are shown in Figure 3.3.The H-TRIS Mark 1 apparatus as used in Phase 2 of the experimental work carried out in this project is shown in Figure 3.4 (not in operation as shown).

Figure 3.3: H-TRIS Mark 1 radiant panel array

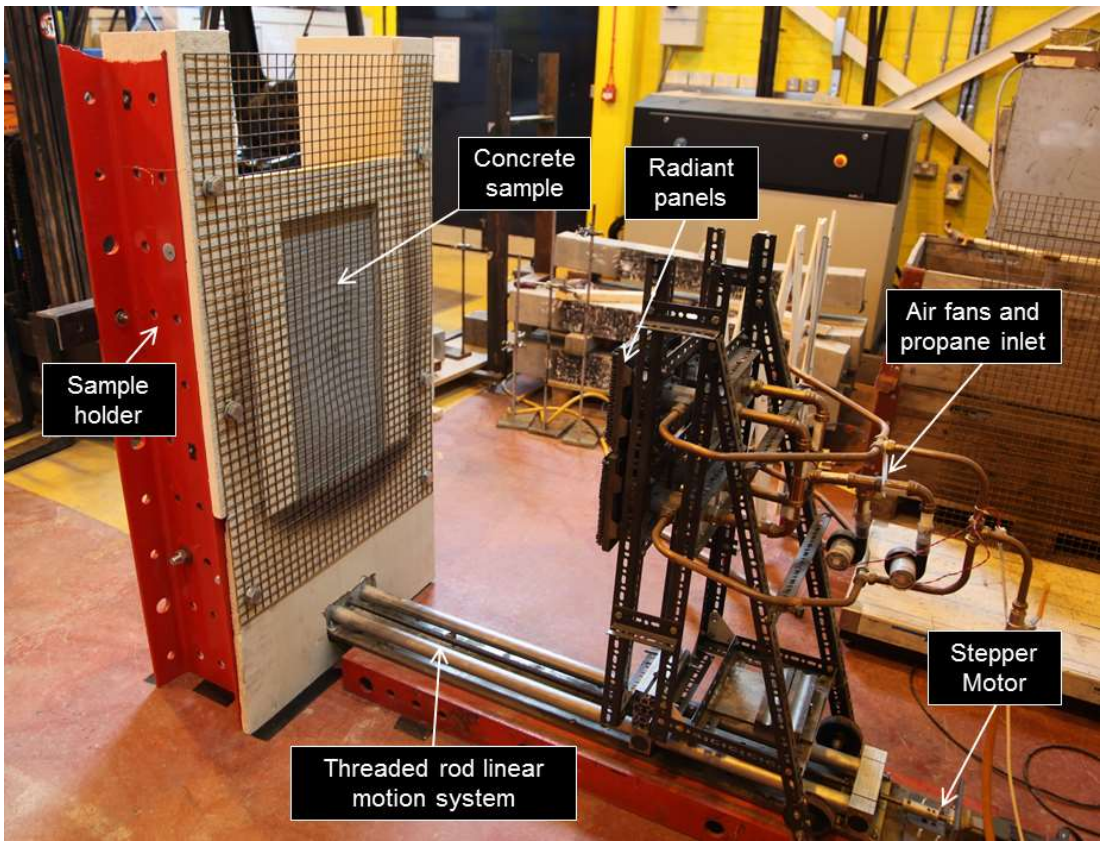

Figure 3.4: H-TRIS Mark 1 setup as used in Phase 2 of experimental work

As can be seen in Figure 3.4, the frame of the apparatus itself was made from steel angle sections bolted together to create a trolley holding the radiant panels above the linear motion system. Each row of the four propane-fuelled radiant panels had its own fan and propane input giving the premixed propane and air required. For the radiant panels used in both H-TRIS Mark 1 and H-TRIS Mark 2 (described later) the combustion occurs within a porous media. For the radiant panels used on H-TRIS Mark 1 the porous media is a sintered matting. This matting has proved to be resilient to harsh testing conditions in comparison with other radiant panels and many tests can be carried out before the matting eventually deteriorates to the level that it needs to be replaced (assessed by obtaining and comparing calibration curves). A gradual deterioration was observed for this combustion medium, but this was corrected for by calibration of the apparatus. When the porous media needed to be replaced it was typically a crack or hole which developed in the matting and this would be visible with the eye. The radiant panels are fully serviceable however, and the matting, protective mesh and gasket can be easily replaced and repaired.

The radiant panels were calibrated using a Schmidt-Boelter heat flux gauge attached to a bespoke water-cooled mounting sleeve which protects the hoses and cable of the gauge. This method was developed by Dr Maluk (Maluk, 2014) during his PhD work and was used for early calibrations in Phase 2 of the experimental programme presented in this thesis. More recently, a heat flux mapping robot has been developed (with input and assistance from the author of this thesis) which allows automated positioning of the gauge in front of the radiant panel array. This is discussed in detail in Section 3.7. The calibration process creates a curve of incident heat flux versus standoff distance from the radiant panel array. This is used as the input when controlling H-TRIS experiments and a point or average of points on the panel array must be used. The tests using H-TRIS Mark 1 were carried out based on a calibration taken at the centre of the top right radiant panel.

3.5.1 Issues with experimental apparatus

H-TRIS Mark 1 was, for the most part, a tried and tested experimental apparatus when the early experiments for the current project were carried out. The sintered matting in the radiant panels proved to be robust and survived repeated severe spalling incidents reasonably well without damage or deterioration. It did require periodic replacement, but the service life of the sintered matting is estimated to be around 200 hours of running time for undertaking spalling tests. This of course depends on the specific conditions being experienced, but it is usual for these sintered mats to last for multiple experimental programmes without any significant changes in heating performance. As mentioned previously, the matting has been observed to crack or develop a hole eventually, and this is when replacement is necessary.

3.6 H-TRIS Mark 2

The central aim of the current research project was to develop a rational, robust, and repeatable test method to study the heat-induced explosive spalling of concrete, with a particular focus on spalling of concretes used in tunnel linings. The H-TRIS Mark 1 apparatus therefore needed to be upgraded in order to be able to test to the high incident heat flux time-histories that might be experienced in a furnace test carried out to a temperature versus time curve developed for tunnels. These standard curves developed for tunnels are more severe when compared against the cellulosic standard fire curves (International Organisation for Standardization, 1999) used for building applications.

This second version of H-TRIS (Mark 2) had a larger manufacturing budget than the original, which was largely fabricated on a small budget from spare and borrowed parts. As a result of the significant budget for the second generation of H-TRIS, it was possible to improve the entire apparatus, not only the radiant panels.

The radiant panels selected for H-TRIS Mark 2 were GoGas Radimax panels (GoGaS Goch GmbH & Co, 2018). This is a similarly sized panel to those used on H-TRIS Mark 1, and is also intended for industrial uses such as paper drying. The difference being that they burn with a higher surface temperature (quoted as 1450 °C, compared to 1050 °C for H-TRIS Mark 1 panels) and therefore produce a higher heat flux. These were the most powerful (i.e. hottest burning) radiant panels which could be reasonably sourced at the time of manufacture of H-TRIS Mark 2. The GoGas panels were fitted along with a large fan and a manifold system, allowing mixing of propane and air and promoting an even distribution of fuel (and hence surface temperature) between the four panels that made up the radiant array. A number of new safety features were also incorporated into the burners of H-TRIS Mark 2, these were;

- electronic spark starters to avoid any requirement for manual ignition of the radiant panels;
- flame sensors to cut the propane supply should the combustion within the porous media stop for any reason; and
- emergency anti-blowback valves which shut off gas supply in the event of a flame propagating back into the manifold (with associated safety concerns).

Some problems were encountered with the flame sensors and the emergency valves throughout the testing performed during the current project and these are discussed

in Section 3.6.1. The H-TRIS Mark 2 apparatus, complete with uniaxial compressive loading frame (which is described in Section 3.8) is shown in Figure 3.5.

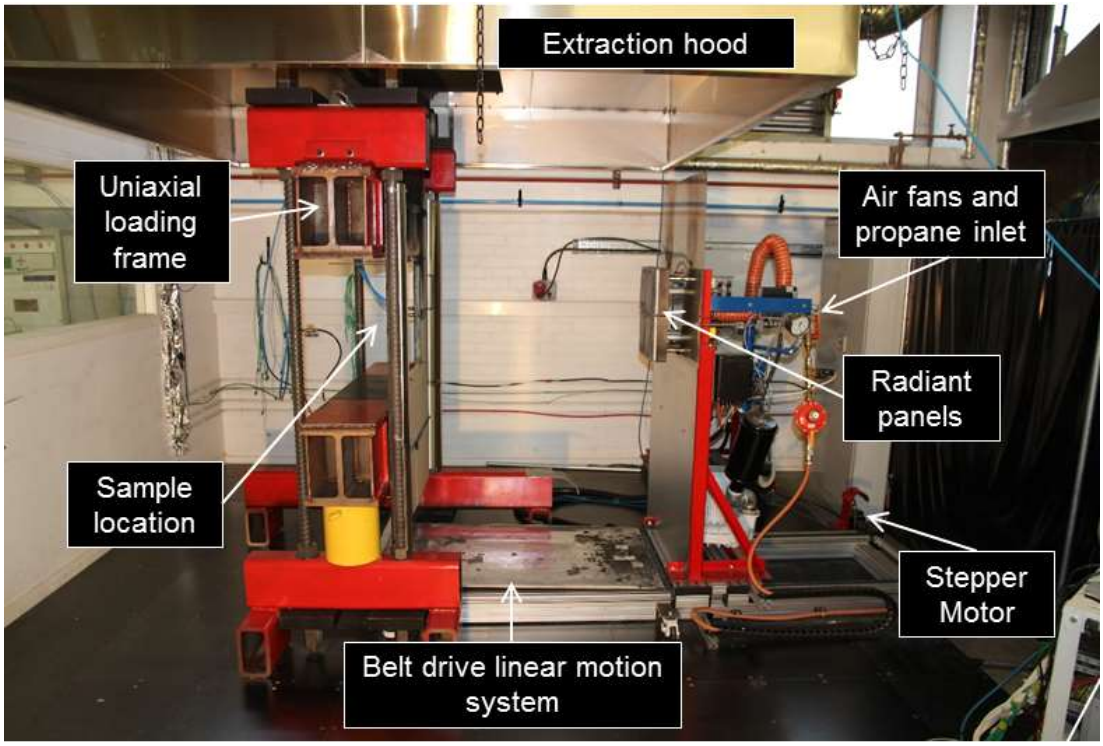

Figure 3.5: H-TRIS Mark 2 and compressive uniaxial loading frame

The fan required for the GoGas radiant panels is much larger than those used for H-TRIS Mark 1. The GoGas panels also require a propane mass flow rate of approximately four times that of the H-TRIS Mark 1 panels. This increased demand on propane and air meant that the propane supply had to be upgraded and that the linear motion system needed to be able to support the larger mass fan. In order to reduce the moving mass, the power supply and electronics were separated and mounted in a control box on the wall behind H-TRIS. The linear motion system used on H-TRIS Mark 2 is a belt driven extruded aluminium system that is also controlled by a stepper motor but allows much faster and smoother movement of the radiant panel assembly when compared to the threaded rod drive of H-TRIS Mark 1.

3.6.1 H-TRIS Mark 2 experimental apparatus – Issues and Challenges

It is important to explain in detail the issues encountered during the development of H-TRIS Mark 2, as a number of tests presented in this thesis were cut short as a result of several challenges. Through extensive testing experience, the sources of all the problems were identified and, where possible, measures were taken to prevent the problems re-occurring (mostly successfully).

3.6.2 Failure of flame sensors

After experiencing few serious problems initially, the radiant panels in H-TRIS Mark 2 started to cut out after a few minutes of radiant panel use. Flame sensors (one for each row of the array of radiant panels) were supplied and installed in the panels by the panel manufacturer. The flame sensor probes are fitted within the panels and are monitored by sensors in the ignition box supplied with the panels. The flame sensor probe is a simple rod which is insulated, except for the tip, within a ceramic sleeve and connected to an AC power source. When functioning properly the flame sensors produce a small DC signal when the probe is in contact with a flame. The AC power to the probe is rectified to DC through a process called flame rectification. After considerable investigation, the cut out of the radiant panels was found to be due to oxidation of the probes impeding this flame rectification. The oxidation eventually built up to the extent that the DC current being produced when the probe was in contact with a flame was below the critical limit set within the apparatus. The DC current dropping below this critical limit is interpreted by the sensor as there being no flaming and results in the propane supply to the panels being automatically halted.

It was found that the flame sensor probes must be replaced periodically, and this is now done after approximately every 30 hours of testing. This replacement cycle has proved to be sufficient to prevent them malfunctioning. The array of radiant panels is separated into top and bottom rows with a sensor in each row and an ignition/shutoff system for each row. In some of the experiments carried out one of the rows of panels shutoff due to this flame sensor issue and caused the experiment to be cut short.

Figure 3.6 shows an oxidised flame sensor probe which falsely indicates absence of flaming. To function properly the probe should be relatively free from oxidation, as it is close to the insulated ceramic part in this figure. The oxidised tip is the area which

is exposed to the most severe heating as, when in use, it is located within the very high temperatures of the porous media of the radiant panels.

Figure 3.6: Oxidised and malfunctioning flame sensor probe

3.6.2.1 Failure of emergency valves

In some of the early spalling testing undertaken using H-TRIS Mark 2, the radiant panels were found to stop working after an incident of violent explosive spalling. Upon dismantling the apparatus, this was found to be a result of activation of the emergency valves within the system designed to prevent flame propagation and panel blowback. The emergency valves were located within the manifold pipework behind the radiant panels and consisted of a glass bulb that held open a spring valve. In theory, the increase in temperature due to a flame propagating back into the manifold could break this glass bulb.

The emergency valves were designed to close in the event of a flame propagating back into the manifold and pipework of the system. Testing of concrete caused violent explosive spalling which was sufficient to shake the radiant panel assembly sufficiently or to generate an overpressure within the system that these glass bulbs

broke and the emergency valves closed irreversibly. As spalling is unavoidable during spalling testing, and there are many other safety measures in place, these glass bulbs were replaced with metal blanks to hold open the valves. Removing the valve assembly entirely was found to alter the flow rate of propane to the panels and resulted in surface flaming on the panels. Since experiments are stopped at the first spalling incident this issue did not cut any of the experiments short. It did, however, result in a large downtime and delay to the testing performed during the Phase 3 experimental work of the current project, and resulted in greater age differences between specimens at time of the experiments than had originally been planned (or was desired).

As the panels were calibrated before experiments, the presence of either a glass fusible, or identically sized metal spacer is not believed to have had any impact on the experiments. The glass bulbs were used up to their failure when they were replaced by metal spacers.

3.6.2.2 Blowback of combustion into panel body

During some of the testing the combustion occurring in the porous media of the radiant panels propagated back into the chamber of the radiant panel itself. This was not prevented by the emergency valves mentioned above in Section 3.6.2.1. The result of this propagation of the combustion into the panel was a loud droning noise and a reduction in the combustion occurring in the surface of the panels, this was visible as the panel would darken. It was not possible to quantify this change in heat flux as to keep running the panels with combustion within the semi sealed chamber of the panel is dangerous. Experiments were manually stopped immediately if this blowback occurred.

The source of the problem and the reason for this blowback starting to occur was found, again after considerable investigation and unintended downtime in testing, to be due to degradation of a ceramic rope that was placed around the edges of the individual radiant panels that made up the radiant panel array. The seal provided by the rope was lost when it degraded, and air could be drawn in from underneath the sides of the porous media. The GoGas panels are not designed to be disassembled or serviceable, however a method of replacing the porous media and the ceramic rope was developed by the author.

Replacing the rope prevented this blowback. The blowback cut short a number of experiments that were carried out using H-TRIS Mark 2 (as described in Chapter 5

and Chapter 6). After the testing described in this thesis had been completed, it was found that using an additional fan to keep the reverse side of the radiant panels cool is an effective method to prevent blowback – the testing apparatus has now been modified to make use of this discovery. Figure 3.7 shows a GoGas panel being serviced and the degraded ceramic rope around its edge.

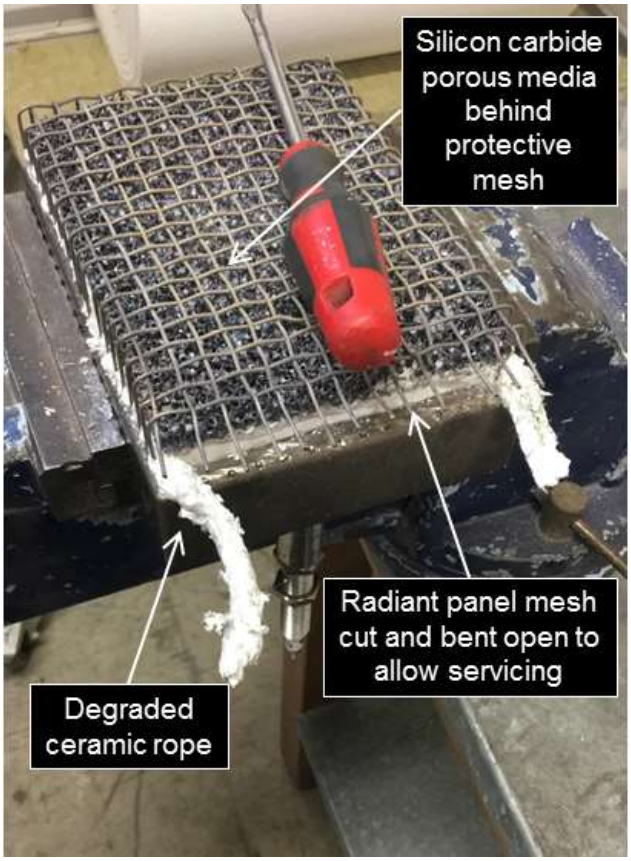

Figure 3.7: GoGas radiant panel being serviced

3.6.2.3 Degradation of porous media within the radiant panels

Whilst small changes in the performance of the radiant panels can be accounted for by periodically adjusting the calibration curve, a more severe degradation of the porous media was periodically observed. This could not be accounted for only by re-calibrating the apparatus. A dark area, burning less brightly, would appear on the radiant panels. This dark area would then move around on the face of the radiant panel.

After considerable investigation, it was found that the porous media itself can break down (for reasons that remain unknown), forming a ‘foam’ which influences the flow of propane and air through the surface of the panel. Having carried out extensive

experiments on non-spalling or non-concrete specimens – for which no degradation of the porous media has yet been observed – it appears that this degradation is triggered by concrete dust from spalling events getting into the porous media of the radiant panels. The extreme temperatures of the combustion in the panels then appears to cause a degradation reaction which produces this foam. Once this reaction has begun it is not possible to reverse it or to clean out the foam (based on various attempts by the author and colleagues). The porous media on the panels has to be replaced when this degradation occurs. A typical darker area on a burning radiant panel is shown in Figure 3.8. A section of the porous media that has started to degrade and contains the silica foam is shown in Figure 3.9.

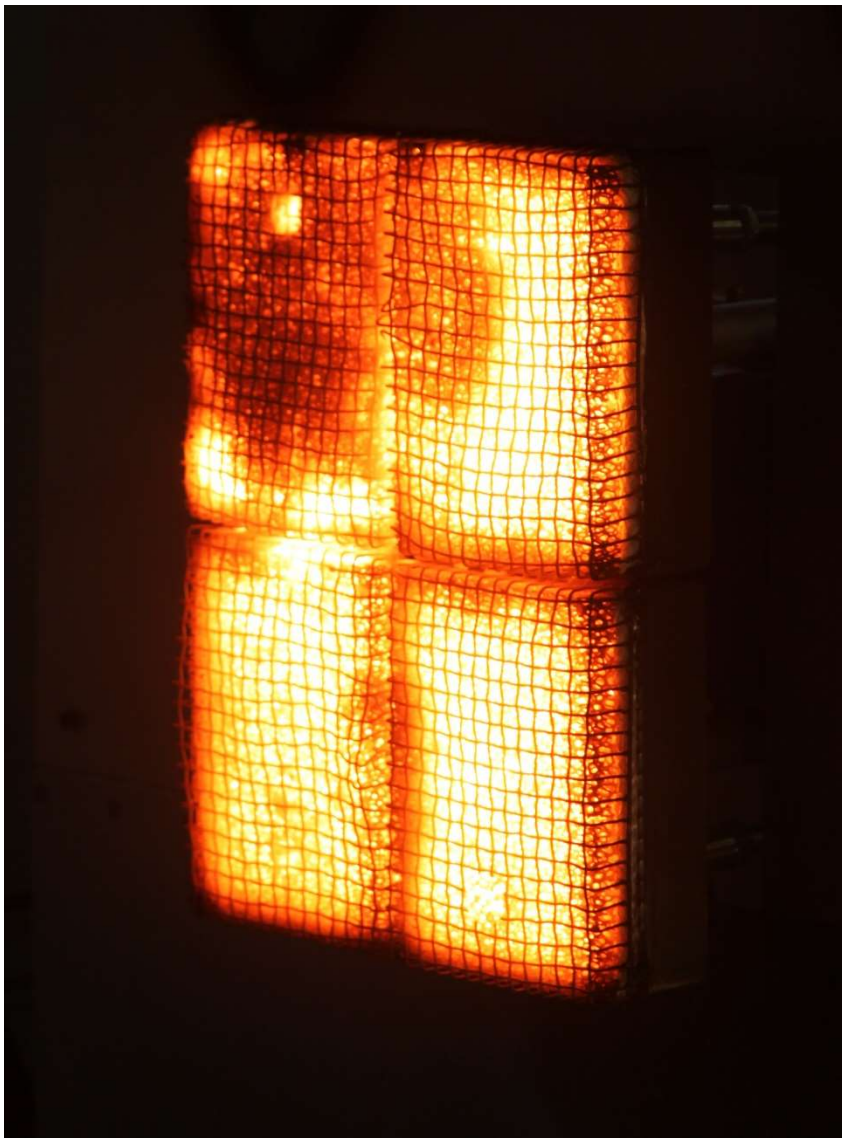

Figure 3.8:H-TRIS Mark 2 panels with degraded porous media

Figure 3.9: Degraded porous media from H-TRIS Mark 2 radiant panel

Whilst no tests were cut short because of this panel degradation, it is possible that the degradation may have started during a test and influenced heating. The degradation however appeared to usually begin during the initial warmup and stabilisation stage of experiments after a period were the radiant panels were left unused. Some delays to the experimental programme were encountered as a result.

Now that spare parts have been sourced and a method has been developed for refurbishing the panels, all four panels in an array can be refurbished in one day. A second set of radiant panels is now in rotation on H-TRIS Mark 2 so that down time is reduced and experimental programmes can be completed without these delays. This was not the case during the early tests on H-TRIS Mark 2, and this issue contributed significantly to delays to experiments with there being a long lead time on ordering parts from the manufacturer.

3.6.2.4 Non-uniformity of heating

Non-uniformity of heating is an issue faced by all experimental setups which impose a thermal exposure on a sample through incident heat flux to a sample surface (i.e. a cone calorimeter or FPA). This issue is also faced when carrying out experiments using H-TRIS Mark 1 or Mark 2. Non-uniformity of heating, due to a range of factors, is discussed further and quantified in Section 3.7.

3.6.2.5 Convective flow at close proximity

At close proximity to the sample, hot air from the radiant panels may impinge on the target sample surface. This is a result of the forced flow of combustion gases through the porous media of the panel and is an issue faced by all propane and air radiant panels. The influence of any hot air being expelled from the radiant panels will increase with the decrease in separation between the radiant panels and the sample surface (increase in incident heat flux). This means that there is higher uncertainty in the net heat flux into the sample at higher heat fluxes. Separation of the convective and radiative heat fluxes, and the quantification of the convective portion, is challenging. Characterisation of the radiation from the radiant panels and the potential influence of the forced flow remains a subject of ongoing research at The University of Edinburgh.

The uncertainty associated with the hot gases is present both during the calibration stages, and through experiments. The heat flux gauge used is calibrated to ISO 14934 (British Standards Institution, 2014) which involves calibration in a purely radiative environment and the convection is likely to influence the readings obtained during calibration. Again, decoupling of the convection and radiation was not possible and remains an area of research.

While the presence of any convective heat flux is undesirable, it important that this unknown is consistent in every test since the panels are operated in the same way. This means that while there is some uncertainty as to the convective and radiative portions of the incident heat flux, the heating remains repeatable from test to test.

3.7 Heat flux mapping

In order to evaluate the uniformity of thermal exposure that the surface of a sample receives from the H-TRIS Mark 2 experimental apparatus, a map of the thermal exposure, in terms of heat flux, can be produced.

3.7.1 Heat flux mapping robot

In an effort to quantify the variation of heat flux from the radiant panels a three-axis motion system was developed to allow precise automated movement of a Hukseflux SBG01 Schmidt-Boelter style heat flux gauge in front of the radiant panels. Without an automated system, mapping of the heat flux from the panels is prohibitively time-consuming, since for each point at which the heat flux is to be measured the gauge has to be manually repositioned. This means stopping the radiant panels and allowing everything to cool down fully before moving the gauge. With the use of a computer-controlled motion system and water cooled arm, however, the heat flux gauge can be moved while the radiant panels are burning continuously. If positions relative to the radiant panels are set before calibration it is possible to accurately move the heat flux gauge to known locations without having to stop the operation of the panels. If heat fluxes are to be measured at multiple locations the gauge must be allowed to stabilise in the new location before taking a reading of heat flux. A delay of 20 seconds was found to be an appropriate time to allow for stabilisation and accurate reading in a new location.

The apparatus used to map the heat flux is shown in Figure 3.10. While it is capable of moving in three axes it was only moved in two axes when being used for H-TRIS calibration, the linear motion system of H-TRIS is used to vary the distance between the radiant panels and the heat flux gauges mapping plane. The gauge used is calibrated in the range of 100 – 200 kW/m^2 but is capable of reading heat fluxes of 50% outside its calibration range. This means that reading for heat flux of over 300kW/m^2 will have some unquantified error in the measurement. A gauge calibrated to higher heat fluxes was not available at the time of calibration, however heat fluxes greater than 300kW/m^2 are not possible within H-TRIS Mark 2 in any case. Heat flux gauges calibrated in the range of 0 – 100 kW/m^2 were used for calibration at lower heat fluxes, particularly for the H-TRIS Mark 1 apparatus.

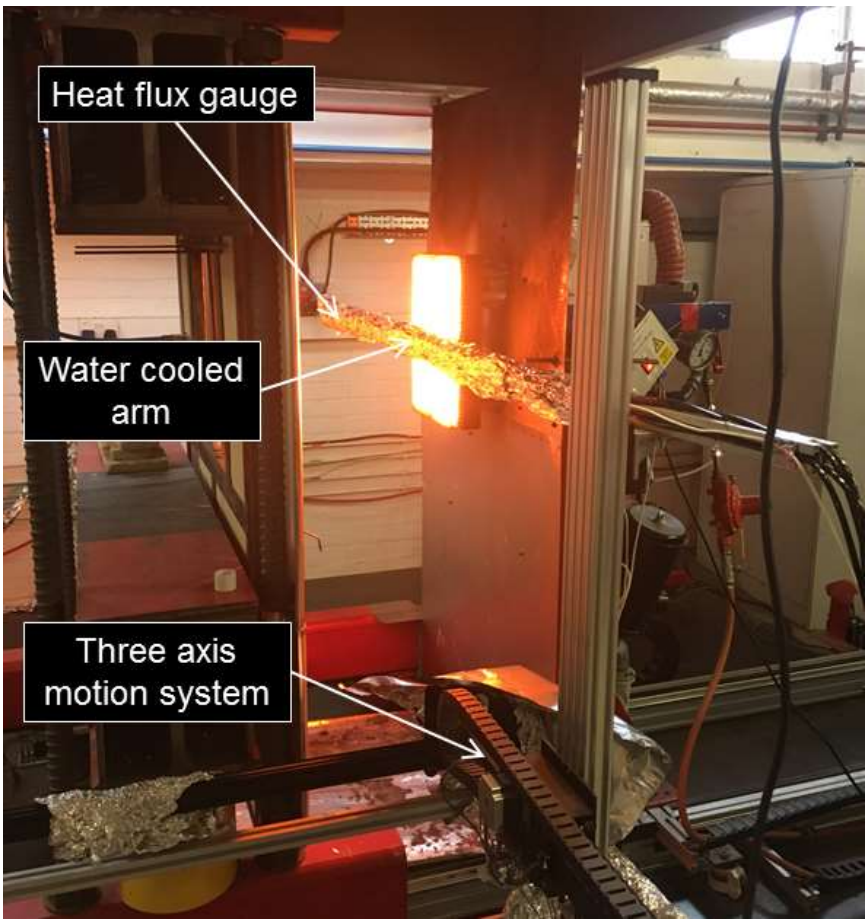

Figure 3.10: Calibration robot being used to map heat fluxes for H-TRIS Mark 2

3.7.2 Mapping of the thermal exposure from H-TRIS Mark 1

The heat flux mapping apparatus was not developed at the time of testing using H-TRIS Mark 1. As a result, detailed mapping for that test setup was not carried out. H-TRIS Mark 1 as used in Phase 2 (Chapter 5) of the experimental work for this project no longer exists in the same form that it did previously.

3.7.3 Mapping of the thermal exposure from H-TRIS Mark 2

The heat flux over a 500 x 500 mm area, slightly larger than is typically heated in any of the experiments reported in this thesis, was mapped for different heat flux levels with the position of the panels being determined based on an average control calibration of the centre of the top two panels in the array. These are referred to as the right control point and the left control point in the explanation in this section. These points have been found to give the peak incident heat fluxes for the radiant panel array and H-TRIS is controlled to the peak incident heat flux. The calibration curve obtained from the pre-test mapping calibration and used to determine mapping positions is shown in Figure 3.11. It can be seen that the calibration curves differ the

most at high heat fluxes when the heat flux gauge is at close proximity to the radiant panels.

As mentioned in Section 3.6.2.5 the convective flow interacts increasingly as the distance between the radiant panels and the heat flux gauge decreases. During control calibrations the heat flux was measured 20 times at each point and the value given is the average value measured. The average values and standard deviations are shown in Table 3.1. The standard deviation in heat flux measurement is higher when the heat flux gauge is close to the panels but the variation in measured values is insufficient to account for the differences in recorded heat fluxes. In this characterisation exercise the calibration location on the panel on the right is producing a higher heat flux than that on the panel on the left. The left and right control calibration locations are shown in Figure 3.12

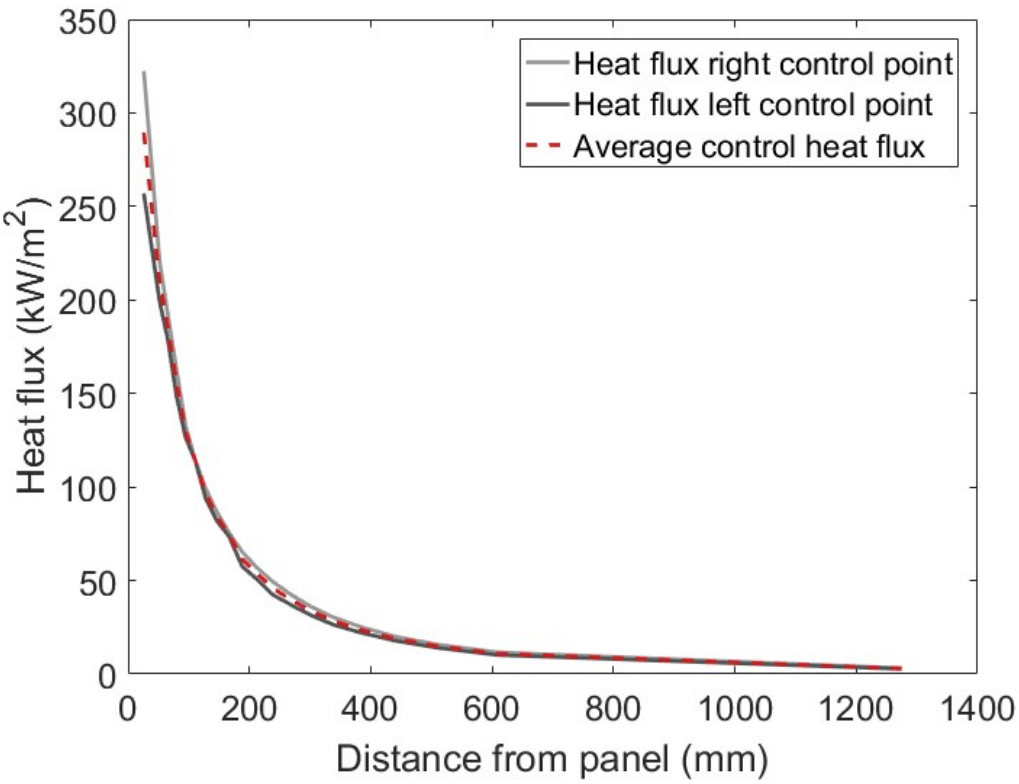

Figure 3.11: Graph of calibrations used for mapping control

Table 3.1: Calibration data from control points

Distance from panels (mm)	Heat flux left control point (kW/m^2)		Heat flux right control point (kW/m^2)	
	Average	Standard Deviation	Average	Standard Deviation
1275	2.72	0.26	3.18	0.30
608.6	10.18	0.23	11.60	0.27
509.5	14.03	0.24	15.75	0.33
438.7	17.93	0.31	20.14	0.24
383.6	22.12	0.33	25.15	0.31
338.5	26.35	0.40	30.31	0.34
300.3	31.57	0.22	36.18	0.46
267.1	37.25	0.72	42.75	0.31
237.9	42.51	0.25	49.51	0.23
211.7	50.88	1.74	57.04	0.44
188	57.55	2.15	65.33	0.45
166.4	73.59	1.28	75.57	0.67
146.5	81.79	3.87	86.60	0.97
128	93.76	4.69	99.07	1.42
110.9	113.96	2.87	114.02	2.53
94.8	126.45	6.69	132.72	1.38
79.7	148.86	5.21	163.01	6.65
65.5	178.96	5.41	192.33	11.95
52	199.09	4.54	220.47	3.76
26	256.99	1.22	322.35	8.64

The incident heat fluxes mapped in two dimensions over the target surface were 50, 100, 150, 200 and 250 kW/m^2. The chosen peak mapping heat flux of 250kW/m^2 corresponds to approximately the peak heat flux that samples experienced during HCM equivalent experiments performed as part of the current project. This peak heat flux varies with panel condition and is corrected for with regular re-calibrations. While the panels were theoretically capable of delivering a higher peak incident heat flux than this value, the presence of the insulation shield in front of the concrete spalling samples (see Section 3.8.5.6) and protective mesh prevented the distance between the panels and the sample being reduced further during the experiments.

The heat flux mapping was carried out in a ten by ten grid over a 500 x 500 mm area (i.e. in 50 mm increments). The largest exposed surface area of the samples heated was 450 x 450 mm while the sample size was 500 x 500 mm. Figure 3.12 shows the mapping grid used and its location relative to the H-TRIS Mark 2 radiant panel array and the control calibration points. It is important to note that the target heat fluxes are based on the control calibrations carried out at the points indicated in Figure 3.2. These locations were not precisely picked up in the grid of points used for heat flux mapping.

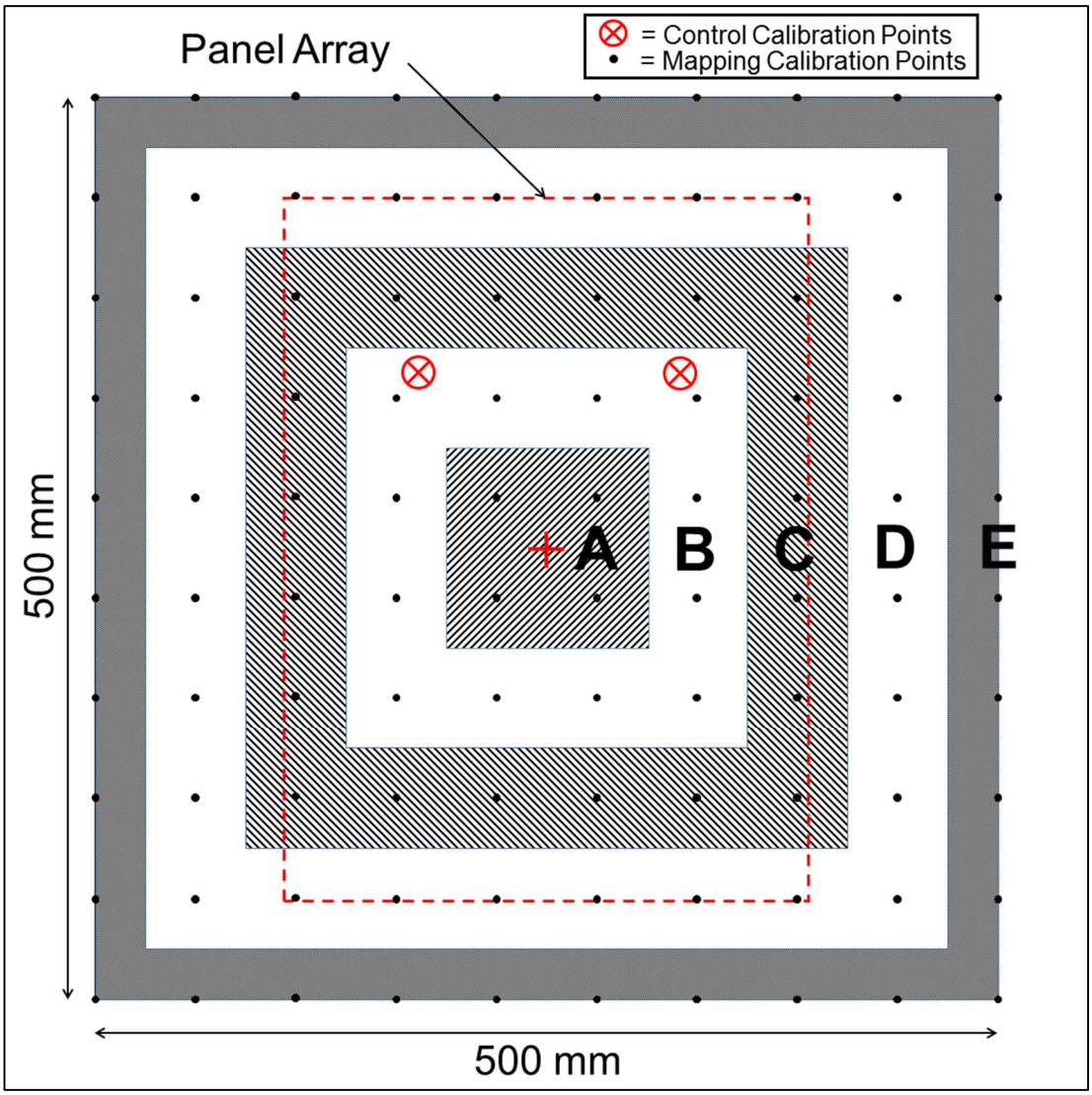

Figure 3.12: H-TRIS heat flux mapping layout showing H-TRIS panel location, calibration points used for control and the grid of mapping calibration points. Calibration carried out in parallel plane to radiant panel surface with distance to radiant panels varied.

The variation of the potential incident heat flux across a 500 x 500 mm target surface at different peak target incident heat fluxes can be assessed by splitting the calibration mapping grid into different areas. This grid was broken up into the areas A through to E shown in Figure 3.12. The average and standard deviation of the recorded heat fluxes for the different areas was then calculated in an attempt to quantify the spatial variation of the thermal exposures for different target heat fluxes based on the calibration. Table 3.2 shows the average and standard deviations of the heat flux measurements taken during the heat flux mapping. The areas A through to E correspond to the areas shown in Figure 3.12. The heat fluxes recorded during the control calibrations were not used in the calculations.

Table 3.2: Average and standard deviations of heat fluxes for different heated areas

Target heat flux (from callibration)	Measured Heat fluxes points within defined area (kW/m^2)									
	A		B		C		D		E	
	Average	SD	Average	SD	Average	SD	Average	SD	Average	SD
50	52.98	0.73	47.14	2.41	37.04	3.77	26.15	4.58	17.36	3.88
100	108.12	6.63	91.59	8.25	63.94	12.51	35.91	11.69	18.37	6.94
150	151.37	11.21	130.41	16.39	82.86	23.98	37.05	15.65	15.70	7.21
200	189.71	18.66	172.91	23.44	103.83	37.44	37.39	19.12	12.86	6.51
250	210.13	19.84	211.60	23.91	128.44	53.31	36.53	23.00	10.48	5.31

As would be expected, the heat fluxes measured in the outer areas which are further out from the radiant panel array – and therefore have a smaller radiation view factor with respect to the radiant panel array – are lower than those in the central areas. The difference increases with increasing target heat flux, since the close proximity of the radiant panels to the plane of measurement further reduces the view factor to the outer calibration points. The close proximity also increases the influence of the non-uniformity of source irradiance due to the fact that the radiant panel array is made up of four distinct radiant panels with a small gap between them (which is colder).

For this mapping, when the panels were set to a target peak incident heat flux of 50 kW/m^2 the panels were 225 mm away from the plane of heat flux measurement. By comparison, when the target peak incident heat flux was 250 kW/m^2 the plane of measurement of the heat flux gauge was only 39 mm away from the radiant panel array. It can be seen from Table 3.2 that the uniformity of heating reduces with increasing heat flux. The heat flux distribution, at high heat fluxes is characterised by a severe thermal exposure central to the panels and comparatively very low thermal exposures to the edges of the measurement grid. For the mapping carried out at 250kW/m^2 there is a 95% reduction in heat flux from the central area, A, to the outer edge area of the measurement grid, E, a difference of almost 200kW/m^2.

Beyond a certain panel location these low outer heat fluxes also reduce as the radiant panels get closer to the plane of measurement.

Whilst the above variation is important to be aware of, it is not strictly problematic, since it is highly repeatable once characterised. This is one of the great advantages of the H-TRIS testing method (which it has in common with other fire science testing methods based on incident radiation heat flux, such as the cone calorimeter (British Standards Institution, 2015)and the FPA (ASTM, 2013).

The last column of Table 3.2 shows a decrease in average heat flux in area E with increasing target peak heat flux. This issue could be resolved in part by increasing the size of the radiant panel array to be at least as large as the sample surface being heated. This would mean that the view factor reduction with close proximity would be reduced. This is an area for future improvement of the experimental setup and is a clear next step now that the workings and limitations of the current four panel array are better understood. The primary challenges associated with increasing the size of the radiant array are associated with the size of the lab required, providing the requisite supply of propane, and various health and safety concerns with larger, more powerful arrays.

Contour maps of the measured incident heat flux distributions are shown in Figure 3.13 to Figure 3.17. The orientation of these figures is as if facing the radiant panels, with the right hand side of the heat flux maps corresponding to the right hand side of the panels if facing them from the front. The measurement points are as shown in Figure 3.12.

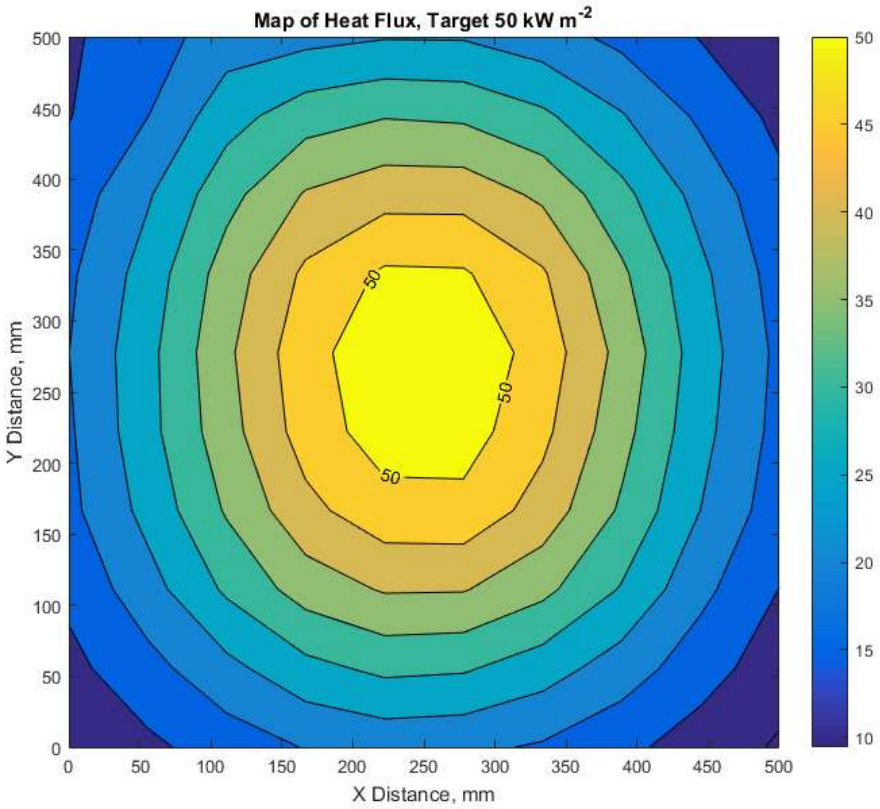

Figure 3.13: Heat flux map for target heat flux of 50kW/m^2

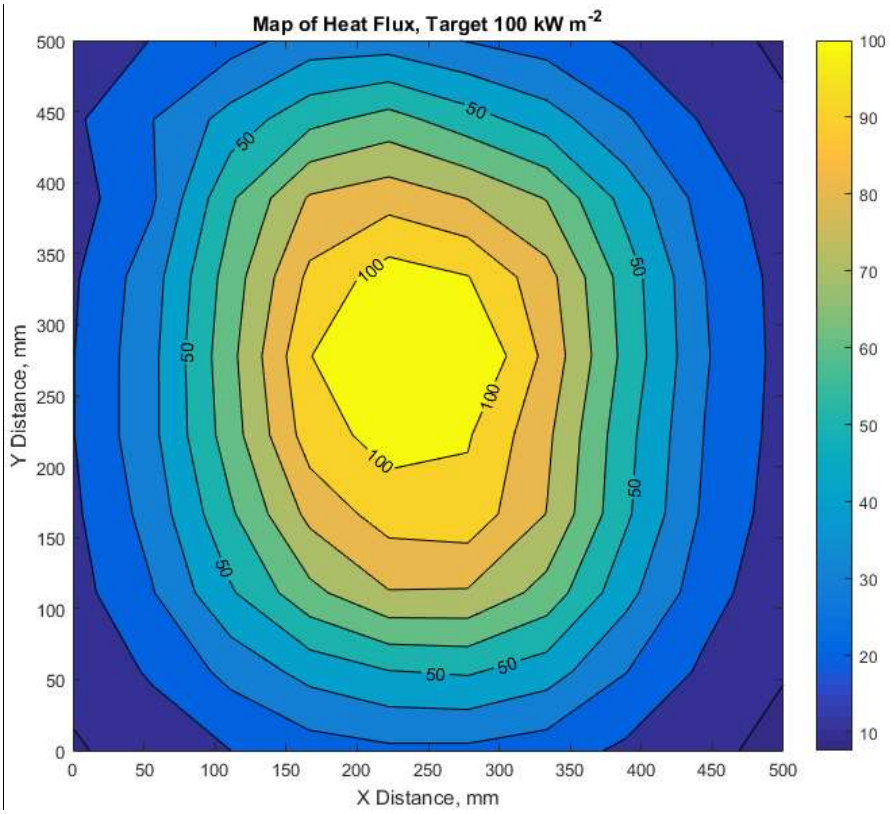

Figure 3.14: Heat flux map for target heat flux of 100kW/m^2

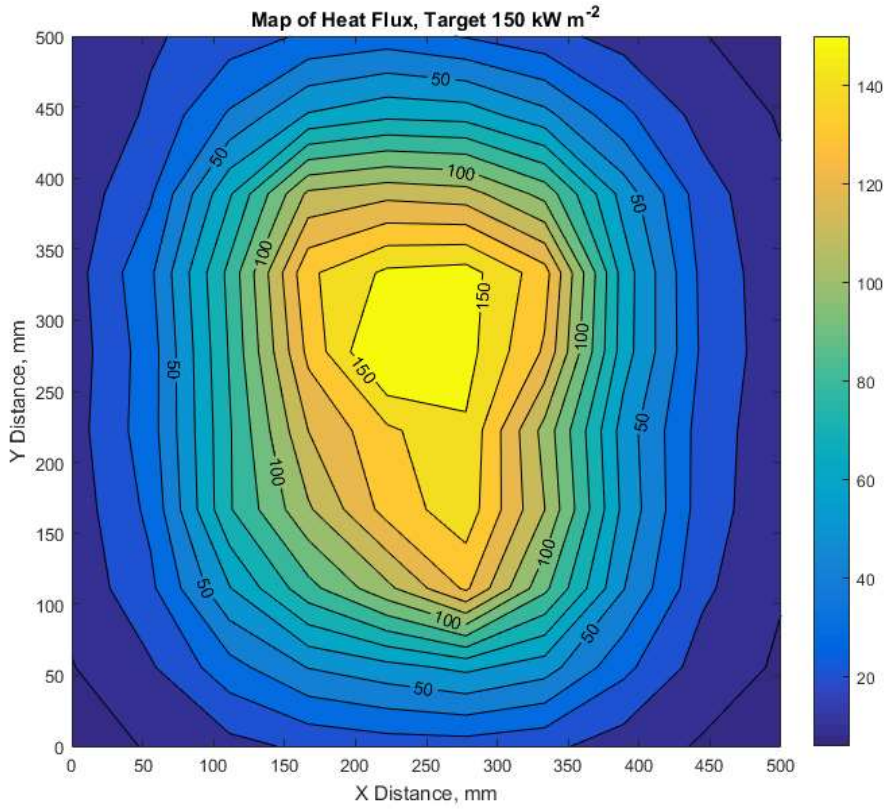

Figure 3.15: Heat flux map for target heat flux of 150kW/m^2

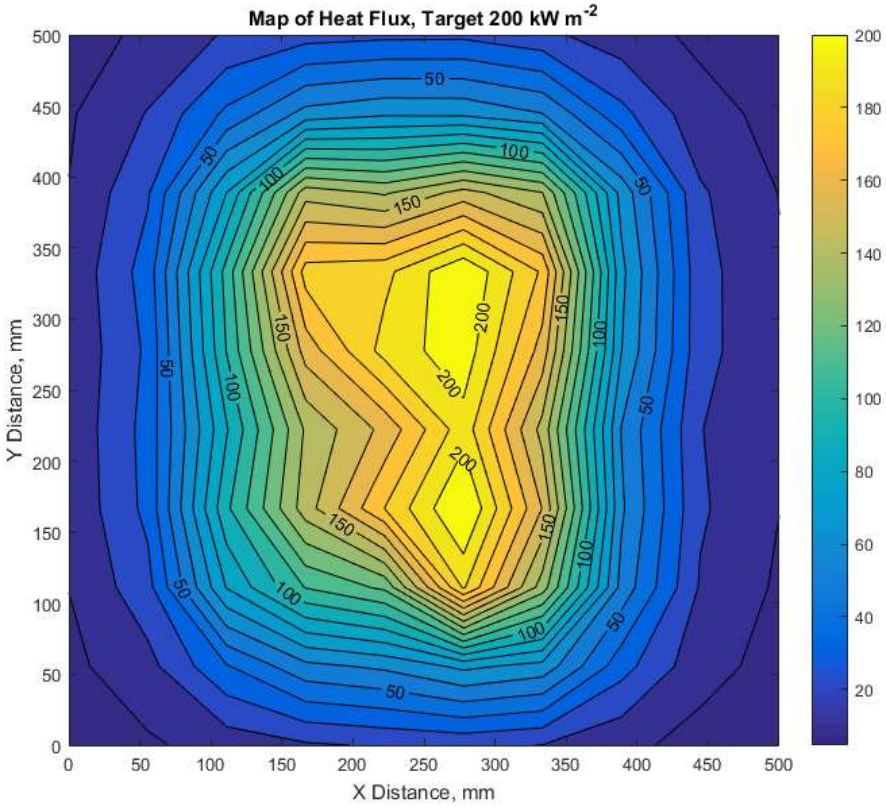

Figure 3.16: Heat flux map for target heat flux of 200kW/m²

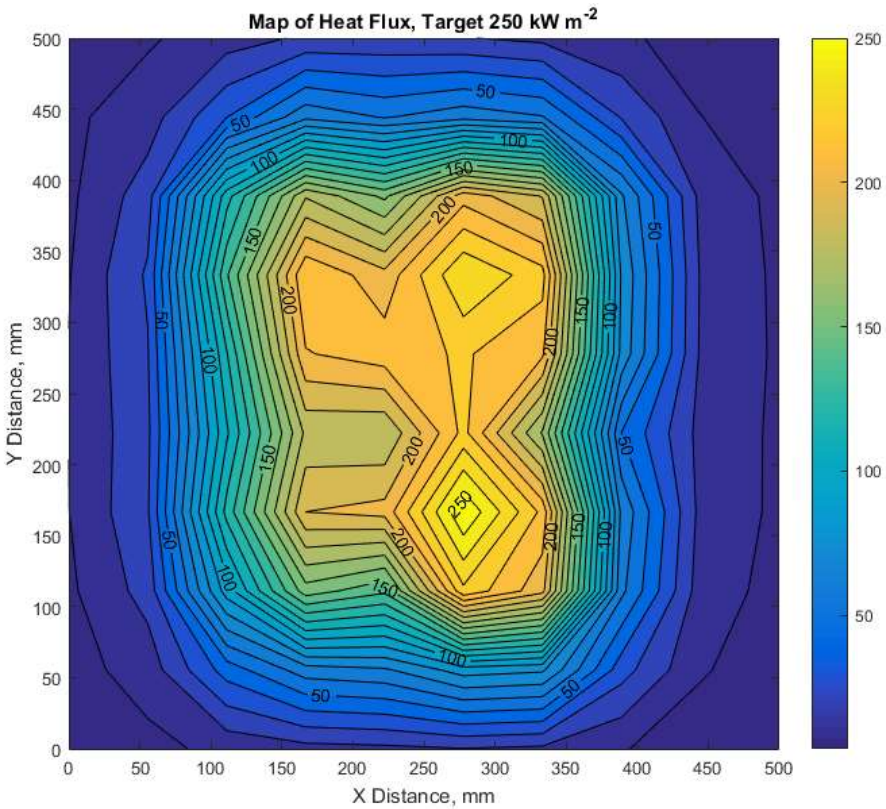

Figure 3.17: Heat flux map for target heat flux of 250kW/m²

The heat flux contour maps provide an additional visual representation of the uniformity of heat flux across the mapping area. The shape of the radiant panel array is clear in the mapping carried out for a target heat flux of 250 kW/m^2, see Figure 3.17 and Figure 3.12 for panel location. As already mentioned, the uniformity of incident heat flux over this area would be improved at close proximity by increasing the size of the radiant panel array. It is also of interest that the radiant panels themselves are not completely uniform with the right hand panels producing a higher heat flux. It may be possible to improve upon this lack of uniformity by improving the design of the radiant panels or regulating the flow to each panel more accurately. The manifold maintains a constant pressure resulting in a flow of propane and air to the panels. Individual mass flow controllers could ensure that the panels all receive the same propane and air mix even if the flow resistance of the panels is slightly different. This approach is untested and it may be that the panels are not produced with enough accuracy to all burn in the same way. This is an area for future work, however simply increasing the size of the radiant panel array (to allow for higher and more uniform heat fluxes at greater stand-off distances) is clearly the best approach for the future.

3.8 Sample loading

3.8.1 Introduction

As discussed in Chapter 2, the loading conditions experienced by a concrete sample during severe thermal exposure are widely considered to influence the propensity for high temperature explosive concrete spalling (Jansson and Boström, 2013; Rahim *et al.*, 2013). As the project presented herein aimed to investigate the performance of concrete with a focus on concrete used in tunnelling applications, an approach to loading of samples was required.

A uniaxial loading frame was developed and used during the experiments carried out in Phase 3 of the experimental work presented in this thesis (Chapter 6). The basis for this approach and the apparatus developed are described in the following sections. To provide context to the approach taken, some of the basic concepts of tunnel design are covered first in Section 3.8.2. Following this Section 3.8.3 describes the adopted approach.

3.8.2 Understanding the tunnel design process

In order to gain an understanding of the way in which tunnels are designed and the stresses which could be expected in a tunnel lining, the author spent six weeks working alongside engineers in the Arup London offices from October - December, 2014. The time spent working with the tunnels team was particularly valuable and special thanks must be given to Michele Mangione and Hyuk-Il Jung for sharing their knowledge and enthusiasm, and devoting so much time to explaining some of the basics of tunnel design.

This section aims to summarise the key outcomes of discussions that took place during this time and the basis for the approach to loading which was adopted in the experimental work described in this thesis. The focus was on cylindrical precast concrete tunnels installed using a tunnel boring machine, TBM. Not having any knowledge of structural design of tunnels prior to the time spent at Arup it had been thought it would be possible to define a representative load condition that would apply to most tunnels. There are a number of design considerations which result in this not being possible, mostly relating to the construction method. The key considerations are covered in the sections below which aim to provide high-level summaries of design considerations. This is not an exhaustive list of tunnel design considerations and the author does not profess to be a tunnel engineer. For further information on

any of the areas discussed the textbook “Mechanized Tunnelling in Urbanised areas” (Guglielmetti et al., 2007) is recommended. Some diagrams from this textbook have been reproduced in the sections below to demonstrate key concepts.

Cylindrical tunnel linings are formed from curved segments; these segments are installed in rings by the TBM as the tunnel is bored. The curvature of the segments depends upon the diameter of the tunnel. This diameter generally ranges from single line subway tunnels to large road tunnels with diameters ranging from around 6 m to 17 m respectively. The thickness of the tunnel lining segments could be expected to be 250 mm or thicker depending on the diameter and ground conditions.

The most obvious loading on tunnel segments is that which comes from the ground and water that the tunnel passes through. Geotechnical engineering involves dealing with large uncertainty as surveys are usually limited and can miss localised ground conditions. As a result, tunnel design involves safety factors and conservatism in design. Figure 3.18 reproduced from the paper by Vu et al. (Ngan Vu, Broere and Bosch, 2017) shows a simplification of the stresses on a cylindrical tunnel from the ground where σ_v is the vertical stress and σ_h is horizontal stress. Depending on the ground conditions, the pressure on the outside of the tunnel will vary along its length. This pressure will also be non-uniform around the circumference of the tunnel due to:

- depth underground (being deeper at the tunnel base than at the crown);
- the influence of the water table; and
- changes in soil or rock conditions.

As the pressure is non-uniform the tunnel lining experiences both a compressive hoop stress and some bending moment.

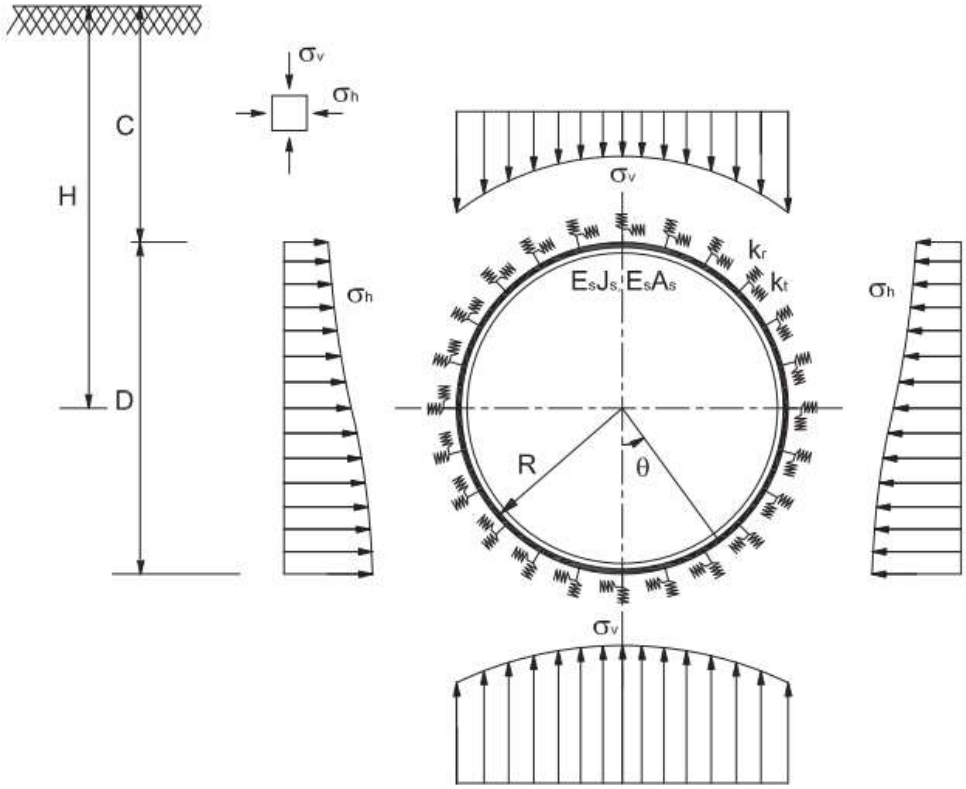

Figure 3.18:Stresses on a concrete tunnel as considered in a proposed model reproduced here from paper (Ngan Vu, Broere and Bosch, 2017).

In addition to the stresses described, there is potential for there to be some longitudinal stress down the length of the tunnel. This is more likely to occur in the case of a sloping tunnel. Due to the construction methodology and the design requirements, this longitudinal stress was considered likely to be low in most tunnels. Construction considerations influencing tunnel design and final in service stress state are described in Sections 3.8.2.1 to 3.8.2.3.

3.8.2.1 Segment design

The tunnel construction process involves making a bespoke TBM that both bores the tunnel and installs segments of a certain size as the tunnel boring progresses. Typically, these tunnel segments will all be designed to be suitable for the most severe ground conditions. Changing segment design for areas of different ground is not usually viable due to the complexity and cost; in addition, ground conditions may not be the driver of segment design as covered in Section 3.8.2.2 and Section 3.8.2.3.

Due to the same segment specification being used over extended lengths of tunnel, a short section of a long tunnel could result in over engineering of the rest of the tunnel and low stresses in tunnel segments. Figure 3.19, reproduced from the textbook "Mechanized Tunnelling in Urbanised areas", shows the different layers of rock, gravel and clay that the EOLE tunnel in France passes through. For a tunnel like this, it is likely that there will be worst-case ground conditions and the segment design will remain constant throughout.

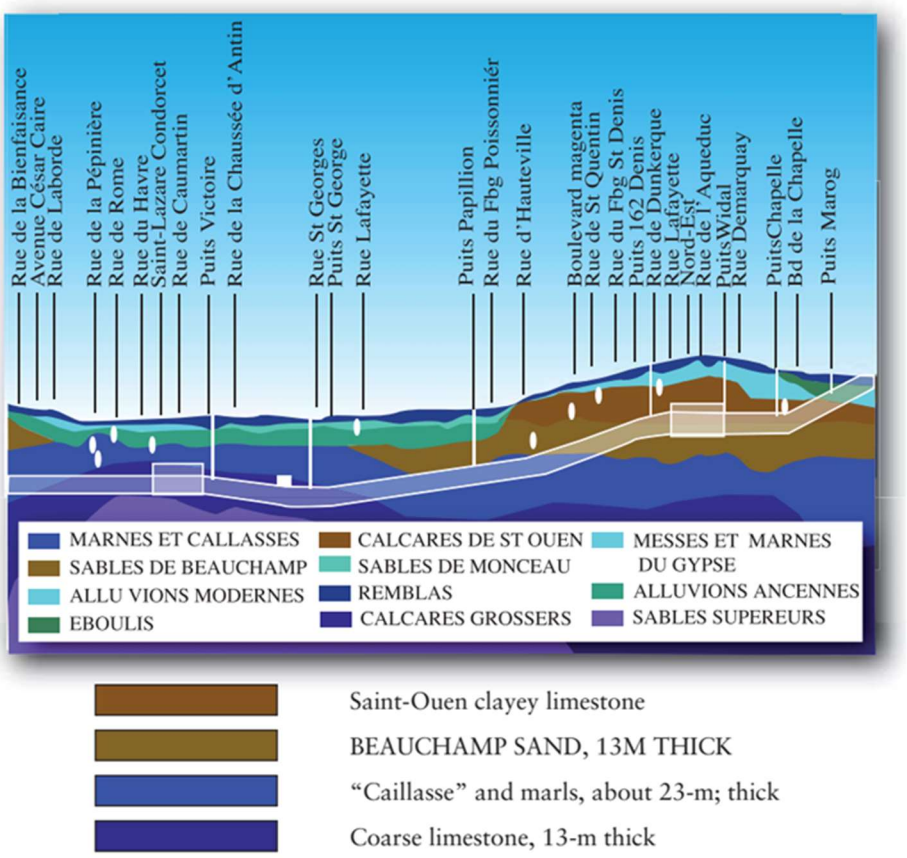

Figure 3.19: Longitudinal cross section of EOLE tunnel, France. (Guglielmetti *et al.*, 2007)

3.8.2.2 TBM thrust forces

When drilling a tunnel the application of pressure to the cutterhead of the TBM, and ultimately the progression of the TBM, involves the boring machine pushing off from the segments that are in place. Once sufficient progress is made, further segments are installed and the process repeats. Thrust jacks located around the perimeter of the tunnel are used to apply this force. These can be seen in Figure 3.20, which provides a simplified overview of the front of a tunnel being bored by TBM.

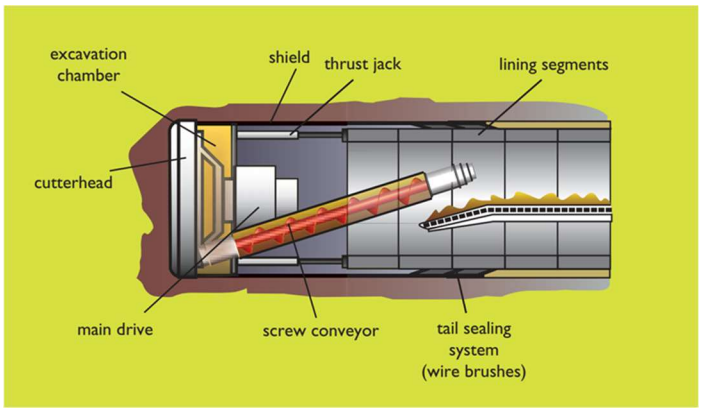

Figure 3.20: Overview of tunnel boring process (Figure reproduced from Guglielmetti et al., 2007)

The tunnel segments must be designed to resist the longitudinal compressive load from the TBM thrust jacks during construction. The force required to progress the TBM and the resultant, temporary, longitudinal loading on the precast segments could be the critical load case and drive segment design.

During the progression of the TBM the EPDM gaskets which are used as seals between rings are compressed and the concrete of the segment rings of will contact. After the thrusting jacks are released and the applied longitudinal stress is removed, the gap between rings can then open again. Figure 3.21 shows the behaviour of gaskets during these stages. The longitudinal loading is at its greatest when the TBM thrust jacks are active. If the segments have been enhanced to resist the thrust jack loading they may be “over engineered” for the final use as tunnel structure.

Figure 3.21: EPDM gaskets during boring process (Figure reproduced from Guglielmetti et al., 2007)

3.8.2.3 Casting, curing, storage and transport

In addition to the design considerations mentioned above, the pre-construction requirements can further influence the design of the tunnel segments. Prior to the boring of a tunnel thousands of segments must be cast, cured, and stored.

It must be possible to remove these segments from their moulds, move them around, and store them stacked, without damage or cracking occurring. The suitability of the segments is assessed and designs may need to be altered to ensure that the likelihood of defective segments being produced is reduced. Figure 3.22 shows segments for the Crossrail tunnel in London being stored prior to installation (Crossrail Ltd, 2020)

Figure 3.22: Crossrail tunnel segments (Crossrail Ltd, 2020)

3.8.3 Proposed sample configuration and loading for experiments

The following sections provide discussion around the basis for the design of the experimental setup and loading frame. The decisions made were informed by discussions with Arup tunnel engineers. Please refer to Section 3.8.2 for further information on factors influencing tunnel design.

3.8.3.1 Sample Curvature

For a large diameter tunnel the curvature of each segment is low. For a 12 m diameter tunnel, for example, the dimensions of a 500 mm high section of a tunnel lining of this diameter can be assessed using basic trigonometry. Figure 3.23 shows the naming convention for key dimensions assessed; note this diagram is not to scale. Table 3.3 shows the calculated dimensions.

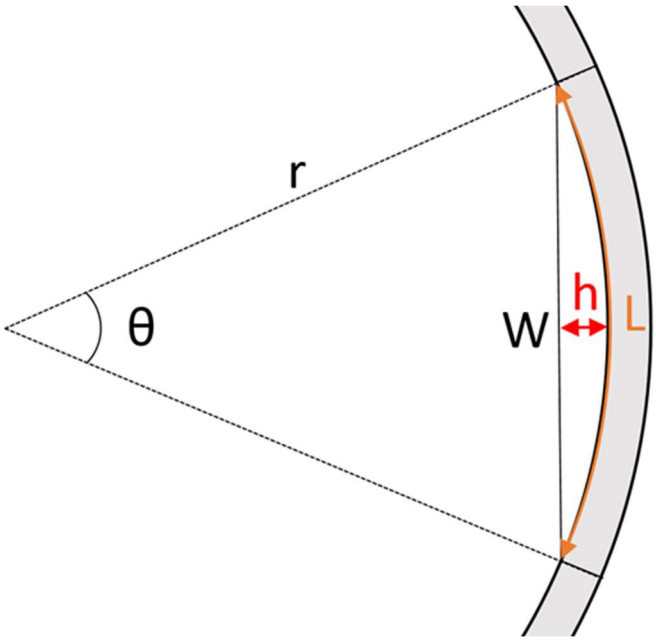

Figure 3.23: Diagram showing naming convention for curvature assessment

Table 3.3: Dimensions of tunnel segment

Dimension	Symbol used	Value	Units
Length of arc	L	0.5	m
Radius	r	6	m
Angle subtended by arc	θ	4.77465	degrees
Height of arc	h	0.00521	m
Width of arc	W	0.49986	m

As shown in Table 3.3, a 500 mm section of tunnel lining from a 12 m diameter tunnel would have an arc height of 5.2 mm.

A 500 mm sample was considered a manageable size for experimental work. For a sample of this length it was considered that approximating as flat, while not strictly correct, provides a reasonable approximation of shape. In addition, attempting to create multiple samples, by hand, to the precision required to replicate a 5.2 mm arc height would be unrealistic with handmade timber formwork at The University of Edinburgh. The approach of disregarding curvature also means that samples are not specific to a particular diameter of tunnel.

3.8.3.2 Loading

Aside from the unknowns associated with geotechnical surveys, and the challenges characterising ground conditions, there are practical constraints placed on tunnel design by the construction method and processes used. Some of these were discussed in briefly in Section 3.8.2 in order to convey why it is not possible to determine a representative load condition for a typical tunnel.

It would in fact not be possible to define a loading condition representative of the full length of a single tunnel, let alone multiple tunnels. Around one ring of segments the compressive hoop stress and bending moment vary depending on the ground conditions and whether the tunnel is being forced inwards or outwards. Figure 3.24 shows an example of hoop stress and bending moment distribution around a tunnel lining.

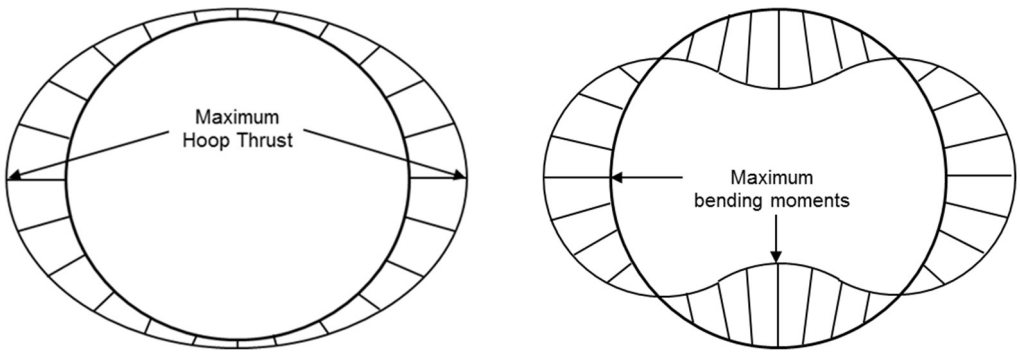

Figure 3.24: Hoop thrust and bending moment around a tunnel (tunnel being squashed vertically)

Bending moment has the effect of either increasing or decreasing the compressive stress at the inner surface of the tunnel lining. As covered previously compressive stress is thought to be critical for spalling. Due to the challenges with defining a

representative stress state it was decided to carry out the planned spalling experiments at a range of compressive stresses. It was thought that this would give an insight into the importance of load and inform decisions for future work. It is also important that different areas of a tunnel will be under different loading so an appreciation of the behaviour of concrete under a range of loads is valuable.

Following discussions with tunnel engineers at Arup, it was agreed that applying a uniaxial compressive stress during heating would provide a credible load case. This is based on the expectation of there typically being low in service longitudinal stresses as a result of the tunnel construction process and presence of gaskets. This has been discussed in Section 3.8.2.2.

Carrying out experiments on concrete at a range of load levels up to 30% of the compressive strength of the concrete was considered a reasonable approach following discussions with Arup tunnel engineers.

3.8.3.3 Restraint

Based on discussions with Arup tunnel engineers it was hypothesised that, in the event of a fire occurring within a tunnel, restrained thermal expansion of the inner surface of the precast lining will result in increased compressive hoop stress at the inner surface of the tunnel lining.

The potential increase in longitudinal stress due to heating was thought not to be as significant due to the expansion that could occur with compression of the gaskets as in the installation process described in Section 3.8.2.2.

In the event of a fire occurring, the resultant stress state in the tunnel lining depends upon:

- the severity of the thermal exposure;
- the ground conditions and the resistance provided to expansion of the tunnel (This could be very high in the event of an area passing through rock, for example).
- the restraint provided by the cool concrete at the ground facing side of the segment

Determining a representative stress state for a tunnel at elevated temperatures is not possible for the same reasons that it is not possible to determine a representative ambient temperature stress state.

As the restraint to thermal expansion is unknown, it was decided that carrying out experiments with a constant, controlled, externally applied load would be a rational approach, rather than attempting to replicate a specific tunnel. Using this approach to load control and a range of compressive loads allows a more general understanding of potential spalling behaviours to be built up.

3.8.4 Loading frame design

Based on the tunnel design information detailed in Sections 3.8.2 and 3.8.3. It was decided to develop a uniaxial loading frame, for flat samples, in which applied load can be maintained constant throughout experiments.

A number of design constraints influenced the loading frame design. An alternative, more structurally efficient loading frame construction may have been possible if some of these limitations could have been removed. The primary design considerations for the loading frame are given in the following sections.

3.8.4.1 Fabrication

Due to budget restrictions, the loading frame had to be designed so that it could be fabricated in-house at The University of Edinburgh. In order for in house fabrication to be viable, welded, standard steel sections and components were used where possible.

3.8.4.2 Location and assembly

The loading frame had to be designed to apply a uniaxial load to samples at the same time as they are being heated using H-TRIS Mark 2. Since H-TRIS Mark 2 is not mobile, this meant that the loading frame needed to be able to fit within the space underneath the H-TRIS Mark 2 extraction hood. Furthermore, since there is no crane within The Rushbrook Fire Laboratory at the University of Edinburgh (where H-TRIS Mark 2 is located), the loading frame also had to be modular and the design had to allow for assembly (and disassembly) without assistance from an overhead crane. This restricted the permissible size and mass of the various frame components.

3.8.4.3 Loading control

Heating of a concrete sample causes (differential) thermal expansion. It was decided that the overall loading on any sample should be maintained at a desired level throughout an experiment (i.e. sustained loading in a load-control mode) rather than having an unknown average compressive stress within the sample as a result of the thermal expansion. The loading system therefore had to be designed to enable the externally applied load to be held constant, adjusting in real time for any drop or increase in pressure in the hydraulic system due to thermal expansion or load-induced contraction of the sample.

3.8.4.4 Heat from H-TRIS Mark 2

The loading frame, made from structural steelwork and high-tension rods, had to be protected from the severe thermal exposures that the samples were exposed to during testing, so that it was not damaged (or deformed) by the repeated heating and cooling that would occur when running multiple experiments. Any hydraulic equipment also had to be kept sufficiently cool during testing under severe thermal exposures.

3.8.5 Loading frame details and specification

Working with the design constraints mentioned above a loading frame shown in Figure 3.25 was designed and constructed. The first assembly of the loading frame is shown in Figure 3.26, this was a trial assembly using a crane to make sure the fabrication was correct and to practice the assembly order within the more constrained Rushbrook Fire Laboratories. Figure 3.27 shows the loading frame painted and in situ within the Rushbrook Fire Laboratory. The separate aspects of the design are discussed in the sections below.

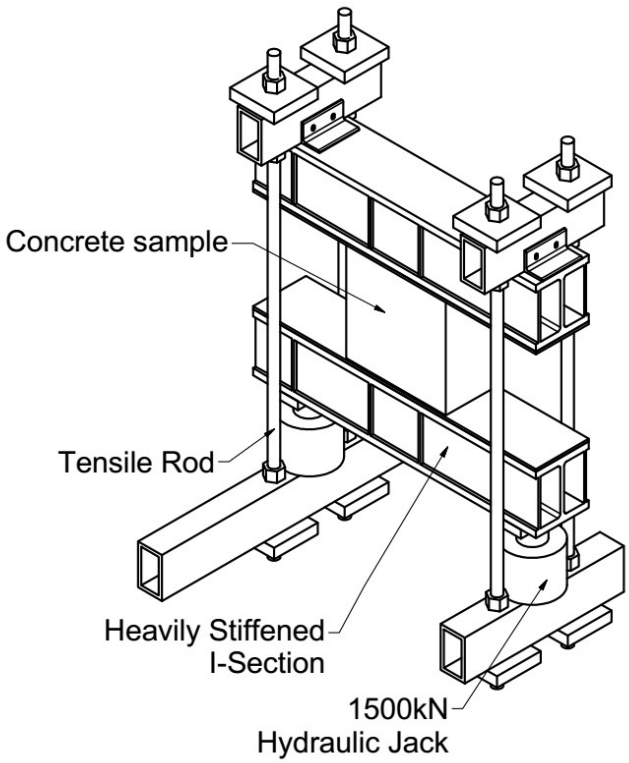

Figure 3.25: Isometric view of loading frame

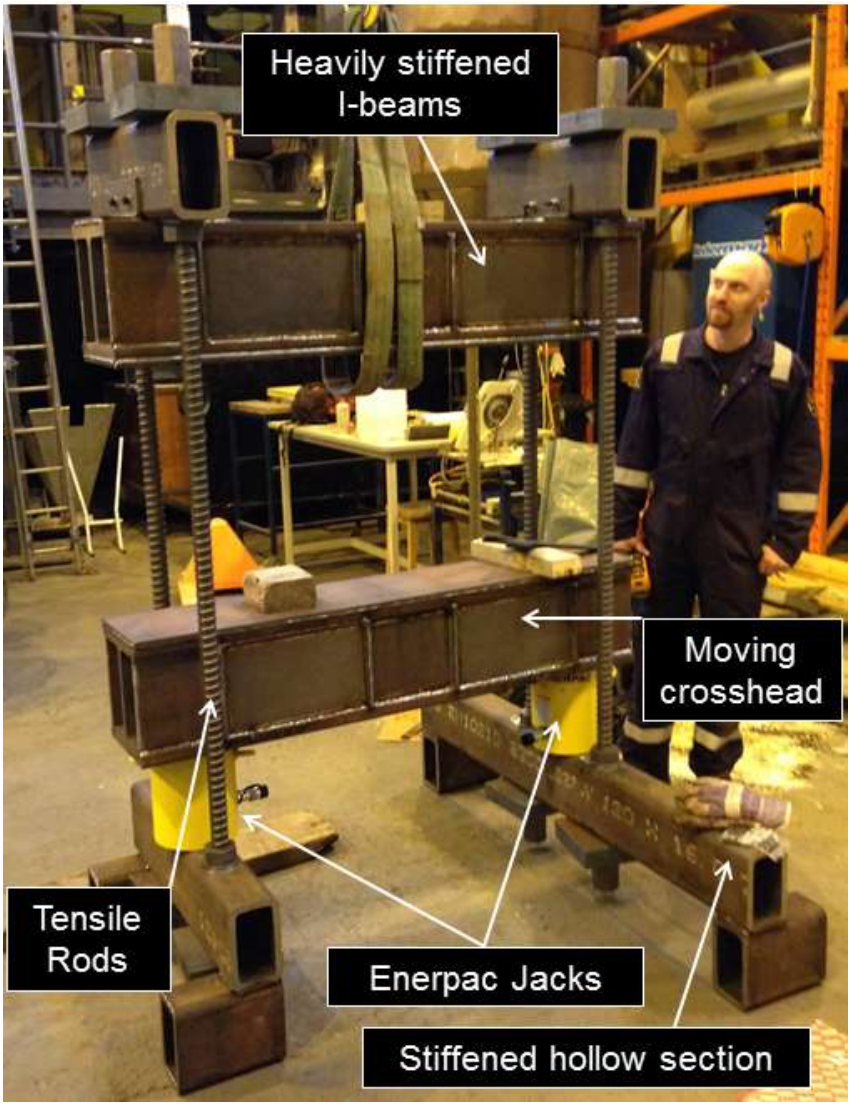

Figure 3.26: Trial assembly of loading frame in structure laboratory

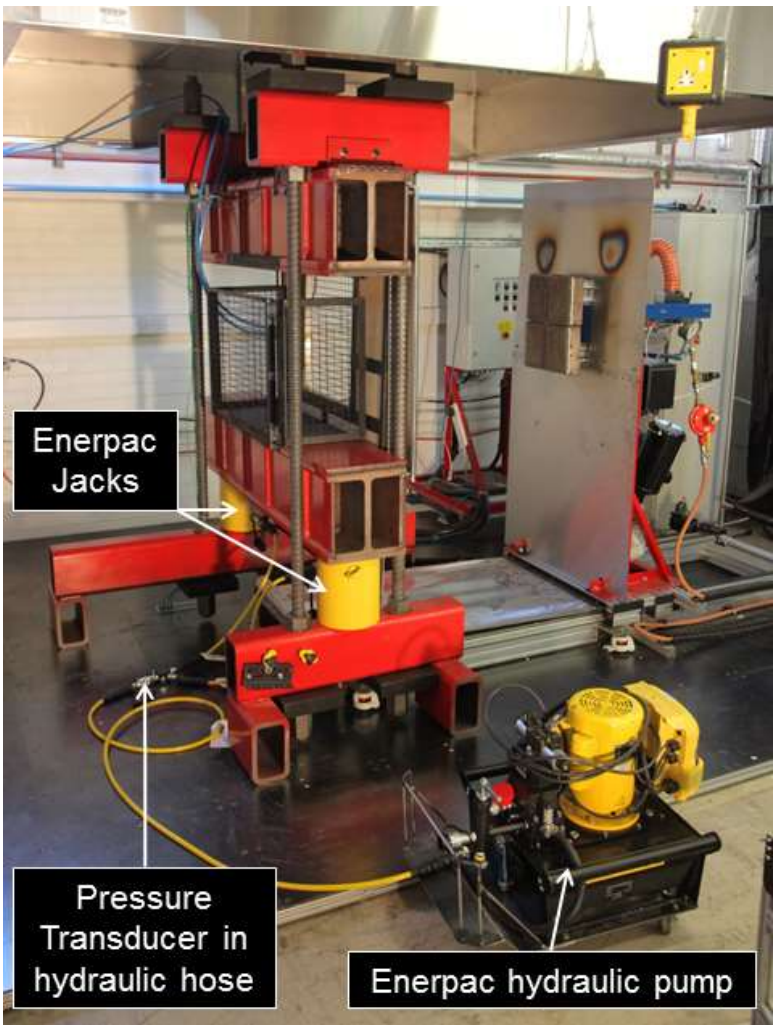

Figure 3.27: Loading frame with hydraulics in position under the extraction hood.

3.8.5.1 Key principles of the loading frame

The uniaxial loading frame is a self-reacting tension frame comprising of two heavily stiffened I-beam sections linked by high-tensile steel rods. The lower I-beam crosshead moves vertically on two 1.5 MN hydraulic Enerpac jacks to apply a compressive load to a sample which is located between the two crossheads. The upper crosshead is held stationary at the correct height for H-TRIS heating. The upper crosshead is supported by four high-tensile rods, which are in compression when no sample is being loaded but act in tension between the two crossheads when load is applied to a sample. Designing for the lower crosshead to move up into place aids the positioning of samples in the frame without a crane. With extensive stiffening of the I-sections it was possible to design the frame to safely allow a uniform compressive stress of 15MPa to be applied to a sample with a cross-section of 250 x 500 mm. This

requires a total compressive load of 1.875 MN. Initially it had been desired to achieve up to 20 MPa of compression in the 250 x 500 mm samples tested in the current project, but it was not practical to build a loading frame that could achieve such high loads whilst also fitting within the laboratory space available. With the frame that was developed there is only 30 mm of clearance between the top of the loading frame and the inside of the H-TRIS Mark 2 extraction hood.

The frame was constructed in as many parts as possible to allow it to be moved into place and assembled by hand. This also resulted in a modular design which can easily be adapted for other uses. Using longer tension rods or changing the I-section cross heads would allow for testing of samples with different geometries. The details of the current assembly are provided in Sections 3.8.4.2 to 3.8.5.6.

3.8.5.2 Primary stiffened steel I-section cross beams

The primary structural elements of the loading frame are the two large cross beams (i.e. crossheads). These are heavily-stiffened S355 254x254x167 UKC sections. The two 1420 mm lengths are each stiffened with eight in number 10 mm thick vertical stiffners, 2 diagonal web stiffeners made from 100x100x10 UKA section, and 10 in number 10 mm thick sideplates welded between the vertical stiffners. To complete the crosshead beams there is an additional 12 mm thick plate welded to the loading surface.

For the upper crosshead 4 tabs were added to allow bolting on to the upper secondary beams. The tabs were slotted so that the bolts are not loaded when there is a sample under compression. Drawings of the upper crosshead are shown, the lower crosshead is the same but without the addition of attachment tabs. Figure 3.28 gives an overview of the upper crosshead, complete with the tabs used to attach to the secondary cross beams of the loading frame.

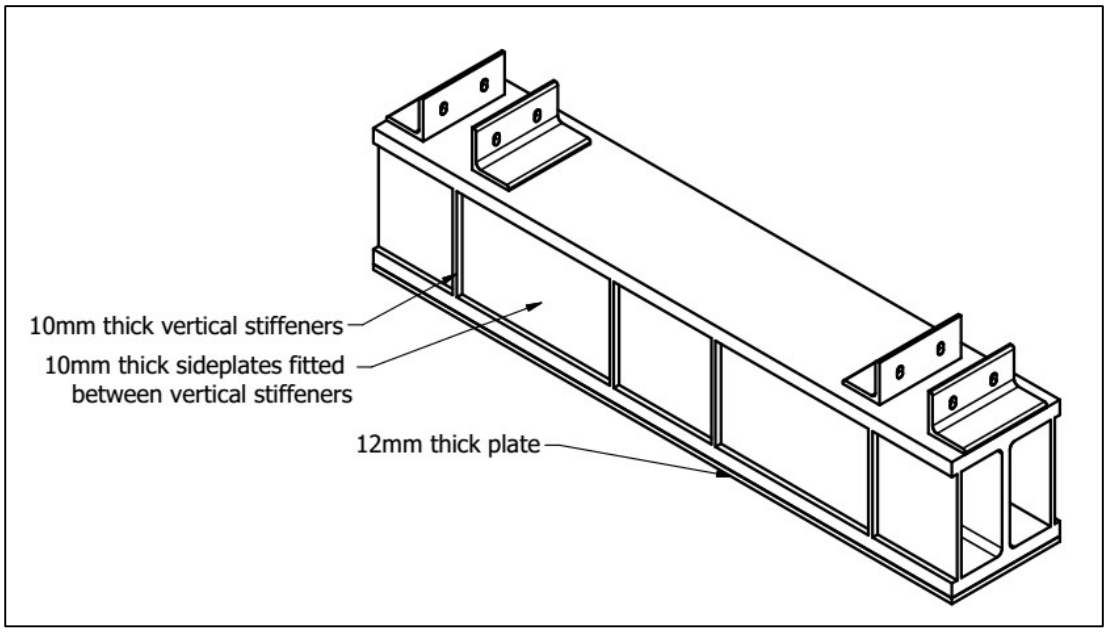

Figure 3.28: Isometric view of loading frame upper crosshead

The location of the 20 stiffeners mentioned previously are shown more clearly in Figure 3.29 and Figure 3.30. The welding of the stiffeners is shown in Figure 3.31. After welding is complete the diagonal stiffeners are sealed into the section between the side plates and the web of the UKC section so are not visible on the completed frame. Figure 3.32 shows the stiffened I-sections just before the diagonal stiffeners were blocked in.

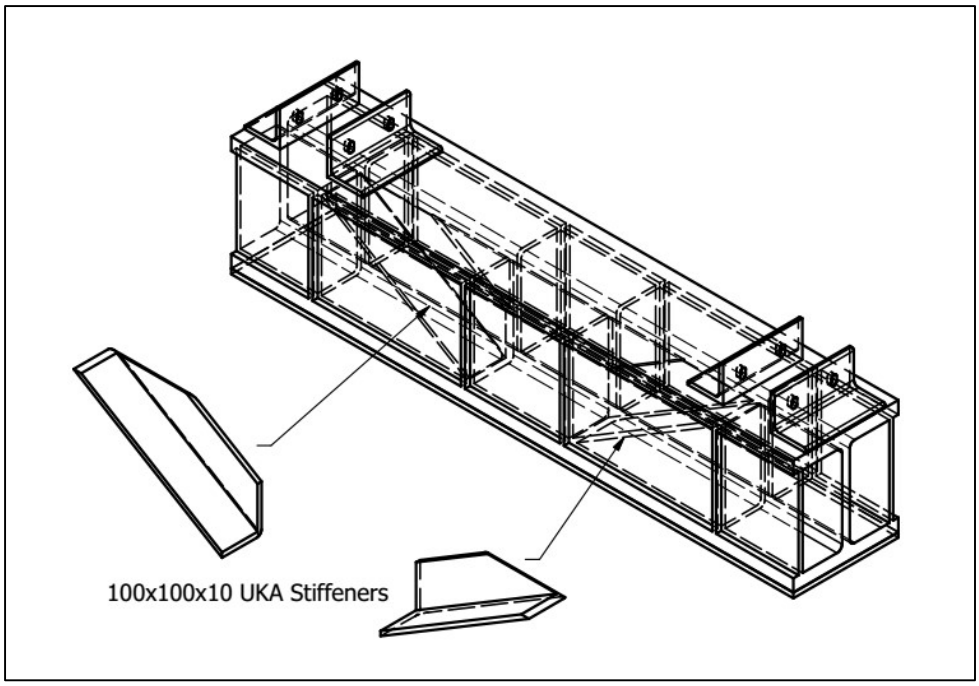

Figure 3.29: Part-exploded isometric view of crosshead showing internal stiffener locations

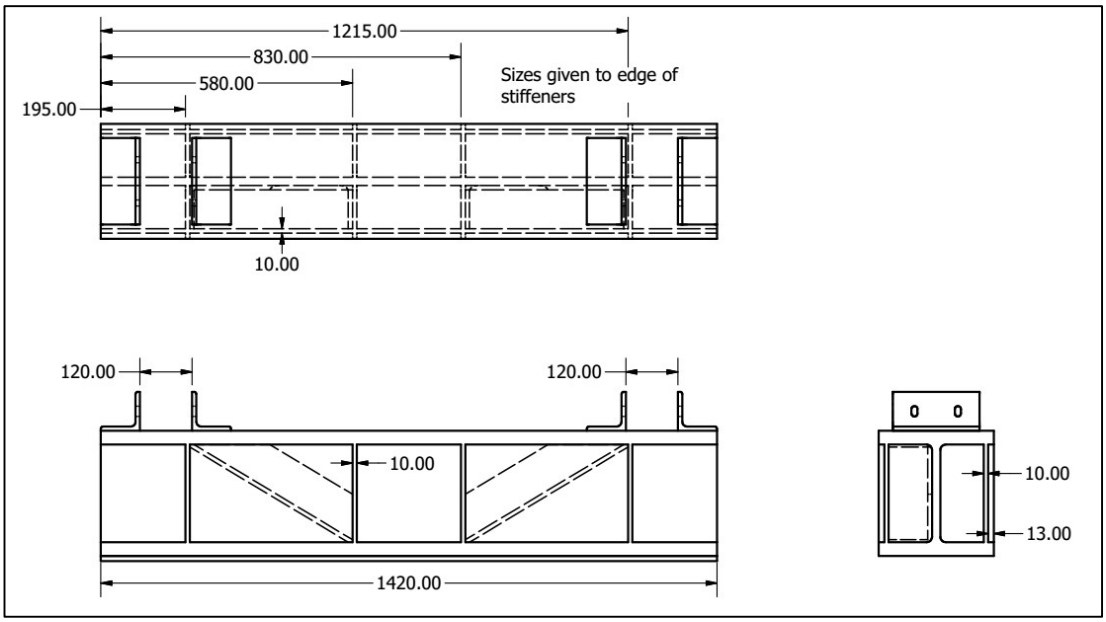

Figure 3.30: Plan and elevation drawings of upper crosshead all sizes in mm

Figure 3.31:Welding of stiffeners to the I-section

Figure 3.32: Stiffened I-sections before closing in the diagonal stiffeners

3.8.5.3 Secondary cross beams

The secondary beams transfer the load to the high tensile rods. They were fabricated from S355 grade, 200 x 120 x 16 mm rectangular hollow section. In order to prevent crushing of the hollow section they were stiffened with a steel tube with internal diameter of 47 mm and external diameter of 70 mm. The two upper rectangular hollow section beams were drilled to allow the upper stiffened I-section crosshead to be bolted in place and their construction is shown in Figure 3.33.

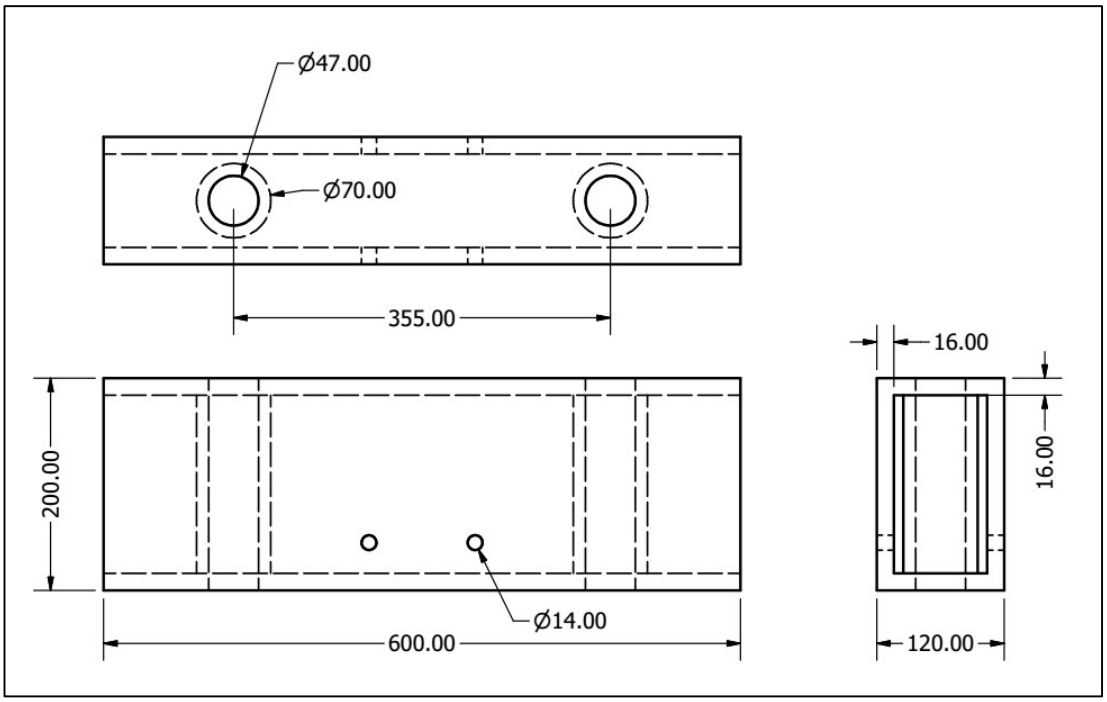

Figure 3.33: Plan and elevations of upper rectangular hollow section beams

The lower rectangular hollow section beams are stiffened in the same way but are longer and were drilled to allow attachment of the hydraulic jacks. The base beam closest to the wall is 1600 mm and the lab side base beam is 800 mm long. The beams sit on feet made from the same rectangular hollow section. This configuration with the longer base beam at the back-wall side of the frame is to provide stability whilst allowing samples to be moved in and out on trolleys from the lab.

3.8.5.4 Tensile Rods

The tensile rods used are high-tensile prestressing steel deformed threadbar, with a nominal diameter of 40mm and a yield strength of 950 MPa. The four bars are 2200 mm long. In order to be able to reduce the build height of the frame, the locknuts were positioned on the inside of the hollow section beams with the washers and nuts on the outside. This enabled a reduction in the loading frame height of 100 mm. This detail is shown in Figure 3.34.

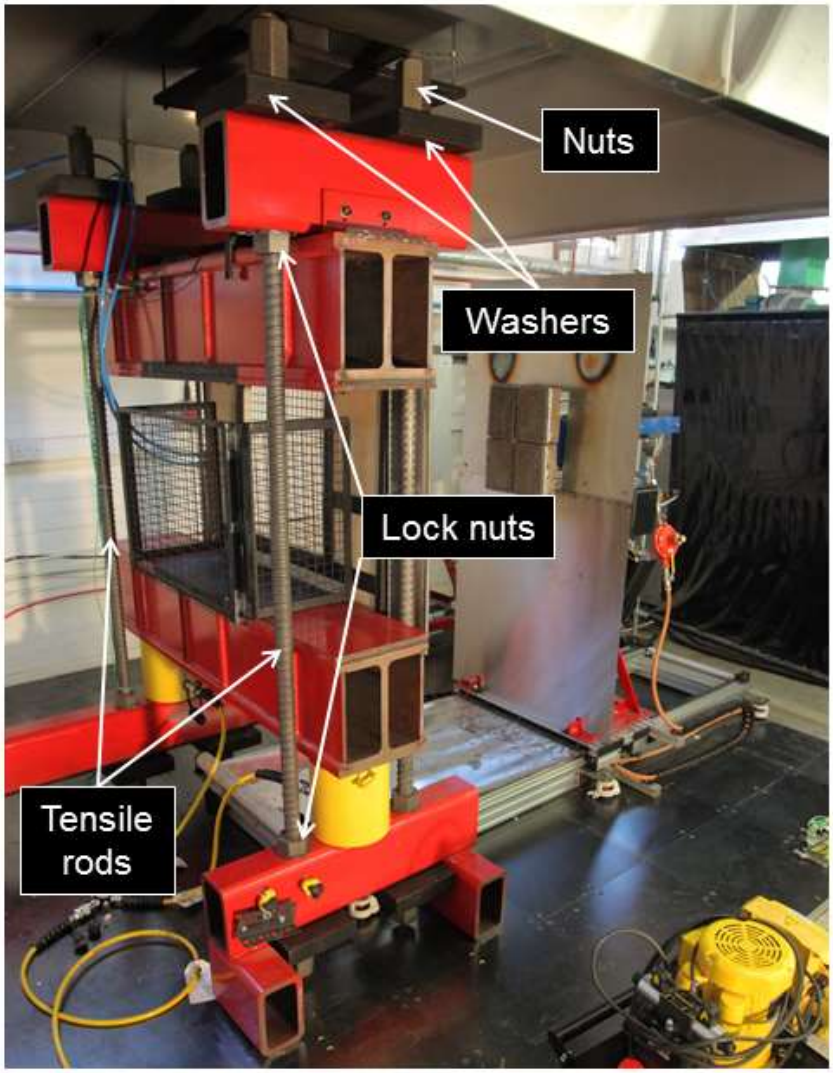

Figure 3.34: Loading frame showing tensile rod configuration

The location of the lock nuts means that, as well as acting as lock nuts, they also hold the upper assembly up when there is no sample in the frame. Since the entire length of the rods are threaded the assembly of the frame was much easier and safer. It was possible to raise the 600kg upper assembly slowly using hydraulic jacks and moving the lock nuts up underneath as the movement progressed. The full-length threads also mean that it is possible to adjust the crosshead spacing and carry out loaded experiments on smaller samples.

3.8.5.5 Hydraulic system

The hydraulic system used consists of two 1.5 MN Enerpac CLSG 1504 jacks connected to an Enerpac Z class E3 pump. The pump has a load-control function which is able to compensate for any drops in the hydraulic system pressure that may

occur. The load control function is not able to adjust for an increase in the load in the system which results in an increase in hydraulic pressure. The thermal expansion of the heated concrete samples has the potential to increase the load in the system in this way. In order to prevent this increase in load from happening a manual pressure relief valve was fitted to the pump.

The manual pressure relief valve can be set to the required pressure whilst attached to another hydraulic system. For the experiments carried out in this project a small hydraulic jack was confined within a section of rectangular hollow section to allow the pressure limit to be set. Once this pressure limit is set the pump can be connected to the loading frame again and the load that can be applied to samples is limited. Also setting the hydraulic pump to maintain load results in the load level remaining constant regardless of whether settlement or thermal expansion occurs and needs to be adjusted for. An Omega PX309-10KG5V in-line pressure transducer was used to set pressure relief valve and to monitor the pressure within the hydraulic system during loaded tests. It was found that the system was able to maintain a target compressive stress to within 0.25 MPa. This equates to ±1.25% of the maximum stress which can be applied.

3.8.5.6 Insulation shielding

The steel loading frame must be protected from the thermal exposure from the H-TRIS apparatus while allowing centrally located samples to be heated. In order to protect the frame an insulation shield with a sample heating window was made from 25 mm thick vermiculite board supported on a steel frame. This insulation shield hooks over the top of the loading frame and allows free movement of the lower crosshead. Stainless steel guards were also made for the tensile rods closest to the radiant panel array. These guards are spaced out from the tensile rods and deflect both convective and radiative heat.

Permanent thermocouples are fitted to the loading frame crosshead and tensile rods and the temperatures at these points are monitored thoughout experiments. If the temperature of the frame begins to rise quickly the test is stopped to prevent permanent damage. The first version of the vermiculite insulation shield bent when subjected to high heat fluxes and opened up a gap exposing the loading frame causing a test to be cut short. This bending of the insulation shield was a result of the edge of the steel insulation support frame being exposed. This problem was resolved

by installing a water cooled rim around the opening in the insulation shield. The latest version of the insulation sheild can be seen in Figure 3.35.

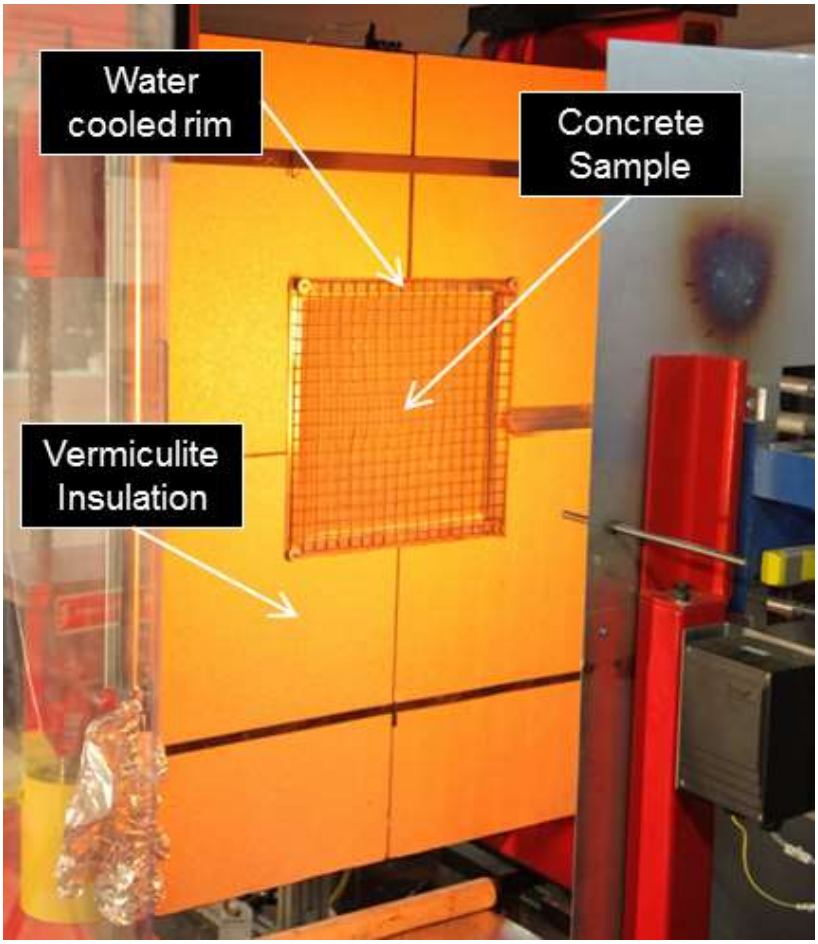

Figure 3.35: Front view of a sample during an experiment showing the current insulation shield

3.8.6 Contact between concrete samples and steel loading frames

Samples to be loaded must be capped to ensure that there is an even contact between the sample and the loading frame. In this project the samples were placed on a 5mm thick cork pad and capped using dental plaster. In most cases this cap was between 1 and 4 mm depending on the interface angle between the concrete sample and the loading frame crosshead. Since the loading frame moves very slowly the dental plaster caps were made inside large Ziplock bags. A plaster filled bag can be slid in to a small gap between the sample and upper crosshead. The gap needed to be small enough that it could be closed before the dental plaster started to cure.

3.9 Future work

Many of the areas for improvement of H-TRIS have been mentioned through the discussion of the apparatus and issues encountered. Key areas for immediate future work are further characterisation of the radiant panels, increasing the size of the radiant panel array and, the development of an improved, more serviceable, radiant panel.

The radiant panels have been assessed using a heat flux gauge in open conditions. However when the radiant panels are used to heat a sample there will be feedback from the sample. It is unknown if this feedback influences the combustion in the radiant panels but it is possible that the feedback alters the combustion and therefore the heat flux emitted by the panels. Characterisation of this potential difference in performance is challenging. The gauges currently used would not be suitable as they can only be heated from one side.

The size of the radiant panel array should be increased if larger samples are to be tested. The work described in Section 3.7.3 showed that the radiant panel array should be at least the same size as the desired heated area on the samples to be used. Increasing the size of the radiant panel array should be quite straightforward now that the limitations and behaviour of the radiant panels are understood and it would increase the uniformity of heating greatly.

The radiant panels themselves could be improved upon. The need for the panels to be serviceable combined with the desire to improve the uniformity of heating is enough to justify design of an improved radiant panel for use with H-TRIS.

4 Phase 1 experimental work – CERIB furnace tests

4.1 Summary

This chapter discusses the testing carried out to establish an appropriate thermal exposure for H-TRIS experiments allowing experiments to be carried out using a thermal exposure comparable to that experienced in furnace tests. This process involved carrying out four furnace tests at CERIB, in Epernon, France, on concrete slabs under two different standard fire curves. These were the ISO 834 and French modified hydrocarbon curves. These tests were carried out primarily in order to gather reliable through-thickness temperature data to allow the absorbed heat flux – time history to be calculated which allows the incident heat flux – time curve to be determined. This incident heat flux – time curve is the required input for H-TRIS testing. During the furnace tests the influence of sample geometry in terms of both sample thickness and plan area were investigated along with the addition of polypropylene fibres and the influence of curing condition/moisture content.

4.2 Introduction

As discussed in Chapter 3, the H-TRIS test method controls the thermal exposure imposed on a test specimen directly by controlling the incident heat flux – time history. This differs from conventional standardised furnace tests that control the heating of a large furnace volume to a furnace gas temperature – time curve. The focus of the work described in this chapter is obtaining the necessary data to allow experiments to be carried out using H-TRIS to an equivalent thermal exposure to that experienced by samples in a furnace test. It is important to note that the H-TRIS test method is able to recreate almost any incident heat flux – time history with some limitation to the maximum incident heat flux achievable and the maximum heat flux increase rate. This flexibility gives great potential for future research and facilitation of performance based design of concrete structures by testing to realistic worst-case thermal exposures for specific applications.

In these early stages of spalling research with this experimental apparatus, it was desirable to benchmark against existing standard temperature time curves. This allows comparison of results with existing literature and maximises the possibility for early application of research findings and use of the developed test method. The development of equivalent incident heat flux – time curves enables the test method, in the immediate future, to be used to screen candidate concrete mixes before the,

currently necessary, expensive furnace tests are carried out for approvals purposes. In effect H-TRIS can act as a screening test for immediate usefulness.

The concept of developing a screening test method for these purposes is now becoming increasingly popular in the spalling research community. The RILEM Technical Committee 256-SPF has a specific task group investigating test methods. There were also a number of papers on this topic at the 2017 International Workshop on Concrete Spalling (Jansson McNamee and Boström, 2017) including an international collaborative paper between four institutions for which the author carried out testing using the H-TRIS apparatus (Jansson McNamee *et al.*, 2017).

This chapter describes the testing that was carried out to allow the through-thickness temperatures to be obtained and the results and observations that could be made from the Prometheus furnace tests.

4.3 Test apparatus

4.3.1 Large Prometheus furnace

The Prometheus test facility at CERIB in Epernon, France comprises primarily of a state of the art standard fire-resistance testing furnace with an advanced active loading system. The facility was first operational in 2008 and was hailed in a NIST report in 2012 as

> *"Probably the best example of a structural testing facility which is currently available for large-scale non-standard structural fire testing*" (Almand, 2012).

The Prometheus furnace is a large, modern, modular, gas fuelled furnace with dimensions of 6 x 4 x 2.7 m. The modular nature of the furnace allows it to be reconfigured to test taller or longer samples. For the tests described in this section, the standard configuration was used with simply supported slabs placed over the open top of the furnace. No loading was applied to any samples. The furnace is controlled using 18 plate thermometers positioned within the furnace. The Prometheus test facility complies with EN17025 (British Standards Institute, 2017). This furnace is primarily used for fire-resistance testing for approvals purposes and, as a modern high quality furnace, is an ideal candidate furnace to use for a benchmark equivalent thermal exposure. The Prometheus furnace is shown in Figure 4.1 and Figure 4.2. This furnace was the primary test apparatus and was used to test 28 samples; eight additional samples were tested in two tests using the small furnace at CERIB.

Figure 4.1: Samples positioned over the Prometheus Furnace at CERIB

Figure 4.2: Elevation view of the Prometheus Furnace

The concrete slab samples being tested were placed horizontally over the furnace with any samples not large enough to span the furnace width being simply supported either on a central beam or within a bespoke sample holder frame. All samples were

tested unloaded, as it was not possible to load samples in the configuration used. For the Prometheus furnace tests, identical samples were tested in the same locations over the furnace in both the ISO 834 and French modified hydrocarbon, HCM, furnace tests. This allowed direct comparison between the two thermal exposures. Figure 4.4 shows the sample layout over the furnace used in both tests, plate thermometer locations, and the side naming convention.

Samples 2.14 m x 1.45 m and above sample sizes were simply supported at each end by 250 mm. Samples smaller than this were simply supported on all four edges by 50 mm within a sample holder frame. The bespoke frame, necessary to allow small samples to be tested over the large furnace, was cast from concrete and protected with insulation board resulting in a 130 mm down stand around the heated face of each small sample. The small samples in the frame prior to testing are shown in Figure 4.3 and the location of this frame is shown in Figure 4.4.

Figure 4.3:Sample holder frame for small samples.

The burner locations on each side wall of the furnace are shown in Figure 4.5, Figure 4.6, and Figure 4.7. Note that there are no burners on the fourth side and the large burners on Side B were only used in the furnace test to the HCM temperature time curve.

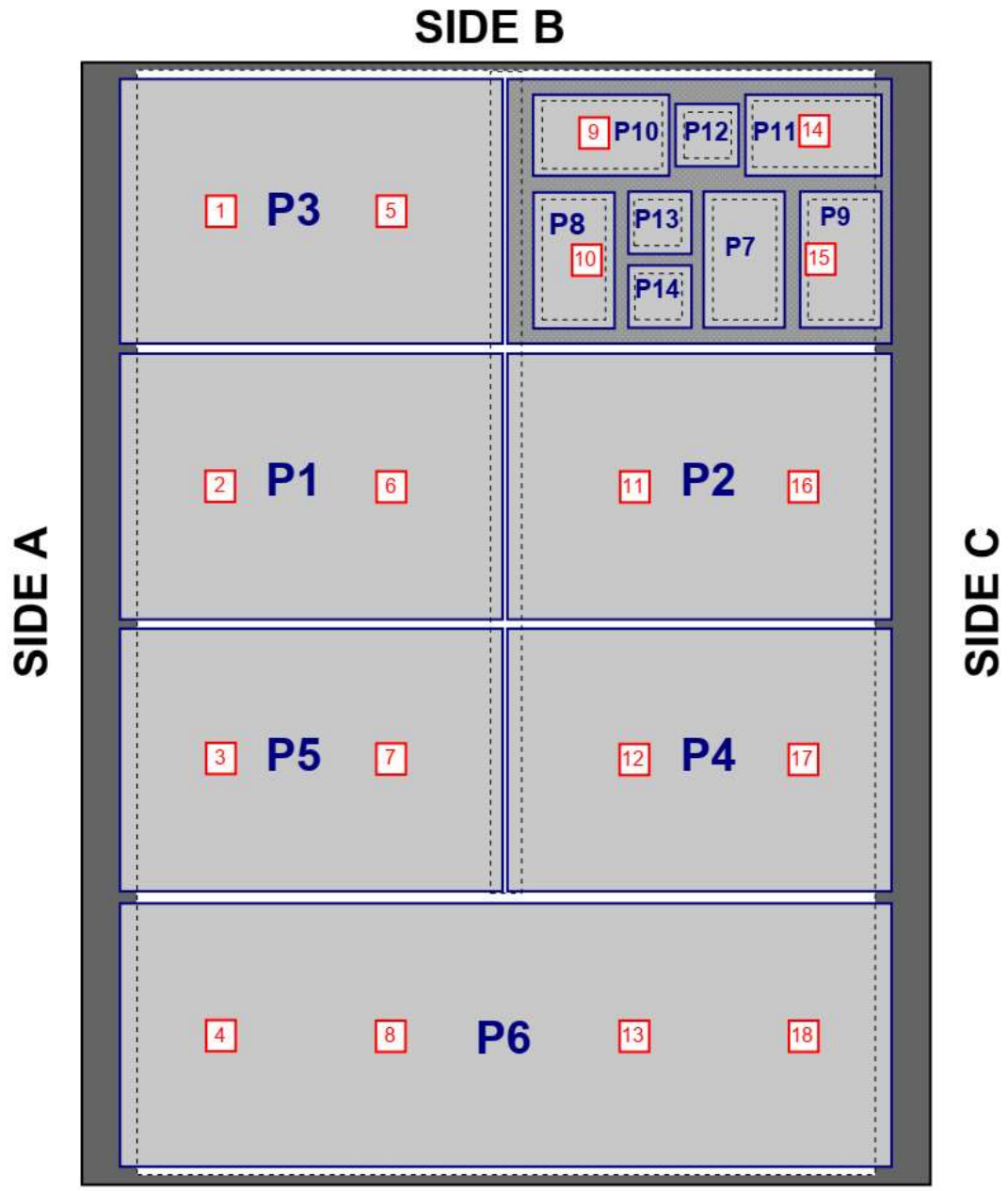

Figure 4.4: Sample locations over Prometheus furnace (from above) for both ISO 834 and HCM experiments. Red boxes indicate plate thermometer locations within furnace (approximately 150 mm below sample face).

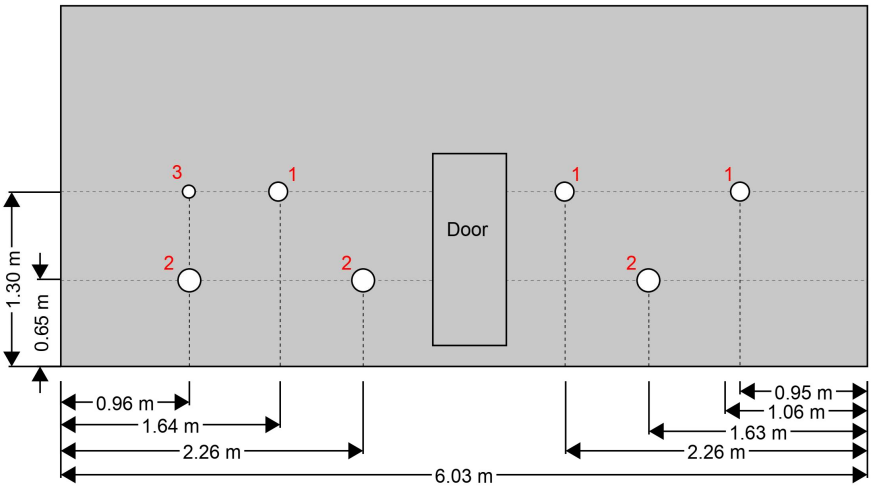

Figure 4.5: Side A of Prometheus furnace from inside showing burners with diameters 1) 140mm 2) 170mm 3) 95mm

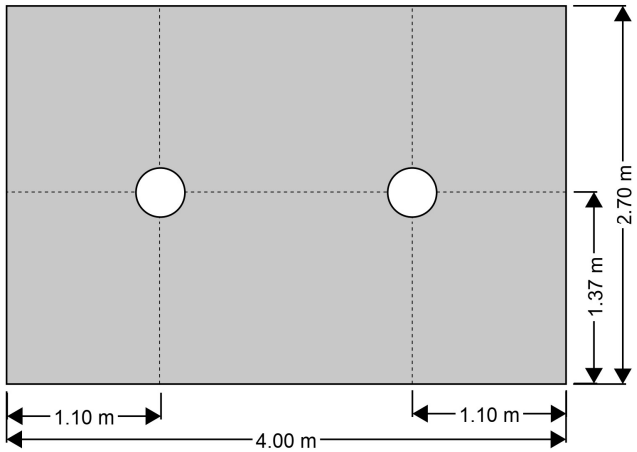

Figure 4.6: Side B of Prometheus furnace - from within showing 350mm diameter burners

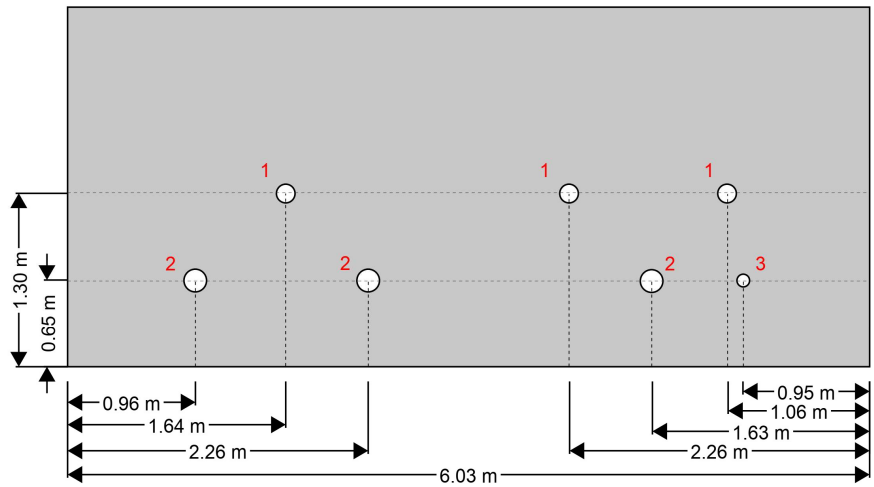

Figure 4.7: Side C of Prometheus furnace from inside showing burners with diameters 1) 140mm 2) 170mm 3) 95mm

4.3.2 Small furnace

The small furnace is only capable of recreating the ISO 834 thermal exposure and is used for what CERIB call “Intermediate scale orientation tests” it was also referred to in correspondence as the “spalling furnace” (email 21/03/2014). The use of this furnace was intend to give a comparison between the two furnaces and the thermal exposures the samples experienced. The small furnace was capable of testing four 750 x 450 mm samples per test and the samples sit on the floor of the furnace during testing. This removes the influence of sample self-weight as would be present in the simply supported Prometheus tests. This simplification of the stress within the sample could be considered beneficial for comparison of results. Figure 4.8 shows the inside of the small furnace prior to testing. The four plate thermometers used to control the furnace are shown above the samples. Temperatures of the plate thermometers were recorded at 5 second intervals.

Figure 4.8: Small furnace prior to testing

4.4 Sample preparation

4.4.1 Instrumentation

The samples were very heavily instrumented using thermocouple trees which were manufactured at The University of Edinburgh and some inconell thermocouples provided by CERIB. Over 700 thermocouples were installed in the samples during testing resulting in over 336 thermocouples per large furnace test. The target location for the thermocouples in the thermocouple trees manufactured at The University of Edinburgh within the samples was at depths of 1, 5, 10, 20 and 50 mm from the heated sample surface with additional thermocouples at a depth of 100 mm in samples with thicknesses greater than 100mm. The thermocouple trees which were made by the author at The University of Edinburgh are shown in Figure 4.9. These are the same design of thermocouple trees that were used in all experimetal work in this thesis and Figure 4.10 shows how these thermocouple trees are installed within the formwork. Figure 4.11 gives and overview of the first cast carried out at CERIB and shows the thermocouple trees in the sample formwork.

Figure 4.9: Thermocouple trees manufactured at The University of Edinburgh

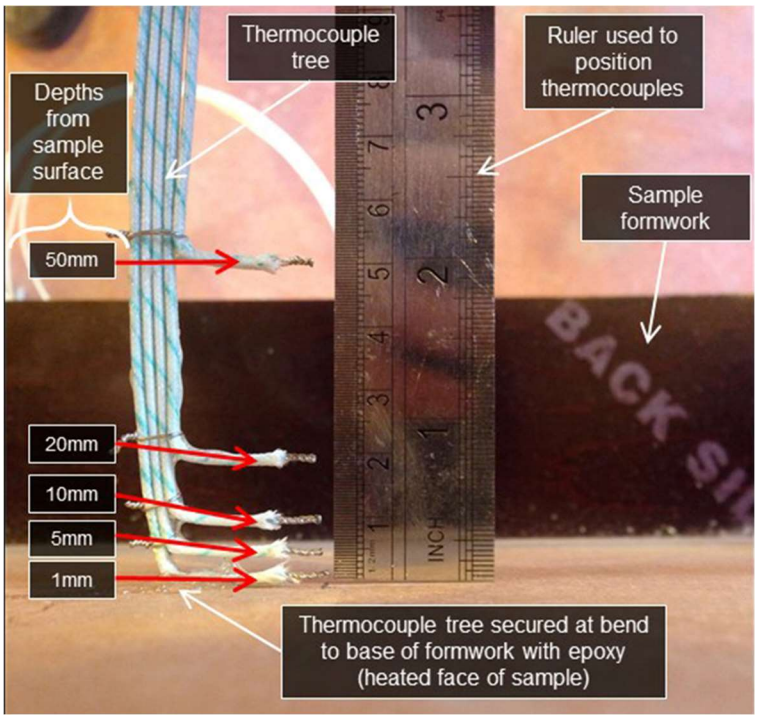

Figure 4.10: Thermocouple tree of the same type installed in formwork ready for casting

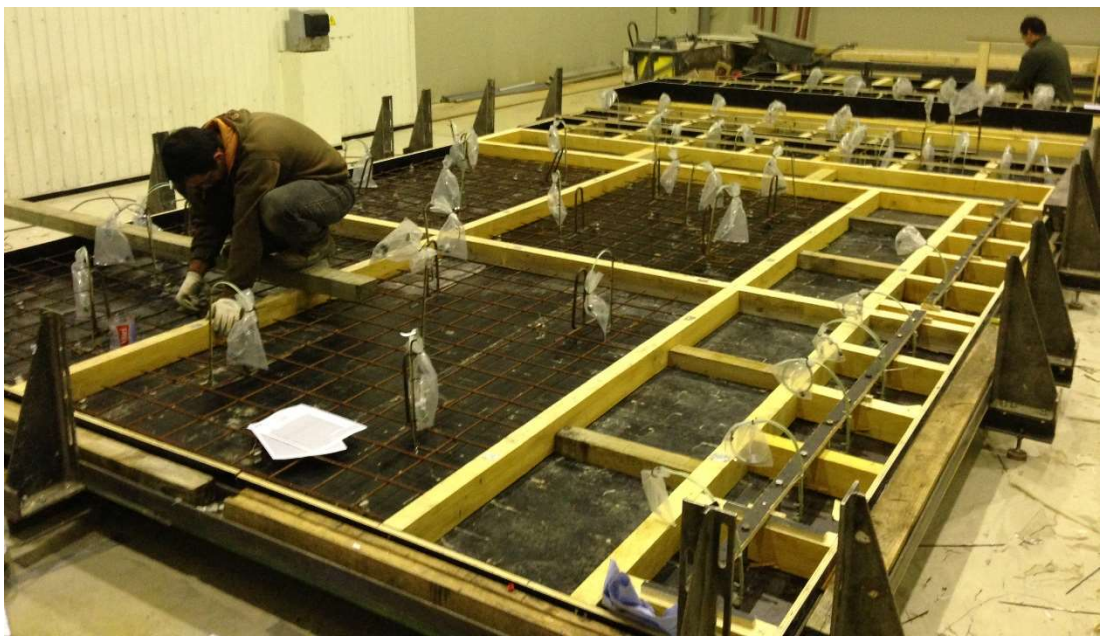

Figure 4.11: Thermocouple trees being installed in formwork at CERIB, France

4.4.2 Thermocouple locations within samples

Thermocouples were positioned within samples in a variety of configurations. The difference was due to the number of thermocouple trees being produced in time for cast not being sufficient to instument all samples with 5 or more thermocouple trees. Where additional thermocouples were used these were installed centrally. Specific thermocouple locations are not reffered to in this thesis but these diagrams are included for completeness. In each plan view the blue crosshair marks the themocouple tree location.

4.4.2.1 Layout A

The layout shown in Figure 4.12 was used for the following sample types (both ISO 834 and HCM sample sets)

1450 x 2140 mm samples – P1, P2, P4, P5

450 x 750 mm samples – P7, P11

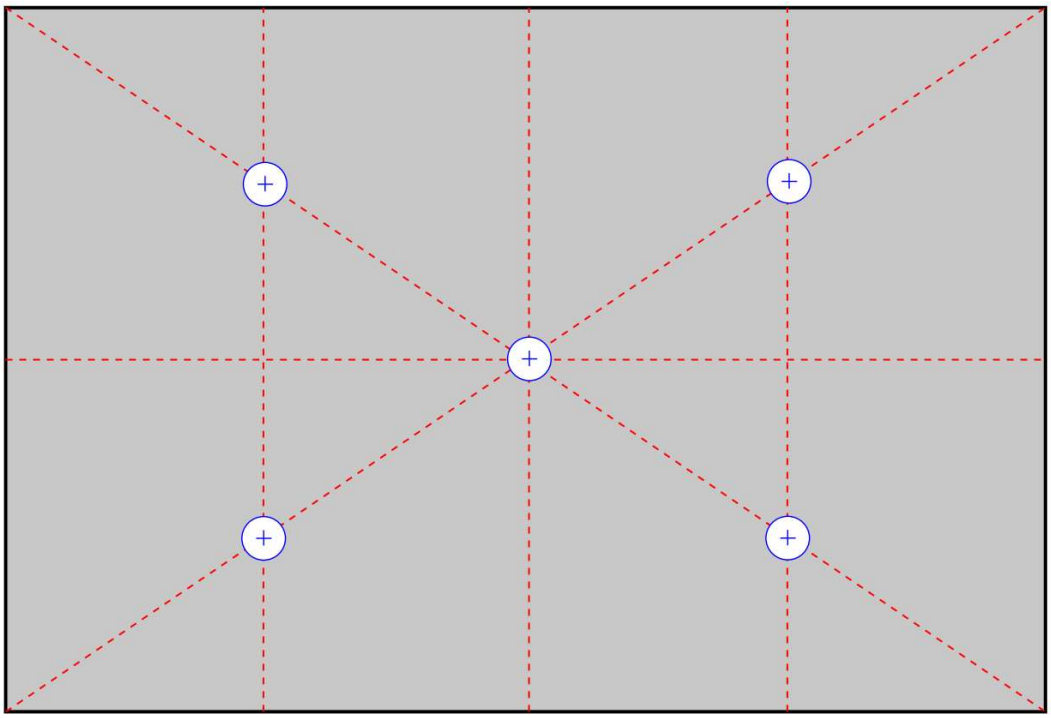

Figure 4.12: Thermocouple layout A

4.4.2.2 Layout B

The layout shown in Figure 4.13 was used for the following sample types (both ISO 834 and HCM sample sets)

450 x 750 mm samples – P8, P9, P10

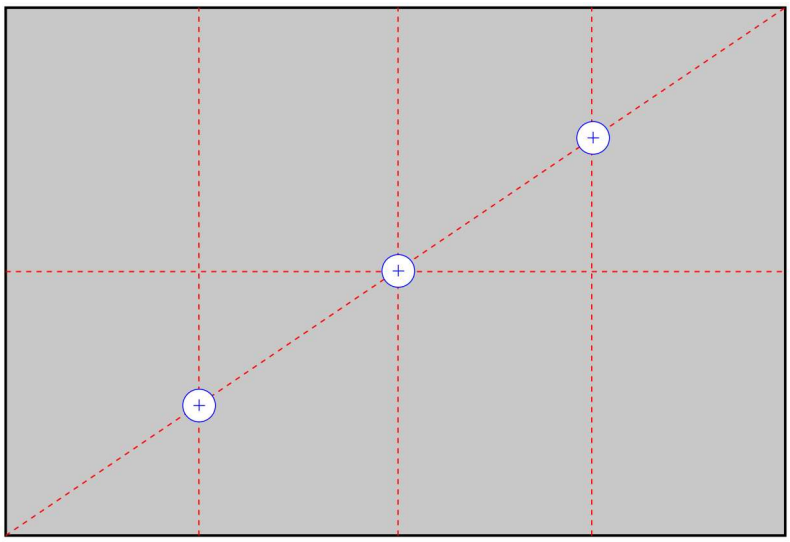

Figure 4.13: Thermocouple layout B

4.4.2.3 Layout C

The layout shown in was used for the following sample types (both ISO 834 and HCM sample sets)

1450 x 2140 mm samples – P3

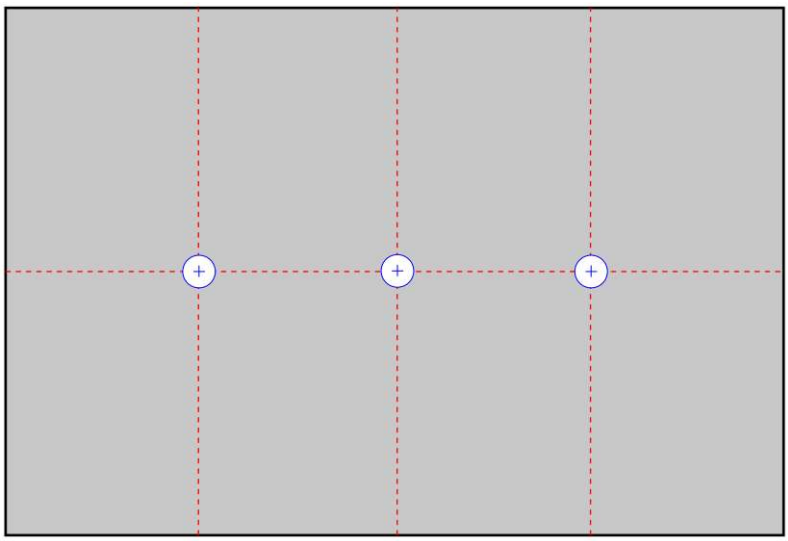

Figure 4.14: Thermocouple layout C

4.4.2.4 Layout D

The layout shown in Figure 4.15 was used for the large 4380 x 1450 mm samples.

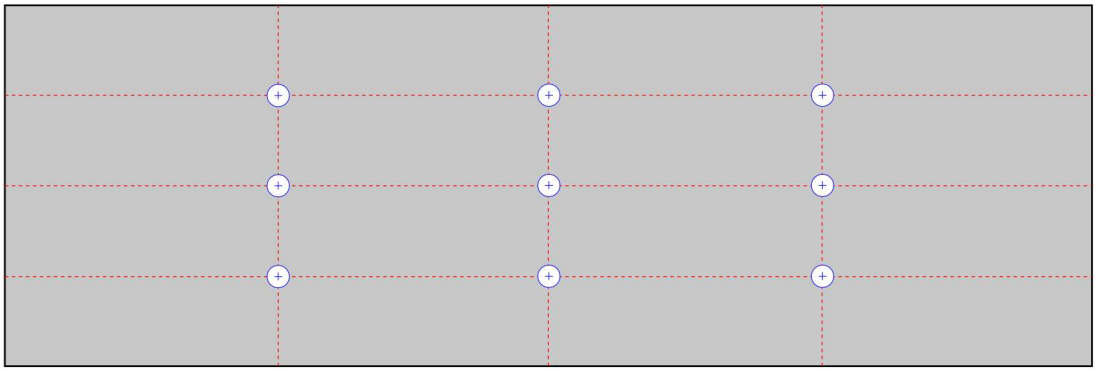

Figure 4.15: Thermocouple layout D

4.4.2.5 Layout E

The layout shown in Figure 4.16 was used for the small 350 x 350 mm samples, these being P12, P13 and P14.

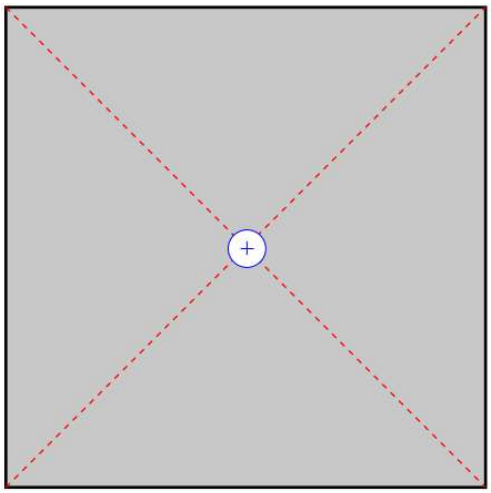

Figure 4.16: Thermocouple layout E

4.4.3 Casting

The samples were cast in three casts. These casts took place on the 13 December 2013, the 20 December 2013 and the 10 January 2014. The mix design is shown in Table 4.1. The SikaFibre Antifissure polypropylene fibres were only added to the final cast on the 10th of January. The Sikaplast techno 7 plasticiser was specified as 0.7% by mass of cement, which equates to 3.05 kg/m^3. This is normally added in the range of 0.3% to 3% by mass of binder so this is a moderate dosage. The plasticiser was added to increase the concrete workability.

Table 4.1: Concrete mix design

Mix Ingredient	Quantity (kg/m^3)
Portland Cement CEM 1 52.5	435
Fine Sand 0/2	500
Sand 0/4	300
4/10mm Limestone aggregate	820
SIKAPLAST® TECHNO 7	3.05
Water	180
SikaFibre Antifissure 12mm Ø:34 µm	2

It is not ideal to have samples of the same mix cast in different casts. It is likely that the resultant mix will not be exactly the same and there is also a difference in age. The breakdown of which sample types were cast in which cast is given in Table 4.2.The sample types P and SF refer to whether they are intended for the Prometheus furnace or for the small furnace. This lettering was selected at Cerib and maintained for clarity.

Table 4.2: Concrete cast schedule

Cast	Sample Types Cast	
Cast 1 13/12/2013	P1	
	P2	
	P7	SF1
	P9	SF2
	P13	
	P14	
Cast 2 20/12/2013	P3	SF3
	P6	SF6
	P8	SF7
	P10	SF8
Cast 3 10/01/2014	P4	
	P5	SF4
	P11	SF5
	P12	

The influence of slight changes in actual poured concrete between casts was reduced by casting all samples of one type in the same cast.

4.4.4 Curing

The samples were cured in the large conditioning room of the Prometheus lab at CERIB. The curing conditions were varied by keeping some samples wrapped in plastic for the curing period whilst the majority of samples were open to the controlled environment of the conditioning room. The conditioning room was set to maintain a 50% relative humidity and a temperature of 23°C. Samples were cured for between 96 days and 132 days based on which cast they were from and in which furnace test they were tested.

Additional samples cast at the same time were wrapped in plastic and shipped to The University of Edinburgh to be used for the Phase 2 experimental work using the H-TRIS apparatus. These experiments are described in Chapter 5.

4.5 Test programme

The furnace testing programme tested a total of 36 samples. These varied in size from the largest at 4.38 m by 1.45 m with a thickness of 250mm to the smallest of which were 0.35 x 0.35 m and 100mm thick. In addition to varying the sample size

and thickness, the standard temperature-time curve, furnace used, polypropylene fibre content, reinforcement, and curing conditions were varied. In the Prometheus tests the small samples did not contain any internal reinforcement but all of the large samples (2.14 m x 1.45 m and above) contained a reinforcement mesh to protect the furnace. The test matrix for the Prometheus tests is shown in Table 4.3. The samples were all cast in duplicate with one set being tested using the ISO 834 temperature versus time curve (International Organisation for Standardization, 1999) and the other tested using the HCM temperature versus time curve (Ministère de l'Equipement, 2000). Samples were positioned in the same location over the furnace in both tests. This means that a total of 28 samples were tested over the two Prometheus tests. One set to each temperature versus time curve.

Table 4.3: Test matrix for ISO and HCM Prometheus furnace tests

Sample	Size (mm)	Thickness (mm)	PP Fibre Dosage (kg/m^3)	Curing Conditions	Reinforcement
P1	2140x1450	100	0	standard	yes
P2	2140x1450	100	0	standard	yes
P3	2140x1450	250	0	standard	yes
P4	2140x1450	250	2	standard	yes
P5	2140x1450	250	2	sealed	yes
P6	4380x1450	250	0	standard	yes
P7	750x450	100	0	standard	no
P8	750x450	250	0	standard	no
P9	750x450	100	0	sealed	no
P10	750x450	250	0	sealed	no
P11	750x450	250	2	standard	no
P12	350x350	100	2	standard	no
P13	350x350	250	0	standard	no
P14	350x350	100	0	standard	no

A further eight samples were tested in two tests in the small furnace to the ISO 834 temperature versus time curve. The test matrix for the two small furnace tests is shown in Table 4.4. Some samples tested in the small furnace are identical to samples being tested in the Prometheus furnace, which allows comparison between the two furnaces. The potential influence of the reinforcement on the spalling performance was also investigated in the small furnace tests with the same reinforcement mesh being used in both cases. All samples tested in the small furnace were 750 x 450 mm.

Table 4.4: Test matrix for small furnace tests

	Sample	Thickness (mm)	PP Fibre Dosage (kg/m^3)	Curing Conditions	Reinforcement
Test 1	SF1	100	0	Standard	No
	SF2	100	0	Standard	No
	SF6	250	0	Sealed	No
	SF7	250	0	Sealed	Yes
Test 2	SF3	250	0	Standard	No
	SF4	100	2	Standard	No
	SF5	250	2	Standard	No
	SF8	250	0	Standard	Yes

The testing can be broken down into sets of samples allowing direct comparison of the influence of the key parameters being investigated and these will be discussed in the following sections. Due to the use of identical samples in the Prometheus ISO 834 and HCM tests, where a comparison of the influence of a variable can be made for one heating regime it can also be made for the other.

4.5.1 Thermal exposure

Identical sets of samples were tested in the Prometheus furnace to different thermal exposures. This gave a direct comparison of the influence of the thermal exposures on spalling performance. These samples are shown in Table 4.3 The eight samples tested in the small furnace to ISO 834 were designed to investigate any differences in sample behaviour when tested to the same fire curve in a different furnace. These tests are shown in Table 4.4. Direct comparisons of the performance of the samples under the different thermal exposures can be made between ISO and HCM Prometheus tests and also between the small furnace samples.

4.5.2 Slab sample thickness

The thickness of a sample heated on one face influences both the distance through which moisture must travel to escape from the cool face and also the restraint against thermal expansion and bowing provided by the cool unheated concrete. In the Prometheus furnace tests comparison of sample types P1, P2 and P3 gives a direct comparison in both the ISO and HCM tests of the influence of sample thickness. Direct

comparison of the influence of thickness can also be seen by comparing sample types P7 and P8, sample types P9 and P10 and sample types P13 and P14. This gives direct comparison of the influence of the thickness of the concrete slab sample at three different sample sizes and using two different moisture contents. The test types mentioned are shown again in Table 4.5 for clarity

Table 4.5: Direct comparisons of sample thickness

Sample	Size	Thickness	PP Fibre Dosage	Curing Conditions
	(mm)	(mm)	(kg/m^3)	
P1	2140x1450	100	0	standard
P2	2140x1450	100	0	standard
P3	2140x1450	250	0	standard
P7	750x450	100	0	standard
P8	750x450	250	0	standard
P9	750x450	100	0	sealed
P10	750x450	250	0	sealed
P13	350x350	250	0	standard
P14	350x350	100	0	standard

Samples from the small furnace tests also give a comparison of the influence of sample thickness on spalling performance. Samples SF1 and SF2 can be compared with the results of sample SF3 and samples SF4 and SF5 can be compared. These comparisons give insight into the influence of thickness with and without PP fibres. Table 4.6 shows the small furnace tests mentioned.

Table 4.6: Direct comparisons of sample thickness from small furnace tests

Test	Sample	Thickness	PP Fibre Dosage	Curing Conditions	Reinforcement
		(mm)	(kg/m^3)		
1	SF1	100	0	Standard	No
1	SF2	100	0	Standard	No
2	SF3	250	0	Standard	No
2	SF4	100	2	Standard	No
2	SF5	250	2	Standard	No

It is important to note that sample SF3 was tested in the second of the two small furnace tests so did not experience exactly the same heating conditions. This is an additional variation to that associated with sample positioning during the tests.

4.5.3 Slab size

In the Prometheus furnace, four different sample sizes were tested in the two thicknesses mentioned to give a total of seven different sample geometries. The influence of sample size/geometry is an important parameter to understand when trying to develop a test method as it is desirable to use samples of manageable size and not waste resources yet their behaviour needs to be representative of that of a "full scale" sample. The range of sample sizes was chosen to allow comparison from a "full scale" slab over 4 m long to smaller scale test slabs 0.35 m square. Comparison of the influence of the sample size on spalling performance can be made in both ISO and HCM furnace tests for 100mm thick samples, 250mm thick samples, and 250mm thick samples with PP fibres. The sets of sample types for comparison are shown in Table 4.7.

Table 4.7: Direct comparisons of the influence of sample slab size

Sample	Size	Thickness	PP Fibre Dosage	Curing Conditions
	(mm)	(mm)	(kg/m^3)	
P1	2140x1450	100	0	standard
P2	2140x1450	100	0	standard
P7	750x450	100	0	standard
P14	350x350	100	0	standard
P3	2140x1450	250	0	standard
P6	4380x1450	250	0	standard
P8	750x450	250	0	standard
P13	350x350	250	0	standard
P4	2140x1450	250	2	standard
P11	750x450	250	2	standard

Sample size was not varied in the two small furnace tests however the sample thickness was varied as mentioned in Section 4.5.2 above.

4.5.4 Curing conditions

The test program was designed to allow direct comparison of the influence of increased moisture content on the spalling performance of the concrete. This increased moisture content was achieved by altering the sample curing conditions. As mentioned in Section 4.4.4, comparison of the influence of moisture content can be made both in the Prometheus furnace test and in the small furnace tests. The sample comparison sets are shown for the Prometheus furnace tests in Table 4.8 and for the small furnace tests in Table 4.9.

Table 4.8: Direct comparisons of the influence of curing conditions in Prometheus tests

Sample	Size	Thickness	PP Fibre Dosage	Curing Conditions
	(mm)	(mm)	(kg/m^3)	
P4	2140x1450	250	2	standard
P5	2140x1450	250	2	sealed
P7	750x450	100	0	standard
P9	750x450	100	0	sealed
P8	750x450	250	0	standard
P10	750x450	250	0	sealed

Table 4.9: Direct comparisons of the influence of curing conditions in the small furnace tests

Test	Sample	Thickness	PP Fibre Dosage	Curing Conditions	Reinforcement
		(mm)	(kg/m^3)		
1	SF6	250	0	Sealed	No
2	SF3	250	0	Standard	No
1	SF7	250	0	Sealed	Yes
2	SF8	250	0	Standard	Yes

4.5.5 Polypropylene fibre content

Polypropylene, PP, fibres are often used to mitigate against explosive spalling of concrete. Comparison of the Prometheus tests summarised in Table 4.10 gives comparison of the efficacy of the fibres in mitigating spalling when tested to the both ISO834 and HCM standard fire curves.

Table 4.10: Direct comparisons of the influence of polypropylene fibre content in Prometheus tests

Sample	Size	Thickness	PP Fibre Dosage	Curing Conditions
	(mm)	(mm)	(kg/m^3)	
P3	2140x1450	250	0	standard
P4	2140x1450	250	2	standard
P8	750x450	250	0	standard
P11	750x450	250	2	standard
P12	350x350	100	2	standard
P14	350x350	100	0	standard

Comparison of the small furnace results shown in Table 4.11 also gives a comparison of the influence of PP fibres on the spalling performance of the concrete.

Table 4.11: Direct comparisons of the influence of polypropylene fibre content in small furnace tests

Test	Sample	Thickness	PP Fibre Dosage	Curing Conditions	Reinforcement
		(mm)	(kg/m^3)		
1	SF1	100	0	Standard	No
1	SF2	100	0	Standard	No
2	SF4	100	2	Standard	No
2	SF3	250	0	Standard	No
2	SF5	250	2	Standard	No

4.5.6 Reinforcement

In the small furnace tests, some samples were tested with and without reinforcement. This allows the influence of the reinforcement mesh to be assessed. The reinforcement mesh in the small samples was a mesh 15 cm × 15 cm, Ø 7 mm, and the cover was 30 mm. Table 4.12 shows the small furnace samples that can be compared.

Table 4.12: Direct comparisons of the influence of reinforcement in small furnace tests

Test	Sample	Thickness (mm)	PP Fibre Dosage (kg/m^3)	Curing Conditions	Reinforcement
1	SF6	250	0	Sealed	No
1	SF7	250	0	Sealed	Yes
2	SF3	250	0	Standard	No
2	SF8	250	0	Standard	Yes

4.6 Testing

The furnace testing was carried out in accordance with ISO 834 (International Organisation for Standardization, 1999) and CETU guidance for HCM tests (CETU, 2017).

4.6.1 Test control and instrumentation

4.6.1.1 Control of thermal exposure

The temperatures in the furnace tests were controlled by plate thermometer readings, and the gas burners were adjusted to maintain furnace gas temperatures within the target range for the chosen temperature versus time curve. Eighteen plate thermometers were used to control the Prometheus furnace tests and four plate thermometers were used to control the small furnace tests.

4.6.1.2 Instrumentation during testing

Thermocouples within the samples were used as mentioned when discussing the sample preparation.

Additonal thermocouples were placed within the furnace to measure gas temperature. These additional thermocouples were not used for furnace control but instead to have a record of the time at which the burners were started. The furnace control was carried out using 18 plate thermometers meeting the requirements given in the relevant testing guidance (International Organisation for Standardization, 1999; CETU, 2017). The locations of the plate themometers can be seen in Figure 4.4.

The temperatures measured by the plate thermometers used for furnace control were also recorded. Strain pot gauges were used to measure the central deflection of the largest slabs during the Prometheus furnace tests and this data was later used in research carried out by another PhD student at The University of Edinburgh (Baharudin *et al.*, 2017).

4.6.2 Test procedure

Samples were removed from their conditioning room (and plastic wrapping in the case of the sealed samples) and placed on the furnace the day before testing. This time prior to testing could not be reduced further as it is time-consuming to position all the samples over the furnace. In the Prometheus furnace tests, instrumentation was connected up to one of two data loggers; the CERIB data logger or an additional data logger from The University of Edinburgh, which was required as the CERIB data logger had insufficient channels for the number of thermocouples being used. Tests lasted an hour based on a defined start time being the point at which the average plate thermometer temperature reaches 50°C. This start condition was inbuilt into the software of the furnace control system and the thermocouples on the CERIB data logger do not record before this defined start point.

The Prometheus tests were observed from a control room above the furnace. After testing the samples were left to cool for a few hours before being removed, photographed, and spalling depths measured. While representatives from The University of Edinburgh were present for both of the Prometheus tests, the majority of the post-test measurements and photographs were taken by staff at CERIB with no one from the University of Edinburgh on site. This has meant that the measurements are not as comprehensive as was desired, however the focus of this test series was to obtain through-thickness temperatures and characterise the thermal exposure and this part of the work was not impacted.

4.6.3 Spalling measurements

The depth of spalling was measured by using a straight edge and ruler across the surface of the sample. Measurements were taken by CERIB staff after those from the University of Edinburgh had returned to Edinburgh. In addition to limited measurements of spalling depth, observations of the severity of spalling can be made from the post-test photographs.

4.7 Results – Concrete properties

4.7.1 28 Day Cylinder Strength

The compressive strength and moisture content of the concrete was measured at 28 days and at the time of testing. Table 4.13 gives the 28 day compressive strengths for the three casts and two curing conditions. It is interesting to note that the addition of the polypropylene fibres in cast three, with no modification to the mix design, served to lower the compressive strength of the concrete. The risk of spalling is believed to increase with an increase in a concrete's compressive strength. This means that the samples containing polypropylene fibres benefited from the supposed spalling-reducing effects of the fibres as well as the lower concrete strength.

Table 4.13: 28 day test results for the concrete casts

Cast	Curing	f_c (MPa)	f_{cm} (MPa)
1	Sealed	48.6	48.9
		49.0	
		49.1	
	Unsealed	47.7	49.8
		52.9	
		48.8	
2	Sealed	56.9	53.9
		55.1	
		49.7	
	Unsealed	58.0	55.4
		52.4	
		55.9	
3	Sealed	42.0	42.7
		44.6	
		41.4	
	Unsealed	47.4	44.8
		41.7	
		45.3	

4.7.2 Moisture content

The moisture content at the time of testing was measured, close to the time of testing, on the 17th of April 2014, by weighing and oven drying standard cylinders that were cast and cured in the same way as the samples. This corresponds to a concrete age of 125 days for the first cast, 118 days for the second cast and, 97 days for the concrete from the third cast

The moisture contents measured are shown in Table 4.14. This method of measuring the moisture content of the concrete only gives an indication of the moisture content. It does not give a true value of moisture content for the large samples and cannot capture a difference in moisture content that may be caused by a difference in sample size and thickness. It can be seen that wrapping the samples in plastic during the curing process resulted in an increase in moisture content of between 1.8% and 2.8% by mass depending on the mix.

Table 4.14: moisture content by mass at time of testing for the different casts and curing conditions

Cast	Curing	Moisture Content (%)	Average Moisture Content (%)
1	Sealed	5.6	5.9
		6.5	
		5.5	
	Unsealed	4.5	4.1
		3.9	
		3.8	
2	Sealed	5.4	5.8
		5.9	
		6.2	
	Unsealed	3.3	3.5
		3.8	
		3.3	
3	Sealed	6.8	6.8
		6.9	
		6.7	
	Unsealed	4.2	4.0
		4.2	
		3.7	

4.8 Results – Test validity

The requirements for temperature control within a furnace during testing are set by the relevant guidance documents for the specific temperature time curve being followed (International Organisation for Standardization, 1999; CETU, 2017). The data from the plate thermometers can be compared against these requirements to confirm the acceptability of the furnace tests. Since one of the primary aims of this phase of testing is to establish a thermal exposure to use for future testing, it is important to make sure that these furnace tests meet the relevant standards. For reference, plate thermometer locations in Prometheus tests are shown in Figure 4.4. Plate thermometer locations in the small furnace tests can be seen in Figure 4.8.

For tests to the ISO 834 temperature-time curve, the standard (International Organisation for Standardization, 1999), gives limits of allowable variation in Section 6.1.2. There are no limits on temperatures within the furnace for the first five minutes of a test. Following this, the variation between the area under the temperature time curve and the area under the average furnace temperature curve is limited to 15% at a time of 5 to 10 minutes. Between 10 and 30 minutes the allowable deviation, d_e, as a percentage can be expressed as:

$$d_e=15-0.5(t-10)\%$$

Where t is the test time in minutes. Between 30 and 60 minutes, this allowable deviation can be expressed as:

$$d_e=5-0.083(t-30)\%$$

A limit on the maximum allowable deviation of an individual plate thermometer of 100°C from the standard temperature-time curve after a time of ten minutes is also set.

For the modified hydrocarbon, HCM, curve the CETU guide (CETU, 2017) gives a maximum allowable deviation for an individual plate thermometer from the curve of 130°C after a time of ten minutes. The acceptability of the control of the furnace is also judged based on the difference between the area under the HCM curve and the area under the average plate thermometer reading. The allowable variation in area is given as 20% for a time of 5 to 10 minutes, 15% from 10 to 20 minutes, 10% from 20 to 30 minutes, and 5% for 30 to 60 minutes. After a test time of 60 minutes, the allowable percentage difference in the area under the curves is 2.5%.

The acceptability criteria of the area under the temperature time curve is interesting, as it has no physical meaning. It is thought that initially the idea may have been to try to equate the input energy between tests; the gas temperature within the furnace however is not the correct measurement of this. If the test were heat flux controlled the area under the curve would equate to the energy input into the furnace.

The requirements on temperature control are set in an attempt to harmonise furnace testing but are limited by the realistic capabilities of the furnaces to control the temperatures during the test. It would be better to have much less variation and higher level of control of the heating than is prescribed but this is not possible in most furnaces. The variation in the early test may not be so critical for all materials being tested but spalling, which often occurs within these first uncontrolled minutes, has been seen to be very sensitive to the early thermal exposure. When researching spalling it is desirable that the heating is controlled accurately throughout the entire test.

4.8.1 ISO 834 Prometheus test

The ISO 834 checks can be carried out for the Prometheus ISO tests and are shown in Figure 4.17. A total of 18 plate thermometers were used to control the Prometheus furnace. It can be seen in Figure 4.17 that, while initially there is a large spread of temperatures, this is acceptable as there is no restriction on the temperature range during the first 5 minutes. There is also no restriction on individual plate thermometer readings until a test time of 10 minutes, after which the individual temperatures recorded are within the allowable maximum deviation of 100°C from the curve. The areas under the curves shown in Figure 4.17 are also in good agreement and well within the allowable range, although again this does not really have any physical meaning.

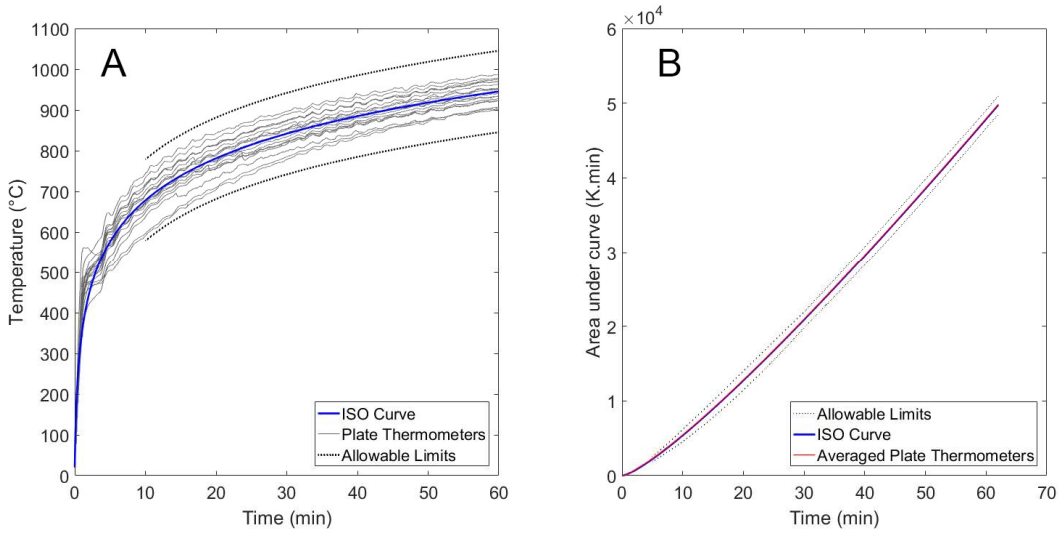

Figure 4.17: Acceptability checks for Prometheus ISO 834 test. A) Plate thermometer temperature check B) Area under temperature – time curve check

During the Prometheus ISO 834 test, the temperatures recorded by plate thermometers were highest at plate thermometers numbers 12 and 16 and lowest at plate thermometers 1 and 5 (see Figure 4.4). It is possible that the plate thermometer numbering provided by CERIB was incorrect but there does not appear to be any obvious link between gas temperature and proximity to burners (see Figure 4.5 to Figure 4.7).

4.8.2 HCM Prometheus test

The requirements for the control of a furnace to the HCM curve are different to that of the ISO 834 curve and can be found in a CETU guide (CETU, 2017). The requirements on the temperature deviation and the allowable difference in area under the curves are more relaxed than those for the ISO 834 temperature versus time curve. The HCM furnace temperatures can be checked against this guidance and the results are shown in Figure 4.18. One of the plate thermometers exceeded the allowable deviation of 130°C at a time of 10 minutes and recorded a temperature 131.3°C lower than the temperature specified by the curve. This means that the test did not meet the requirements. It was decided that this minor discrepancy could be ignored. It should be noted that 11 of the 18 plate thermometers broke during testing due to the very high temperatures. This is an issue when attempting to run tests to temperature time curves that exceed the temperatures of the standard fire curves for which these plate thermometers were developed. It does not seem appropriate to be controlling the temperatures within a furnace, and thermal exposure to a test specimen with instrumentation that cannot withstand the test conditions.

The plate thermometers were specified, supplied, and installed by CERIB as part of the standard test control for their furnace during an HCM test. CERIB are an accredited testing laboratory and it is understood that this is their standard approach to temperature control measurement. As a result, it was not anticipated that plate thermometer failure would be an issue. Other temperature measurements to corroborate were not available due to data acquisition issues.

The author is not aware of the temperature rating or high temperature accuracy of the plate thermometers used by CERIB as part of their furnace setup. The approach used is consistent with a standard test to the HCM temperature time curve, which was desired for this phase of the experimental work.

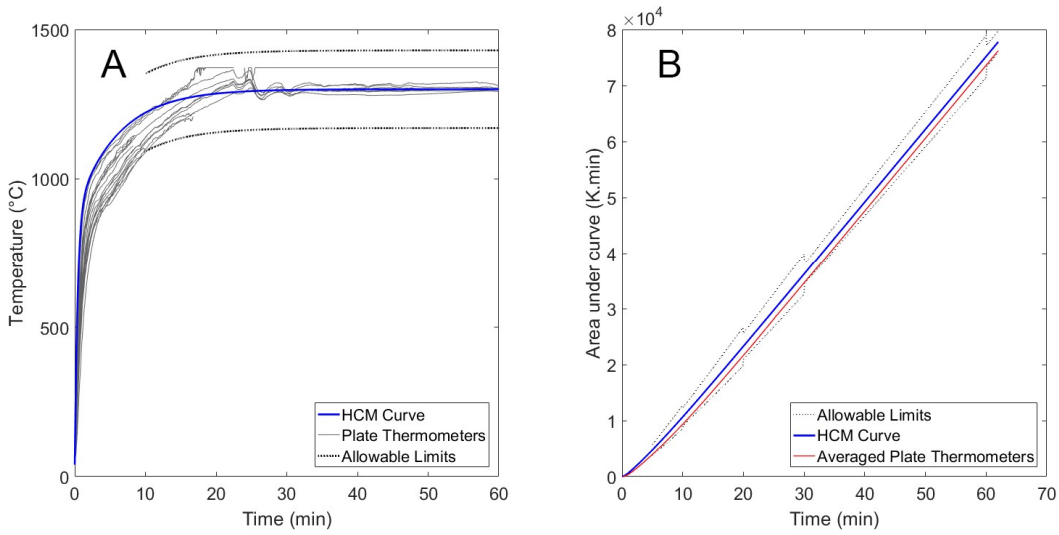

Figure 4.18: Acceptability checks for Prometheus HCM test. A) Plate thermometer temperature check B) Area under temperature – time curve check

During the Prometheus HCM test, the temperatures recorded by plate thermometers were highest at plate thermometers numbers 7 and 13 and lowest at plate thermometers 9 and 16 (see Figure 4.4). It is possible that the plate thermometer numbering provided by CERIB was incorrect but there does not appear to be any obvious link between gas temperature and proximity to burners (see Figure 4.5 to Figure 4.7). This was also observed in the ISO 834 Prometheus furnace test.

4.8.3 Small furnace ISO 834 tests

The small furnace tests can be checked against the ISO 834 criteria. Four plate thermometers control the small furnace. It can be seen that there is a smaller spread in the plate thermometer temperatures than in testing carried out in the Prometheus furnace. Both of the small furnace tests' temperature-time histories meet the acceptability requirements.

4.8.3.1 Small furnace test 1

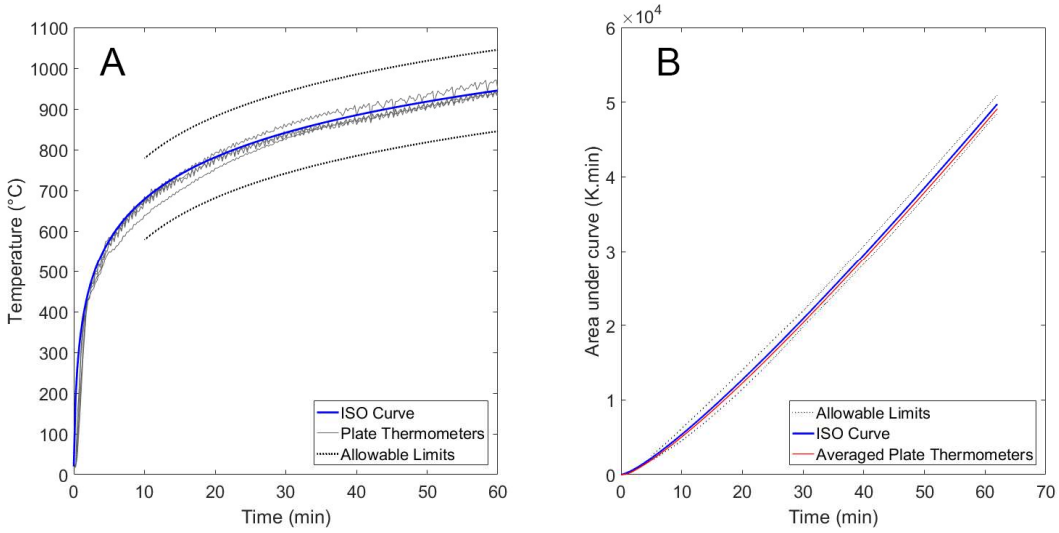

Figure 4.19: Acceptability checks for small furnace test 1. A) Plate thermometer temperature check B) Area under temperature – time curve check

4.8.3.2 Small furnace test 2

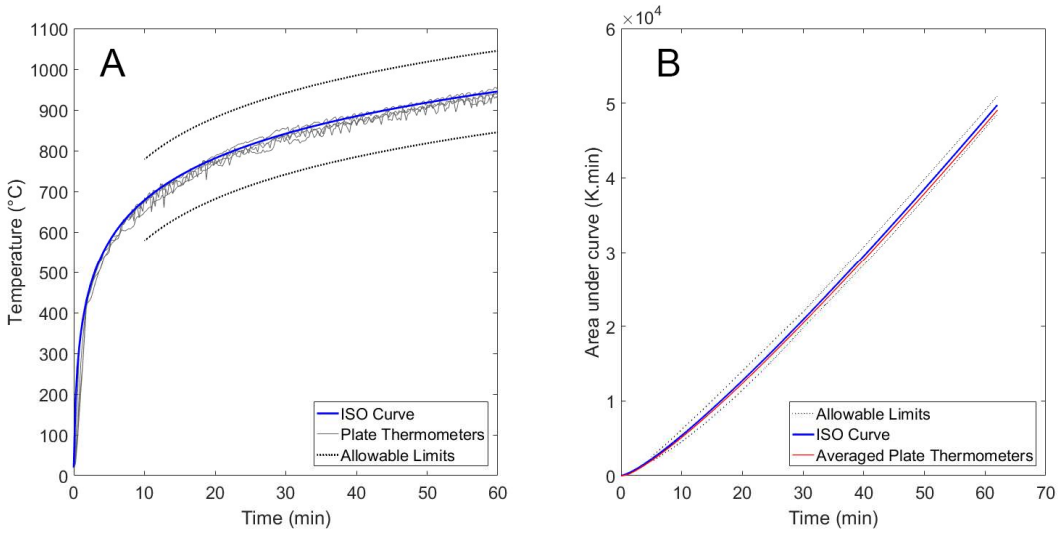

Figure 4.20: Acceptability checks for small furnace test 2. A) Plate thermometer temperature check B) Area under temperature – time curve check

4.9 Results – spalling observations

4.9.1 Notes during and immediately after testing

The two tests carried out in the Prometheus furnace were observed both from the control room at CERIB that looks onto the furnace, and using the furnaces internal camera, although this camera had a very limited view of the samples during the test. During the testing spalling was often loud enough to be heard from the control room. The tables of crude observations below from the Prometheus tests include anything that was noted down during or immediately after the tests. No representatives from The University of Edinburgh were present at the small furnace tests or for the removal of the samples following the ISO curve test in the Prometheus furnace. As a result, the observations are not documented here. All spalling observations were taken on the day of testing prior to concrete rehydration, sloughing off, and the resultant surface loss.

4.9.1.1 ISO 834 Prometheus test

Spalling incidents were audible from the control room; these, along with observations from the camera positioned within the furnace, are given in Table 4.15.

Table 4.15: Spalling observations from control room in ISO 834 Prometheus test

Test Time (mm:ss)	Observations from Internal Camera
09:00	Spalling heard
09:30	Spall seen on sample P6 behind support column
10:00	Spall heard
10:20	P6 Spall closer to edge of sample
11:55	P6 Spall
12:30	P6 Spall behind column right of the first spall
12:55	P6 spall next to plate thermometer
13:42	P6 near edge
14:26	P3 spall
17:00	P2 spall (heard not seen)
28:40	Moisture escaping from 100mm thick samples
36:50	P2 water spraying from central thermocouple tree. Moisture pooling clearly showing sample curvature

4.9.1.2 HCM Prometheus test

Spalling during the HCM testing was almost constant and it was hard to identify specific instances of spalling. A lot of material was dropping from the samples located at the ceiling of the furnace making it hard to see on the camera which sample it was coming from. Observations from the HCM test and immediately after the test are given in Table 4.16

Table 4.16: Spalling observations from control room in HCM Prometheus test

Test Time (mm:ss)	Observations from test
10:00	Violent spall on sample P3 for 5 minutes
15:00	Violent spalling on sample P6
20:00	Thermocouples burning south-west corner due to gap opened between samples and hot gas escaping
22:00	P6 top surface spalling hot gases escaping over cool back face of sample
After Test	Initial observations P6 spalling severe with depth varying from 10-40mm difficult to measure due to the curvature of the bowed sample. P3 spalling reached a depth of 63mm

4.9.2 Prometheus ISO 834 test

The results of the ISO tests are summarised in Table 4.17. Detailed information on the spall dimensions in terms of area, volume and depth are not available. Photographs of the spalled samples are shown in Figure 4.21, Figure 4.22, and Figure 4.23. It can be see that the spalling is not severe and no reinforcement has been exposed. All spalling observations were taken on the day of testing prior to concrete rehydration, sloughing off, and the resultant surface loss.

Table 4.17: Results summary after testing - Prometheus ISO test

Sample	Spalling	Notes
P1	No	
P2	No	
P3	Yes	Spalling in two locations close to the edge of the sample
P4	No	
P5	No	
P6	Yes	Five occurrences of spalling. Shallow and localised
P7	No	
P8	Yes	Full heated surface. Shallow spalling, 5mm thermocouple exposed.
P9	Yes	One localised spall
P10	Yes	Shallow spall in two locations covering most of the surface
P11	No	
P12	No	
P13	No	
P14	No	

Figure 4.21: Samples P3 and P6 after Prometheus ISO test

Figure 4.22: Samples P8 and P9 after Prometheus ISO test

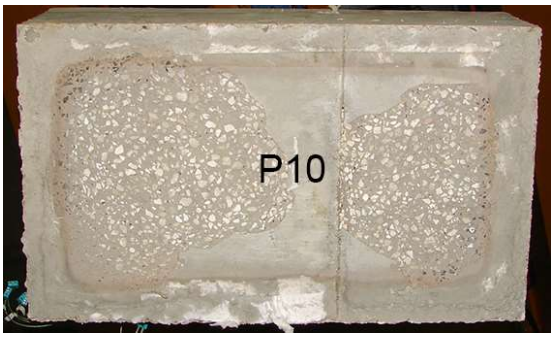

Figure 4.23: sample P10 after Prometheus ISO test

4.9.3 Prometheus HCM test

The spalling observations from the HCM test are shown in Table 4.16. Photographs of the spalled samples are shown in Figure 4.24 to Figure 4.29.

Table 4.18: Results summary after testing - Prometheus HCM test

Sample	Spalling	Notes
P1	Yes	Very minor spall
P2	Yes	Six minor localised spalls
P3	Yes	Severe spalling exposing the reinforcement mesh
P4	Yes	Full surface "sloughing off"
P5	Yes	Full surface "sloughing off"
P6	Yes	Full surface "sloughing off"
P7	Yes	Localised
P8	Yes	Almost full heated area, 35mm depth. Large cracks in sample.
P9	Yes	Most of the surface
P10	Yes	Full surface. 30mm depth
P11	Yes	most of surface 15mm deep
P12	No	
P13	Yes	Full heated area 17mm deep
P14	No	

Figure 4.24: Samples P1 and P2 after Prometheus HCM test

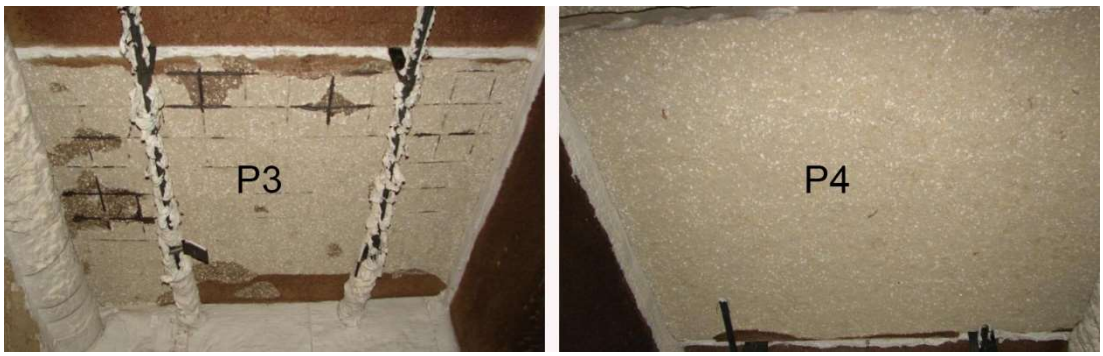

Figure 4.25: Samples P3 and P4 after Prometheus HCM test

Figure 4.26: Samples P5 and P6 after Prometheus HCM test

Figure 4.27: Sample P7 and P8 after Prometheus HCM test

Figure 4.28: Sample P9 and P10 after Prometheus HCM test

Figure 4.29: Sample P11 and P13 after Prometheus HCM test

All photographs of spalling shown above were taken on the day of testing prior to concrete rehydration, sloughing off, and the resultant surface loss.

4.9.4 Small furnace tests 1 and 2

The spalling observations from the two small furnace tests are given in Table 4.19. Both of the small furnace tests were to the ISO 834 temperature versus time curve.

Table 4.19: Results summary after testing small furnace ISO tests

	Sample	Spalling	Notes
Test 1	SF1	No	
	SF2	No	
	SF6	Yes	Two large spalls
	SF7	Yes	One spall, some aggregate spalling.
Test 2	SF3	Yes	Severe spalling of most of the exposed face
	SF4	No	
	SF5	No	
	SF8	No	

It should be noted that samples SF1 and SF2 were supposed to be a control sample with one tested in each of the small furnace tests yet they both were tested in the first furnace test. This still provides a meaningful repeat of the test and both samples performed similarly with no spalling occurring in either. Images of the spalled samples can be seen in Figure 4.30, Figure 4.31, and Figure 4.32.

Figure 4.30: Sample SF6 after testing

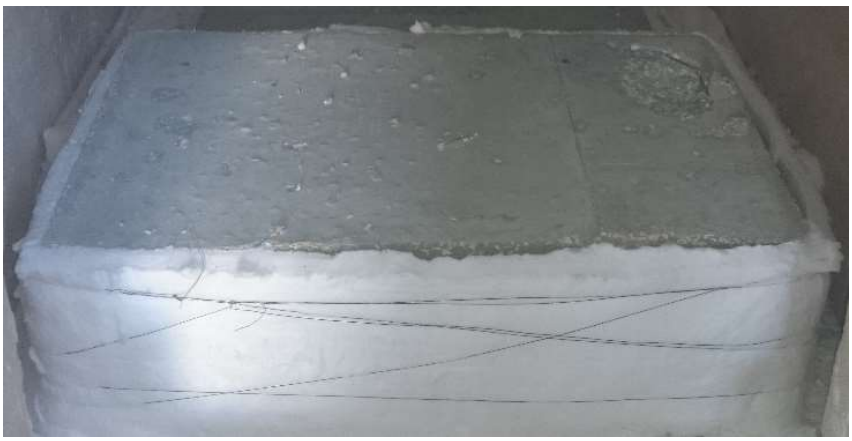

Figure 4.31: Sample SF7 after testing

Figure 4.32: Sample SF3 after testing

4.9.5 Comparisons of the influence of key parameters

The result of the furnace tests are shown above. Discussions of the influence of the key parameters being investigated, based on the results obtained, are discussed in the sections below.

4.9.5.1 Thermal exposure

Fourteen direct comparisons of the influence of thermal exposure are possible from the Prometheus furnace tests. The two identical sets of 14 samples were tested to the ISO 834 temperature versus time curve in one test and to the HCM temperature versus time curve in the other. Summaries of the results for the ISO 834 Prometheus furnace test are given in Table 4.17 and the HCM Prometheus test results are

summarised in Table 4.18. Comparison between the two furnace tests shows the influence of the French modified hydrocarbon curve, HCM, in comparison to the ISO 834 curve. Five of the fourteen samples experienced some spalling In the ISO 834 test while twelve of the fourteen samples spalled in the HCM test. It is also noteworthy that the more severe heating under the HCM thermal exposure led to more severe spalling. In the samples that spalled under both fire curves, the spalling was more severe in the HCM test. These results indicate that the more severe HCM thermal exposure increases both the likelihood of spalling occurring and the severity of spalling if it does occur.

4.9.5.2 Slab sample thickness

The influence of the sample thickness on its spalling propensity can be assessed in the Prometheus tests by comparing the sample groups shown in Table 4.20. These sample groups give comparisons for both the ISO 834 and HCM temperature versus time curves.

Table 4.20: Prometheus sample thickness results summary

Sample	Size (mm)	Thickness (mm)	PP Fibre Dosage (kg/m^3)	Curing Conditions	Spalling ISO 834	Spalling HCM
P1	2140x1450	100	0	standard	No	Yes
P2	2140x1450	100	0	standard	No	Yes
P3	2140x1450	250	0	standard	Yes	Yes
P7	750x450	100	0	standard	No	Yes
P8	750x450	250	0	standard	Yes	Yes
P9	750x450	100	0	sealed	Yes	Yes
P10	750x450	250	0	sealed	Yes	Yes
P13	350x350	250	0	standard	No	Yes
P14	350x350	100	0	standard	No	No

Looking at samples P1, P2, and P3 in the ISO test there was no spalling of P1 or P2, yet the thicker sample P3 did spall. While no measurement of the slab deflection was taken for these samples, the thinner samples visibly bowed and it is thought this bowing could help reduce the internal stresses due to the high thermal gradient. See Section 2.5. In the HCM test, all three of these samples spalled but the spalling on sample P3 was much more severe than that in the other two. This again indicates that the thicker, 250 mm thick samples provide a worse case for spalling than the 100 mm thick samples.

The same observation can be made for samples P7 and P8. Sample P7 did not spall in the ISO test yet in the same test, P8 experienced some spalling. In the HCM test both spalled, yet sample P8 spalled more severely. Sample types P9 and P10, and P13 and P14 also show more spalling in the thicker of the two samples (if spalling occurred in either of the samples).

In the Prometheus tests, thicker samples were the most prone to spalling across all the sample sizes and curing conditions investigated. The thicker samples spalled more severely, where spalling occurred in both tests, and when spalling occurred in only one of the comparison samples the thicker samples were the samples that spalled.

Comparison of the influence of thickness on the spalling behaviour based on the small furnace tests can also be made. Table 4.21 gives an overview of the comparisons of the influence of thickness that can be made. While no spalling occurred in the samples containing PP fibres the results of standard mix samples support the results from the Prometheus tests with the thicker sample SF3 spalling while neither of the 100 mm thick samples spalled.

Table 4.21: Small furnace sample thickness results summary

Test	Sample	Thickness (mm)	PP Fibre Dosage (kg/m^3)	Curing Conditions	Reinforcement	Spalling
1	SF1	100	0	Standard	No	No
1	SF2	100	0	Standard	No	No
2	SF3	250	0	Standard	No	Yes
2	SF4	100	2	Standard	No	No
2	SF5	250	2	Standard	No	No

Through the ten sets of samples that allow direct comparison of the influence of the sample thickness on the spalling performance the following summary can be made:

- Two of the comparisons are inconclusive with no spalling occurring (P13 and P14 in the ISO 834 Prometheus test and SF4 and SF5 in the small furnace tests).
- The remaining eight direct comparisons show that the 250 mm thick samples are a worse case for spalling than the 100 mm thick samples with spalling always occurring in the 250 mm thick samples. If spalling occurred in both

sample thicknesses, the most severe spalling occurred in the 250 mm thick samples.

It is thought that the observation of thicker samples being a worse case for spalling could be due to the thicker samples having more resistance to deflection. A slight bending of the samples would result in the stress due to the thermal expansion of the concrete on the heated face being relieved. See Section 2.5.

4.9.5.3 Slab size

The influence of the sample size in terms of the exposed slab face size can be seen in the Prometheus tests by comparison of the groups of sample types shown in Table 4.22. No comparison of the influence of slab size is possible from the small furnace tests as all small furnace samples were 750 x 450 mm. The samples were unloaded and simply supported over the furnace, and the results may be specific to this test arrangement.

Table 4.22: Prometheus slab size results summary

Sample	Size (mm)	Thickness (mm)	PP Fibre Dosage (kg/m^3)	Curing Conditions	Spalling ISO 834	Spalling HCM
P1	2140x1450	100	0	standard	No	Yes
P2	2140x1450	100	0	standard	No	Yes
P7	750x450	100	0	standard	No	Yes
P14	350x350	100	0	standard	No	No
P3	2140x1450	250	0	standard	Yes	Yes
P6	4380x1450	250	0	standard	Yes	Yes
P8	750x450	250	0	standard	Yes	Yes
P13	350x350	250	0	standard	No	Yes
P4	2140x1450	250	2	standard	No	Yes
P11	750x450	250	2	standard	No	Yes

For the 100 mm thick samples P1, P2, P7 and P14 all slab sizes with the exception of largest size (4380 x 1450) were tested. In the ISO 834 Prometheus test, none of these samples spalled. In the HCM Prometheus test, with identical samples, there was no spalling in sample type P14, the smallest sample, but some localised, shallow spalling in all of the other samples. This result would indicate that the 350x350 mm samples were too small with their behaviour not being representative of the behaviour of larger, more realistically sized slabs. This is discussed further in Section 4.11.2.2.

The 250 mm thick samples with no polypropylene fibres P3, P6, P8 and P13 spalled much more than the 100 mm thick samples. In the ISO 834 test, the sample types P3 P6 and P8 all spalled and P13 did not spall at all. Sample type P8 spalled the most severely in the ISO 834 test. The reason for this is unclear. It is hypothesised that the self-weight of the larger samples may have caused them to bow into the furnace which would relieve stress in the heated surface. See Section 2.5. It is not possible to verify this theory as the deflections of the samples were not measured.

When looking at the results of the HCM test all of these samples spalled. The most severe spalling occurred in sample type P3 where spalling exposed the reinforcement mesh. The spalling observed in sample types P6, P8 and P13 was also severe. This comparison yet again suggests that the smaller sample size does not give a result representative of that which could be expected in full scale sample.

For sample types containing polypropylene fibres, P4 and P11, neither spalled in the ISO 834 test and both spalled in the HCM test. The severity of the spalling was similar in both sample types. The whole heated surface of sample P4 spalled and most of the heated surface of sample type P11 spalled. The maximum spall depth was similar.

It is difficult to draw a conclusion about the “worst case” sample size for spalling. It appears that sometimes the smaller samples do not spall when the larger ones do. It is also not the case that the largest samples experience the most severe spalling. The presence of reinforcement in the larger samples is not thought to be a primary influencing factor here as sample P8 spalled yet did not contain reinforcement.

While no load was applied to the samples, the self-weight of the slabs is not insignificant during these severe furnace tests. The largest sample had a higher span to depth ratio than the smaller ones. The variation in performance due to size is likely to be a result of the differing stiffness and self-restraint of the sample as well as the influence sample size has on moisture transport and heat transfer. The edge effects on moisture transport and heat transfer will decrease with increasing sample size.

The largest samples were seen to bow which will relieve thermal stresses in the heated surface. It appears that the size of the sample is not as critical to spalling as the other parameters varied in these tests.

4.9.5.4 Curing conditions

The pairs of sample types shown in Table 4.23 give a direct comparison of the Influence of curing conditions in Prometheus tests.

Table 4.23: Prometheus curing conditions results summary

Sample	Size (mm)	Thickness (mm)	PP Fibre Dosage (kg/m^3)	Curing Conditions	Spalling ISO 834	Spalling HCM
P4	2140x1450	250	2	standard	No	Yes
P5	2140x1450	250	2	sealed	No	Yes
P7	750x450	100	0	standard	No	Yes
P9	750x450	100	0	sealed	Yes	Yes
P8	750x450	250	0	standard	Yes	Yes
P10	750x450	250	0	sealed	Yes	Yes

Sample types P4 and P5 containing polypropylene fibres did not spall when tested to the ISO 834 curve but both spalled when tested to the HCM curve. The P4 and P5 samples tested to the HCM curve experienced a very similar damage with some material loss across the entire surface of the sample. This material loss appeared to be more of a “sloughing off” than violent localised spalls.

Sample types P7 and P9 showed a difference between spalling behaviour with curing conditions. In the ISO 834 test, the sample cured under standard conditions, type P7, did not spall but the sample sealed during curing, P9, spalled with one localised spall. In the HCM test sample P7 spalled in one location while P9 spalled most of the heated surface, again demonstrating that, for these samples, the sealed curing conditions provide a worse case for spalling.

For the 250 mm thick sample types of the same size in the ISO 834 Prometheus test, sample P8 spalled over the entire heated surface and sample P10 spalled in two locations. When these sample types were tested to the HCM curve, sample P10 spalled over the complete heated surface with a spalling depth of 30 mm and sample P8 spalled over the complete heated area but to a depth of 35 mm. This greater spalling depth in the sample cured under standard conditions was unexpected. It would be interesting to compare the volume of spalling but this information is not available.

Comparison of the influence of curing conditions is also possible from the small furnace tests. Table 4.24 gives a summary of these results.

Table 4.24: Small furnace curing conditions results summary

Test	Sample	Thickness (mm)	PP Fibre Dosage (kg/m^3)	Curing Conditions	Reinforcement	Spalling
1	SF6	250	0	Sealed	No	Yes
2	SF3	250	0	Standard	No	Yes
1	SF7	250	0	Sealed	Yes	Yes
2	SF8	250	0	Standard	Yes	No

The results of the small furnace tests show more severe spalling occurring in the SF3 sample than in the SF6 sample. Again this more severe spalling in the sample cured under standard conditions rather than the sealed sample is unexpected. The second sample set which provides a direct comparison of the influence of the curing conditions on the spalling behaviour indicated again that the sealed curing condition provides a worst case for spalling.

Through the eight direct comparisons that can be made on the influence of the curing conditions on the spalling performance the following can be observed;

- Two of the eight comparisons are inconclusive (P4 and P5 in ISO and HCM Prometheus tests).
- Three of the direct comparisons indicated that a sealed curing condition is the worst case for spalling (P7 and P9 ISO 834 and HCM Prometheus tests and SF7 and SF8 tested to ISO 834 in the small furnace).
- Three of the direct comparisons indicate that standard curing conditions provide a worse case for spalling (P8 and P10 in ISO 834 and HCM Prometheus tests and SF6 and SF3 tested to ISO 834).

These comparisons are made between samples of the same concrete mix, tested in the same furnaces, in tests that meet the testing standards, and at the same time. There are no external factors that should have influenced the results. Based on these results no conclusions can be made about the influence of curing conditions. While there are multiple samples that allow this comparison, there are no repeats of the specific samples in each furnace test. Further repeats may have given confirmation of these results. Had fewer samples been tested, the inconsistent behaviour may not have been captured and the results may have led to inappropriate conclusions being made. These observations highlight the importance of carrying out repeat tests.

4.9.5.5 Polypropylene fibre content

Direct comparison of the effects of polypropylene fibres on the concrete samples in Prometheus testing to ISO 834 and HCM curves can be made by comparing the pairs of sample types shown in Table 4.25.

Table 4.25: Prometheus PP fibre content results summary

Sample	Size (mm)	Thickness (mm)	PP Fibre Dosage (kg/m^3)	Curing Conditions	Spalling ISO 834	Spalling HCM
P3	2140x1450	250	0	standard	Yes	Yes
P4	2140x1450	250	2	standard	No	Yes
P8	750x450	250	0	standard	Yes	Yes
P11	750x450	250	2	standard	No	Yes
P12	350x350	100	2	standard	No	No
P14	350x350	100	0	standard	No	No

In ISO curve testing sample type P3 spalled in two locations while type P4 did not spall. In the test to the HCM curve sample P3 experienced very severe spalling exposing the reinforcement while P4 lost a thin layer of concrete from the entire heated surface. While spalling was reduced, the presence of the PP fibres was not sufficient to prevent spalling entirely in testing to the HCM curve. Although the failure mode may have been more of a “sloughing off” of the surface rather than the violent spalling seen from sample type P3 on the in-furnace camera.

Sample type P8 spalled over the entire heated surface when tested to the ISO 834 curve yet sample type P11 did not spall. When tested to the HCM curve both samples spalled over the entire heat surface. The spall depth for type P8 was 35mm while it was only 15mm for sample type P11.

Neither sample type P12 nor P14 spalled when tested to the ISO curve or the HCM curve.

The direct comparison results shown in Table 4.26 allow comparison of the influence of PP fibre content from the small furnace tests carried out using the ISO 834 temperature time curve.

Table 4.26: Small furnace PP fibre content results summary

Test	Sample	Thickness (mm)	PP Fibre Dosage (kg/m^3)	Curing Conditions	Reinforcement	Spalling
1	SF1	100	0	Standard	No	No
1	SF2	100	0	Standard	No	No
2	SF4	100	2	Standard	No	No
2	SF3	250	0	Standard	No	Yes
2	SF5	250	2	Standard	No	No

No spalling occurred in the first comparison set, comprising of samples SF1 SF2 and SF3, and as such, no conclusions can be drawn from these tests. In the second comparison set SF3 the sample containing no PP fibres spalled yet the SF5 sample containing PP fibres did not spall.

Through the eight direct comparisons that can be made on the influence of polypropylene fibres on the spalling performance the following can be observed;

- Three of the eight comparisons are inconclusive (P12 and P14 in ISO and HCM Prometheus tests and SF1, SF2 and SF4 in the small furnace tests).
- Five of the direct comparisons indicated that the addition of PP fibres either prevented or reduced spalling (P3 and P4 ISO 834 in ISO 834 and HCM Prometheus tests, P8 and P11 in both ISO 834 and HCM Prometheus tests and SF3 and SF5 tested to ISO 834 in the small furnace).

4.9.5.6 Reinforcement

A direct comparison of the influence of the reinforcement on testing can be made by comparing the results of the small furnace tests shown in Table 4.27.

Table 4.27: Small furnace reinforcement results summary

Test	Sample	Thickness (mm)	PP Fibre Dosage (kg/m^3)	Curing Conditions	Reinforcement	Spalling
1	SF6	250	0	Sealed	No	Yes
1	SF7	250	0	Sealed	Yes	Yes
2	SF3	250	0	Standard	No	Yes
2	SF8	250	0	Standard	Yes	No

The in first sample set SF6 and SF7, sample SF6 experienced two large spalls while SF7 spalled in one location with some minor aggregate spalling elsewhere. The more

severe spalling occurred in the sample SF6 that did not contain reinforcement. The same conclusion can be drawn for the second set of direct comparisons with SF3 spalling while SF8, containing reinforcement, did not spall.

In both of the direct comparisons, the presence of reinforcement was observed to reduce the spalling. It should be noted that this might not be the case for other reinforcement configurations or mix designs. In addition, these samples were unloaded and would not have experienced self-weight as they were positioned on the furnace floor.

4.10 Results – through-thickness temperatures

The primary outcome desired from the test series was to establish through-thickness temperature versus time profiles for the concrete as tested in the furnace tests. These in depth temperature versus time profiles can then be used as inputs to an inverse model to create an incident heat versus flux time curve that corresponds to this thermal exposure experienced by the samples when tested during the Prometheus furnace tests.

Determining the through-thickness temperatures to use for the model input was challenging as thermocouple failure and thermocouple placement accuracy combined with spalling meant that much of the data recorded was unsuitable. The following sections give an overview of how the temperature data was analysed and selected as a basis for future testing.

It was decided that averaging the temperatures artificially removes any more severe exposures, and it was thought important to select credible through-thickness temperatures representative of the worst case thermal exposure experienced in each furnace test. Rather than averaging, the approach to thermocouple tree selection was qualitative, with visual comparisons made between the measured through-thickness temperatures over different thermocouple trees. The selection process is described in the following sections and Chapter 7 provides analysis of the influence of thermocouple placement accuracy on the theoretical range of temperatures.

4.10.1 ISO 834 Prometheus furnace test

In the ISO test data was recorded both by CERIB on their logging system and by an additional data logger from The University of Edinburgh. Instrumentation included:

- 18 plate thermometers used to control the furnace
- 14 point thermocouples located 100mm below the samples.
- 336 thermocouples located in 60 trees inside the samples.

Both data loggers were set to record temperatures at 1 second intervals. Since there was no extensive spalling or damage to the thermocouples during the testing, the data from the different thermocouple trees across all the samples can be compared. If this is done by depth then the temperature time curves can all be compared clearly. Starting with the 1mm graphs shown in Figure 4.33.

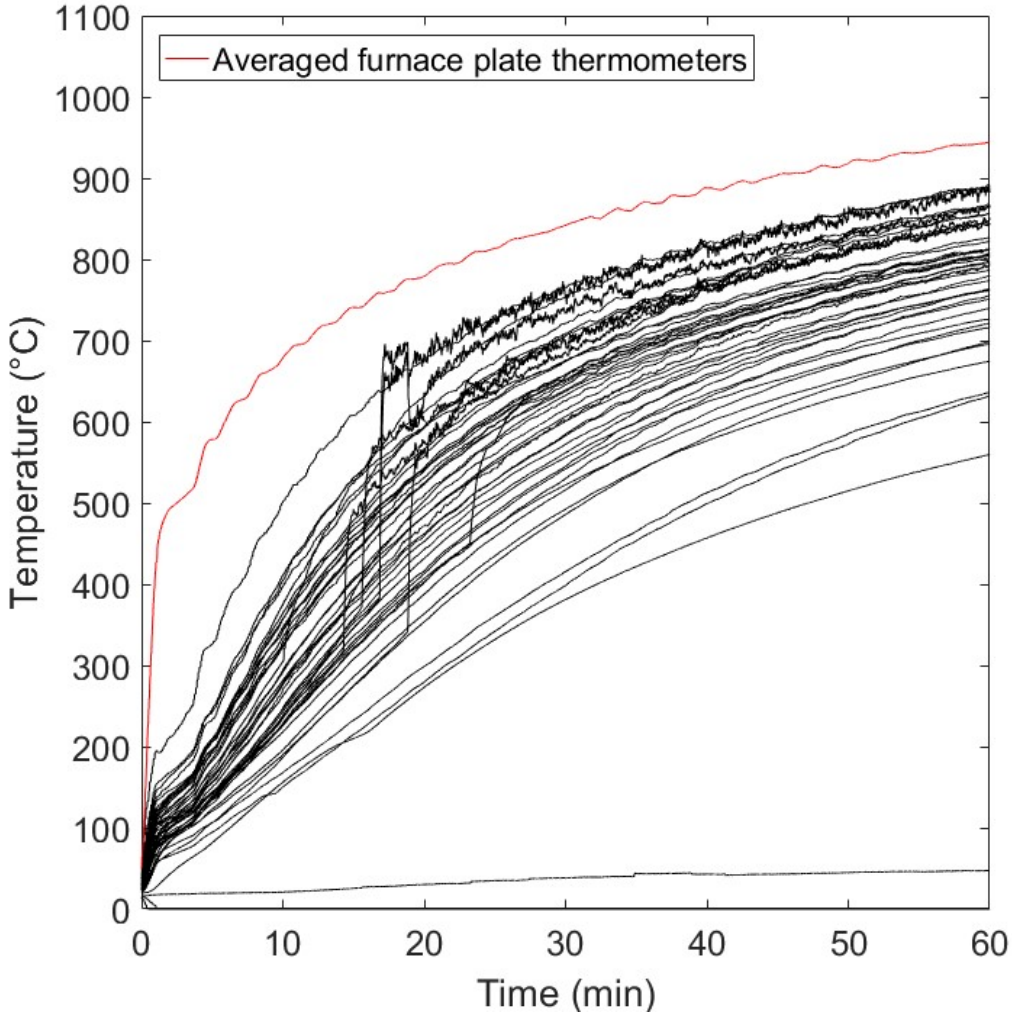

Figure 4.33: Temperature data recorded in ISO 834 Prometheus tests at a target thermocouple depth of 1mm

Figure 4.33 shows all the data for thermocouples at 1mm depth in the samples. The occurrence of spalling can be seen where the temperature time curve spikes and suddenly starts to read a much higher temperature. It can also be seen that some of the thermocouples give results that are much lower than others. This has been attributed to the thermocouple trees becoming dislodged during casting of the samples. When these lower readings are compared to others, they correspond to a temperature profile observed for thermocouples located at a depth of around 20mm. It can also be seen that some of the thermocouples were too close to the surface and are likely measuring gas temperatures although the temperatures measured remain below the averaged plate thermometer temperatures. The rapid fluctuation in temperature readings is not possible within a sample of concrete.

The spalling time at different thermocouple tree locations can be approximated based on the spikes in temperature readings. The approximate spalling times at the thermocouple tree locations can be determined as shown in Table 4.28. It is important to note that spalling close to a thermocouple tree could alter the temperatures recorded in depth yet may not cause such a sudden spike as when the thermocouple is suddenly exposed to the gas temperature of the furnace.

Table 4.28: Spalling times in the ISO 834 Prometheus test at thermocouple tree locations based on temperature measurements

Thermocouple Tree	Spalling Time (min)
P6E*	10.08
P8A	16.87
P8B	16.87
P8C	18.85
P10A	15.6

For the purpose of identification, the thermocouple trees have been named. The naming convention can be explained by providing an example. Thermocouple tree P8A refers to thermocouple tree A within sample P8. Where an asterisk is used, as in the case of P6E* above, the thermocouple tree comprised of Inconel thermocouples. In some cases there is an asterisk and non-asterisk variant. These are located next to each other.

The temperature readings after the occurrence of spalling were removed as well as the readings for thermocouples from trees that appeared to have been dislodged from their desired position during casting. These were identified as thermocouple trees P1C, P1B, P6B, P6D, P6I*, P9B, P10B, P11D. The selection of these outliers, while somewhat arbitrary, was done qualitatively by comparing the temperature versus time curves. Comparison between the remaining temperatures are shown in Figure 4.34.

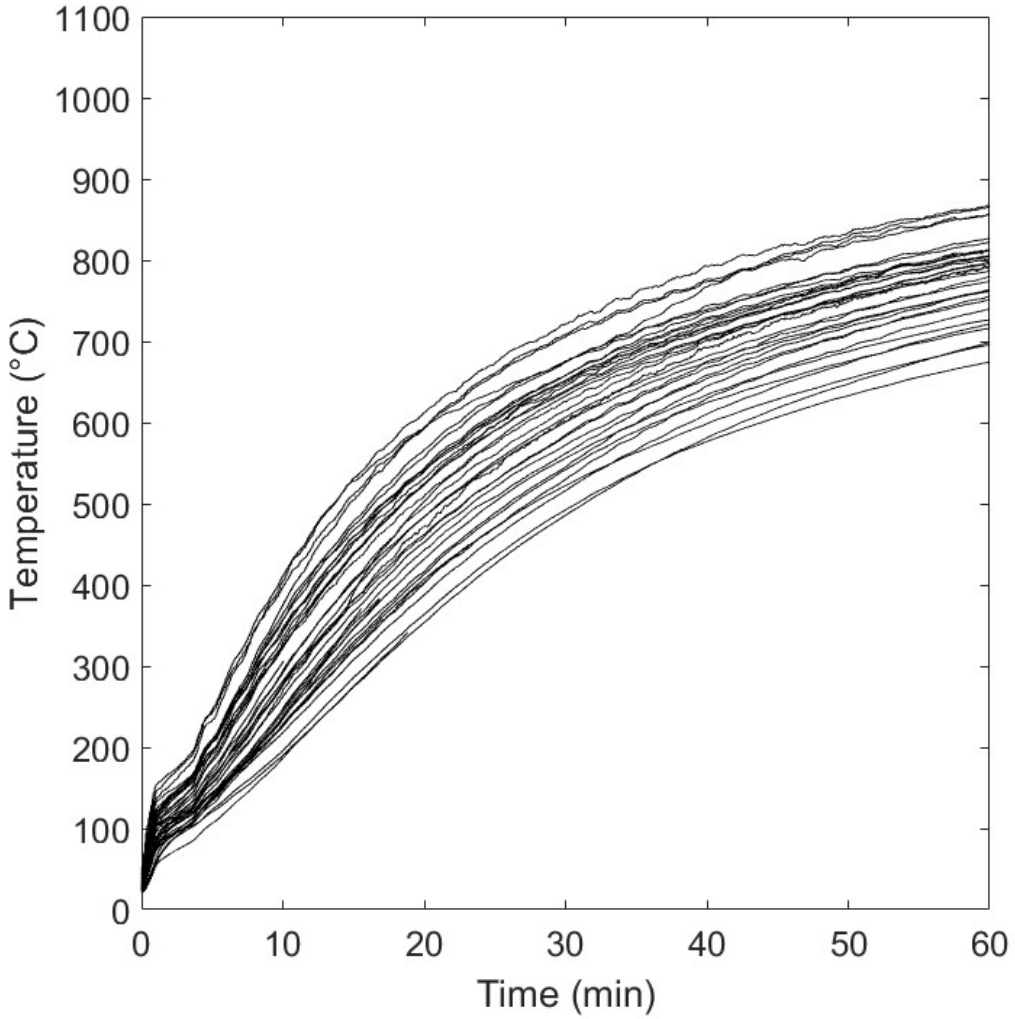

Figure 4.34: Temperature data recorded in ISO 834 Prometheus tests at a target thermocouple depth of 1mm – cleaned data

The same process of data cleaning was followed for thermocouples at other depths. Data was removed after the estimated time of spalling from those thermocouple trees affected and the trees that were believed to have moved considerably during casting were also removed.

It is noteworthy that there remains a large range of temperatures within this cleaned data. The spread in data could be a result of both different thermal exposure and errors in thermocouple placement, it is not possible to separate these. It was therefore not felt appropriate to further reduce this data based on an assumed parameter or opinion. Presentation of the data as shown provides an honest depiction of the range of “sensible” data and the precision achieved in thermal exposure and placement. If

tests are carried out with fewer thermocouples this kind of data spread is not seen. The cleaned data for 5mm depth can be seen in Figure 4.35.

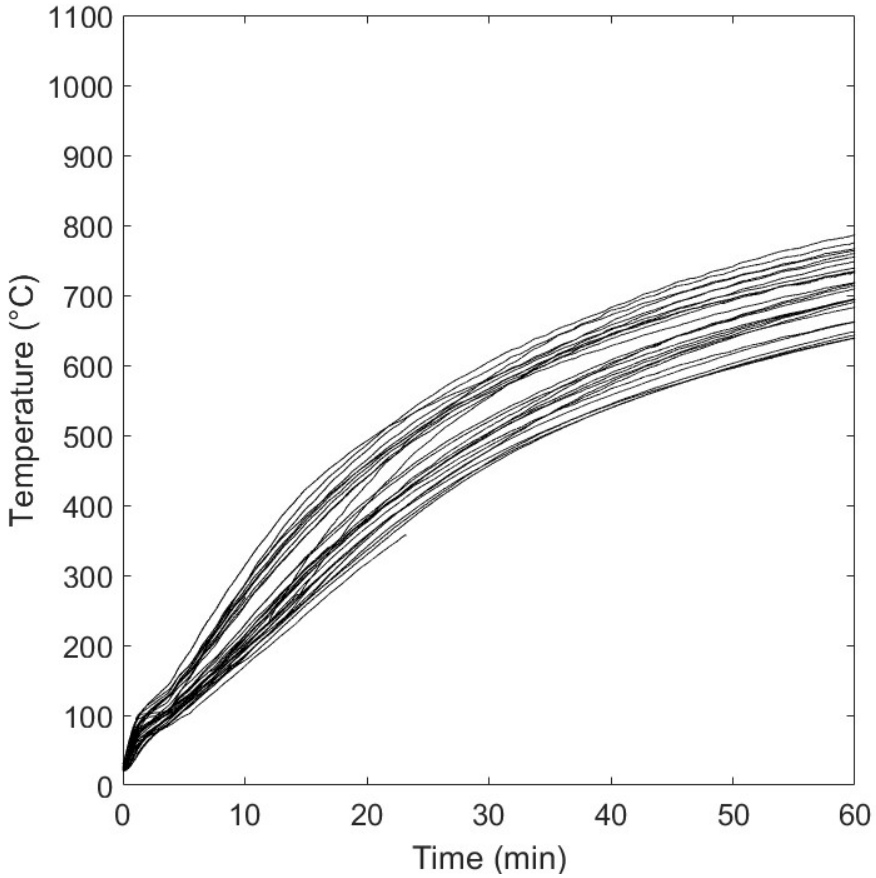

Figure 4.35: Temperature data recorded in ISO 834 Prometheus tests at a target thermocouple depth of 5mm – cleaned data

The decision of which thermocouple data to use for further testing was based on the data from the 5mm thermocouples. Thermocouples located at 1 mm depth were very challenging to place and, due to the thermal gradient close to the surface, a small error in positioning has a greater influence on the temperatures recorded than further in depth. This issue is a constant throughout the experimental work reported in this thesis, the temperature range associated with placement is assessed in Section 7.3. At a time of ten minutes at a depth of 1 mm the expected range of temperatures associated with a thermocouple placement accuracy of ±0.5 mm is around 30°C. At a depth of 5 mm this reduces to around 20°C.

It was seen in the tests that a more severe thermal exposure provided a worse case test environment for spalling than a gentle thermal exposure. While wishing to be able to replicate the ISO 834 thermal exposure it was also desirable for the thermal

exposure replicated to be a severe example of the thermal exposure experienced during the ISO 834 furnace test. The thermocouple tree P2A, which is thermocouple tree A of sample P2, was chosen as all of the thermocouples appeared to have remained in the correct location, based on the spread of data from the other trees, and they were on the more severe side of the spread of temperatures. Thermocouple tree P2A recorded some of the highest through-thickness temperatures at 5 mm particularly in the early stages of the test and, when compared, the thermocouples located at other depths in tree P2A also gave sensible results. The data from thermocouple tree P2A at a depth of 5 mm is highlighted in Figure 4.36.

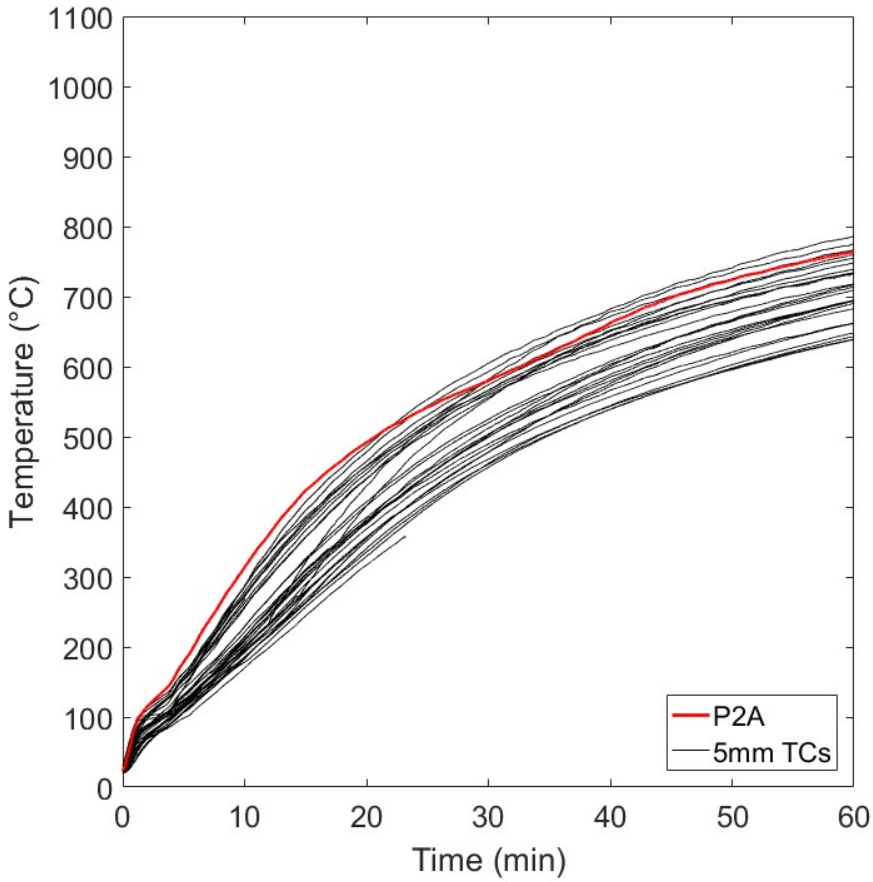

Figure 4.36: Temperature data recorded in ISO 834 Prometheus tests at a target thermocouple depth of 5mm – cleaned data, thermocouple P2A highlighted

The thermocouple tree selected is also located in one of the sample types that did not spall in the HCM furnace test meaning that the data chosen for both the HCM and ISO tests could be for the same concrete mix with the same strength, age, moisture content, thickness and geometry.

The full temperature data for the thermocouple tree selected is shown in Figure 4.37

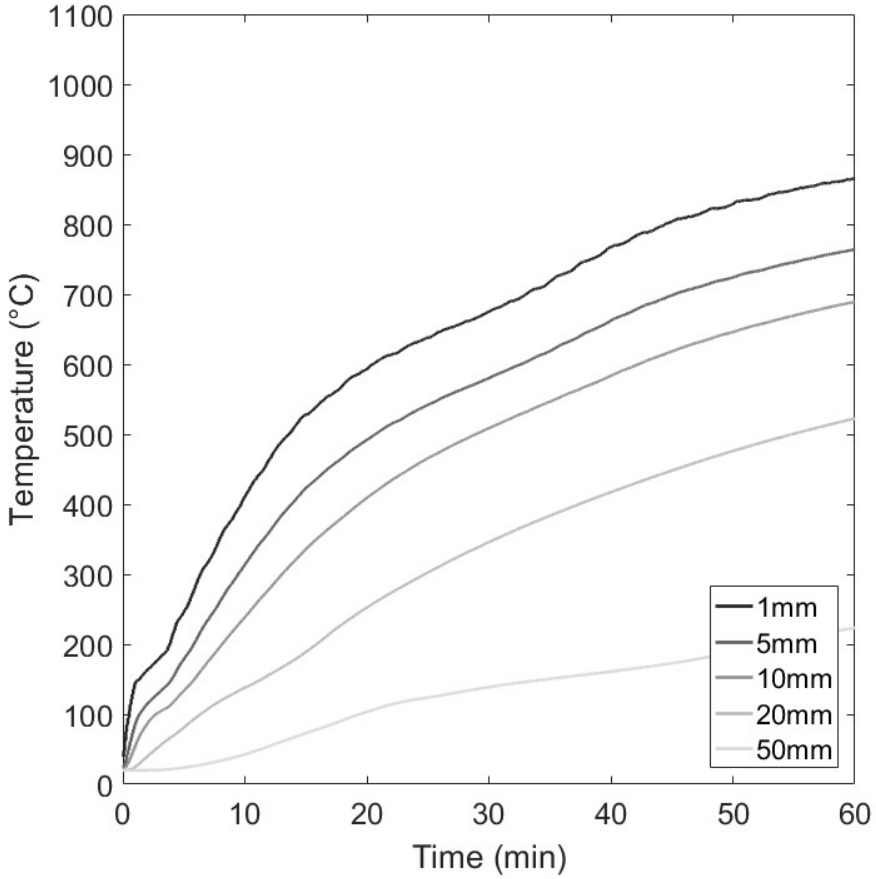

Figure 4.37: Temperature data at different target depths for the thermocouple tree P2A in the ISO 834 Prometheus furnace test

4.10.2 HCM Prometheus furnace test

The process for selecting which temperature data to use to replicate the HCM thermal exposure was similar to that described for the ISO 834 exposure except that a lot of spalling occurred in the furnace test. Therefore, there was less complete data to select from.

During the HCM test, there was a problem with one of the data loggers meaning that data was only obtained from 42 of the 57 thermocouple trees installed. This problem meant that some of the samples did not have any working thermocouples within them and also that there were no point thermocouples within the furnace.

The instrumentation left after the data logger fault included:

- 18 plate thermometers used to control the furnace
- 244 thermocouples located in 42 trees inside the samples

During the testing there was a large amount of spalling and the extreme temperatures caused many of the plate thermometers controlling the furnace and thermocouples located within the samples to fail. The raw data from the plate thermometers is plotted in Figure 4.38 as well as the HCM temperature versus time curve and the allowable limits for temperatures (CETU, 2017). This raw data for thermocouples at a target depth of 1mm from the sample surface can be seen in Figure 4.39 along with the HCM curve for reference. The spalling, broken thermocouples and thermocouples that are out of place are shown.

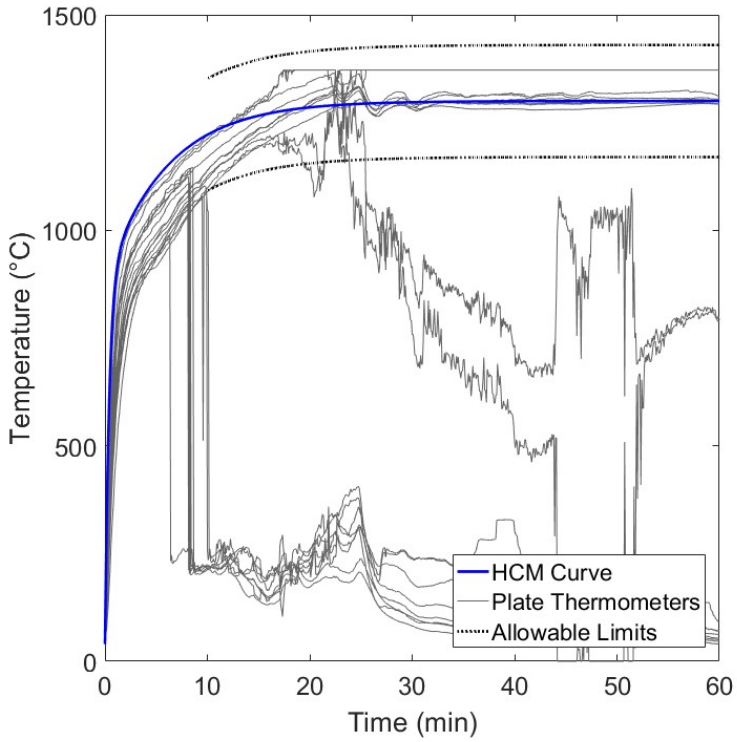

Figure 4.38: Raw data from plate thermometers in the Prometheus HCM test. HCM curve and allowable limits for temperatures also shown

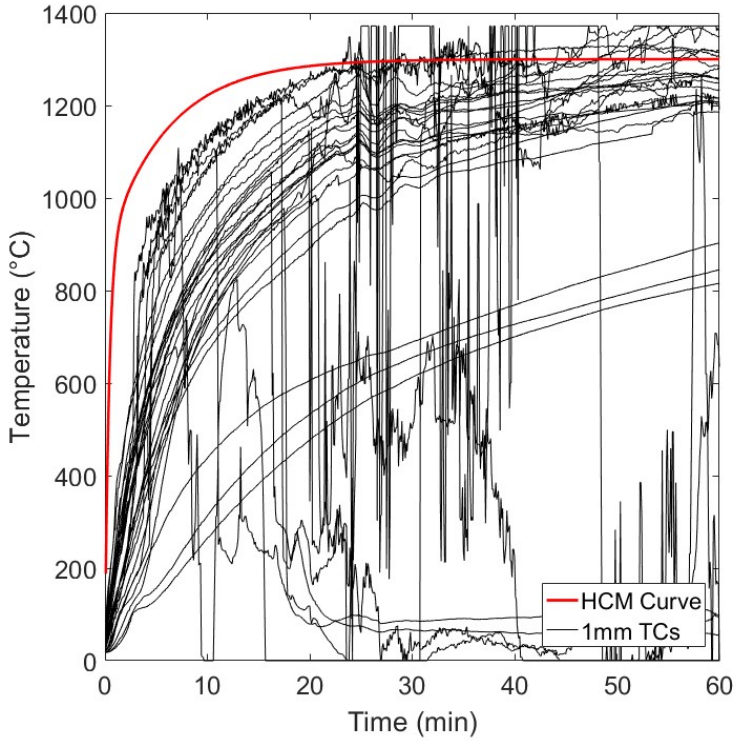

Figure 4.39: Raw data from thermocouples at a target depth of 1mm in the Prometheus HCM test. Red Line indicating HCM curve

During the test, most samples experienced extensive spalling over their entire surface. Of the large samples, only samples P1 and P2 experienced almost no spalling. Focus was shifted to the thermocouple trees in samples P1 and P2, as the purpose of this analysis is to obtain representative through-thickness temperatures for the duration of the test. This means the thermocouple trees selected must be located in an area were spalling did not occur. It is not possible to create a full heat flux versus time curve for a location where unquantified spalling occurred during the furnace test.

Given that the severity of thermal exposure is a parameter which influences spalling it is important to ensure that temperature data chosen from the unspalled samples is comparable with the initial pre-spalling temperature data for the samples that did spall. It is possible that these samples that did not spall received a less severe thermal exposure and that was an influencing factor in their not spalling. It is important to check this was not the case. The heat flux versus time curve created should be representative of the thermal exposure experienced by all samples when tested to the HCM curve in the Prometheus furnace not just the least severe exposure.

The data for thermocouple trees located in samples P1 and P2 was compared in a similar way to those of the ISO test. All of the data from these samples is shown in Figure 4.40. After extensive comparison of the data from the thermocouples, it was apparent that thermocouple trees P1B, P1C, and P2C moved deeper into the samples. Thermocouples at 1mm depth in trees P2A and P1A appear to have broken and the 20mm thermocouple in tree P2E had been bent close to 10mm depth based on the readings. As a result, these thermocouples were removed.

Figure 4.41 shows the thermocouples removed and Figure 4.42 shows the thermocouple of P2E which appears to have been dislodged, recording temperatures close to those of the 10mm thermocouples. Plotting the remaining thermocouples as shown in Figure 4.43 shows the variation in the results.

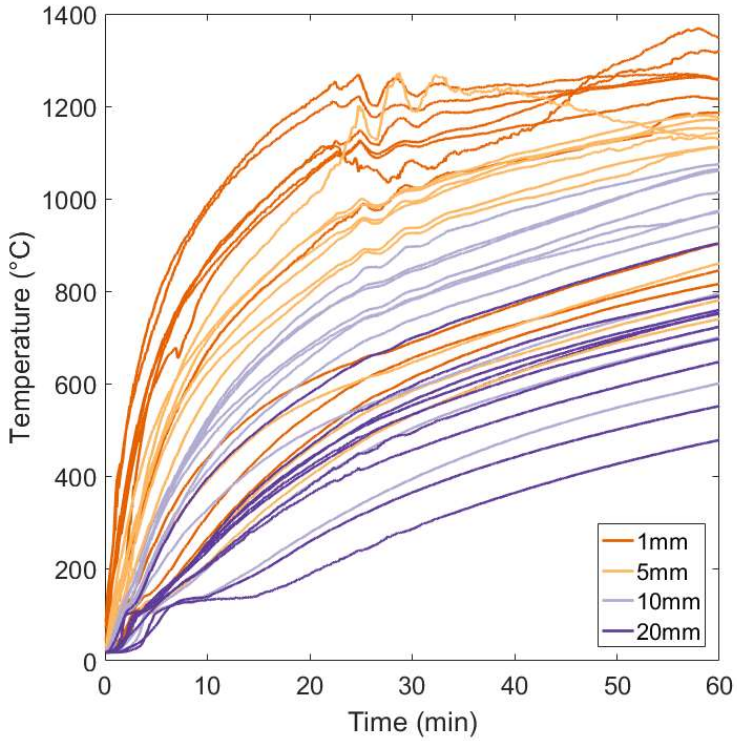

Figure 4.40: Raw temperature data from samples which did not spall in HCM Prometheus test

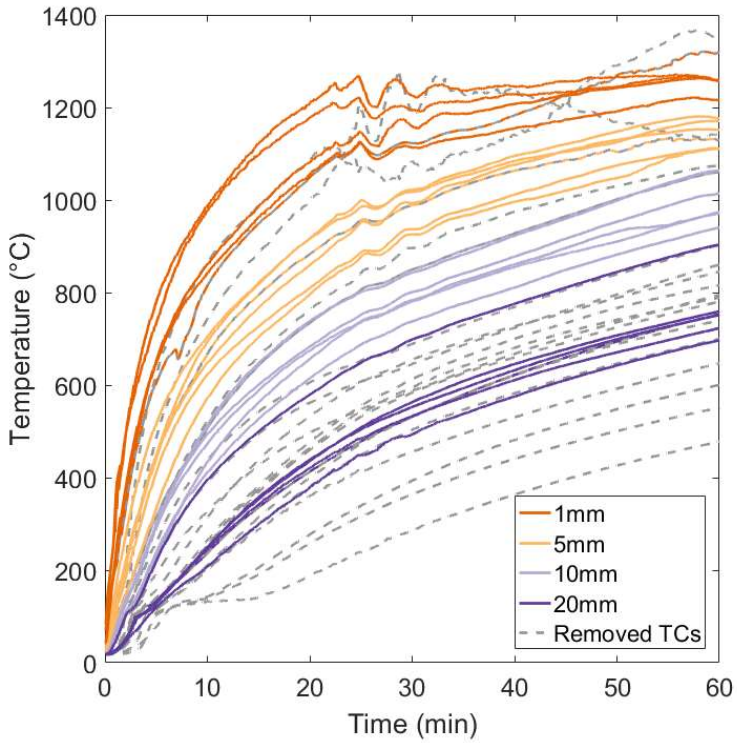

Figure 4.41: Temperature data from HCM Prometheus test showing thermocouples retained and removed.

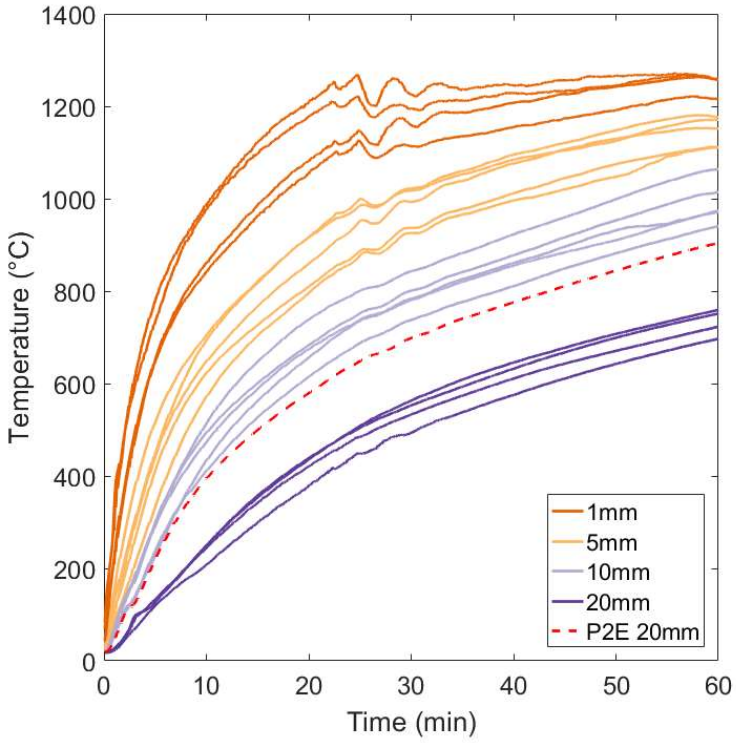

Figure 4.42: P2E 20mm thermocouple highlighted within temperatures from selected thermocouples

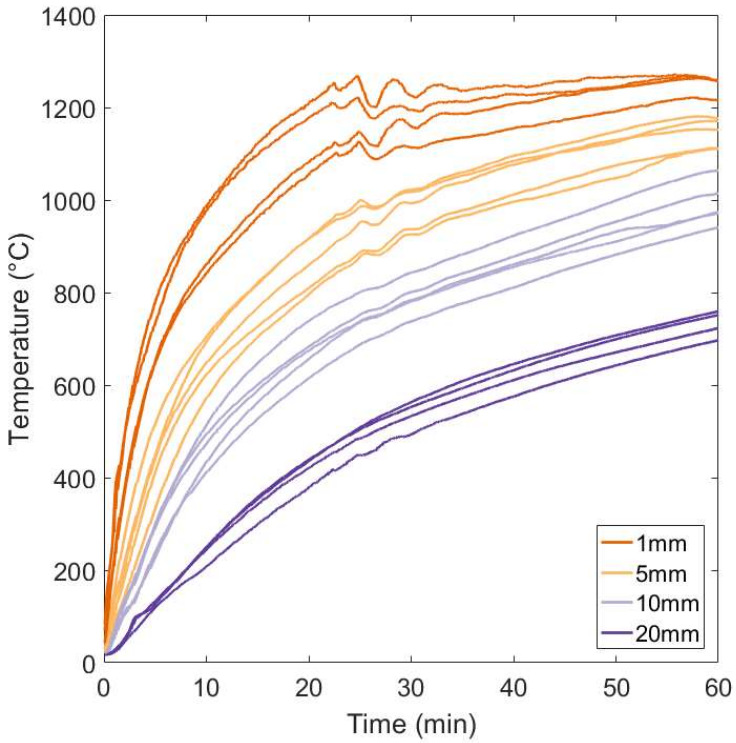

Figure 4.43: Temperature data from HCM Prometheus test for selected thermocouple trees located in samples that did not spall

The thermocouple trees shown in Figure 4.43 are P1D, P1E, P2B, P2D and P2E. It is interesting to note the drop in temperature at around 25 minutes. In this case this is taken to be a real drop in temperature as it is recorded across all the thermocouples at a target depth of 1mm and can be seen influencing the temperatures recorded at a target depth of 5mm. It is also shown in the plate thermometer data shown previously in Figure 4.18. This is a result of the furnace not following the temperature versus time curve accurately.

Based on comparison of the data, thermocouple tree P1E was selected to use for inverse modelling. The temperatures recorded are in the upper range for the HCM exposure and all of the thermocouples appear to have remained in the target location. The temperatures from tree P1E are shown in Figure 4.44 and compared against the cleaned data from all the thermocouple trees in Figure 4.45 to Figure 4.48. The temperatures recorded at thermocouple tree P1E at the target depths of 1 mm and 5 mm are some of the highest and above those recorded by thermocouples in samples that spalled. This means that the thermal exposure experienced by sample one at the location of tree P1E should be no less severe than that experienced by samples that spalled.

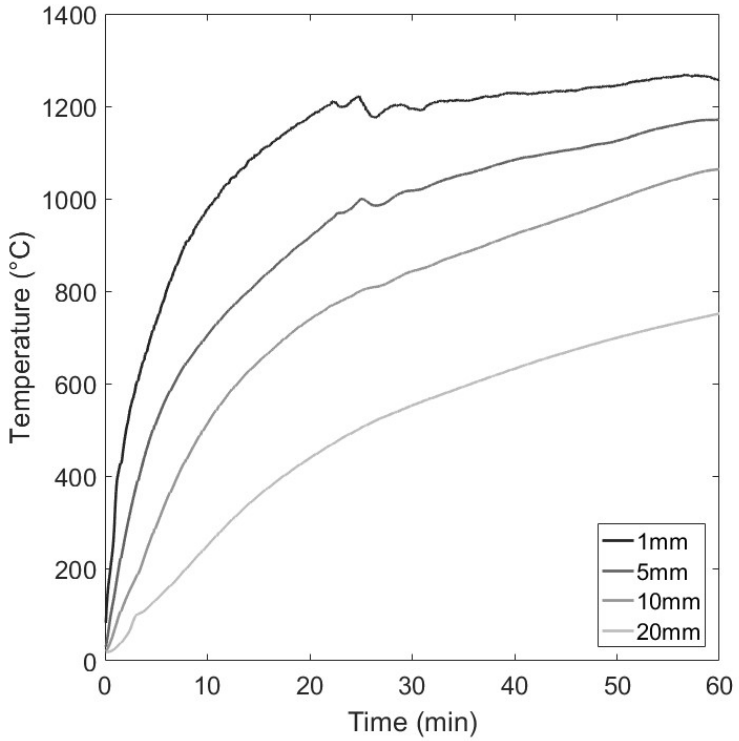

Figure 4.44: Temperatures recorded in Prometheus HCM test for thermocouple tree P1E

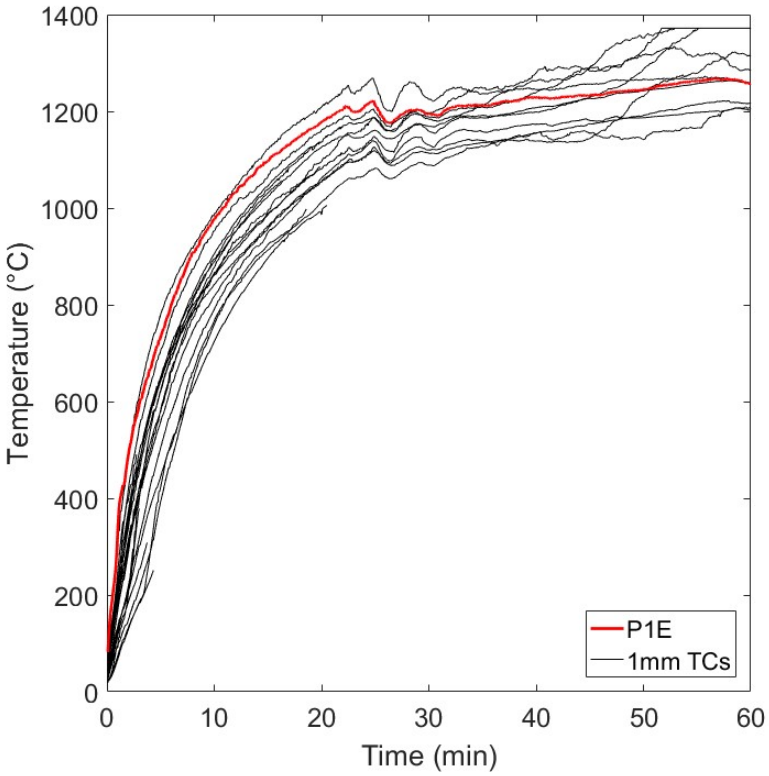

Figure 4.45: Cleaned thermocouple data for thermocouples at a target depth of 1mm in Prometheus HCM test. Thermocouple from tree P1E highlighted.

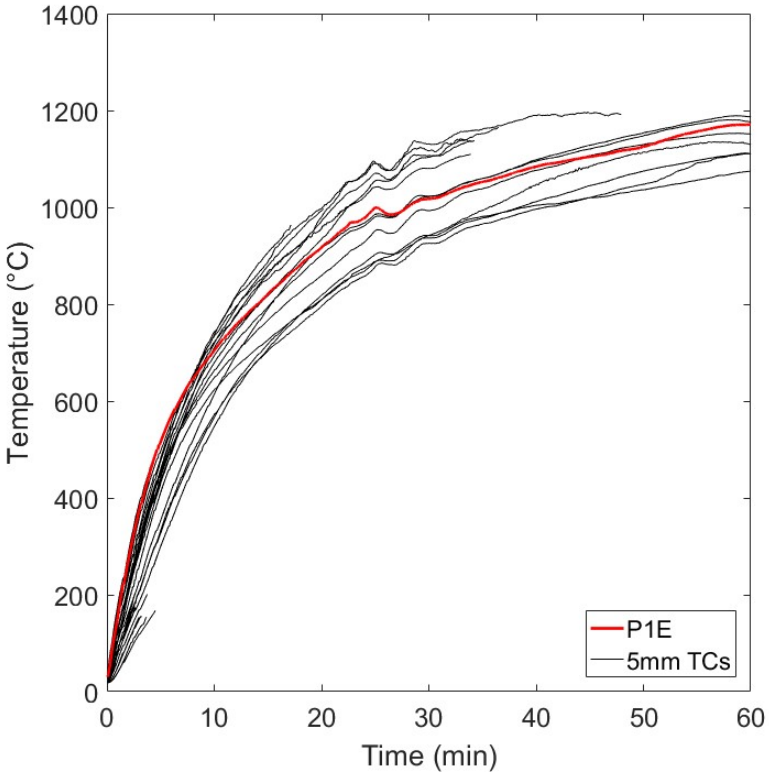

Figure 4.46: Cleaned thermocouple data for thermocouples at a target depth of 5mm in Prometheus HCM test. Thermocouple from tree P1E highlighted.

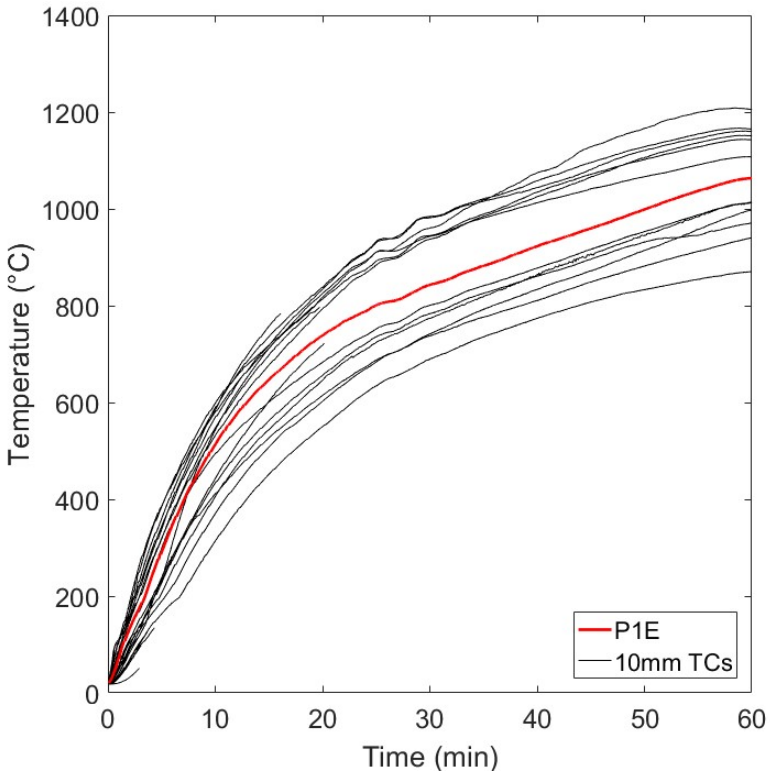

Figure 4.47: Cleaned thermocouple data for thermocouples at a target depth of 10mm in Prometheus HCM test. Thermocouple from tree P1E highlighted.

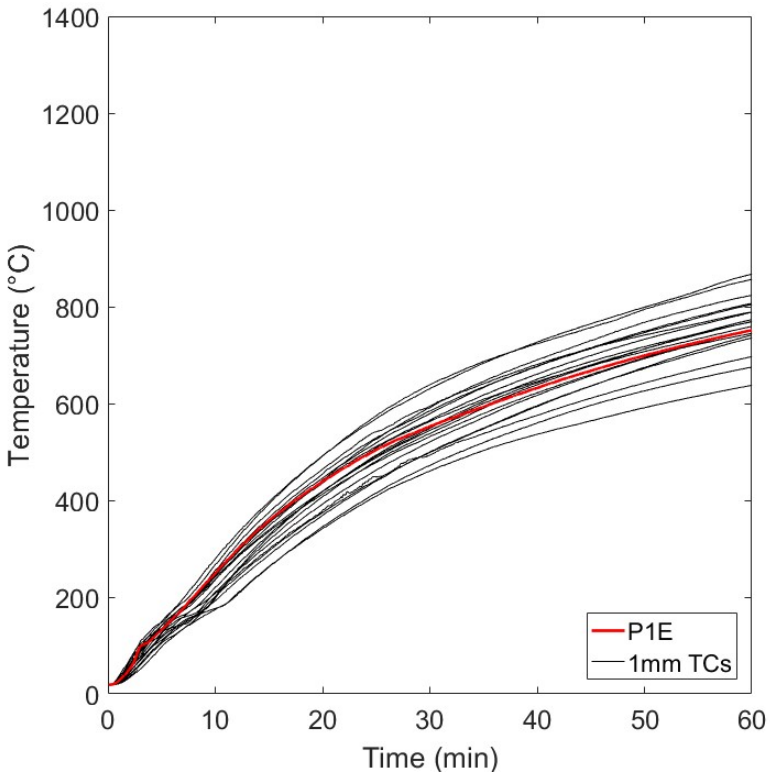

Figure 4.48: Cleaned thermocouple data for thermocouples at a target depth of 20mm in Prometheus HCM test. Thermocouple from tree P1E highlighted.

Again, the dip in temperatures that is seen within the samples is a real temperature drop rather than a malfunction with the thermocouples. Looking at the data from the plate thermometers used to control the furnace shows a drop in the furnace temperature so the drop in sample temperature is logical.

4.11 Discussion

4.11.1 Polypropylene fibres

The 2 kg/m^3 of polypropylene fibres were able to reduce the risk of spalling in the HCM tests but were not sufficient to prevent all spalling. The dosage of 2kg/m^3 of PP fibres to prevent spalling is given in Eurocode 2 (British Standards Institution, 2005) and the guidance is not intended for use with temperature time curves other than ISO 834 (International Organisation for Standardization, 1999). It is however the case that manufacturers of tunnel segments use PP fibres with dosages in the region of, and lower than 2 kg/m^3 and demonstrate that for their test conditions and concrete mix the dosage is sufficient to prevent spalling. The testing described in this chapter demonstrated that it is not appropriate to assume that a fibre dosage of 2 kg/m^3 is sufficient to prevent spalling. Until our understanding of spalling has improved samples of a candidate concrete mix should be tested in conditions as close to those that the concrete will be faced with in its end use application and repeat tests should be carried out.

4.11.2 Sources of error

4.11.2.1 Samples

Whilst there was in principle only two different concrete mixes that were then cured in two ways, the samples had to be cast in three casts due to space limitations. Despite best efforts to ensure the same concrete mix was used each time there is likely to be some variation between casts. There is also a small difference in age between the samples of different casts. There does not appear to have resulted in any observable variation in spalling behaviour. There is some difference in the 28 day strengths and the moisture content of cylinders cast from different casts at the same time as the samples. The breakdown of the different concrete casts is shown in Table 4.2 in Section 4.4.3.

It is likely that the true location of thermocouples within the samples cast varied somewhat from the target thermocouple locations. For some of the thermocouple

trees it was clear from the much lower temperatures recorded during testing that the actual location of the thermocouple tree was far from the target location. In this case, the thermocouple tree was removed from the analysis. The difficulty arises when the thermocouples appear to be in a reasonable location based on the temperature data but may be just slightly displaced from the target depth. It is impossible to tell if a slight difference in recorded temperatures is due to slightly different thermal exposure to the sample within the furnace or due to inaccuracy with the thermocouple positioning. The positioning of thermocouples is discussed further in Chapter 7.

The temperatures recorded can also be influenced by spalling during testing. A small spall in close proximity to a thermocouple tree could lead to an effectively reduced thermocouple depth. When spalling results in a large loss of cover it is possible to see this in the temperature readings. In order to avoid error due to spalling the temperatures selected to be representative where from samples or areas of samples which were observed not to have spalled. It is possible that these samples received a slightly less severe thermal exposure and this played a contributing role in their not spalling.

4.11.2.2 Influence of the sample holder

The smaller samples were supported on all four edges by a concrete sample holder frame. This sample holder frame was protected using insulation board and when in position for testing the samples were effectively recessed by 130 mm. It was thought that this method of supporting the samples could have resulted in shadowing of the samples from the thermal radiation from burner flames during the early stages of the furnace test. The through-thickness temperatures used to calculate the incident heat flux – time curve used for testing was based on temperatures from the larger samples in the furnace so should be more representative and unaffected by this shadowing. The spread of data and thermocouple placement issues, as discussed previously, mean it is not possible to quantify this shadowing effect. Figure 4.49 shows the area of the furnace where the smaller samples were supported and Figure 4.50 shows the small samples in their support frame.

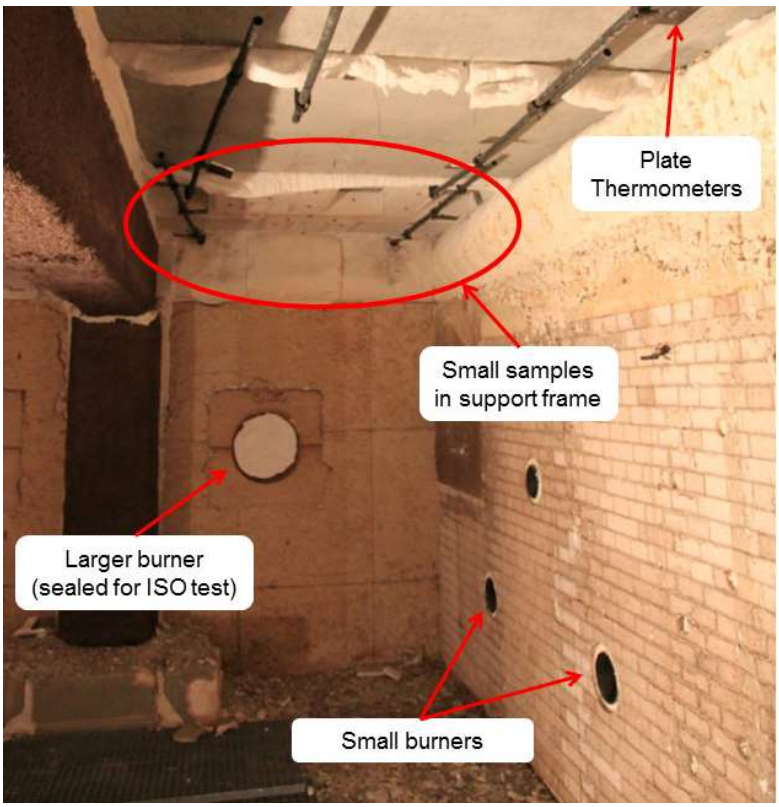

Figure 4.49: Inside of Prometheus furnace showing the location of the small samples relative to the burners

Figure 4.50: Small samples supported over Prometheus furnace

The edges of the support frame have a down stand of 130mm that is enough to shield the samples from having clear visibility of the burners, particularly the small burners located along the long side of the furnace. The method of supporting the small

samples during the tests could have had an influence on the concrete behaviour. In these furnace tests, it was however not possible to support so many small samples in any other way given the short amount of time available. Further repeat testing with a different sample configuration would allow greater confidence in the results from the small samples.

4.11.2.3 Small furnace direct flame impingement

The staff at CERIB had concerns over the possibility of direct flame impingement on the samples in the small furnace test. If there was not direct flame impingement on the sample, it is likely that the flames from the burners were close enough that the heating was more severe for those samples than the others during the early stages of the test when the radiation from the burner flame is a key component of the heat transfer. It was of the opinion of CERIB that the small furnace tests results be discounted based on this presumed direct flame impingement. The results of these tests have been included in the comparison but it is important that this issue is not forgotten. Spalling behaviour may not have been seen if the furnace arrangement was different, however; the results do seem to agree with those from the Prometheus testing.

4.12 Concluding remarks

This chapter described four furnace tests carried out at CERIB in France. The primary goal of this testing was to obtain through-thickness temperatures for the tests in order to be able to recreate the thermal exposure at The University of Edinburgh. Through-thickness temperature profiles were obtained for both the ISO 834 and HCM standard temperature versus time curves. This temperature data will be used for testing for the rest of this project.

A total of 36 samples were tested and various parameters were varied between the samples. It is possible to draw the following conclusions from the testing although due to the variability in spalling performance, which has been seen with repeat testing since, caution should be taken with the use of the results. It is also important to note that these conclusions only apply to the concrete that was tested and only in the test conditions it was tested in. Other concrete mixes that are tested in other test apparatus are likely to perform differently.

- The more severe HCM curve was a worse case for spalling than the ISO 834 curve for the tests carried out in the Prometheus furnace.
- The 250 mm thick samples are more prone to spalling than the thinner 100 mm thick samples
- The addition of 2kg/m3 of PP fibres can reduce spalling but is not necessarily enough to prevent spalling when testing to the HCM curve. It is recommended in the Eurocode as a method for avoiding spalling when testing/designing to the ISO 834 temperature time curve and not the HCM temperature time curve and these results show that it is not a definite solution to spalling.
- Reinforcement bar had a positive influence on spalling with samples identical, apart from the presence of reinforcement, spalling when no reinforcement was present and not spalling when reinforced.
- The moisture content was controlled in these tests by altering the curing conditions. It is unclear whether increased moisture content provides a worse case for spalling; the results of the samples that could be compared were inconclusive. Three sets of samples suggested that the increased moisture content increased spalling. The other three comparisons suggested the opposite was true.

- The need to carry out repeat testing and be cautious when analysing spalling results was demonstrated by the variation in spalling performance with moisture content.

It is difficult to make any conclusions about the influence of the sample size on spalling. In the tests that allow a direct comparison of the influence of sample size there is not a clear worst case sample size for spalling. It is encouraging for ease of future testing that it seems possible to assess the spalling propensity of a concrete by testing a small sample. Between the two thicknesses tested, thickness of a sample had a greater influence on spalling in these tests than the sample size.

4.13 Recommendations and further work

Since it was not possible to carry out multiple repeats of these tests, it would be desirable to repeat this work to test the validity of the conclusions made. It is also of value to investigate the performance of other concrete mixes tested in the same way. More recent work described in Chapter 6 has shown the potential variation of result with repetition.

One parameter that is believed to be important when assessing spalling is the loading/restraint. In these furnace tests, no load was applied to the samples during testing. This choice was so that the number of samples being tested could be maximised. Having carried out testing since these furnace tests it is believed that all tests should include representative/realistic load. Carrying out loaded tests in line with the tests described in this chapter would be a worthwhile addition to assess the influence of load. While it may influence the spalling behaviour, it would not influence the thermal exposure. The characterisation of thermal exposure was the primary goal of these tests.

Positioning so many thermocouples accurately when carrying out casting of samples on this scale is challenging. Great care must be taken at this stage and it would be worthwhile to carry out further testing with an improved system of securing thermocouples.

5 Phase 2 experimental work - establishing thermal exposures and H-TRIS experiments on CERIB samples

5.1 Summary

This chapter describes Phase 2 of the experiments undertaken as part of this thesis project, which was carried out using samples which were cast by the author at CERIB, France at the same time as the samples which were used in the large-scale furnace tests described in Chapter 4 (also performed by the author, in collaboration with CERIB). These samples were transported to The University of Edinburgh and tested using H-TRIS. Through-thickness temperatures recorded during the large-scale furnace tests at CERIB were used to determine the time-history of equivalent incident heat flux versus time curve. Comparison of through-thickness temperatures during the H-TRIS experiments allowed validation of the acceptability of the thermal exposure as a reasonable replication of the exposures to which samples were exposed within the Prometheus furnace tests at CERIB. The experiments presented in this chapter also allow some further comparison of the influence of some of the widely accepted key parameters on heat-induced explosive concrete spalling.

5.2 Introduction

The principal aim of Chapter 4 was to collect high-fidelity data on the through-thickness temperatures within concrete slabs during exposure to both standard cellulosic and hydrocarbon fire exposures, such that these could be used to calculate equivalent thermal exposures to enable testing in H-TRIS that would be comparable to the standard furnace testing which is widely carried out elsewhere. This chapter describes the second stage of that testing. Taking the through-thickness temperatures and calculating the equivalent heat flux versus time thermal exposures, and then undertaking experiments on samples of concrete, cast from the same batches as those of the CERIB samples, using the H-TRIS apparatus and methodology. The aim is to validate use of H-TRIS by comparison against both calculated through-thickness temperatures and between the two test methods. In addition, further investigation is undertaken into the influences of various key parameters on heat-induced explosive concrete spalling.

5.3 Inverse modelling to determine heat flux versus time curves

An inverse heat transfer model, developed by Dr Cristian Maluk in his PhD under the supervision of Professor Luke Bisby at the University of Edinburgh, was applied in an attempt to determine the incident heat flux versus time curves to be using H-TRIS that would produce the same temperature time histories as those recorded during the large-scale furnace tests at CERIB. This inverse model is described in detail in Cristian Maluk's doctoral thesis (Maluk, 2014); only a summary of the model is presented here.

The author did not develop or contribute to this model and does not have access to the model to carry out further analysis or sensitivity assessments. The model has previously been validated allowing thermal exposures experienced by samples in furnaces to be recreated using the original H-TRIS heating apparatus. Comparison of through-thickness temperatures measured in samples tested by Cristian Maluk in furnace tests at EMPA and at The University of Edinburgh showed an impressive agreement between the target and achieved through-thickness temperatures and hence thermal exposures (Maluk, 2014). The sensitivity assessments carried out by Maluk are documented in full in his PhD and reproduction of selected figures here was not deemed appropriate. If the reader would like to understand the details of this model they should consult Cristian Maluk's thesis for a complete account.

Inverse models are not direct and solutions may not be unique. The inverse model calculates potential curves of absorbed heat flux versus time that would yield close approximations to the through-thickness temperatures measured in the samples during furnace tests.

These potential curves are then assessed using a conventional finite difference model and the optimum heat flux versus time history is selected from a number of potential curves by comparing the theoretical resultant through-thickness temperatures with those measured in testing.

Once an appropriate absorbed heat flux versus time curve has been determined, the incident heat flux versus time curve required to recreate this time history of internal temperatures using H-TRIS is determined by taking into account the heat losses at the surface of the sample when subjected to an incident heat flux from H-TRIS. This is done using empirical, temperature dependent correlations (Incropera *et al.*, 2013).

The thermal properties for concrete used in this analysis are those suggested within the French National Annex of Eurocode 2 (AFNOR, 2007). These were used at the request of CERIB.

Using the temperature profiles recorded from testing in the Prometheus furnace at CERIB (see Chapter 4), the incident heat flux versus time curves shown in Figure 5.1 were determined. These curves were used as the inputs for the H-TRIS experiments presented in this chapter.

Validation of their appropriateness and reproducibility is undertaken through the testing and analysis given in this chapter. Note that after a time of 50 minutes the heat flux was approximated as constant. This period during the test was not thought to be of concern for spalling and in the case of the HCM equivalent curve is beyond the physical limits of the apparatus.

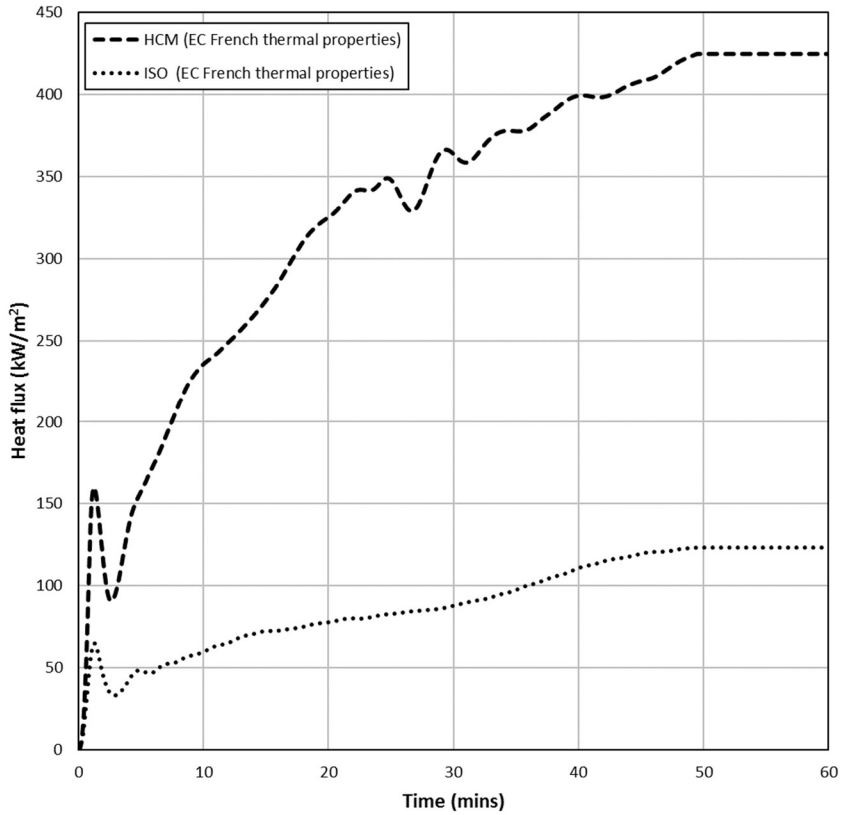

Figure 5.1: Incident heat flux vs time curves for the Prometheus furnace tests carried out to ISO 834 (International Organisation for Standardization, 1999) *and HCM* (Ministère de l'Equipement, 2000) *temperature versus time curves calculated using French Eurocode, EC, thermal properties* (AFNOR, 2007)

The accuracy of any heat transfer modelling is dependent on both the thermocouple placement and the appropriateness of any assumed thermal properties. Chapter 7 provides an assessment of the theoretical influence of different parameters on the recorded temperatures within concrete samples when subjected to these thermal exposures and provides some discussion on the predominant sources of error.

It should be noted that, with hindsight, the author does not believe that attempting to recreate the thermal exposures of a furnace test is the correct approach to experimental spalling research and would not recommend that this approach is taken in future. This is discussed in further detail in Chapter 8.

5.4 Experimental apparatus

The experiments described in this chapter were carried out at The University of Edinburgh using two different incarnations (and an extension) of the H-TRIS experimental apparatus and methodology initially developed by Dr Cristian Maluk during his PhD (Maluk, 2014). The apparatus is described in more detail in Chapter 3. A brief summary is repeated here. The primary advantage of the H-TRIS method is that the thermal exposure is highly repeatable and is controlled directly – in terms of incident heat flux rather than gas phase temperature.

The two different versions of H-TRIS used are called Mark 1 and Mark 2 and these are described in the following sections.

5.4.1 H-TRIS Mark 1

Mark 1 is the original H-TRIS apparatus developed by Dr Cristian Maluk (Maluk, 2014), and described in more detail in Chapter 3. The apparatus is capable of imposing a peak incident heat flux of around 100 kW/m^2. This allows testing to thermal exposures equivalent to the ISO 834 (International Organisation for Standardization, 1999) for up to 35 minutes, after which the maximum heat flux is reached, and the incident heat flux must be kept constant. This results in divergence between H-TRIS Mark 1 testing when compared with furnace testing, beyond about 35 minutes when simulating furnace tests carried out to the ISO 834 fire curve (International Organisation for Standardization, 1999).

A total of 24 concrete samples were tested using H-TRIS Mark 1 and are reported within this chapter. The H-TRIS Mark 1 setup used for the experiments described is shown in Figure 5.2. Because this experimental setup is ‘portable’, it was located

within the Structures Testing Laboratory at The University of Edinburgh. This allowed use of the overhead crane to move the comparatively heavy concrete samples.

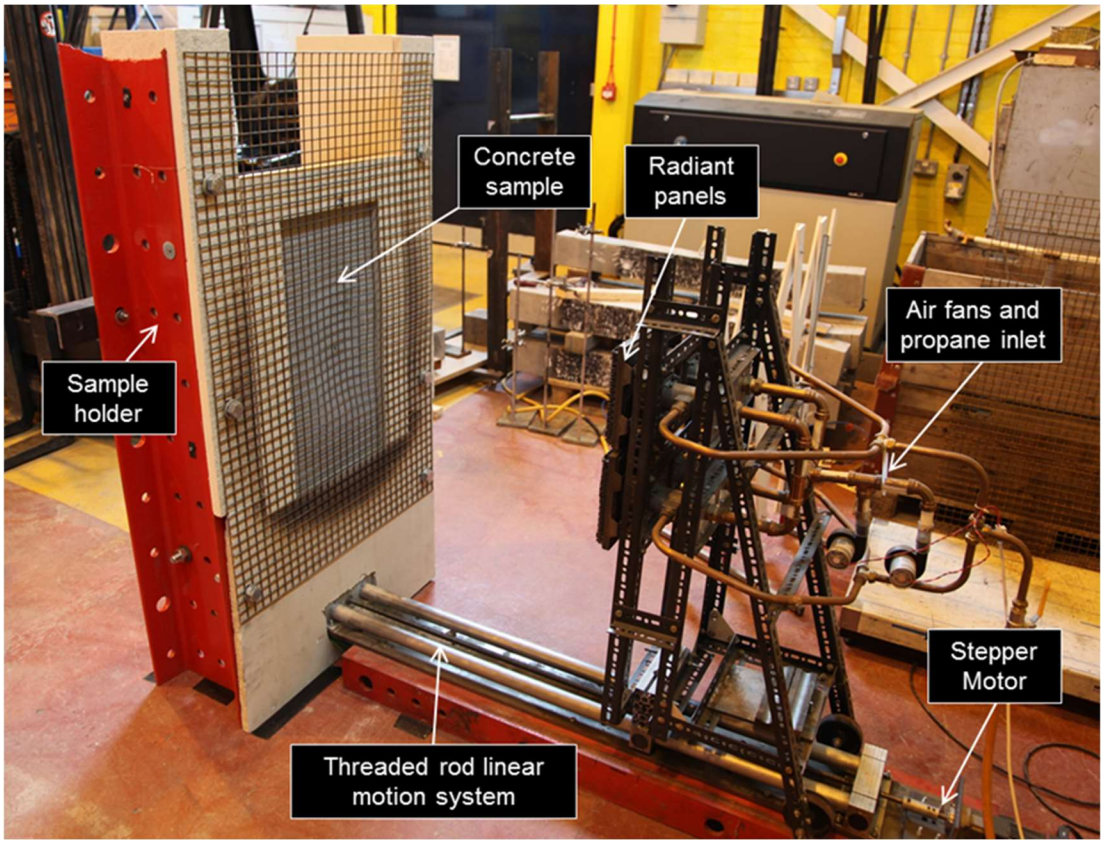

Figure 5.2: H-TRIS Mark 1, with unloaded concrete sample placed within the sample supporting frame

5.4.2 H-TRIS Mark 2

The original H-TRIS Mark 1 apparatus design was modified and improved upon to enable higher incident heat fluxes to be achieved at greater sample standoff distances. This new version of H-TRIS, referred to as H-TRIS Mark 2, was developed during the series of experiments presented in this chapter, along with a bespoke loading frame for Phase 3 experimental work. Chapter 3 describes the apparatus in more detail.

The use of higher output propane-fuelled radiant panels allows a peak incident heat flux approaching 300 kW/m^2, which means that it is possible (in theory) to simulate the same time-history of absorbed heat flux in a concrete sample as in a standard French modified hydrocarbon, HCM, furnace test (Ministère de l'Equipement, 2000) or other severe standard fire curves. The French modified hydrocarbon, HCM,

equivalent thermal exposure can be replicated for about 16 minutes before holding the heat flux at a constant level. This is as close as possible to the HCM standard furnace exposure as is possible to replicate with the current apparatus. It should be clear, with reference to Figure 5.1 above, that it is not possible to test to the equivalent HCM thermal exposure for any meaningful duration using H-TRIS Mark 1 (less than two minutes in fact).

A total of nine concrete samples were tested in H-TRIS Mark 2 and are reported within this chapter. The experimental setup used for the H-TRIS Mark 2 series of experiments is shown in Figure 5.3. This version of H-TRIS considerably larger and more massive than H-TRIS Mark 1, and is therefore permanently located within the Rushbrook Fire Laboratory at The University of Edinburgh.

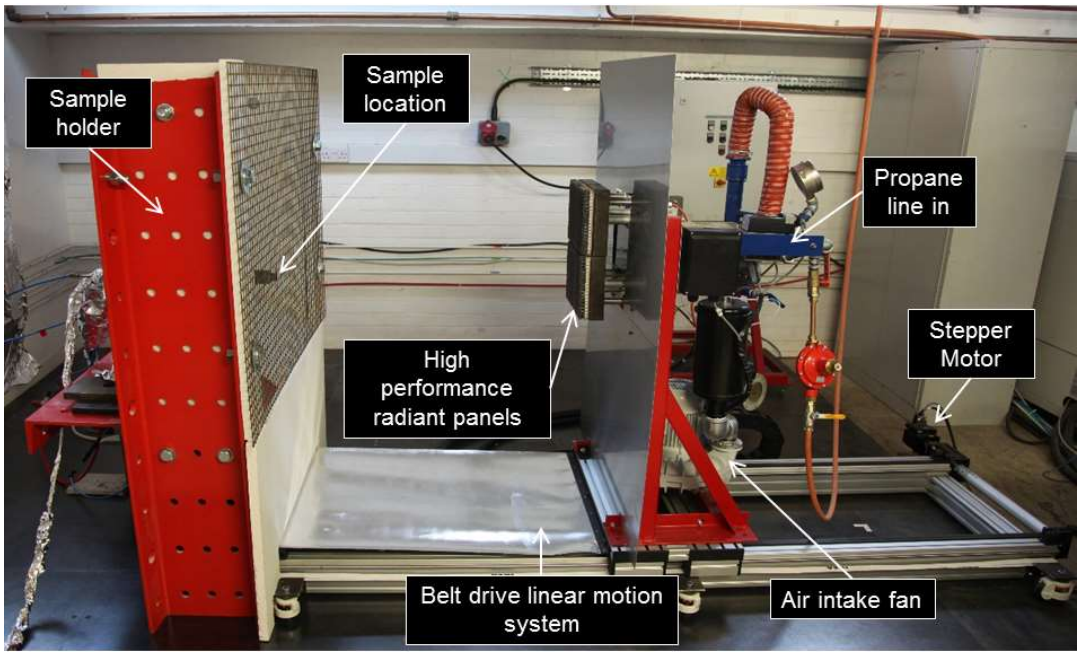

Figure 5.3: H-TRIS Mark 2 experimental apparatus with original unloaded sample holder

The same sample holder frame was used in both sets of experiments presented in this chapter, with some minor adjustments being made to simplify sample installation within the Rushbrook Fire Laboratory without the use of an overhead crane. These adjustments did not significantly influence the positioning of the sample during testing or the thermal exposures that it experienced. In both experimental setups, samples were aligned so that the centres of the samples were level with the centre of the array of radiant panels (i.e. with the vertex of the cross, formed by the edges of the four individual panels).

5.5 Sample preparation

The samples used for the experiments described in this chapter were cast at CERIB, France, alongside the samples used in the furnace tests described in Chapter 4. The samples were cast from the same concrete at the same time and instrumented in the same way. This section will summarise the sample preparation process.

5.5.1 Instrumentation

The samples were instrumented with the same thermocouple trees as the samples tested in the Prometheus and Small furnace tests which were described in Chapter 4 and shown in Figure 4.10. These thermocouple trees give in-depth thermocouples, within the concrete, at target depths of 1, 5, 10, 15, and 20 mm from the heated surface. For the samples to be used in H-TRIS experiments the thermocouple trees were positioned at the centre of the heated surface. All samples were cast in triplicate, but the centrally located thermocouple trees were present only in two of every three samples. This is both because of the time and cost associated with adding thermocouple trees to all of the already large number of experimental samples, and because it was decided that instrumenting two of three samples allowed sufficient confirmation of suitable thermal exposures. Omitting thermocouples from one of the samples in each set of three also allowed some assessment of the potential influence of the presence of the TC trees on spalling to be investigated.

5.5.2 Casting

In addition to the 36 samples which were tested in the furnace tests described in Chapter 4 a further 33 samples were cast at CERIB for experiments in H-TRIS. The concrete samples for this test series were all cast using the same batches as the samples used in the CERIB furnace tests. These casts took place on 13th December 2013, 20th December 2013, and 10th January 2014. The mix designs are as shown in Table 5.1. The mix design was undertaken by CERIB and meant to be representative of a typical concrete mix which might be used for manufacturing precast concrete tunnel lining segments. The only variation in the mix ingredients was the addition of the SikaFibre Antifissure[1] polypropylene, PP, fibres. These were added at a dosage

[1] Specific proprietary trade names are used in some places in this thesis. This is done purely for the purposes of factual accuracy, rather than as any endorsement of a particular manufacturer or supplier.

of 2kg/m^3 which is the dosage of PP fibres recommended in Eurocode 2 (British Standards Institution, 2005) to reduce spalling. Having some samples with PP fibres and some without allows their effectiveness to assessed. The fibre type was chosen by CERIB due to availability. Fibres were only added to the final cast on the 10th of January. The Sikaplast techno 7 plasticiser was specified as 0.7% by mass of cement, which equates to 3.05 kg/m^3. This is normally added in the range of 0.3% to 3% by mass of binder so this is a moderate dosage. The plasticiser was added to increase the concrete workability.

Table 5.1: Mix design for CERIB concrete casts (polypropylene fibres only added in one of the three batches)

Mix Ingredient	Quantity (kg/m^3)
Portland Cement CEM 1 52.5	435
Fine Sand 0/2	500
Sand 0/4	300
4/10mm Limestone aggregate	820
SIKAPLAST® TECHNO 7	3.05
Water	180
SikaFibre Antifissure 12mm Ø:34 µm	2

Ideally, all samples within a given spalling research study of the same nominal mix design would be cast together from a single concrete batch to ensure that the samples are as identical as possible. When a single batch cannot be achieved, as in the current project due to the large volumes of concrete involved and capacity of the local ready-mix suppliers in France, care must be taken to ensure that the same mix design is followed, including aggregate sources and size. Despite efforts to control variation, it is likely that the properties of the resultant concrete will not be precisely the same, and of course there will also be a small difference in sample age. Due to the short spacing between batches and the care taken to use the same aggregates, this variation was minimised. When the furnace tests were carried out on the same concrete there was no noticeable influence of the different concrete batches. The age difference at time of testing in these Phase 2 tests is affected more by the experimental setup times than by the time between concrete batches. A summary of which H-TRIS samples types were cast from which batch (at CERIB) is given in Table 5.2. All of the samples were cast in triplicate. The sample type names have no direct meaning and were decided by CERIB technical staff with the H indicating H-TRIS

sample and the numbers corresponding to the sample set. Sample type H1 consists of three samples; H1a, H1b and, H1c. The sample dimensions, curing conditions, and mix design (PP fibres or no PP fibres) vary between of the different sample types.

Table 5.2: Summary of specimens cast for Phase 2 experiments

Concrete Batch (Date)	Sample Type
Batch 1 (13/12/2013)	H1
	H2
	H3
	H9
	H10
	H11
Batch 2 (20/12/2013)	H4
	H8
	H12
Batch 3 (10/01/2014)	H5
	H6
	H7
	H13

5.5.3 Curing

The samples for experimentation within H-TRIS at Edinburgh were cured alongside the other large-scale samples that were tested within the Prometheus furnace at CERIB, and were then shipped to Edinburgh in June 2014 (some six to seven months after casting). During shipping the samples were sealed in plastic so as to avoid uncertainties in moisture content changes, once the samples arrived at The University of Edinburgh the outer plastic was removed and the samples were placed in a conditioning room.

In order to investigate the effect of curing condition of the samples (and thus pore moisture content), samples were maintained in both “sealed” and “unsealed” conditions. Samples to be tested after curing in a “sealed” condition were kept wrapped in plastic after shipping and up until the time of testing.

The conditioning room at Edinburgh was maintained at a target temperature and relative humidity of 20 °C and 50 % RH for the duration of the sample storage. The basic humidifier and dehumidifier setup is able to maintain this target temperature to within ±5 °C and the humidity to ±10 %.

5.6 Experimental programme

The test matrix for the Phase 2 samples is shown in Table 5.3. The numbering of samples is non-consecutive, since samples were numbered by technical staff at CERIB and the test program changed slightly as the work progressed. Sample types H9 and H10, which are listed in Table 5.2 but missing from Table 5.3, were used to test the functionality of the new H-TRIS Mark 2 apparatus but were not used for reportable experiments. It had been planned to undertake experiments on these samples under sustained uniaxial compressive stresses, however this was not possible due to delays in design and procurement of the loading frame (discussed in more detail in Chapter 3).

Table 5.3: Experimental programme for Phase 2 tests

Sample Type	**Size** (mm)	**Thickness** (mm)	**PP Fibre Dosage** (kg/m^3)	**Curing Conditions**	**Equivalent Thermal Exposure**
H1	350 × 350	100	0	Standard	ISO 834
H2	350 × 350	250	0	Standard	ISO 834
H3	750 × 450	100	0	Standard	ISO 834
H4	750 × 450	250	0	Standard	ISO 834
H5	750 × 450	100	2	Standard	ISO 834
H6	750 × 450	250	2	Standard	HCM
H7	750 × 450	250	2	Sealed	ISO 834
H8	750 × 450	250	0	Sealed	ISO 834
H11	350 × 350	250	0	Standard	HCM
H12	750 × 450	250	0	Standard	HCM
H13	750 × 450	250	2	Standard	ISO 834

These experiments allow direct comparison against the results from samples tested in the standard fire testing furnaces at CERIB. The samples tested are the same concrete cast at the same time, the only difference in the samples between the experiments presented in this chapter and those (of identical geometry) presented in the previous chapter is their age at the time of testing. Samples used in experiment at The University of Edinburgh were 150 to 350 days older depending on cast and experiment see Table 5.8.

5.7 Experiments

The Phase 2 experiments were all carried out at The University of Edinburgh using either H-TRIS Mark 1 or the enhanced H-TRIS Mark 2. This section provides details on the experimental procedures used.

5.7.1 Control of thermal exposure

The thermal exposure applied to samples during Phase 2 experimentation was controlled based on calibrations undertaken throughout the experimental series. These calibrations were carried out at the beginning of the series of experiments, and then at intervals during the series. This was typically every two to three experiments, or more often if spalling occurred resulting in possible damage to the radiant panels. Based on investigatory experimentation with both H-TRIS rigs, this was sufficient calibration to enable a high degree of confidence that the thermal exposure being applied was consistent between experiments and that any deterioration in the performance of the radiant panels was being corrected for on an ongoing basis.

The calibrations were carried out using a water-cooled Hukseflux Schmidt Boelter gauge. Details of the calibration and characterisation of the thermal exposure from H-TRIS are discussed further in Chapter 3.

5.7.2 Instrumentation during testing

The instrumentation applied during Phase 2 experimentation was comprised of the thermocouples cast within the samples as detailed in Section 5.5.1 and an additional thermocouple attached to the back (i.e. unexposed) face of the samples. This was attached using aluminium tape and a small patch of ceramic paper insulation installed over the thermocouple tip. The purpose of this was to ensure it was measuring the surface temperature of the sample rather than the temperature of the surrounding ambient temperature atmosphere.

5.7.3 Experimental procedure

All samples were stored in the conditioning room until they were ready to be tested since the samples were on pallets a few were brought out together. This meant that some samples were tested immediately after being removed from the conditioning room whereas others may have waited in the laboratory for up to 2 days before being tested. This was unavoidable due to availability of a heavy-lifting forklift. It is not anticipated that this small period of time out of the conditioning room had any significant impacts on the experimental results, as the conditions in the lab are broadly

similar to those of the conditioning room (i.e. 15-25C and 50-70%RH). The duration of exposure to conditions outside the conditioning room was also extremely short in comparison with the specimen ages.

All samples were photographed, and lifted into place before the internal thermocouples were connected to the data acquisition system. All samples were tested in a vertical orientation, with the centre of the samples aligning with the centre of the radiant panel array. No applied load or external restraint was supplied to the samples by the sample holder frame during Phase 2 experimentation.

Ceraboard insulation, 25 mm thick, was fitted so that the outer 25mm edge of the heated face of the samples was shielded both from direct radiation from the radiant panels and from convection by exposure to ambient air. This was necessary both to protect the sample holder from heating and to ensure that the samples were heated only over a well-defined area on their front faces. Insulating in this way also gave similar thermal boundary conditions (in terms of absorbed radiation at least) as the small samples (Sample types P7 to P14) tested in the Prometheus furnace experienced. These are described fully in Chapter 4. An example of the insulation configuration for 750 x 450 mm samples is shown in Figure 5.4 and Figure 5.5. The smaller samples were insulated in the same way resulting in an exposed heated surface of 300 x 300 mm on a 350 x 350 mm sample.

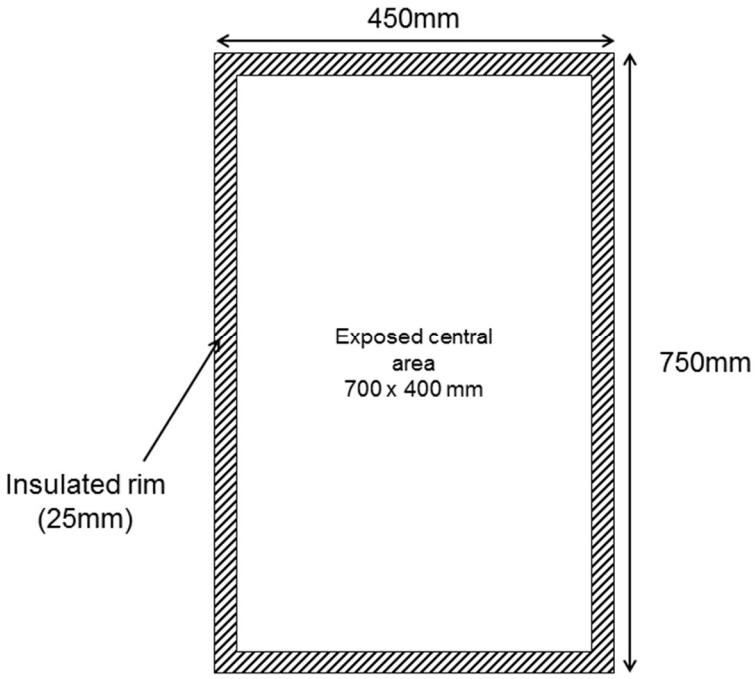

Figure 5.4: Insulation configuration around heated face of samples

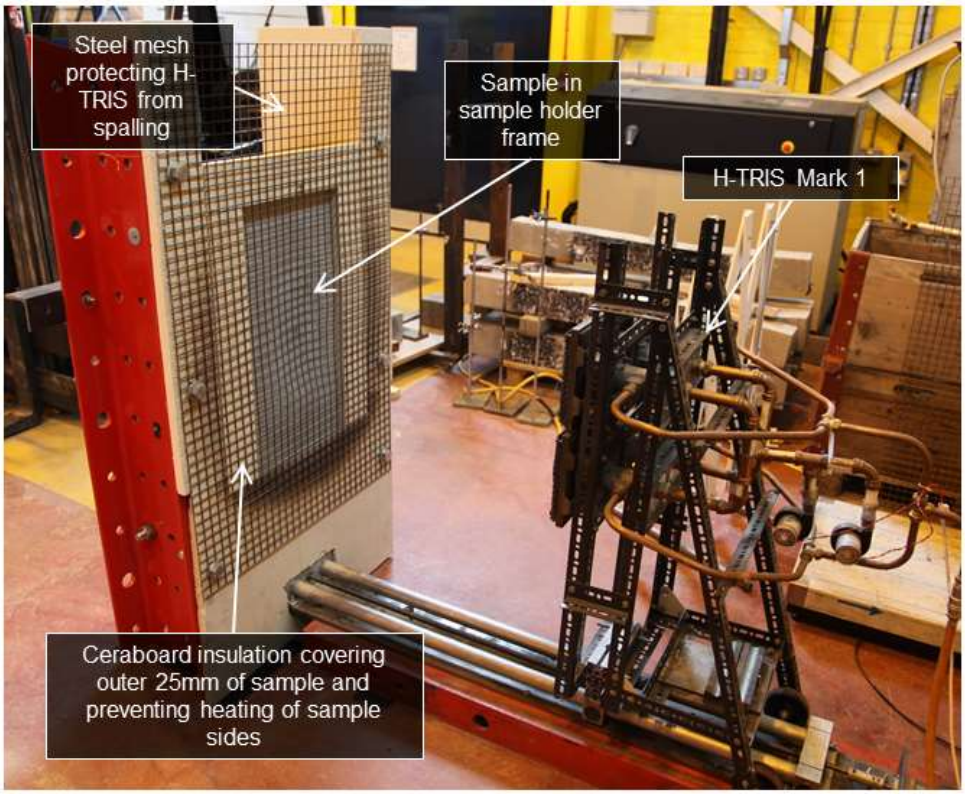

Figure 5.5: Sample in the sample holder frame showing the insulation configuration

Once the samples were positioned in the sample holder, the thermocouples were connected and the edge insulation installed as shown in Figure 5.5. A large vermiculite insulation board was then placed between the sample and the radiant panels. This allowed the radiant panel array in the H-TRIS apparatus to be ignited and to stabilise, avoiding exposure of the sample to an unknown lesser heat flux.

Once the panels had stabilised, the experiment could begin. The radiant panels were moved to a position of known heat flux, 5 kW/m^2, and the insulation board was then removed at the start of the experiment. The requisite incident heat flux versus time exposure was generated by controlling the movement of the radiant panel array both towards and away from the sample, to points of known heat flux established during the calibrations. The experiments were run until the point of first spalling, or for thirty minutes (whichever occurred first).

The experiments were terminated after the initial significant explosive spalling event in which the spall was sufficient to impact shake the apparatus, an explosive spall

rather than a localised aggregate spall. See Section 2.2.1.1.This approach is necessary for two reasons:

- Damage to the radiant panels – Violent spalling introduces aggregate particles into the combustion media of the radiant panels which has been observed to react when heated. Additionally, the impact itself could also damage the panels and safety must be considered.
- Thermal exposure control – When spalling occurs an unknown thickness of the heated front face of the concrete is lost. H-TRIS imposes an incident heat flux controlled by varying the distance between the radiant panels and the sample surface. The loss of the heated surface changes the heat transfer boundary condition at the surface and resultant net heat flux into the sample. In addition the offset between the sample face and the radiant panel is increased and hence incident heat flux is reduced.

Stopping the experiment upon first spall allows a time to spalling to be created and the first spall of each sample to be assessed.

5.7.4 Spalling measurements

If spalling occurred the time to spalling was recorded along with the peak depth of spalling which was measured by using a straight edge and a Vernier calliper.

5.8 Experimental results

The experimental results are discussed in this section, by partitioning the discussion into sections dealing with concrete properties (Section 5.8.1), thermal exposures experienced (Section 5.8.2), and spalling observations (Section 5.8.3); this last section is further partitioned on the basis of the various parameters varied amongst specimens.

5.8.1 Concrete properties

The concrete used for these tests was from the same mix design and three batches as the concrete discussed for the large-scale furnace testing at CERIB (i.e. Phase 1 experiments) in Chapter 4. The properties of the mix concrete at 28-days from casting have already been given in Chapter 4 but are repeated below. Table 5.4 gives the 28 day cylinder strengths for the different mixes and casts, and Table 5.5 gives the moisture contents at the time of the furnace tests.

Table 5.4: 28 day cylinder strengths for CERIB concrete cast

Cast	Curing	f_c (MPa)	f_{cm} (MPa)
1	Sealed	48.6	48.9
		49.0	
		49.1	
	Unsealed	47.7	49.8
		52.9	
		48.8	
2	Sealed	56.9	53.9
		55.1	
		49.7	
	Unsealed	58.0	55.4
		52.4	
		55.9	
3	Sealed	42.0	42.7
		44.6	
		41.4	
	Unsealed	47.4	44.8
		41.7	
		45.3	

Table 5.5: Moisture content by mass loss from cylinders for CERIB cast

Cast	Curing	Moisture Content (%)	Average Moisture Content (%)
1	Sealed	5.6	5.9
		6.5	
		5.5	
	Unsealed	4.5	4.1
		3.9	
		3.8	
2	Sealed	5.4	5.8
		5.9	
		6.2	
	Unsealed	3.3	3.5
		3.8	
		3.3	
3	Sealed	6.8	6.8
		6.9	
		6.7	
	Unsealed	4.2	4.0
		4.2	
		3.7	

No additional cylinders were available to send to Edinburgh along with the concrete samples for H-TRIS testing. As a result it was not possible to carry out additional tests on the concrete at time of testing. It was also not possible to evaluate its moisture content at time of testing by dehydration of concrete cylinders. While not the preferred method of measuring moisture content, an estimate of the moisture content at the time of testing was made by breaking chunks from the unheated back edge of some samples and drying them in the oven. This was only possible for samples that were tested briefly meaning that the back face of the sample did not get hot and should not have been affected by moisture transport.

Pieces broken from the back of samples H2a and H2b, which were cast in Cast 1, gave an average moisture content at time of H-TRIS testing (concrete age 304 days) of 3.2% by mass, a reduction of 0.9% from the moisture content at the time of furnace testing (132 days). Based on this crude assessment of the moisture content it would

be expected that concrete from the other two casts would have experienced a similar decrease in moisture content during storage at the University of Edinburgh.

5.8.2 Thermal exposure

The suitability of the applied variation of incident heat flux with time for recreating the thermal exposures experienced by the samples tested in the Prometheus furnace at CERIB can be assessed by comparing the through-thickness temperatures from the furnace tests with those recorded during the subsequent H-TRIS testing at Edinburgh. This was done for both the ISO 834 (International Organisation for Standardization, 1999)equivalent thermal exposure and the HCM (Ministère de l'Equipement, 2000) equivalent thermal exposure.

5.8.2.1 ISO 834 equivalent thermal exposure

A comparison of through-thickness temperatures recorded for the ISO 834 (International Organisation for Standardization, 1999) tests is shown in Figure 5.6 and Figure 5.7. These plots show the temperatures recorded at various target depths in separate H-TRIS tests, along with the different temperature versus time histories recorded within multiple different samples during the single Prometheus furnace test when operated to follow the ISO 834 thermal exposure. The dashed red lines show the temperatures selected from the furnace data that became the target temperature versus time history within H-TRIS experiments. See Chapter 4.

It can be seen that for the ISO 834 furnace exposure the temperatures recorded within the concrete samples during H-TRIS experiments are in general higher than those recorded in the furnace tests. There is also considerable spread in both the furnace data (around 300°C for 1mm thermocouples) and H-TRIS data (around 150°C for 1mm thermocouples). This can be partly attributed to inaccuracies in the target thermocouple position during casting which is discussed in Chapter 3 with additional analysis in Chapter 7.

The thermal exposure imposed by H-TRIS when attempting to replicate the ISO 834 furnace test appears to be more severe than that experienced by samples in the Prometheus furnace. This may be in part due to the selection of a thermocouple trees that recorded high temperatures for the model input. Possible explanations for the discrepancies are proposed in Section 5.8.2.3. Further discussion and analysis is provided in Chapter 7. The use of a slightly more severe but comparable thermal

exposure was deemed an acceptable outcome as it creates a worst case condition with regards to propensity for heat-induced explosive concrete spalling.

Spalling has generally been found to increase in likelihood with the severity of thermal exposure and this was observed in the tests in Chapter 4. In addition, consistency of heating for the experiments was preferred over iteration in an attempt to better match the furnace.

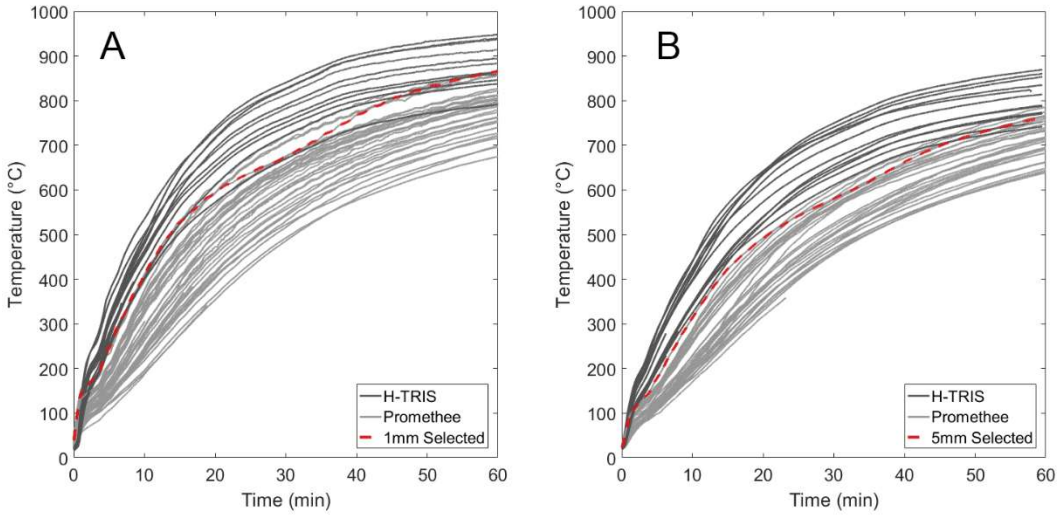

Figure 5.6: Through-thickness temperature comparisons for Prometheus ISO 834 (International Organisation for Standardization, 1999)*(14 samples, 60 thermocouple trees, one test) and H-TRIS ISO 834 equivalent experiments (16 samples containing thermocouples of the 24 experiments carried out) at A) 1mm nominal depth thermocouples, and B) 5mm nominal depth thermocouples*

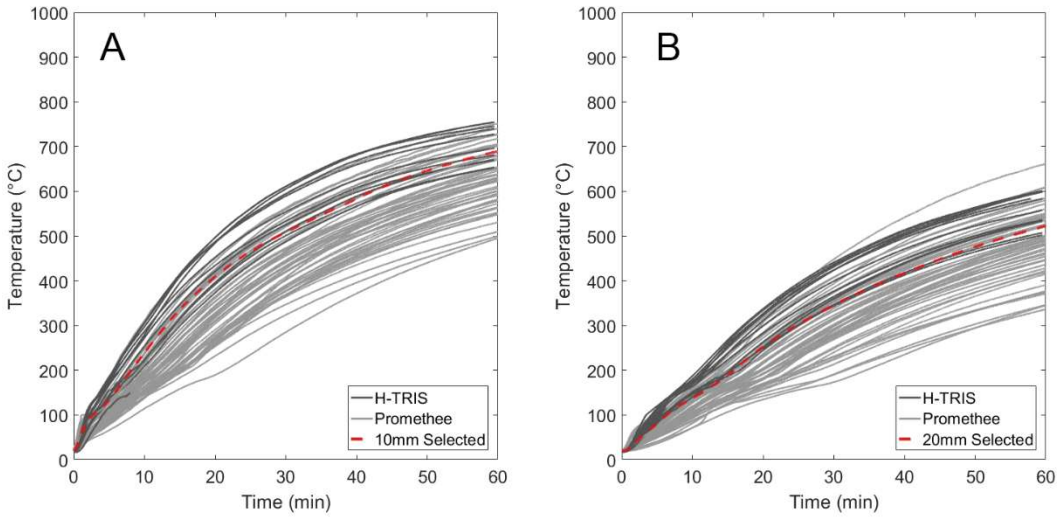

Figure 5.7: Through-thickness temperature comparisons for Prometheus ISO 834 (International Organisation for Standardization, 1999) *(14 samples, 60 thermocouple trees, one test) and H-TRIS ISO 834 equivalent experiments (16 samples containing thermocouples of the 24 experiments carried out) at A) 10mm nominal depth thermocouples, and B) 20mm nominal depth thermocouples*

The spread of the temperature data can be compared by plotting the mean and standard deviations of the temperatures recorded at each time during the tests/experiments. Figure 5.6 shows the means and standard deviations of the H-TRIS experiments and Prometheus ISO 834 (International Organisation for Standardization, 1999) test. It can again be seen that the temperatures recorded during H-TRIS testing are higher than recorded in the furnace tests. However, the spread of temperatures for the separate H-TRIS experiments is lower than the spread of temperatures from thermocouples in different samples in the Prometheus tests. For a target thermocouple depth of 1mm a maximum standard deviation of the temperatures measured across the thermocouples in the ISO 834 furnace test was 75°C compared to 54°C for the maximum standard deviation in temperatures at 1 mm across the H-TRIS experiments. At a depth of 5 mm the maximum standard deviation was 52°C for both the ISO 834 furnace and H-TRIS temperatures. This gives confidence that running multiple single sample experiments using the H-TRIS apparatus and methodology is at least as repeatable as running a single large-scale furnace test incorporating multiple individual samples.

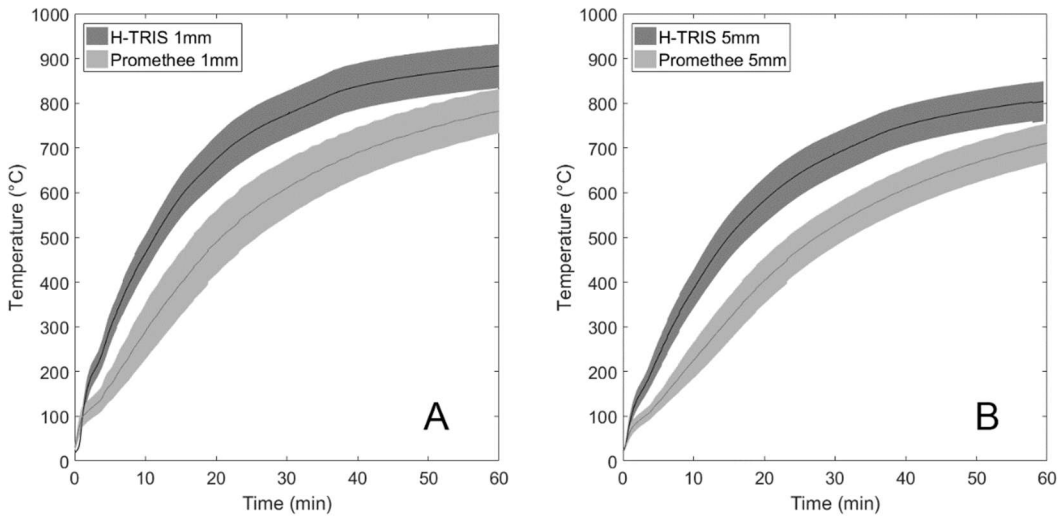

Figure 5.8: Means and standard deviations for temperatures recorded at a nominal depth of (A) 1mm and (B) 5mm in the ISO 834 Prometheus furnace test (International Organisation for Standardization, 1999) *and H-TRIS ISO 834 equivalent experiments*

5.8.2.2 HCM equivalent thermal exposure

A comparison of the recorded HCM (Ministère de l'Equipement, 2000) temperature versus time histories in both the furnace tests and the H-TRIS experiments can be carried out in the same manner as for the ISO 834 tests. The resulting plots are given in Figure 5.9 and Figure 5.10.

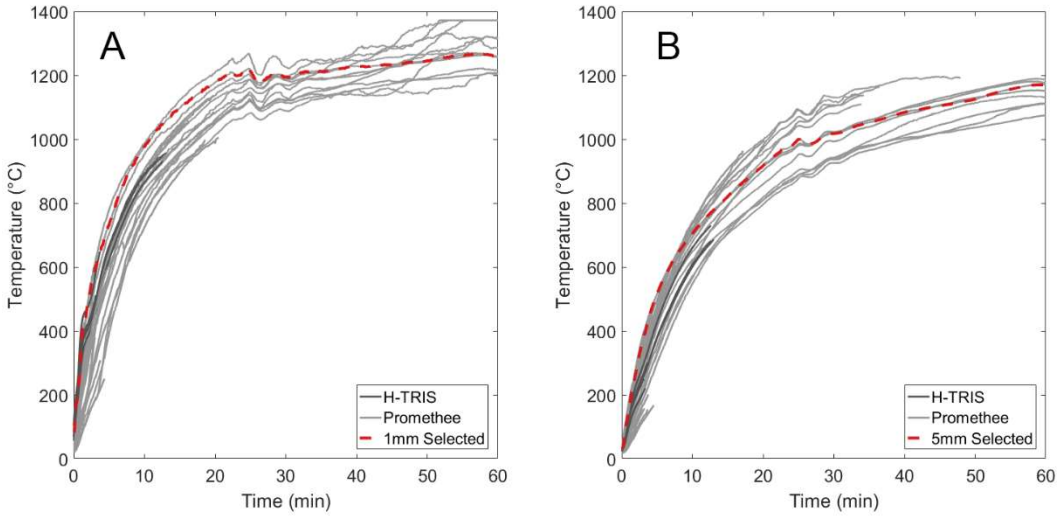

Figure 5.9: Through-thickness temperature comparisons for Prometheus HCM (Ministère de l'Equipement, 2000) *(14 samples, 24 thermocouple trees after data cleaning, one test) and H-TRIS HCM equivalent tests (5 samples, 5 thermocouple trees) at A) 1mm nominal depth thermocouples, and B) 5mm nominal depth thermocouples*

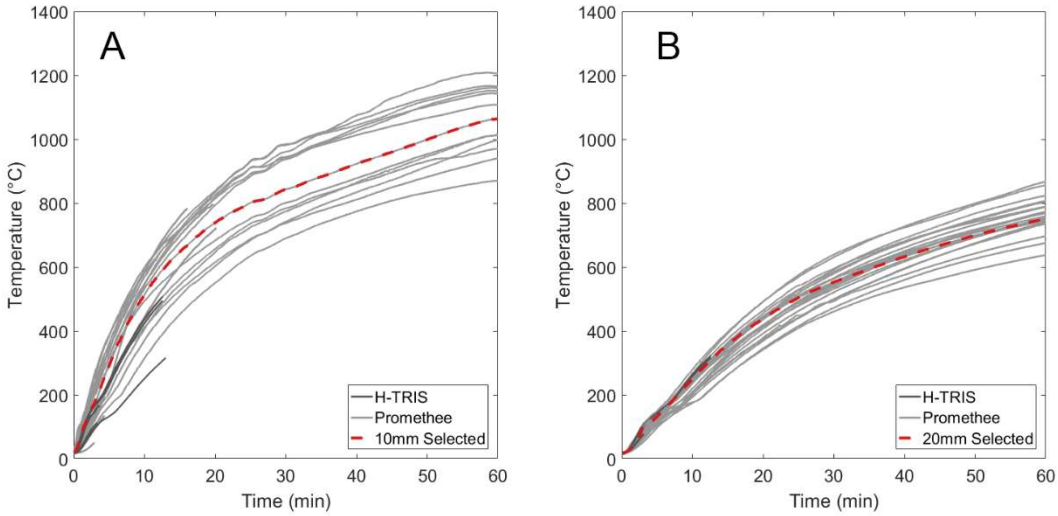

Figure 5.10: Through-thickness temperature comparisons for Prometheus HCM (Ministère de l'Equipement, 2000) *(14 samples, 24 thermocouple trees after data cleaning, one test) and H-TRIS HCM equivalent tests (5 samples, 5 thermocouple trees) at A) 1mm nominal depth thermocouples and B) 5mm nominal depth thermocouples*

There is limited data from H-TRIS HCM equivalent tests in the above plots, since only six of the nine samples tested contained thermocouple trees and measurement of temperatures failed in one of those experiments. The data from thermocouples was also cut short if spalling occurred or the thermocouples failed. This failure of the thermocouple is typically due to spalling resulting in the thermocouple tip being damaged. In one of the experiments the data acquisition system malfunctioned and did not record temperatures. From the available through-thickness temperature data it can be seen that the temperatures experienced by samples during H-TRIS testing to an equivalent HCM (Ministère de l'Equipement, 2000) exposure lie within the range of the temperatures recorded in the Prometheus tests but are generally lower. This is a more satisfactory agreement than observed for the ISO 834 (International Organisation for Standardization, 1999) tests/experiments in the previous section. Reasons for the discrepancies are discussed in Section 5.8.2.3. It is important to note that there is very little data for the HCM equivalent H-TRIS tests so it is likely that some variation is not captured. The uncertainty in thermocouple locations again introduces difficulty when making comparisons. Uncertainty in the position of thermocouples is discussed in more detail in Chapter 7.

Since the temperatures measured in the H-TRIS experiments and Prometheus tests are similar, this heat flux versus time curve was deemed suitable for recreating the thermal exposure that the samples experienced in the Prometheus furnace when tested to the HCM (Ministère de l'Equipement, 2000) temperature versus time curve. It is important to note that in these tests data from H-TRIS testing were only available for the first 13 minutes. Testing was stopped after this point, either because of issues with the test setup or because spalling occurred. The issues which occurred during this experimental program were blowback, and sensor malfunction. These issues and the steps taken to avoid them in future testing are discussed in detail in Chapter 3. These HCM H-TRIS experiments were amongst the first tests carried out using the new H-TRIS Mark 2 apparatus, and as a result these unforeseen challenges had to be overcome. It was not possible to redo the tests that experienced problems, since a severely limited number of samples was available.

5.8.2.3 Discrepancies in thermal exposures

During the period between Prometheus and H-TRIS experiments the concrete had cured further and the moisture content of the concrete had decreased by around 1%. The thermocouples were installed in the these samples using the same method as

the samples tested in the Prometheus furnace and the expected temperature range due to inaccuracies discussed in Section 7.3. While there was confidence that the H-TRIS apparatus was applying the desired thermal exposure, based on calibrations using a heat flux gauge, there was still an observed spread of temperatures measured which was attributed to the thermocouple placement error. This variation in temperatures recorded has been shown.

Chapter 7 provides further analysis and considerations on this topic but, while it is unclear, it is thought that the discrepancy between the target internal temperatures and those recorded could be attributed to a number of factors:

- Assumed thermal properties of the concrete based on Eurocode may have resulted in the calculated incident heat flux being incorrect. This seems unlikely to be a primary contributing factor as it does not account for the HCM equivalent exposure being more accurate than the ISO 834 equivalent exposure - particularly with ISO 834 exposure appearing to be too severe and the HCM equivalent exposure slightly low.
- The concrete thermal properties changed with ongoing curing. Again, this does not account for the difference in accuracy of the ISO 834 and HCM equivalent exposures.
- The boundary condition and potential for contribution of convection from forced flow combustion in the radiant panels could have had an unforeseen impact on the heat transfer to the samples. Again, this does not explain the HCM equivalent exposure providing a better match to the desired through-thickness temperatures, particularly as the panels are much closer to the concrete samples during HCM equivalent experiments and would experience any convection to a greater extent.
- The heat flux-mapping robot was developed in-between the ISO 834 and HCM experiments. Being able to map the heat fluxes allowed the thermal exposures across the whole surface to be measured at different distances and resulted in the points being used to calibrate the heat flux versus distance being representative of the peak heat flux.

It is unclear what the cause of the discrepancies is. In both cases, it was preferred to impose a consistent thermal exposure between experiments rather than to iterate to improve on the match. It is the view of the author in hindsight that the attempted recreation of these thermal exposures is not the best way to carry out experiments

and that repeatability is more important than exactly recreating a specific furnace on a specific day. See Chapter 8. It is the author's opinion that the testing for comparison generally would have been improved if the H-TRIS experiments had been carried out closer to the time of the furnace tests; however, the apparatus was still under development at that time.

5.8.3 Spalling observations

This section discusses the spalling results from the H-TRIS experiments. The complete results are summarised in Section 5.8.3.1. Splitting down the overall test results allows clearer direct comparison of the influences of various parameters on spalling. Sections 5.8.3.2 to 5.8.3.7 present the results with a focus on each parameter investigated. Comparison of the spalling observations from the Phase 2 experiments with the results of the Prometheus furnace tests carried out during Phase 1 at CERIB is given in Section 5.9. It is important to remember when comparing, that the boundary conditions in H-TRIS experiments are not the same as in the furnace.

5.8.3.1 Results summary

The results of the H-TRIS experiments described in this chapter are summarised in Table 5.6 and Table 5.7. Issues associated with the radiant panels, as described in Chapter 3, were experienced for test type H6. This is believed to be a result of overheating due to the panels running longer than in the experiments which spalled. In all of the experiments that H-TRIS malfunctioned it was at a time of around 18 minutes. By this time the samples had cracked and moisture could be seen escaping, see Figure 5.13. It is not believed that continued testing would have resulted in spalling.

Table 5.6: Results summary from Phase 2 experiments

Sample Type	Plan Dimensions (mm)	Thickness (mm)	PP Fibre Dosage (kg/m^3)	Curing Conditions	Equivalent Thermal Exposure	Spalling
H1	350 × 350	100	0	Standard	ISO 834	No
H2	350 × 350	250	0	Standard	ISO 834	2 of 3
H3	750 × 450	100	0	Standard	ISO 834	No
H4	750 × 450	250	0	Standard	ISO 834	No
H5	750 × 450	100	2	Standard	ISO 834	No
H6	750 × 450	250	2	Standard	HCM	No
H7	750 × 450	250	2	Sealed	ISO 834	No
H8	750 × 450	250	0	Sealed	ISO 834	Yes
H11	350 × 350	250	0	Standard	HCM	Yes
H12	750 × 450	250	0	Standard	HCM	Yes
H13	750 × 450	250	2	Standard	ISO 834	No

Table 5.7: Details of first spall for samples that spalled in Phase 2 testing

Sample Type		Time to Spalling (mm:ss)	Spalling depth (mm)
H2	a	08:33	16.8
	b	06:51	13.2
	c	-	-
H8	a	03:21	10
	b	06:03	9.7
	c	02:31	11
H11	a	04:08	13
	b	02:05	7.4
	c	02:11	9
H12	a	03:53	10.1
	b	04:26	13.5
	c	03:39	8.9

It is important to remember that the Prometheus furnace tests and the tests carried out in the small furnace at CERIB tested multiple samples at the same time in one furnace test. Experiments run using H-TRIS are single sample experiments. As a result of this, the sample age at time of experiment varies both between sample types being tested and also within the sample type set if it was not possible to run the three experiments on the same day. The sample ages at time of testing are shown in Table 5.8 for the ISO 834 equivalent tests carried out using H-TRIS Mark 1 and Table 5.9 for the HCM equivalent tests carried out using H-TRIS Mark 2.

Table 5.8: Sample age at time of experiment for Phase 2 ISO equivalent experiments

			Sample Age (days)
Samples	H1	a	300
		b	300
		c	301
	H2	a	304
		b	304
		c	304
	H3	a	273
		b	276
		c	276
	H4	a	280
		b	285
		c	285
	H5	a	249
		b	249
		c	250
	H7	a	252
		b	256
		c	257
	H8	a	286
		b	286
		c	286
	H13	a	257
		b	258
		c	258

Table 5.9: Sample age at time of experiment for Phase 2 HCM equivalent experiments

			Sample Age (days)
Samples	H6	a	439
		b	452
		c	454
	H11	a	483
		b	483
		c	483
	H12	a	454
		b	458
		c	461

The delay between the furnace tests being completed at CERIB and the experiments being carried out using H-TRIS was a result of the time taken to analyse the data from

the furnace tests, update the H-TRIS Mark 1 experimental setup, and build the H-TRIS Mark 2 apparatus. These being the first experiments carried out using the H-TRIS Mark 2 apparatus also led to a slow turnover between tests with unforeseen modifications being required. The Phase 2 experiments described in this chapter were being carried out over approximately 180 days. These issues encountered with the experimental setup are mentioned in the discussion of these tests in Section 5.9 and discussed in greater detail in Chapter 3.

5.8.3.2 Thermal exposure

Three direct comparisons of the influence of thermal exposure on nominally identical concrete samples are possible from the tests carried out for this chapter. These are shown in Table 5.10. Again, as discussed in Section 5.7.3, it is important to note that the thermal exposure areas used were not the full slab size as the outer 25mm around the edge of the sample face was insulated. This means the heated area for the 350 x 350 mm samples was the central 300 x 300 mm and for the 750 x 450 mm samples, it was the central 700 x 400 mm. This insulation around the edge was necessary to replicate the furnace heating condition where the sample edges, for samples of this size, were supported on all four edges by a sample holder. The insulation was also required to prevent heating of the sample sides and protect the sample holder frame.

Table 5.10: Table of Phase 2 thermal exposure results comparisons

Sample Type	Plan Dimensions (mm)	Thickness (mm)	PP Fibre Dosage (kg/m^3)	Curing Conditions	Equivalent Thermal Exposure	Spalling
H2	350 × 350	250	0	Standard	ISO 834	2 of 3
H11	350 × 350	250	0	Standard	HCM	Yes
H4	750 × 450	250	0	Standard	ISO 834	No
H12	750 × 450	250	0	Standard	HCM	Yes
H5	750 × 450	100	2	Standard	ISO 834	No
H6	750 × 450	250	2	Standard	HCM	No

While no spalling occurred in any of the samples that contained PP fibres during the H-TRIS experiments, the results of the other two pairs of tests indicate that the increased severity of the HCM thermal exposure increased the propensity for spalling. Spalling occurred in all of the HCM samples of H11, yet in only two of three samples of H2. This result for the H2 samples does not agree with the results of the furnace tests described in Chapter 4 this is discussed in Section 5.9. Of the two H2 samples that spalled, the sample that spalled later spalled more severely. All of the H2 samples

were tested on the same day to the same thermal exposure. The variation in the behaviour suggests that perhaps the conditions are close to critical for initiation of spallling. Variation within results is an important consideration when specifying testing.

5.8.3.3 Sample thickness

Three direct comparisons of the influence of sample thickness are possible from the tests carried out in this chapter. These are shown in Table 5.11.

Table 5.11: Table of Phase 2 sample thickness results comparisons

Sample Type	Size (mm)	Thickness (mm)	PP Fibre Dosage (kg/m^3)	Curing Conditions	Equivalent Thermal Exposure	Spalling
H1	350 × 350	100	0	Standard	ISO 834	No
H2	350 × 350	250	0	Standard	ISO 834	2 of 3
H3	750 × 450	100	0	Standard	ISO 834	No
H4	750 × 450	250	0	Standard	ISO 834	No
H5	750 × 450	100	2	Standard	ISO 834	No
H13	750 × 450	250	2	Standard	ISO 834	No

It is difficult to draw any clear conclusion about the influence of sample thickness from these results, because spalling only occurred in two cases. In two of the three sample types tested, no spalling occurred whatsoever. The results from the first pair of sample types would appear to indicate that the thicker samples increase the propensity for spalling. This is thought to be a result of the restraint to deformation and thermal expansion that is provided by the increased cross section, which remains cool during the early testing and more effectively restrains the heated surface of the sample. The results of the testing described in Chapter 4 indicated that the thicker samples provided a worse case for spalling. While this conclusion would be harder to make from the results of this phase of experiments, the results do not contradict this hypothesis.

5.8.3.4 Slab size

The influence of slab size (i.e. plan dimensions) can be assessed by comparison of the results summarised in Table 5.12.

Table 5.12: Table of Phase 2 slab size comparisons

Sample Type	Size (mm)	Thickness (mm)	PP Fibre Dosage (kg/m^3)	Curing Conditions	Equivalent Thermal Exposure	Spalling
H1	350 × 350	100	0	Standard	ISO 834	No
H3	750 × 450	100	0	Standard	ISO 834	No
H2	350 × 350	250	0	Standard	ISO 834	2 of 3
H4	750 × 450	250	0	Standard	ISO 834	No
H11	350 × 350	250	0	Standard	HCM	Yes
H12	750 × 450	250	0	Standard	HCM	Yes

It is interesting to observe that for the comparison of sample sizes it would appear that the smaller 350 x 350 mm samples are more prone to spalling than the larger 750 x 450 mm samples. This observation does not agree with the results from the furnace tests and will be discussed in Section 5.9.

It is important to note that for these H-TRIS experiments with the increased sample size comes an increase in the heated area and a reduction in the uniformity of heating. This reduction in uniformity of heating when imposing high heat fluxes is discussed and quantified in Chapter 3. A reduction in the uniformity of heating may result in increased differential thermal stresses, and in the larger samples an increase in the cool concrete acting to restrain the expansion of the hot surface which is heated centrally, see Section 2.5.

5.8.3.5 Curing conditions

The sealed curing conditions resulted in a concrete moisture content that was, at the time of furnace testing, between 1.8 and 2.8% higher than that of the concrete cured in unsealed conditions. No cylinders were provided to assess the moisture content at the time of H-TRIS experiments but an assessment of the moisture content was made as described in Section 5.8.1. It was found that the moisture content of concrete from the first cast at CERIB, cured in unsealed conditions, dropped by almost 1% in the time between furnace testing and H-TRIS experiments. It is expected that the concrete from the other casts would have experienced a similar reduction in moisture content with the samples cured in sealed conditions maintaining a higher moisture

content than those cured in unsealed conditions. The influence of the curing conditions on spalling in the Phase 2 experiments can be assessed by direct comparison of the samples shown in Table 5.13 below.

Table 5.13: Table of Phase 2 curing condition results comparisons

Sample Type	Plan Dimensions (mm)	Thickness (mm)	PP Fibre Dosage (kg/m^3)	Curing Conditions	Equivalent Thermal Exposure	Spalling
H4	750 × 450	250	0	Standard	ISO 834	No
H8	750 × 450	250	0	Sealed	ISO 834	Yes
H5	750 × 450	100	2	Standard	ISO 834	No
H7	750 × 450	250	2	Sealed	ISO 834	No

The first pair of sample types, H4 and H8, showed that the increased moisture content as a result of the sealed curing was sufficient to cause spalling. In the pair of sample types containing PP fibres spalling was prevented in the 250mm thick sample and again did not occur in the 100 mm thick sample so it is not possible to draw any conclusion about the influence of curing conditions.

5.8.3.6 PP fibre content

The H-TRIS tests allow direct comparison of the influence of PP fibres on spalling through comparison of the sample sets summarised in Table 5.14.

Table 5.14: Table of Phase 2 PP fibre content results comparisons

Sample Type	Plan Dimensions (mm)	Thickness (mm)	PP Fibre Dosage (kg/m^3)	Curing Conditions	Equivalent Thermal Exposure	Spalling
H3	750 × 450	100	0	Standard	ISO 834	No
H5	750 × 450	100	2	Standard	ISO 834	No
H4	750 × 450	250	0	Standard	ISO 834	No
H13	750 × 450	250	2	Standard	ISO 834	No
H6	750 × 450	250	2	Standard	HCM	No
H12	750 × 450	250	0	Standard	HCM	Yes
H7	750 × 450	250	2	Sealed	ISO 834	No
H8	750 × 450	250	0	Sealed	ISO 834	Yes

In the sample pairs allowing direct comparison of the influence of PP fibres, in cases where it occurred, spalling always occurred in the samples, which did not contain any PP fibres. This shows that the concrete mix containing the 2 kg/m^3 of PP fibres is less prone to spalling; this was the case for both thermal exposures used. It is important

to mention that the addition of PP fibres to the mix also led to a reduced strength concrete and it is not possible to isolate in which way the addition of the PP fibres reduced spalling. It is accepted that low strength concretes are less prone to spalling than high strength concretes although this is likely due to a number of properties which change with increasing concrete strength (Clayton and Lennon, 2000).

5.8.3.7 Presence of thermocouple trees

Since the samples were tested in triplicate, with one of the three samples in each of the sample sets not fitted with a thermocouple tree, is was possible to investigate the influence of the thermocouple trees. In previous testing moisture has been seen to escape from the thermocouple tree location during testing, both in furnace tests and in H-TRIS experiments. It was thought that this moisture escape could influence the behaviour of the concrete samples. Throughout this series of experiments, there was no noticeable influence of the thermocouple trees. Moisture was seen to escape from the thermocouple trees but the impact of this was not sufficient to result in a different spalling behaviour between samples with and without thermocouples. Figure 5.11 shows moisture escaping from the thermocouple tree area during the testing of sample H10b.

Figure 5.11: Moisture escaping from thermocouple tree area during testing of sample H10b

5.9 Discussion – Comparison of H-TRIS and Prometheus results

5.9.1 Directly comparable results summary

Comparisons can be made between samples tested in the Prometheus furnace and identical samples tested using the two versions of the H-TRIS apparatus at The University of Edinburgh. While the samples tested were the same, it is important to note that the sample support conditions differ. The samples used in H-TRIS experiments were supported vertically and unloaded. The samples tested in the Prometheus furnace were tested horizontally and simply supported on all sides. It is thought that the influence of this would be low due to the very low span to depth ratio and resultant bending stress on the samples. Further to the sample support differences the thermal exposure was being applied by a different means and, as discussed in Section 5.8.2, the equivalent thermal exposure does not appear to be recreated perfectly.

The comparisons that can be made are summarised in Table 5.15 for the ISO 834 equivalent thermal exposure and in Table 5.16 for the HCM equivalent thermal exposure.

Table 5.15: ISO 834 results - direct comparisons between Prometheus and H-TRIS tests

Sample Number		Properties				Spalling	
H-TRIS	Promethee	Size (mm)	Thickness (mm)	Fiber dosage (kg/m^3)	Curing Conditions	H-TRIS	Promethee
H3	P7	750x450	100	0	Standard	No	No
H4	P8	750x450	250	0	Standard	No	Yes
H8	P10	750x450	250	0	Sealed	Yes	Yes
H13	P11	750x450	250	2	Standard	No	No
H2	P13	350x350	250	0	Standard	2 of 3	No
H1	P14	350x350	100	0	Standard	No	No

Table 5.16: HCM results - direct comparisons between Prometheus and H-TRIS tests

Sample Number		Properties				Spalling	
H-TRIS	Promethee	Size (mm)	Thickness (mm)	Fiber dosage (kg/m^3)	Curing Conditions	H-TRIS	Promethee
H12	P8	750x450	250	0	Standard	Yes	Yes
H6	P11	750x450	250	2	Standard	No	Some
H11	P13	350x350	250	0	Standard	Yes	Yes

The comparisons possible are between one sample tested in the Prometheus furnace, and three samples (identical other than in age) tested using H-TRIS. Since only one sample was tested in the Prometheus furnace, it is possible that variability

in the results was not captured. This could be part of the reason for the discrepancy between the results for the H2 samples and the P13 sample. Two of three samples spalled in the H-TRIS experiments and the one sample tested in the furnace did not spall. Had more samples been tested a similar variation may have been observed.

The differences in results are likely a result of the additional curing time between the furnace tests and the H-TRIS experiments. The age of the samples tested using H-TRIS at the time of testing was significantly greater than the age of the samples tested in the furnace at CERIB. This was a result of the time required to transport samples, create an experimental setup, and in the case of the HCM equivalent tests, build an updated H-TRIS. The sample age in days at time of testing using H-TRIS was between 249 and 483 days. The age of the samples tested using H-TRIS and those tested using Prometheus are summarised in Table 5.17, which also shows the sample cast information.

All of the H-TRIS samples used for the comparison were cast in the same cast as their Prometheus equivalent sample, reducing the potential for slight differences in the mix. However, the large age differences at time of testing are thought to have a potential influence on the test behaviour. The largest age difference between tests on identical samples was 359 days. This was the time between the P13 samples being tested in the Prometheus HCM test and the H11 samples being tested on H-TRIS Mark 2. An additional year of curing (when compared to relatively young 96 day old concrete) could influence the concretes properties significantly. The moisture content will almost certainly have decreased in the additional curing time, as discussed in Section 5.8.1, and the concrete strength is likely to have increased although this could not be measured. Despite the age difference, P13 and H11 samples spalled in both the H-TRIS and Prometheus testing. Comparison of spalling characteristics is not possible as the H-TRIS tests were stopped at time of first spall and the Prometheus tests were left to run for a full hour.

Table 5.17: Sample ages at time of testing for Prometheus and H-TRIS testing

	H-TRIS Sample		Cast	Tested at Age (days)	Promethee Sample	Cast	Tested at Age (days)
ISO Equivalent Tests	H1	a b c	1	300 300 301	P14	1	132
	H2	a b c	1	304 304 304	P13	1	132
	H3	a b c	1	273 276 276	P7	1	132
	H4	a b c	2	280 285 285	P8	2	125
	H5	a b c	3	249 249 250	-	-	-
	H7	a b c	3	252 256 257	-	-	-
	H8	a b c	2	286 286 286	P10	2	125
	H13	a b c	3	257 258 258	P11	3	104
HCM Equivalent Tests	H6	a b c	3	439 452 454	P11 HCM	3	96
	H11	a b c	1	483 483 483	P13 HCM	1	124
	H12	a b c	2	454 458 461	P8 HCM	2	117

5.9.2 Discrepancies in results between test methods

The results of the H-TRIS testing did not match the Prometheus results in three of the nine comparisons of experiments on identical samples that are possible. These results are discussed below along with potential reasons for the variations. It is important to note that based on the through-thickness temperatures recorded during

testing, the H-TRIS ISO equivalent exposure is more severe than the ISO exposure experienced by the samples tested in the Prometheus furnace. This was attributed to the way the temperatures were selected with the desire to create a “worst case” but representative thermal exposure coupled with some uncertainty in the thermocouple positions.

5.9.2.1 H4 samples and P8 from Prometheus ISO

These were the 750 x 450 mm, 250 mm thick samples cured under standard conditions and contained no PP fibres. The P8 sample spalled in the Prometheus furnace test yet the three H4 samples did not spall.

The time difference between the Prometheus and H-TRIS testing was 155 – 160 days depending on the sample tested. It is not clear what the cause of this variation might be, the probable reduction in moisture content of the H4 samples during the extra 155 days of curing may have been sufficient to influence the concrete behaviour. These H4 samples were more than double the age of the P8 sample at time of testing making comparison difficult.

5.9.2.2 H2 samples and P13 from Prometheus ISO

These samples were the smaller 350 x 350 mm size with a thickness of 250 mm, no PP fibres, and standard curing conditions. Two of the three H2 samples spalled in H-TRIS testing yet the P13 sample that was the equivalent sample in the Prometheus furnace test did not spall. The H-TRIS samples were all cast in the same cast as the Prometheus sample but had an additional 172 days of curing, with the H-TRIS samples all being tested on the same day. Only one sample was tested in the Prometheus furnace so it is possible that these samples were around the critical conditions for spalling with one of the H-TRIS samples not spalling. If further samples had been tested in the Prometheus furnace, a similar observation may have been made. The age difference of the samples along with the vertical rather than horizontal orientation for testing could also influence the behaviour.

It was also thought that the method of supporting the smaller samples in the Prometheus tests could result in shadowing of the samples from the thermal radiation in the early stages of the furnace test. This issue was discussed in more detail in Chapter 4.

5.9.2.3 H6 samples and P11 from Prometheus HCM

These samples were the 750 x 450, 250 mm thick samples containing PP fibres. No spalling was observed in the three H6 samples that were tested using H-TRIS Mark 2 however, some spalling was observed in sample P11 in the HCM Prometheus test. Sample P11 after testing is shown in Figure 5.12.

Figure 5.12: Sample P11 after Prometheus HCM testing

The samples tested using H-TRIS were not tested for the full hour as the sample tested in the Prometheus furnace was. Problems with the H-TRIS radiant panels cutting out due to overheating and blowback of the combustion into the panel were encountered during these tests. This panel cut-out occurred at a test time of 13 minutes and 26 seconds for test H6a and tests H6b and H6c were stopped at 14 minutes 56 seconds and 15 minutes 52 seconds. This issue is discussed further in Chapter 3.

It is possible that the spalling witnessed in Prometheus sample P11 may have been more of a thermal degradation and falling off of the damaged surface concrete rather than an explosive spalling incident. In Figure 5.12 it is possible to see concrete that has mostly detached from the surface and is almost peeling off, this could imply that the failure was not violent. However is not possible to be certain as to the failure mechanism. If this was a thermal degradation and sloughing off of the surface then it

is likely that the reduced test times due to H-TRIS issues may have prevented the concrete being damaged to this extent and could explain the different results. It is not thought that explosive spalling would have occurred in H-TRIS experiments if they had been continued for the full hour as, at the point of the experiments being stopped, the samples were cracked and moisture was escaping

In all H-TRIS testing carried out as part of this PhD project, after visible cracking and the resultant stress relief and moisture escape, spalling was not observed to occur. A large crack in the top of sample H6a is shown in Figure 5.13. The tensile cracks allow both compression in the heated front face to be released, and the escape of moisture, and reduction in pore pressures. See Section 2.5.

Figure 5.13: Cracking in the top of sample H6a after H-TRIS testing

5.9.3 General discussion of results

In the Prometheus tests described in Chapter 4, the smaller samples appeared less prone to spalling than the larger samples. The 100 mm thick, 350 x 350 mm samples tested to the HCM curve did not spall when all the other samples sizes spalled at least partially. The same trend was seen with the 250 mm thick samples tested to the ISO 834 temperature versus time curve. All experienced some spalling with the exception of the smallest samples. All of the 250mm thick samples spalled when tested in the Prometheus test to the HCM temperature time curve. This trend of the smaller samples not spalling was not observed in the results of the H-TRIS experiments. As the small samples were the samples thought to be shadowed in the Prometheus furnace tests, these results suggest that the hypothesis of the shadowing of the samples described in Chapter 4 may be correct. It was not possible to determine the worst case sample size for spalling from the furnace tests or the H-TRIS experiments.

In the H-TRIS experiments, two of three of the 250 mm thick, 350 x 350 mm, H2 samples tested to the ISO curve spalled. This result both disagrees with the results of testing the identical, but much younger, P13 sample in the Prometheus furnace and with the finding that the smaller samples did not spall when larger ones did. As discussed earlier the H4 samples did not spall in H-TRIS testing but the equivalent samples spalled in the furnace testing.

Based on the H-TRIS testing alone the results give the impression that the smaller samples may be a worse case for spalling. It is unclear what the cause of the different behaviour was. Possible causes for the variation were discussed in more detail in Section 5.9.2.

In the Prometheus furnace tests the thicker samples were observed to be more prone to spalling. This conclusion is less clear from the H-TRIS tests although the results do not disagree with this hypothesis.

5.10 Conclusions

5.10.1 Thermal exposure

The H-TRIS test setups were able to reasonably reproduce the thermal exposures determined based on through-thickness temperatures from the Prometheus furnace temperatures. The replication of the HCM thermal exposure seems to have been more successful than the replication of the ISO 834 exposure based on the limited data from the HCM equivalent experiments carried out using H-TRIS Mark 2. The thermal exposures determined give a representative, worst case exposure based on comparison of the through-thickness temperatures.

If there is to be an error in the thermal exposure it is desirable that the exposure is more, rather than less, severe. This would be expected to be a more conservative exposure if used to assess the spalling propensity of a particular mix for screening prior to furnace testing.

Improving the understanding of the spalling phenomenon requires repeatable thermal exposures. It is the authors view in hindsight that the attempted replication of thermal exposures from the furnace was not the best approach to this research and this is discussed further in Chapter 8.

Based on the comparison of the performance of the concrete when tested to the ISO 834 and HCM temperature-time curves it has been seen that a more severe thermal exposure increases the likelihood of spalling occurring and the severity of the spalling.

5.10.2 Spalling behaviour

Due to the age difference between samples tested in the Prometheus furnace and using H-TRIS Mark 1 and Mark 2 it is difficult to make comparisons, as the influence of sample age cannot be decoupled from the other variables being investigated. Running experiments using the two methods on samples of a similar age would reduce the uncertainty caused by sample age.

From the stand-alone results of this test series the general conclusions that can be made are as follows

- The more severe HCM equivalent thermal exposure is a worse case for spalling than the ISO 834 equivalent.
- Maintaining sealed conditions through the curing process increased the spalling propensity.

- The addition of 2 kg/m^3 of polypropylene fibres reduced the chance of spalling occurring in tests at both thermal exposures.
- The presence of the thermocouple trees does not appear to influence the spalling behaviour of this concrete mix in H-TRIS experiments
- The 250 mm thick samples appear more prone to spalling than the 100 mm thick samples although spalling only occurred in one of the comparison pairs.
- It appears that the smaller 350 x 350 mm samples are more prone to spalling than the larger 750 x 450 mm samples

6 Phase 3 experimental work - The influence of mechanical load and localised heating

6.1 Summary

This chapter describes Phase 3 of the experimental work. This experimental series makes use of different cast of samples to those used in experimental work previously described. The experiments were carried out with the goal of understanding, and quantifying, the influence of externally applied mechanical loading on explosive spalling. The experimental series also partly investigated the issue of self-restraint within a sample, through application of localised heating, as well as giving further insight into the influence of overall sample thickness.

6.2 Introduction

As discussed in the literature review in Chapter 2, it has been observed both in testing and in real fires that the presence of compressive stress or application of load/restraint to concrete during heating can influence heat-induced explosive spalling. In order to be able to recommend a suitable test method for concrete tunnel linings it is essential that the influence of load is understood more fully. The appropriate load level to be used for a tunnel type application is difficult to determine and varies both on a case-by-case basis and along the length of the tunnel depending on the ground conditions. Therefore, a range of realistic loads were investigated to see how the spalling behaviour is influenced.

Building upon the thermal exposures developed in the first two phases of experimental work the H-TRIS experimental setup was modified to allow the addition of a bespoke loading frame. The uniaxial loading frame was designed to allow 500 x 500 x 250 mm prismatic samples to be loaded whilst simultaneously being heated to the same thermal exposures as the H-TRIS experiments carried out in Chapter 5.

6.3 Modifications to experimental apparatus

The H-TRIS experimental setup described in detail in Chapter 3 was modified from that used previously with the addition of a loading frame. The loading frame was designed to allow a uniaxial load of 15 MPa to be applied to the sample whilst being heated using H-TRIS. Due to the location of H-TRIS, underneath an extraction hood, in the fire laboratory of The University of Edinburgh, there was no crane to assemble the loading frame in addition to space limitations. The frame therefore had to be

modular and fit within the available space. A frame capable of applying larger loads or biaxial loading could be developed for future experiments. Given the restrictions, the loading frame shown in Figure 6.1 was designed and fabricated. A full description of the loading frame design is given in Chapter 3.

Figure 6.1: Uniaxial Loading frame installed in front of H-TRIS Mark 2

In order to prevent the steel frame from overheating during experiments, a water-cooled insulation shield was required. This insulation shield covered the front of the frame and the outer 25mm of the tested samples heated face. This meant that for a 500 x 500 mm sample surface the maximum heated area was 450 x 450 mm. The water-cooled shield was fitted with a mesh guard to protect the radiant panels from spalling debris. In cases where samples were not located in the loading frame immediately behind the insulation shield, vermiculite insulation board was used to insulate samples so that they had the same heated area. The loading frame is fitted with thermocouples to allow the temperature of the frame to be monitored. If the insulation became dislodged and the temperature of the steel frame started to rise rapidly the experiment was stopped. The tensile rods are protected by a stainless steel shield that reflects the radiation from the radiant panel array. The temperature

of the tensile rods were also monitored throughout the experiments. A full description of the apparatus is provided in Chapter 3.

6.4 Methodology

This section covers the methodology used for the experimental work and is broken down into sample preparation, sample positioning before experiments and the experimental procedure. The loading frame described above was used to hold all samples. Dependant on the experiment type the experimental setup varied slightly. Any variations in experimental method are covered in the individual sections.

6.4.1 Sample preparation

6.4.1.1 Instrumentation

Accurate placement of thermocouples within large concrete samples is difficult to achieve. Thermocouple trees were fabricated and installed within the formwork prior to sample casting. They were designed to position thermocouples at 1, 5, 10, 20 and 50 mm and an additional thermocouple at 100 mm was installed in the 250 mm thick samples. The thermocouple trees were made from fibreglass sheathed thermocouple wire, which was stripped and welded at one end. These thermocouples were then bent 90 degrees and fixed together using tie wire to produce thermocouple trees as shown in Figure 6.2. The thermocouple trees were fixed central to the heated face of the samples and the 90-degree bend provided a 20 mm run of thermocouple parallel to the sample surface. In order to increase the stiffness of the thermocouple trees, epoxy adhesive was applied around the bends and along the start of the 20 mm extension out from the tree.

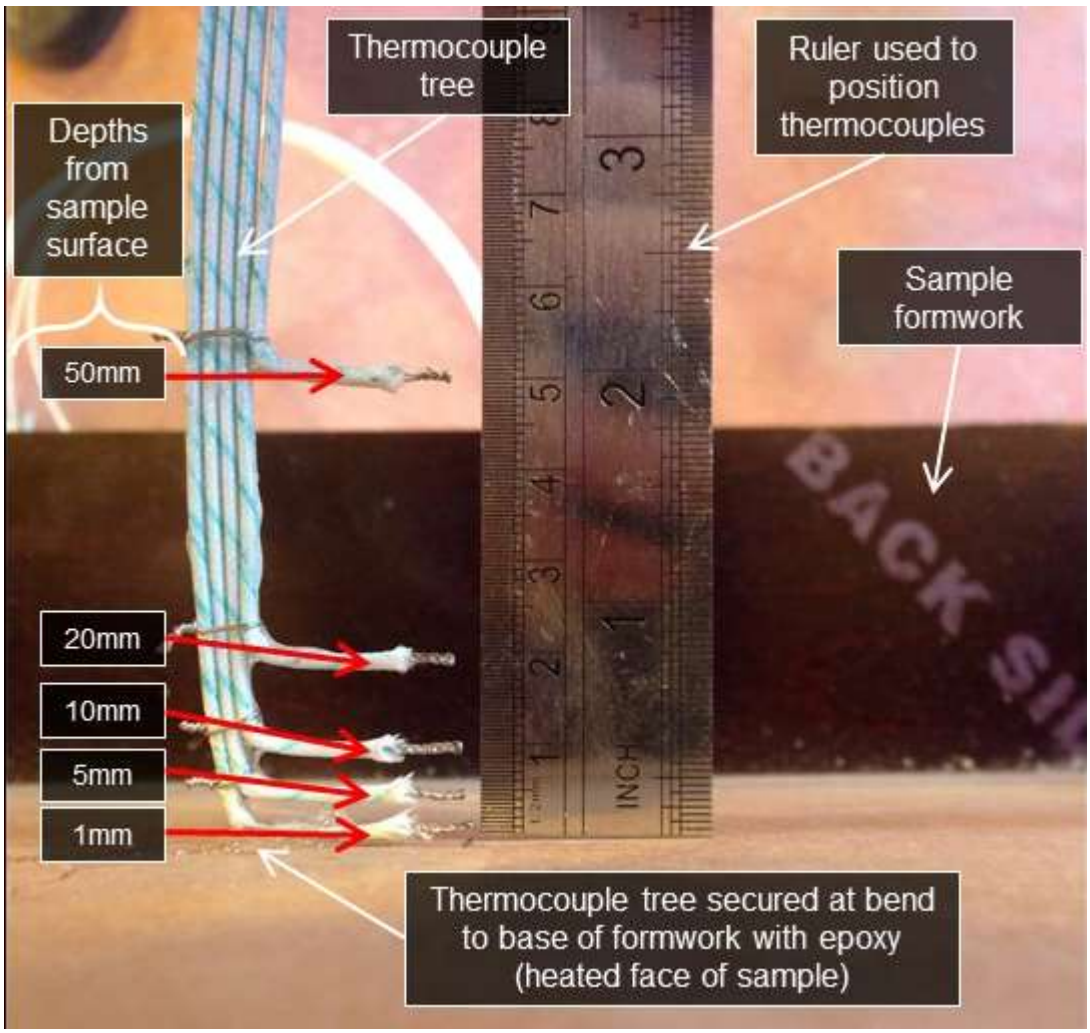

Figure 6.2: Thermocouples installed within formwork in preparation for sample casting

The thermocouple trees were fixed to the base of the formwork using the same epoxy and fixed to a cross member above to keep them rigid during casting. The locations of the thermocouples were checked and corrected after installation into the formwork.

6.4.1.2 Casting

The 45 samples were cast on the 25th of February 2014. The concrete used was ready-mix concrete supplied by Tarmac, Edinburgh. The mix specified was a C50/60 concrete with no polypropylene fibres. This specification was chosen to provide a concrete of compressive strength representative of that which might be used in tunnels. For this phase of experimental work the focus was on the influence of load and restraint so only one concrete mix was used. Polypropylene fibres were omitted both to simplify the mix and in the hope that some spalling would occur allowing meaningful comparison between experiments.

The mix design as obtained from the ready-mix suppliers is shown in Table 6.1

Table 6.1: Concrete mix design for Phase 3 experiments

Mix ingredient	Quantity	Units
Portland Cement	334	Kg/m^3
GGBS	223	Kg/m^3
Sand (moisture content 6.6%)	485	Kg/m^3
4/10mm Aggregate	1140	Kg/m^3
Plastiment 180 Plasticiser	2	Kg/m^3
ViscoCrete 35RM Superplasticiser	2	L/m^3
Water	146	L/m^3

Both the sand and aggregate used in the concrete came from the same Ravelrig Quarry close to Edinburgh. The quarry is a dolerite quarry and the aggregates produced are predominately siliceous dolerite. Results from the ready-mix supplier's chemical analysis of typical aggregates are shown in Table 6.2.This data has not been used but is provided for completeness.

Table 6.2: Chemical analysis or aggregates used

Constituent		%
Iron	as FE_2O_3	10.03
Calcium	as CaO	6.54
Silicon	as SiO_2	53.55
Magnesium	as MgO	4.56
Aluminium	as Al_2O_3	15.12
Phosphorus	as P_2O_5	0.15
Titanium	as TIO_2	2.15
Potassium	as K_2O	1.1
Sodium	as Na_2O	1.98

All samples were cast in formwork made from 18 mm thick phenolic faced plywood. Standard cubes and cylinders were cast alongside the samples cast for H-TRIS experiments in order to allow characterisation of the compressive strength of the concrete as well as estimation of the free moisture content at time of testing. Figure 6.3 shows some of the samples being cast in the yard at The University of Edinburgh.

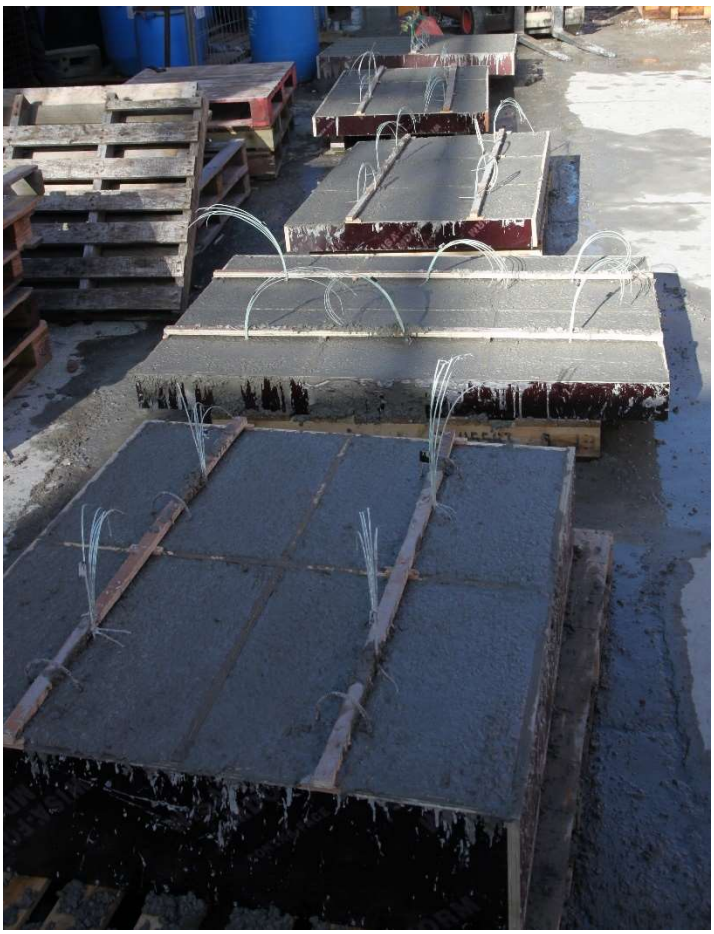

Figure 6.3: Samples being cast at The University of Edinburgh

6.4.1.3 Curing

The samples were demoulded after one week and stored in a conditioning room with approximately 50% relative humidity and a temperature maintained at around 20 °C. Samples were only removed from this conditioning room when they were to be tested. Samples were tested at ages of between 801 and 1176 days. The test series took a long time due to the prototype nature of the test apparatus that broke many times and was repaired and improved upon throughout the testing. The issues encountered are described further in Chapter 3.

6.4.2 Sample positioning during experiments

6.4.2.1 Unloaded samples with a thickness of 100mm

Initially the 100 mm thick samples were placed centrally within the loading frame. The samples were placed on a 5mm thick cork pad and a 2-3 mm gap was left between the top of the sample and the upper crossbeam of the loading frame to ensure that no loading occurred during the experiments as a result of thermal expansion. It was found when carrying out experiments to the HCM equivalent thermal exposure in this central position that the overhang of the frame influenced the thermal exposure experienced by samples. This influence was not quantifiable and is discussed in Section 6.9.2. After initial experiments with unloaded, centrally located samples the remainder of the 100 mm thick samples were positioned, as shown in Figure 6.4, so that their heated surface was located in the same position as that of the full thickness, 250 mm thick samples. The result of this was that it was not possible to apply load to the samples with thickness of less than 250 mm, as the loading frame would not take the eccentricity of load. This is due to the lower crosshead not being fixed rotationally to the jacks.

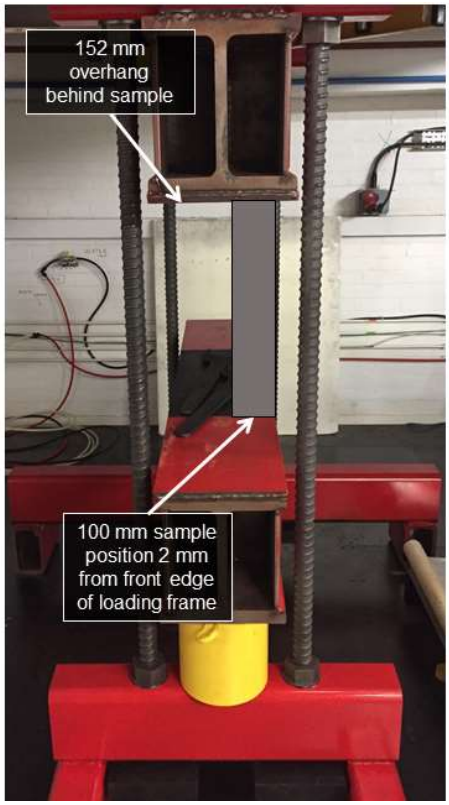

Figure 6.4: Sample position for experiments on 100 mm thick samples. H-TRIS heats from image right.

6.4.2.2 Unloaded samples with a thickness of 175 mm

This intermediate thickness was also not loaded due to the issues discussed for the 100 mm thick samples. The 175 mm thick samples were tested unloaded in the forward position with the heated surface in the same position as for the 250 mm thick samples as shown in Figure 6.5. As in the 100 mm tests, the samples were placed on a 5mm thick cork pad and a 2-3 mm gap was left between the top of the sample and the upper crossbeam of the loading frame to ensure that no loading occurred during testing as a result of thermal expansion.

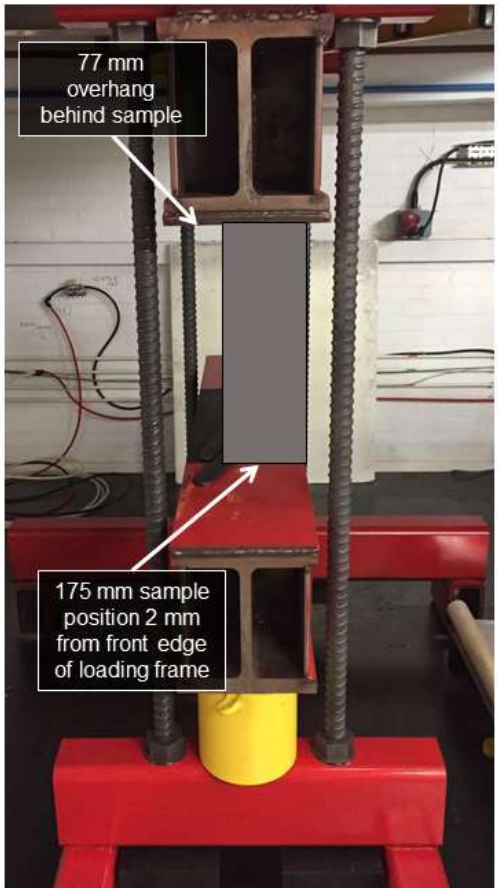

Figure 6.5: Sample position for experiments on 175 mm thick samples. H-TRIS heats from image right.

6.4.2.3 Unloaded samples with a thickness of 250 mm

The 250 mm thick samples filled the loading frame and as such could be positioned centrally as shown in Figure 6.6. In this position they samples could be heated and loaded without the issues mentioned previously. The 250 mm thick samples were used for all the tests investigating the influence of applied load. For the unloaded experiments, as with all unloaded experiments, the samples were placed on a 5mm

thick cork pad and a 2-3 mm gap was left between the top of the sample and the upper crossbeam of the loading frame to ensure that no loading occurred during the experiments as a result of thermal expansion.

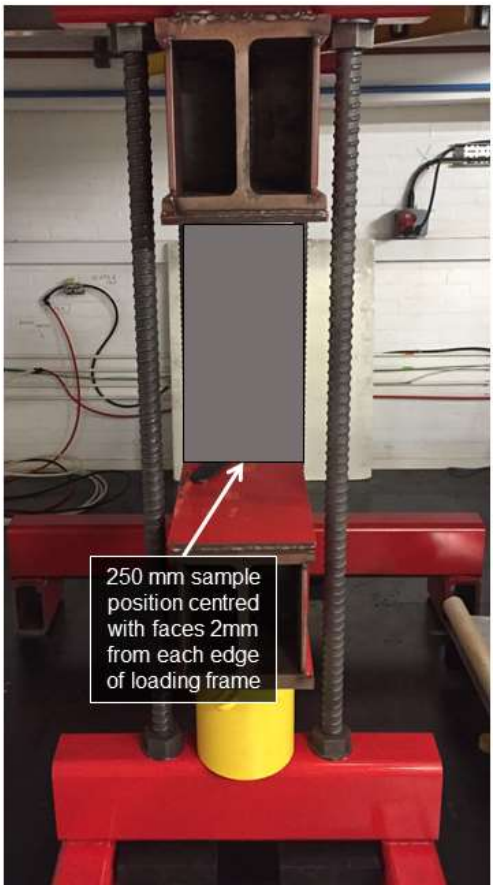

Figure 6.6: Sample position for experiments on 250 mm thick samples. H-TRIS heats from image right.

6.4.2.4 Loaded samples

As previously mentioned, only the 250 mm thick samples were able to be loaded due to issues with thermal exposure preventing thinner samples from being located centrally within the loading frame. When the samples were to be loaded, a 5mm thick cork pad was used underneath the samples as in the unloaded experiments. However, for the loaded samples the top of the sample was capped using plaster to form a good connection with the loading frame. In order to create this plaster cap the wet plaster had to be positioned on top of the sample in a way that the sample could be brought up into its final position before the plaster started to set. Since the loading frame moves very slowly the plaster was placed inside a zip lock bag so that it could be slid into place just before the sample came into contact with the upper beam of the

loading frame. Leaving enough space to apply the plaster to the top of the sample by hand meant that the gap could not be closed before the plaster started to set. During capping, the loading frame was brought up to apply a load of around 5kN to compress the soft plaster in its final position giving a level cap and a good connection between the loading frame and the concrete specimens.

6.4.2.5 Samples with reduced heating area

For samples with a reduced heating area were positioned in the same way as the unloaded and loaded samples with the addition of an extra insulation board shield installed inside the window of the water-cooled insulation shield. The reduced exposure window size of 200 x 200 mm was used.

6.4.3 Experimental procedure

This section briefly discusses the experimental procedure and the method of controlling the different test parameters. Further discussion of the apparatus is given in Chapter 3.

6.4.3.1 Load control

The load applied to samples was controlled by controlling the pressure within the hydraulic lines. An Enerpac hydraulic pump and two CLSG-1504 jacks were used to apply the load. The Enerpac hydraulic pump was fitted with a pressure relief valve and has an automatic load hold function which is able to increase the pressure if it drops. The combination of the load hold and pressure relief valve allow the load level to be set and maintained throughout the test by setting a desired pressure. Any additional load from thermal expansion of samples is released through the pressure relief valve. This method of load control was selected as attempting to fully restrain the thermal expansion would result in uncontrolled/unquantified loading during testing. Whilst the constant external load during heating does not necessarily represent the realistic in service conditions for the concrete, it does allow proper control and repeatability.

The appropriate target pressure and pressure relief valves were set using an Omega PX309-10KG5V pressure transducer in the hydraulic line to the jacks. This same pressure transducer was used to measure any pressure fluctuations during testing.

The combination of the pressure relief valve and load hold function within the Enerpac pump is able to control the pressure to within ±0.25 MPa throughout testing.

6.4.3.2 Control of thermal exposure

The target thermal exposures used came from the tests carried out in the Phase 1 experimental work of this PhD project.

H-TRIS controls incident heat flux by varying the distance between the radiant panels and the test specimen. When controlling the radiant panels to the heat flux–time curves they need to be controlled based on a single heat flux–distance calibration curve. In order to maintain the desired thermal exposure, regular calibrations of the radiant panels were carried out with a Schmidt Boelter heat flux gauge.

Discussion of the thermal exposure from H-TRIS can be found in Chapter 3. The point heat flux measurements used to control H-TRIS for this series of experiments were the average heat flux measurements between the centre points of the top two panels in the array. At close proximity/high heat fluxes these points correspond to the peak heat fluxes of the whole array.

The frequency of the calibrations was determined based upon the nature of the testing being carried out and visual observation of the condition of the panels. The impact force of violent spalling and introduction of concrete dust into the panels had a tendency to damage the porous media of the radiant panels. If the panel was observed to be damaged it was replaced and refurbished. With every replacement or refurbishment of panels, a new calibration had to be carried out.

As discussed in Section 5.7.3, the experiments were terminated after the first spalling event. This approach is necessary for two reasons:

- Damage to the radiant panels – Violent spalling introduces aggregate particles into the combustion media of the radiant panels which has been observed to react when heated in addition the impact itself could also damage the panels and safety must be considered.
- Thermal exposure control – When spalling occurs an unknown thickness of the heated front face of the concrete is lost. H-TRIS imposes an incident heat flux controlled by varying the distance between the radiant panels and the sample surface. The loss of the heated surface changes the heat transfer boundary condition at the surface and resultant net heat flux into the sample. In addition, the offset between the sample face and the radiant panel is increased and hence incident heat flux is reduced.

6.4.3.3 Instrumentation during testing

The instrumentation during the tests comprised of the thermocouples that were cast into the samples and the pressure transducer in the hydraulic line. This allowed measurement of the through-thickness temperatures and applied load. Video cameras were positioned to allow both vertical sides of the samples to be monitored for cracks during the tests. This allowed observation of cracking time and moisture escape during tests. The samples were also photographed immediately before and after testing.

6.4.4 Spalling measurements

The H-TRIS experimental apparatus was used to look for a spall or no spall outcome from experiments. Since the tests are stopped after the first spalling incident, comparison of measurements of spalling is difficult. For example, comparison of a spall that occurred after 2 minutes of heating with one that occurred after 6 minutes of heating is only possible in qualitative sense. It is not certain which of the two samples would have spalled the most in a certain time period. In other test methods, the test is run for a fixed time period regardless of the spalling behaviour and then the performance of all samples can be evaluated afterwards. It is thought that the accurate measurement of the first spalling incident could be used in future to validate models which may be able to predict first occurrence spalling.

6.4.4.1 Spall depth

The maximum spalling depth of the first spall was measured by hand after the samples cooled using a digital calliper and a straight edge steel section as a cross member positioned on the undamaged areas of the sample surface. This allowed comparison between the spall crater depth and the original sample surface location. This was more challenging on samples where a large percentage of the surface spalled. In establishing a reference surface level for some areas of heavily spalled samples, it was only possible to rest the straight edge on one side of the spalled area. In this eventuality, the straight edge was clamped against the surface of the concrete so that it remained parallel and level with whatever remaining undamaged surface was present. In this situation the accuracy of measurement was somewhat reduced.

The average spall depth was determined based on the spalled area and the spall volume. The methods for measuring the spalled area and volume of samples are described below.

6.4.4.2 Spall area

The spalled area was determined digitally using Adobe Photoshop. Images of the samples after testing were input into the software. The length scale can then be set so that the relationship between the pixel size and physical length is known. Simply selecting the spalled area using the mask tool then allows you to measure the area using the scale set previously. The length scale was set based on the known geometry of the samples. Some error may have been introduced into these measurements by lens distortion in the photographs. All spall areas were calculated in the same way using this method.

6.4.4.3 Spall volume

Some investigation into different approaches to measure the spall volume was carried out. This data while not being particularly useful now, other than in direct comparison of the tests, could prove useful in the future for the validation of spalling models. The volume of spalling which occurred in experiments was assessed using one of two methods. The first method was to fill the spalled volume with a sand of uniform particle size and measure the volume of sand both as it was poured in and as it was taken out of the spall crater. Sieving the sand to one particle size was carried out to reduce its compactability. The sand was sieved using standard sieves to give a particle size of between 600 μm and 1.18 mm. Initially measurements were taken multiple times to check repeatability. Over three measurements of one spall volume there was a variation in measurements of 20 ml for an average volume of 550ml.

The second method used to measure the spalled volumes was to scan the sample surface with a 3D scanner. The scanner used was an Artec Space Spider, which has a resolution of 0.1mm and had a quoted accuracy of 0.1 - 0.2 mm in the scans taken. The scanner creates a point cloud of the surface of the concrete, which can then be meshed. Using the scanner's own software and the open source software package Blender it is possible to create a virtual "plug" to fill the meshed spall surface and then output the volume of this "plug" which corresponds to the spalled volume. This process is demonstrated below. Figure 6.7 shows the 3D scan of the spalled surface of a sample. This can be meshed and filled to produce the 3D assembly shown in Figure 6.8. The 3D virtual "plug" can then be removed as shown in Figure 6.9. It was not possible to scan all the samples using this method as the scanner was on a short-term loan and samples with very large spalled areas and missing edges were too computationally demanding for scanning and analysis to be carried out in the available

time period. The measurement of spalled volume using sand is sufficiently accurate for the purposes of this research. It was demonstrated that the use of a 3D scanner could be an effective way to create an archive of detailed data of spalling experiments for future use in models. See Section 6.7 for results and spalling volume measurements.

Figure 6.7: 3D scan of spalled sample surface

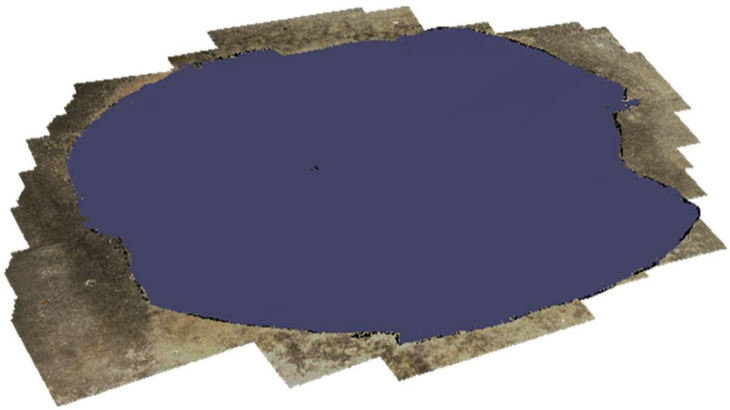

Figure 6.8: 3D scanned spall crater filled with a virtual plug

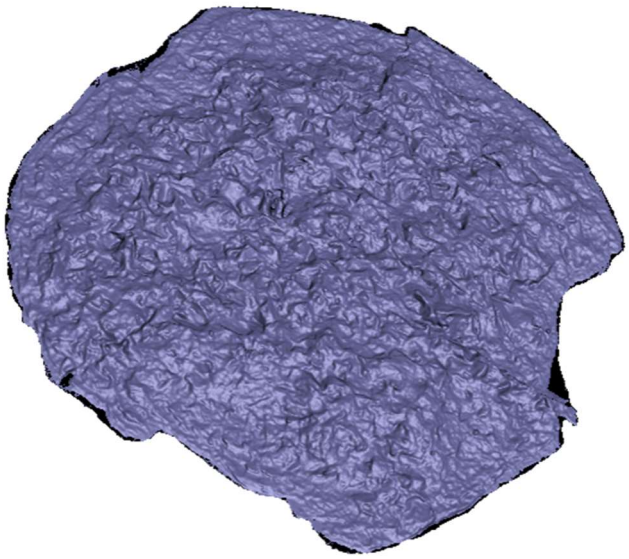

Figure 6.9: Virtual plug removed from the 3D surface. The plug is equal in volume and shape to the spalled concrete

6.5 Experimental programme

The overall test programme for Phase 3 experimental work is shown in Table 6.3. All experiments were carried out in triplicate. As mentioned previously the sample location within the frame was altered after initial issues during testing so only the first six samples were tested in a central location. When referring to the experiments the three repeats of the experiment type are referred to as A, B and C. Experiment 1A refers to the first experiment of Experiment Type 1.

Table 6.3: Overall test programme for Phase 3 experiments

Experiment type	Exposure	Exposure window (mm)	Sample location	Thickness (mm)	Compressive stress (MPa)
1	HCM	450 x 450	Central	100	0
2	ISO	450 x 450	Central	100	0
3	HCM	450 x 450	Front	250	0
4	HCM	450 x 450	Front	250	5
5	HCM	450 x 450	Front	250	10
6	HCM	450 x 450	Front	100	0
7	HCM	200 x 200	Front	250	5
8	HCM	200 x 200	Front	100	0
9	HCM	450 x 450	Front	100	0
10	ISO	200 x 200	Front	100	0
11	HCM	450 x 450	Front	175	0
12	HCM	450 x 450	Front	100	0
13	ISO	450 x 450	Front	175	0
14	ISO	450 x 450	Front	100	0
15	HCM	450 x 450	Front	250	15

The testing can be broken into the key parameters being investigated.

6.5.1 Thermal exposure

The two thermal exposures established in the collaboration with CERIB were used for the experiments described in this chapter. These exposures being the equivalent thermal exposure to that experienced by samples tested in the Prometheus furnace to the French modified hydrocarbon, HCM, and ISO 834 standard fire curves. Some issues arose with the thermal exposure of centrally positioned samples with thicknesses below 250 mm as discussed in Section 6.4.2. Direct comparison of the influence of thermal exposure is possible by comparing Experiment Type 1 and 2, 8 and 10, and 11 and 13.

6.5.2 Sample thickness

Three sample thicknesses, 100, 175 and 250 mm were used. Varying the sample thickness affects the internal self-restraint coming from the cool unheated concrete during experiments. This cool concrete opposes the thermal expansion of the hot heated face. Sample thickness also influences moisture migration moving from the hot heated face to escape from the back and sides of the sample. It is desirable to use thin samples due to ease of handling, however it is necessary to properly evaluate the impact of the sample thickness on heat-induced explosive spalling in order to recommend a suitable experimental method and programme. Experiment types 3, 6, 9, 11 and 12 in the overall experimental programme give a direct comparison of the influence of sample thickness on spalling propensity.

6.5.3 Load level

Four load levels were investigated in the Phase 3 experiments described in this chapter. These were 0, 5, 10 and 15 MPa. This load range was selected based on the capacity of the loading frame that was developed. The primary intention of the loaded experiments was to understand the influence of load rather than to replicate the loading conditions of a particular tunnel. As discussed previously the load on tunnel segments will vary across a tunnel and therefore at this stage in the development of an experimental method it is better to understand the influence of load rather than recreate a condition that will vary from tunnel to tunnel. Depending on the results of the experiments, recommendations about the appropriate load level to use can be made. It was hypothesised that there may be a critical load for spalling for a particular concrete and thermal exposure. If this was the case, and the critical load was low, then samples could potentially be assessed with a load over this critical level rather than the project and segment specific load. Experiment types 3, 4, 5 and 15 give a direct comparison of the influence of load on spalling performance for the 250 mm thick samples exposed to the HCM equivalent thermal exposure.

6.5.4 Thermal exposure window

Variation of the exposure window will induce internal stresses similar to the variation of sample thickness. A reduced exposure window results in cool concrete around the edges of the sample providing some vertical and horizontal restraint to the expanding central heated area. The use of localised heating has the potential to provide results representative of loaded concrete without requirement for a complex loading frame. It is however very difficult to quantify the restraint provided by the cool concrete edge.

The exposure areas used during this experimental series were “fully exposed” 450 x 450 mm and a reduced heating area of 200 x 200 mm. This resulted in a cool edge thickness of 25mm, as a result of the shield used to protect the loading frame and 150 mm due to the additional vermiculite insulation shield. The standard configuration of 25 mm insulated rim is shown in Figure 6.10. The reduced heating area is shown in Figure 6.11.

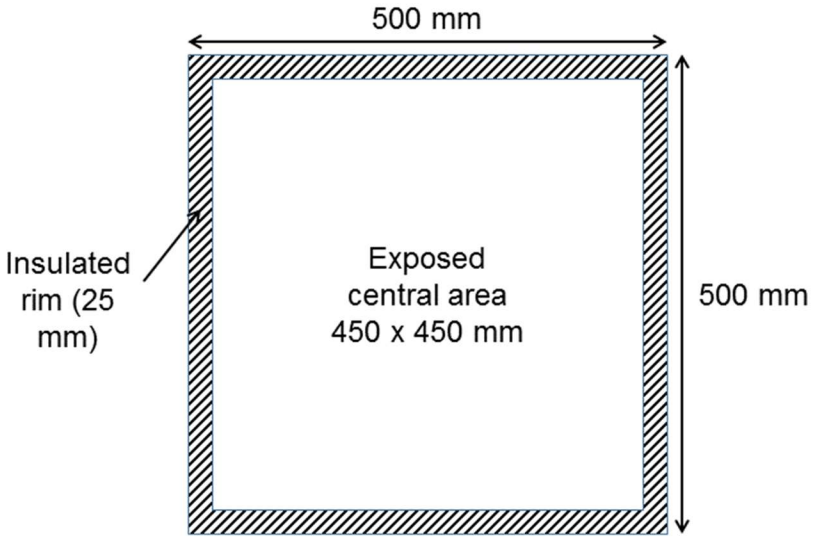

Figure 6.10: Heated face of sample showing area insulated by insulation frame

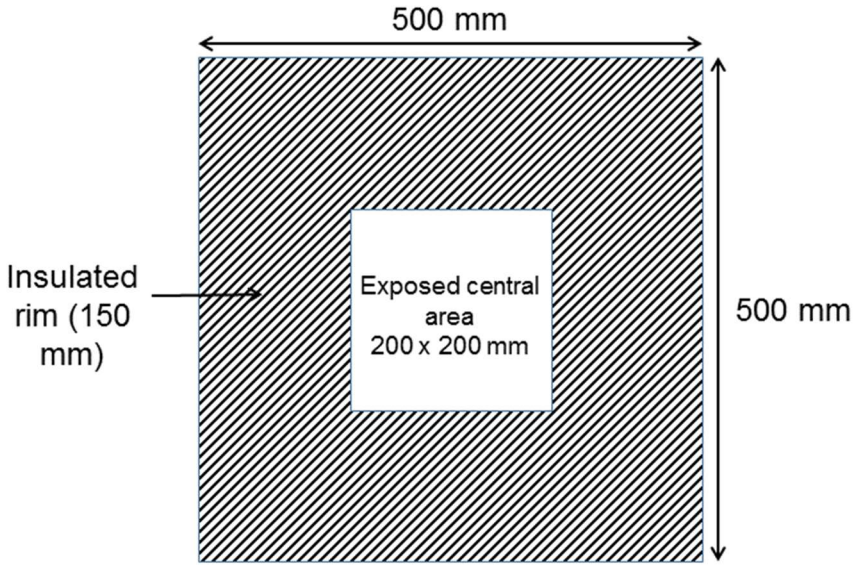

Figure 6.11: Heated face of sample showing area insulated for experiments with reduced heating area

Comparison of the influence of the heating area size can be made for 100 mm thick samples subjected to the HCM and ISO equivalent thermal exposures and for 250 mm thick samples subjected to the HCM equivalent thermal exposure under 5 MPa of compression applied by the uniaxial loading frame.

6.6 Results – Concrete properties

6.6.1 Compressive strength

The compressive strength of the concrete was assessed using standard cylinder tests. The results of these are shown in Table 6.4. The cylinder strength of the concrete increased by 13 MPa in two years. It is expected that most of this strength gain occurred in the early curing period as the strength increased by 11 MPa in the 48 days after the 28 day tests were carried out.

Table 6.4: Concrete cylinder strengths

Concrete age	Cylinder strength, f_c (N/mm^2)	Average (N/mm^2)
28 days	35.4 33.6 37.9	35.7
76 days (time of experiments for a different project)	46.9 48.5 38.8	44.7
815 days (At time of spalling experiments)	43.9 43.7 56.3	48.0

6.6.2 Moisture content

The free moisture content of the concrete was found by dehydration mass loss, standard 100 mm diameter cylinders were dried in an oven at 105°C. Table 6.5 gives the moisture contents measured.

Table 6.5: Free moisture content of concrete

Concrete age	Free moisture content (% by mass)	Average (% by mass)
28 days	4.4 4.8 4.5	4.6
815 days (At time of spalling experiments)	3.0 3.1 3.1	3.1

6.7 Results – Spalling observations

6.7.1 Overview

The results from the tests will be broken down into sub groups given in the test programme explanations. The repeatability of thermal exposure based on through-thickness temperatures will be discussed in Section 6.8. This section provides an overview of the behaviour that was witnessed in the spalling experiments. The performance of the concrete during experiments is assessed based on the occurrence of spalling, another behaviour observed was the development of cracks in the sides of the samples and the escape of moisture.

6.7.1.1 Cracking of samples and moisture escape

The cracking of the sample and moisture escape during Experiment 3A is shown in Figure 6.12. This behaviour was observed at different times for most samples that did not spall, and the cracking times are included in the tables of results. No samples spalled after this cracking had occurred and this is consistent with observations of others in literature (Hertz and Sørensen, 2005). Figure 6.13 shows the cracking that was also observed in Experiment 3B and Experiment 3C. The cracking shown in these images is representative of the cracking that occurred with some variation in crack locations. The crack originated at the edge coinciding with the heated surface and were typically perpendicular to the front edge of the sample (heated face edge). The cracks were observed to allow moisture escape. The photographs shown were not

taken at the same test time so comparison of the volume of water escaping between these experiments is not appropriate.

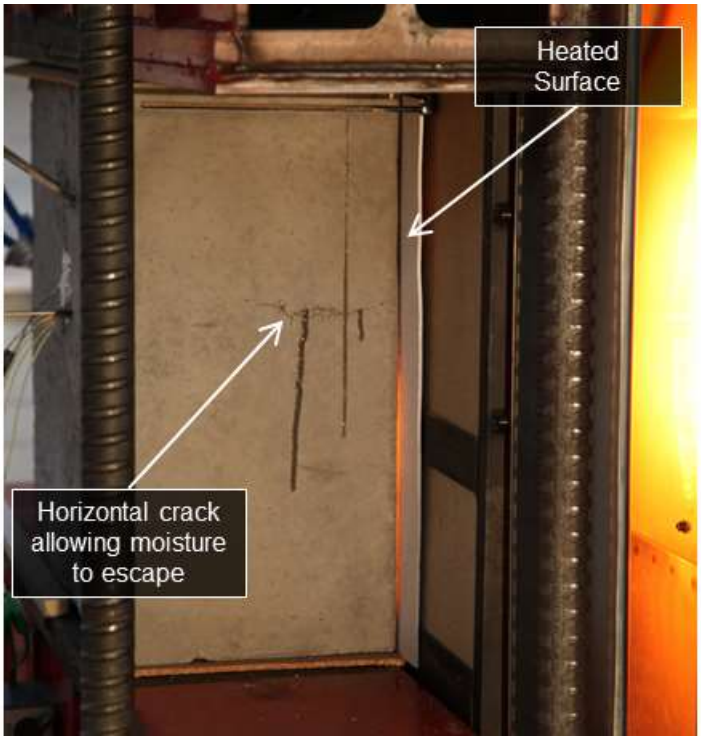

Figure 6.12: Cracking and moisture escape from sample during Experiment 3A

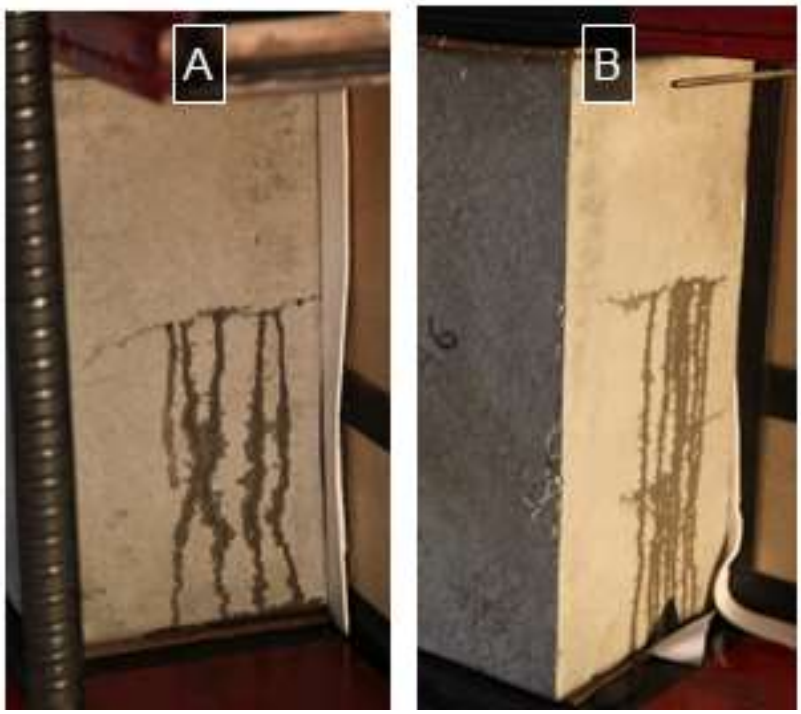

Figure 6.13: Cracking and moisture escape observed in (A) Experiment and 3B (B) Experiment 3C. Note: images not taken at the same time during experiment

6.7.1.2 Spalling of sample surface

The samples that spalled, did so on the front heated face of the sample. Usually the spall remained within the heated area. Spalled sample from Experiment 15A can be seen in Figure 6.14. However, in cases of more severe spalling the damage extended right to the edge of the sample as in Figure 6.15, which shows the spalled sample from Experiment 5A. These images are representative of the type of spalling which occurred during the tests. It is important to remember that these spalls are the first spalls and that the experiment was stopped after the first spalling incident. It is possible that the spalling would have continued for the duration of the experiment.

Figure 6.14: Spalled sample from Experiment 15A. Dashed line indicates edge of the area exposed to heating

Figure 6.15: Spalled sample from Experiment 5A. Dashed line indicates edge of the area exposed to heating

6.7.2 Thermal exposure

The two thermal exposures used were the ISO 834 and HCM equivalent thermal exposures. These were developed in Phase 1 and Phase 2 of the experimental work. See Chapters 4 and 5. Experiment types 1 and 2, 8 and 10, 11 and 13, and 6, 9, 12 and 14 give direct comparisons of the influence of thermal exposure on heat-induced explosive spalling. The experiment types in this comparison are shown in Table 6.6 for clarity and the results of these 30 experiments are summarised in Table 6.7.

Table 6.6: Experiment types allowing comparison of the influence of thermal exposure

Experiment type	Exposure	Exposure window (mm)	Sample location	Thickness (mm)	Compressive stress (MPa)
1	HCM	450 x 450	Central	100	0
2	ISO	450 x 450	Central	100	0
6	HCM	450 x 450	Front	100	0
8	HCM	200 x 200	Front	100	0
9	HCM	450 x 450	Front	100	0
10	ISO	200 x 200	Front	100	0
11	HCM	450 x 450	Front	175	0
12	HCM	450 x 450	Front	100	0
13	ISO	450 x 450	Front	175	0
14	ISO	450 x 450	Front	100	0

It should be noted that six experiments carried out in experiment types 1 and 2, while comparable with each other, are not comparable with the other experiments due to the influence of the loading frame on the heating. The influence of the thermal exposure can be compared with sample thicknesses of 100 mm and heated surface areas of 450 x 450 mm and 200 x 200 mm and also with samples with a thickness of 175 mm. No ISO 834 equivalent heating was carried out on 250 mm thick samples.

In order to assess the influence of different parameters on heat-induced explosive spalling, it is necessary for some spalling to occur. The initial experiments (experiment types 1 and 2) were carried out to determine which thermal exposure to use as the primary exposure for the remainder of the experimental programme. It was desirable to not vary the thermal exposure excessively and be able to focus on the other parameters being investigated. In the experiments described previously in Chapters 4 and 5, the more severe HCM equivalent thermal exposure was seen to produce more spalling. This result was echoed in the results obtained in this series of experiments. No samples tested to the ISO 834 equivalent thermal exposure experienced any spalling.

Table 6.7: Results for the experiment types allowing direct comparison of the influence of thermal exposure

Experiment type		Spalling	Spalling time (mm:ss)	Test duration (mm:ss)	Spall area (%)	Spall volume (cm^3)	Maximum depth of spall (mm)	Average spall depth (mm)	Time of first crack or seeping (visible) (mm:ss)
1	a	Yes	01:07	05:31	12.6	88.8	6.43	2.81	-
	b	Yes	01:02	29:44	6.9	27.1	5.92	1.56	08:26
	c	Yes	01:04	15:40	4.7	22.8	4.85	1.93	08:21
2	a	No	-	30:00	-	-	-	-	-
	b	No	-	30:00	-	-	-	-	-
	c	No	-	30:00	-	-	-	-	27:24
6	a	No	-	09:04	-	-	-	-	04:56
	b	Yes	06:12	06:24	36.5	546	15	6	-
	c	No	-	17:54	-	-	-	-	08:58
8	a	Yes	03:33	03:39	19.6	216	12.3	4.41	-
	b	Yes	04:07	04:14	29.5	396	12.34	5.37	-
	c	Yes	04:05	04:21	32.1	439	14.15	5.48	-
9	a	No	-	17:38	-	-	-	-	04:30
	b	No	-	15:06	-	-	-	-	04:00
	c	No	-	15:05	-	-	-	-	07:50
10	a	No	-	30:00	-	-	-	-	14:42
	b	No	-	30:00	-	-	-	-	13:18
	c	No	-	30:00	-	-	-	-	12:30
11	a	Yes	01:08	02:55	16.18	63	8.44	1.6	-
	b	Yes	01:13	03:47	43.34	258	10.09	2.4	-
	c	Yes	01:07	01:56	16.34	57	10.27	1.4	-
12	a	No	-	18:09	-	-	-	-	05:23
	b	Yes	02:50	03:03	15.1	174	10.86	4.6	-
	c	Yes	03:25	03:27	10.8	92	11.27	3.4	-
13	a	Failed	-	-	-	-	-	-	-
	b	No	-	30:00	-	-	-	-	10:00
	c	No	-	30:00	-	-	-	-	21:00
14	a	No	-	30:00	-	-	-	-	17:55
	b	No	-	30:00	-	-	-	-	19:00
	c	No	-	30:00	-	-	-	-	22:26

*Spall volume determined by sand method

6.7.2.1 Samples heated too severely due to trapped convective gases

The first two sets of experiments were carried out with the 100 mm thick samples positioned centrally in the loading frame. It was not possible to measure the difference in thermal exposure directly, due to the nature of the heat flux gauges available. It was however assumed after observing the experiments that the thermal exposure that samples experienced in this configuration under the HCM equivalent thermal exposure was more severe than that experienced by samples not set back within the loading frame.

The three samples of Experiment Type 1 all experienced localised, early, shallow spalling. This spalling was not deemed sufficient to stop the experiments and so they were not stopped until there were issues with blowback in the radiant panel array due to overheating. This is the same criteria followed for the experiments described in Chapter 5. The problem with blowback is discussed further in Section 6.9.2. After this early spalling, the three samples went on to develop cracks and no further spalling was observed.

In Experiment Type 2 no spalling occurred. Whilst the thermal exposures experienced in experiment types 1 and 2 were not believed to be the desired exposures, they demonstrated, that for a 100mm thick unloaded sample, spalling was unlikely when using the ISO 834 equivalent curve. Based on this result the HCM equivalent thermal exposure was carried forward as the primary thermal exposure in an attempt to ensure that some spalling occurred in the remaining experiments.

6.7.2.2 Samples heated consistently

After the initial issues with thermal exposure, 100 mm thick samples were tested again unloaded, but with the sample positioned so that the sample face was at the front of the loading frame to avoid the large overhang. Experiment types 6, 9 and 12 correspond to 100 mm thick samples exposed to the HCM equivalent thermal exposure. The only difference between the experiment types was the stage during the experimental programme that the experiments were carried out resulting in different sample ages. The nine tests were spread, in sets of three, throughout the overall experimental programme. Experiments of Type 6 were carried out at a concrete age of 960-965 days, Type 9 at an age of 1026 – 1030 days and Type 12 at an age of 1093 – 1130 days. In the majority of experiments spalling did not occur however Experiment 6B and Experiments 12B and 12C spalled. The other six samples did not spall. The reason for this variation in behaviour is not clear.

The variation was not expected but it is not common for nine identical spalling experiments on essentially identical concrete samples to be carried out. As a result the expected variation in spalling performance is not well known. The samples exposed to the ISO 834 equivalent thermal exposure in the same way did not experience any spalling. This supports the theories that the more severe thermal exposure increases spalling however the variation in results from the HCM equivalent experiments brings further questions around the number of repeats that should be carried out to understand the spalling performance of a concrete mix.

The 175mm thick samples originally allocated for loaded tests were used as a further comparison of thermal exposure. All three experiments of Experiment Type 11 exhibited an unusual spalling behaviour unlike that seen in any other experiments during this series or the experiments described in Chapter 5. No spalling was seen in the three experiments of Experiment Type 13 with the ISO 834 equivalent heating curve. This result supports the theory samples are more likely to spall when exposed to the HCM equivalent heating curve. However when compared to the rest of the results, the results do appear to be outliers. In experiments on 12 other unloaded, thicker and thinner samples (experiment types 3, 6, 9 and 12) spalling did not occur with the exception of three tests. The unusual spalling occurring in Experiment Type 11 will be discussed further in Section 6.9.4.

6.7.3 Sample thickness

The experiment types that can be used for a direct comparison of the influence of sample thickness on spalling are summarised in Table 6.8. All of the experiments were unloaded sample exposed to the HCM equivalent thermal exposure.

Table 6.8: Experiments allowing direct comparisons of the influence of sample thickness on spalling:

Experiment type	Exposure	Exposure window (mm)	Sample location	Thickness (mm)	Compressive stress (MPa)
3	HCM	450 x 450	Front	250	0
6	HCM	450 x 450	Front	100	0
9	HCM	450 x 450	Front	100	0
11	HCM	450 x 450	Front	175	0
12	HCM	450 x 450	Front	100	0

Experiment types 6, 9, 11 and 12 have also been given in the Section 6.7.2 in comparison of the influence of different thermal exposures. The results of the tests investigating sample thickness are summarised in Table 6.9.

Table 6.9: Results of experiments allowing direct comparisons of the influence of sample thickness

Experiment type		Spalling	Spalling time (mm:ss)	Test duration (mm:ss)	Spall area (%)	Spall volume (cm^3)	Maximum depth of spall (mm)	Average spall depth (mm)	Time of first crack or seeping (visible) (mm:ss)
3	a	No	-	30:00	-	-	-	-	19:40
	b	No	-	30:00	-	-	-	-	12:46
	c	No	-	30:00	-	-	-	-	12:20
6	a	No	-	09:04	-	-	-	-	04:56
	b	Yes	06:12	06:24	36.5	546	15	6	-
	c	No	-	17:54	-	-	-	-	08:58
9	a	No	-	17:38	-	-	-	-	04:30
	b	No	-	15:06	-	-	-	-	04:00
	c	No	-	15:05	-	-	-	-	07:50
11	a	Yes	01:08	02:55	16.18	63	8.44	1.6	-
	b	Yes	01:13	03:47	43.34	258	10.09	2.4	-
	c	Yes	01:07	01:56	16.34	57	10.27	1.4	-
12	a	No	-		-	-	-	-	05:23
	b	Yes	02:50		15.1	174	10.86	4.6	-
	c	Yes	03:25		10.8	92	11.27	3.4	-

The results of the experiments comparing sample thickness are less conclusive than those investigating thermal exposure. Results of the experiments described in Chapter 4 showed that increased sample thickness resulted in more spalling. This was thought to be due to the thicker concrete samples resisting the thermal expansion and preventing the thermally induced stress in the heated surface being relieved by bowing which was seen in the thinner samples.

When the unloaded 250 mm thick samples did not spall it was be expected that the thinner samples would also not spall. Of the first three 100 mm thick samples (Experiment Type 6) one sample spalled, however when further repeats were carried out in Experiment Type 9 no spalling occurred and then two of the three samples tested in Experiment Type 12 spalled. As mentioned previously the 175 mm samples

displayed an unusual spalling behaviour that was not seen in any other tests; this behaviour is referred to by the author as “popcorn spalling” and discussed in Section 6.9.4. Based on the results from these experiments it is not possible to make conclusions regarding the influence of sample thickness or the appropriate sample thickness to use for experiments, as the variation in results was unable to support any hypothesis. Had further repeats been possible of the 250 and 175 mm thick samples they may have spalled in the same way that three of nine 100 mm samples spalled.

6.7.4 Load level

As discussed previously it was not possible to load any samples other than those which were 250 mm thick. This meant that all experiments for the comparison of the influence of load were carried out using 250 mm thick samples. The experiment types that allowed comparison of the influence of load are shown in Table 6.10.

Table 6.10: Experiments allowing direct comparison of the influence on spalling of externally applied load

Experiment type	Exposure	Exposure window (mm)	Sample location	Thickness (mm)	Compressive stress (MPa)
3	HCM	450 x 450	Front	250	0
4	HCM	450 x 450	Front	250	5
5	HCM	450 x 450	Front	250	10
15	HCM	450 x 450	Front	250	15

The results of the loaded experiments are shown in Table 6.11. It can be seen that the unloaded samples did not spall and the presence of loading was enough to alter the behaviour of the concrete from not spalling to spalling violently. Note for spall volumes an asterisk mean that the volume was measured using the sand method developed by the author. Where there is no asterisk the 3D scanner was used. This is discussed in Section 6.4.4.3.

Table 6.11: Results of experiments allowing direct comparison of the influence on spalling of externally applied load

Experiment type		Spalling	Spalling time (mm:ss)	Test duration (mm:ss)	Spall area (%)	Spall volume (cm^3)	Maximum depth of spall (mm)	Average spall depth (mm)	Time of first crack or seeping (visible) (mm:ss)
3	a	No	-	30:00	-	-	-	-	19:40
	b	No	-	30:00	-	-	-	-	12:46
	c	No	-	30:00	-	-	-	-	12:20
4	a	No	-	26:00	-	-	-	-	-
	b	Yes	06:59	06:59	73.7	1745*	18.4	9.5	-
	c	No	-	30:00	-	-	-	-	-
5	a	Yes	07:49	07:49	93.2	2830*	20.2	12.1	-
	b	Yes	07:48	07:54	83.7	2160*	20.2	10.3	-
	c	Yes	04:51	04:51	39.5	566	12.9	5.7	-
15	a	Yes	03:28	03:31	11.9	82	9.8	5.1	-
	b	Yes	03:54	03:58	52.5	684	12.6	5.8	-
	c	Yes	05:19	05:21	23.1	273	14.9	4.8	-
	d	Yes	04:33	04:37	15.1	168	13.3	6.1	-

*Spall volume determined by sand method

Samples from Experiment Type 3, which were tested unloaded, were seen to crack and moisture escaped from these cracks. The crack times given are times when cracking was visible on the video footage of the experiments, and any very fine cracking or cracking on other surfaces is not accounted for. No spalling occurred in any of the experiments in which visible cracking and moisture escape from the sample occurred.

The application of 5 MPa of uniaxial compressive stress to the 250 mm thick samples, Experiment Type 4, resulted in the prevention of the cracking that was observed in the unloaded tests. One of the three samples spalled violently but the others did not spall at all. It is thought that this load of 5 MPa might represent a load close to a critical load for spalling for this concrete. This theory is backed up by the occurrence of spalling in all the samples tested at load levels of 10 MPa or higher. Interestingly, of all the experiments carried out, the most violent spalling occurred in Experiment 5A

and Experiment 5B, which were loaded to a precompressive uniaxial stress of 10 MPa.

It was originally thought that increasing the externally applied load would increase the severity of spalling. Samples loaded to 15 MPa were observed to spall earlier but less violently than samples loaded to 10 MPa. Since the experiments are stopped after the first occurrence of spalling it is not possible to determine if, in either case, continuous spalling would occur and which of the two load cases would represent a worst case for a concrete structure. Some recent research (Miah *et al.*, 2017) proposed that increased loading over a certain level can lead to increased micro cracking aiding moisture transport. It is possible that an effect like this could be the cause of the reduced spalling severity when the externally applied uniaxial compressive stress increased beyond 10 MPa.

6.7.5 Thermal exposure window

The experiments allowing the comparison of the influence of heating area are summarised in Table 6.12.

Table 6.12: Experiments allowing direct comparison of the influence on spalling of the heated area

Experiment type	Exposure	Exposure window (mm)	Sample location	Thickness (mm)	Compressive stress (MPa)
4	HCM	450 x 450	Front	250	5
6	HCM	450 x 450	Front	100	0
7	HCM	200 x 200	Front	250	5
8	HCM	200 x 200	Front	100	0
9	HCM	450 x 450	Front	100	0
10	ISO	200 x 200	Front	100	0
12	HCM	450 x 450	Front	100	0
14	ISO	450 x 450	Front	100	0

Comparison of the influence of the heated area on the spalling performance can be made for both thermal exposures used and for loaded samples. Table 6.13 shows the results of these tests.

Table 6.13:Results of experiments allowing direct comparison of the influence on spalling of the heated area

Experiment type		Spalling	Spalling time (mm:ss)	Test duration (mm:ss)	Spall area (%)	Spall volume (cm^3)	Maximum depth of spall (mm)	Average spall depth (mm)	Time of first crack or seeping (visible) (mm:ss)
4	a	No	-	26:00	-	-	-	-	-
	b	Yes	06:59	06:59	73.7	1745*	18.4	9.5	-
	c	No	-	06:00	-	-	-	-	-
6	a	No	-	09:04	-	-	-	-	04:56
	b	Yes	06:12	06:24	36.5	546	15	6	-
	c	No	-	17:54	-	-	-	-	08:58
7	a	No	-	10:17	-	-	-	-	-
	b	No	-	12:52	-	-	-	-	09:00
	c	Yes	05:18	05:20	32.1	550*	13.8	6.85	
8	a	Yes	03:33	03:39	19.6	216	12.3	4.41	-
	b	Yes	04:07	04:14	29.5	396	12.34	5.37	-
	c	Yes	04:05	04:21	32.1	439	14.15	5.48	-
9	a	No	-	17:38	-	-	-	-	04:30
	b	No	-	15:06	-	-	-	-	04:00
	c	No	-	15:05	-	-	-	-	07:50
10	a	No	-	30:00	-	-	-	-	14:42
	b	No	-	30:00	-	-	-	-	13:18
	c	No	-	30:00	-	-	-	-	12:30
12	a	No	-	18:09	-	-	-	-	05:23
	b	Yes	02:50	03:03	15.1	174	10.86	4.6	-
	c	Yes	03:25	03:27	10.8	92	11.27	3.4	-
14	a	No	-	30:00	-	-	-	-	17:55
	b	No	-	30:00	-	-	-	-	19:00
	c	No	-	30:00	-	-	-	-	22:26

*Spall volume determined by sand method

For the 250 mm thick samples loaded to 5 MPa (test types 4 and 7), the reduction in the heating area in Experiment Type 7 did not have a clear impact on the spalling behaviour. In both experiment types one in three of the samples spalled. The spall volume and spall area and spall depth were lower in Experiment 7C but this sample also had a smaller heated surface. The spall area in Experiment 7C was double the

heated area. It is not appropriate to attempt to assess which was a more severe spall between Experiment 4B and Experiment 7C.

The cool concrete surrounding the localised central heated area is thought to result in additional thermal stresses as the cool concrete restrains expansion of the heated concrete. It was hypothesised that this additional restraint for a sample under 5 MPa of compression could result in a more severe spalling behaviour, perhaps similar to that observed for the samples with tested under compressive loads of 10 and 15 MPa. This was however not the case when the experiments were carried out. The application of 5 MPa of compression might already outweigh the influence of reduced heating area.

In Experiment Type 8 the 200 x 200 mm heating area and HCM equivalent thermal exposure were sufficient to cause all three samples to spall. This can be compared to the nine 100 mm thick samples subjected to the HCM equivalent thermal exposure of which three samples spalled. In this case the reduced heating area was sufficient to cause spalling. It was unexpected that the unloaded 100 mm thick samples heated over a 200 x 200 mm area all spalled yet the 250 mm thick samples heated in the same way but with the addition of 5 MPa of compressive stress did not spall.

No spalling occurred in any of the samples heated to the ISO 834 equivalent thermal exposure so it is not possible to make any conclusions about the influence of heating area on spalling from those tests.

6.8 Results – Through-thickness temperatures

During experiments, the temperatures were measured at target depths from the heated surface of the samples. Comparison of these temperatures gives an indication of the consistency of the thermal exposures experienced by the samples across the 45 experiments. It is important to note that positioning of these thermocouples during casting is challenging and some variation in the temperatures measured is due to actual thermocouple position differing from target position.

6.8.1 HCM equivalent thermal exposure

The average and standard deviation of temperature measurements for the all HCM equivalent thermal exposure experiments are plotted in Figure 6.16. Data from all thermocouples is used except for thermocouples that broke. In the event of a thermocouple breaking during an experiment, the data for the point until thermocouple broke was retained. Jumps in the plot are due to experiments ending because of

spalling, or panel malfunction, or due to a thermocouple breaking and being cut short at the point they broke. The issues encountered with the apparatus during experiments are covered in Chapter 3.

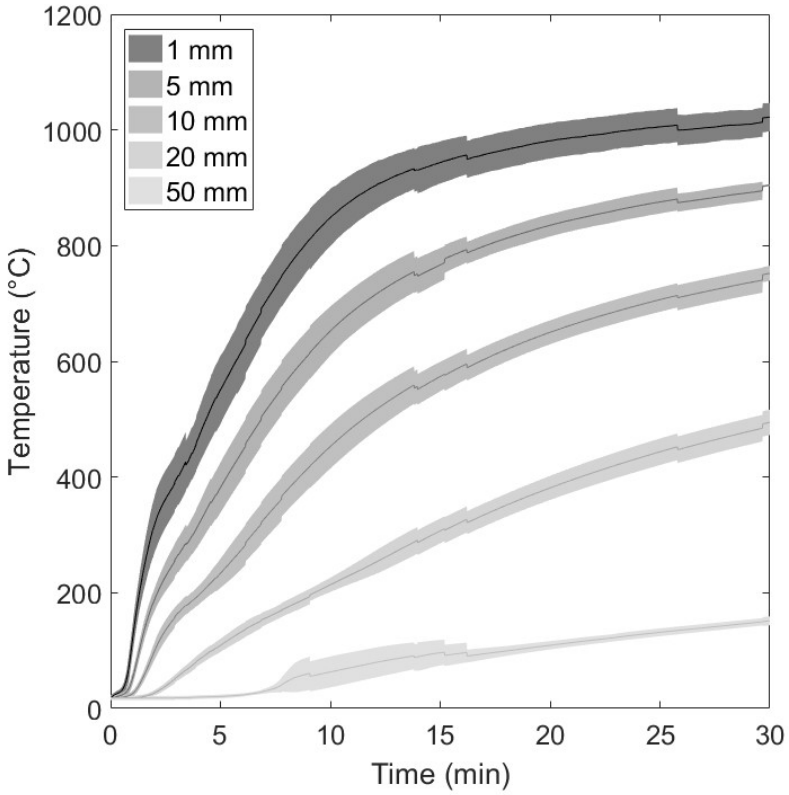

Figure 6.16: Average and standard deviation of through-thickness temperatures from Phase 3 H-TRIS HCM equivalent experiments

It is interesting to note the increase in spread of the 50 mm depth thermocouple readings between of 7 and 17 minutes. Figure 6.17 shows the raw 50 mm temperature data. The sudden rise in temperature to around 100 mm with a long plateau is likely to be due to moisture being transported from the hot surface back into the cool concrete. Internal cracking could allow hot moisture to move back into the sample quickly increasing the temperature in the area of the thermocouple tip. A similar phenomena was observed in some similar experiments carried out by the author (Figueiredo *et al.*, 2017). The differing rates of temperature increase at the 50 mm thermocouples are possibly due differing internal cracking or moisture transport.

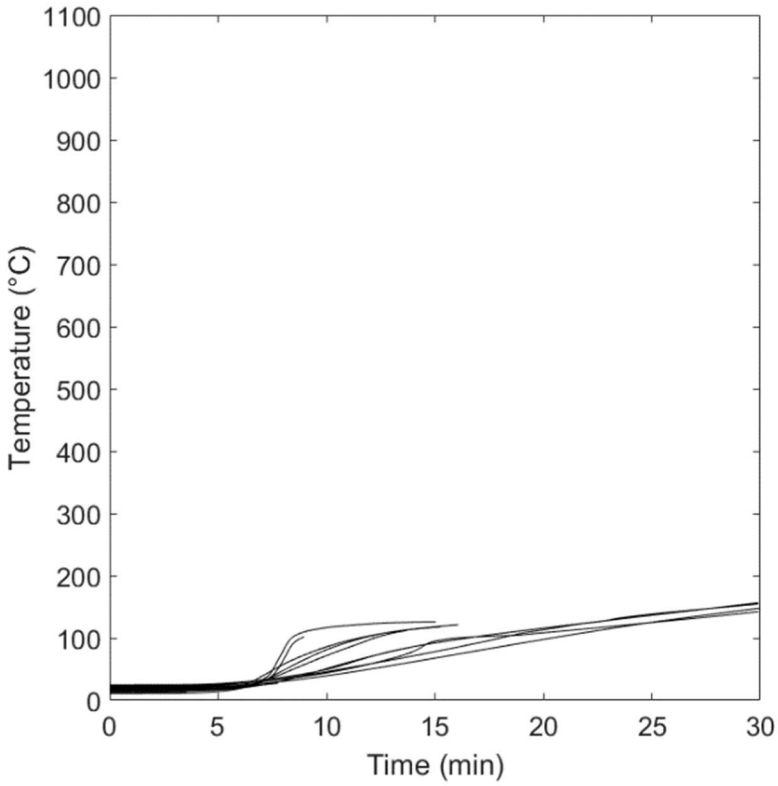

Figure 6.17: Raw data from 50mm depth thermocouples during HCM equivalent experiments

6.8.2 ISO equivalent thermal exposure

The average and standard deviation of temperature measurements for the all but one of the IS0 equivalent thermal exposure experiments are plotted in Figure 6.18. The temperature data shows good repeatability across the ISO experiments. Data from Experiment 13B was not included in this plot as it is believed that the thermocouple tree was dislodged during casting. This will be discussed later in Section 6.9.5.

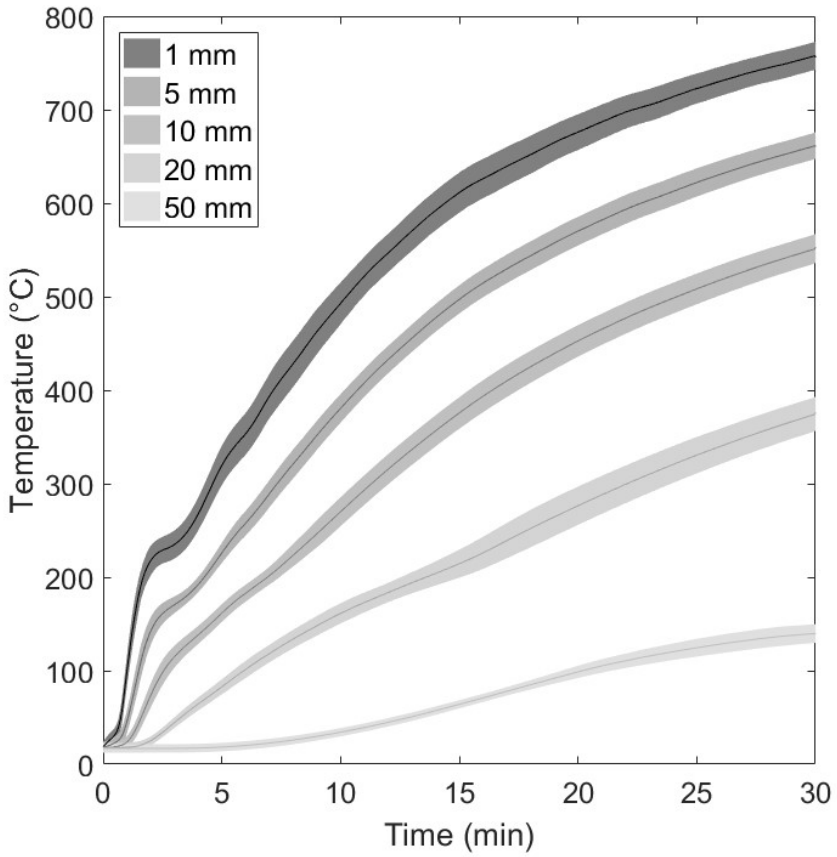

Figure 6.18: Average and standard deviation of through-thickness temperatures from Phase 3 H-TRIS ISO equivalent experiments

6.9 Discussion

This section discusses the primary sources of error during experiments and goes into further detail for the experiments which gave unexpected results either in the spalling behaviour or the measured through-thickness temperatures.

6.9.1 Sources of error

6.9.1.1 Thermocouple Location

The primary source of error with respect to temperature measurement is in placement of the thermocouples. It is very challenging to place thermocouples in a formwork and ensure that they will not move during pouring and vibration of the wet concrete particularly when carrying out large casts. The target depths from the heated surface for the thermocouples were 1, 5, 10, 20 and 50 mm with an additional thermocouple at 100 mm in the 250 mm thick samples. Due to the steep thermal gradient, a very small error in thermocouple position can result in a large change in recorded temperatures for exactly the same thermal exposure. This is discussed further in Chapter 7.

6.9.1.2 Sample age at time of experiment

Due to issues encountered during the development and operation of the apparatus, the experiments were spread over a year. This is not ideal as it is not clear how sample age might affect the results. However, given that the samples were already over 2 years old it is not thought that the properties of the concrete would change much. The ages of the samples are discussed further when discussing unexpected results.

6.9.1.3 Issues with the experimental apparatus

The radiant panels used on H-TRIS during this series of experiments were chosen because of their ability to deliver a high incident heat flux. The peak incident heat flux that a sample can be exposed to with these GoGas panels is around 300kW/m^2. There were however issues with the panels that did not occur when using other less powerful panels such as those which were used on the original H-TRIS. The issues encountered when using the panels are discussed in detail in Chapter 3.

6.9.2 Thermal exposure – centrally located 100 mm thick samples

The overhang of the loading frame can trap convective gases from the radiant panels, particularly when the radiant panels are at close proximity to the sample surface. The overhanging edges of the frame would also heat up and reradiate. The result being that the sample would have experienced a more severe thermal exposure than

samples positioned with the heated face at the front edge of the loading frame. The sample positioning is shown in Figure 6.19.

This increased thermal exposure was evidenced by the melting of aggregates close to the surface, which did not occur in any other tests. In addition, the radiant panels overheated when they moved into this overhanging zone and blowback was observed. At the end of the experiments the samples glowed red, see Figure 6.20. After cooling, the aggregate was seen to have “melted” and seeped from the surface, see Figure 6.21 and Figure 6.22.

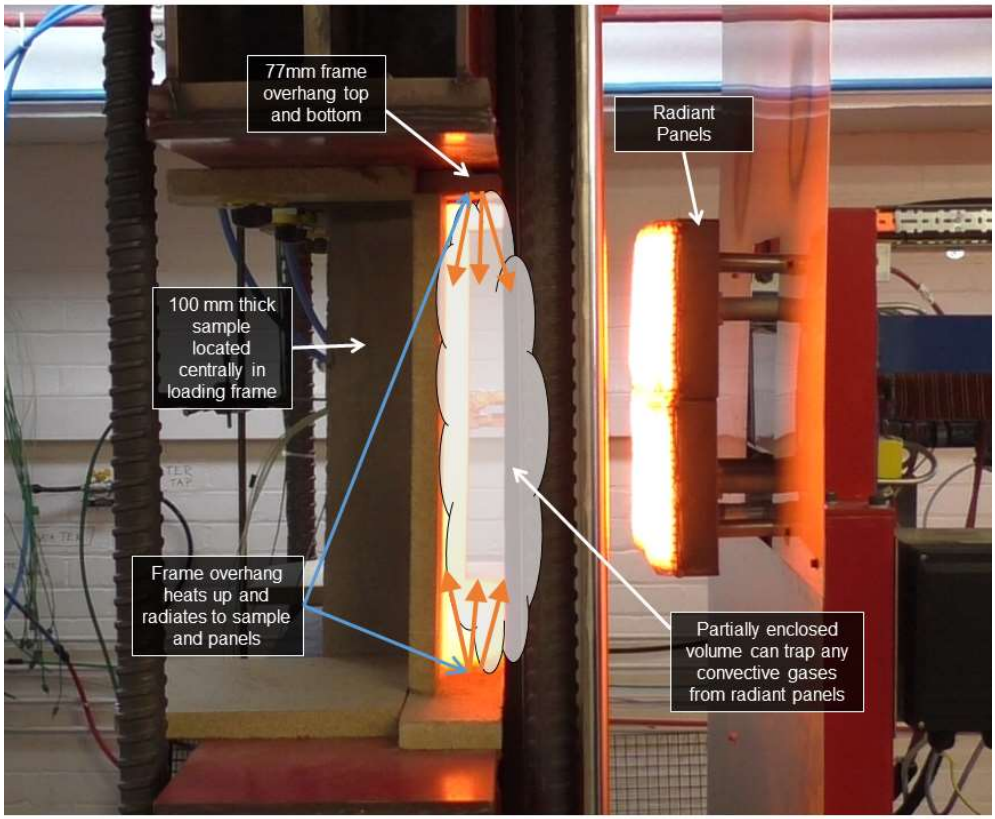

Figure 6.19: Centrally located 100mm thick sample

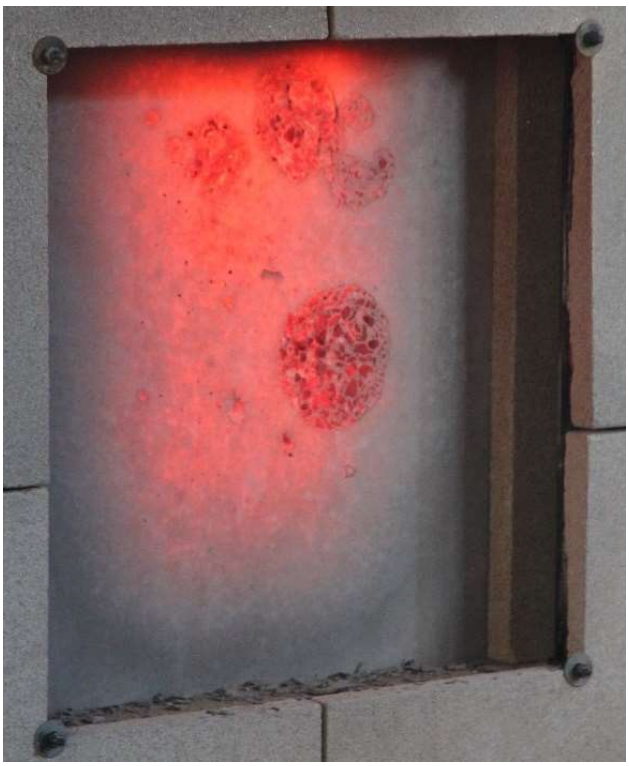

Figure 6.20: Sample glowing red after completion of Experiment 1C

Figure 6.21: Cooled sample after Experiment 1C heated area as per Figure 6.19

Figure 6.22: Melted aggregate, highlighted with arrows, seen seeping from the surface of the sample used in Experiment 1C

Since the thermal exposure does not appear to be correct or in line with the thermal exposure experienced by samples in the other experiments of this series, these experiment types were not used for comparisons other than between each other. Running experiments with the samples in this configuration was an oversight and this kind of experiment should not be repeated as the thermal exposure is unquantified and the apparatus can be damaged by overheating.

6.9.3 Variation in results - 100 mm HCM equivalent experiments

In the nine experiments on 100 mm thick samples exposed to the HCM equivalent thermal exposure (experiment types 6, 9 and 12) a variation in the results was observed. From the nine experiments six samples did not spall and the other three samples did. The samples that spalled were Experiment 6B, and Experiment 12B and 12C.

One hypothesis for the different behaviour is that somehow the samples experienced a more severe or somehow different thermal exposure. The temperatures measured using the internal thermocouples are shown in Figure 6.23 with plots A, B, C and D corresponding to target thermocouple depths of 1, 5, 10 and 20 mm from the heated surface. The temperatures from the three samples that spalled are shown in red. From the graphs, it does not appear that the samples received a different thermal exposure to that experienced by the other tested samples. The Experiment Type 12 experiments were also carried out immediately after a heat flux calibration.

As mentioned previously the only clear variation between these tests was the age of the samples. Typically, in fire-resistance tests, concrete will be tested at minimum age

of around 90 days as the influence of age on the concrete properties decreases with time after an initial curing period. One of the Type 6 experiments and two of the Type 12 experiments spalled. No spalling was observed in the Type 9 experiments that were carried out between the Type 6 and Type 12 experiments. As a result, it seems unlikely that the age is the critical factor. As a side note, if the difference in spalling performance were to be a result of the increase in the age of the concrete being tested from 960 to 1130 days then this would be a concerning result and raise questions about the appropriate age at which concrete should be tested. It is interesting that the spalling that occurred in one of the Type 6 experiments was later and more severe than the spalling that occurred in the Type 12 experiments.

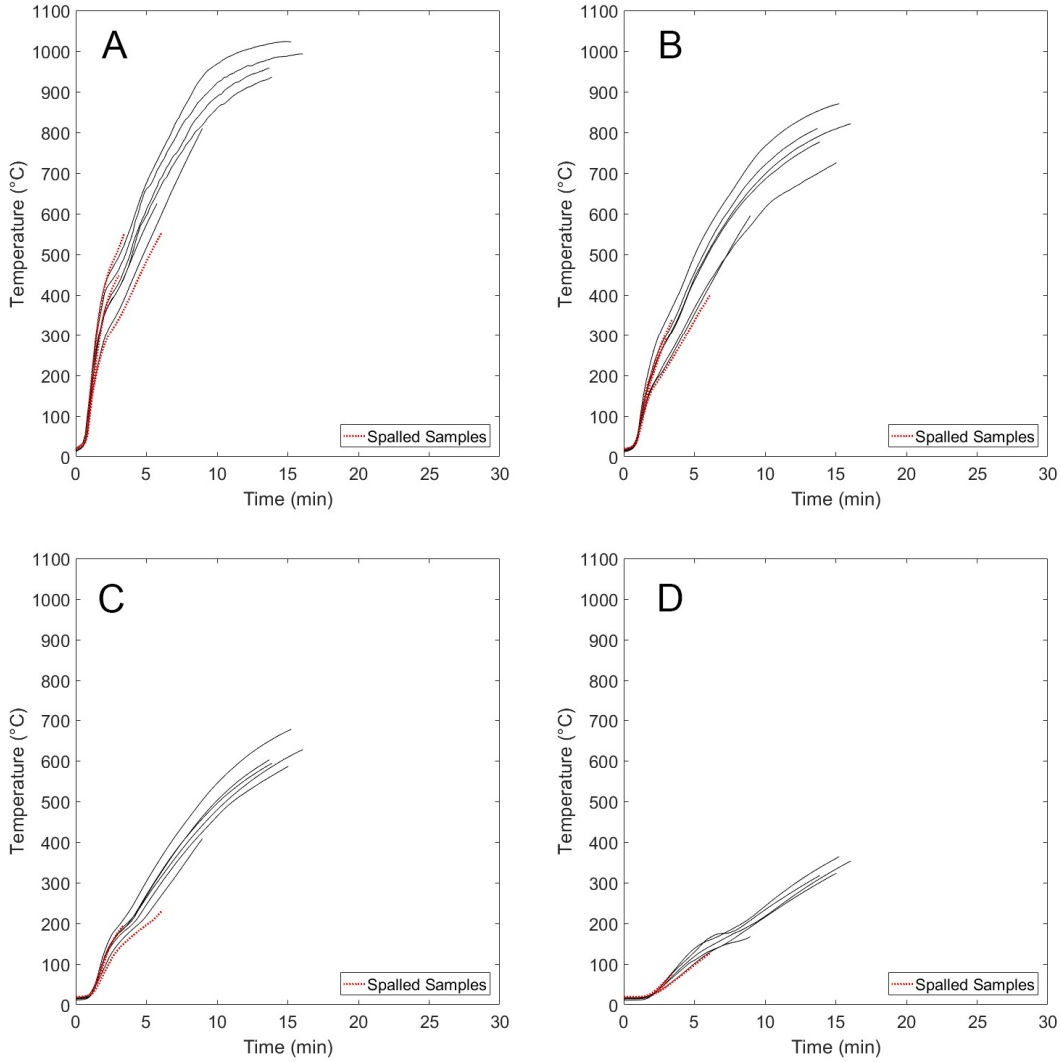

Figure 6.23: Through-thickness temperatures, at depths of (A) 1mm (B) 5mm (C) 10mm (D) 20mm, for the nine 100 mm thick samples tested to HCM equivalent exposure

6.9.4 Popcorn like spalling observed for 175 mm thick samples

The 175 mm thick samples heated using the HCM equivalent thermal exposure spalled in a manner that was not observed in any other experiments, including those carried out in Phase 2 and the many spalling experiments that the author has carried out for other projects. Typically, in other experiments there may be one or two very small aggregate spalls, meaning that a very small, thin piece of aggregate may have popped off the surface of the sample during heating. This very gentle aggregate spalling would not be significant or continuous and a more substantial spall may occur later in the experiment. The experiment would be stopped with the occurrence of the large spall or continued for the full 30-minute duration if no spalling occurred. In the experiments of the 175 mm thick samples exposed to the HCM equivalent thermal exposure there was a phase of fast continuous “popcorn” spalling very early in the experiment. This popcorn spalling consisted of many small spalling incidents occurring rapidly for a prolonged period of time. In all three experiments, this period of popcorn spalling lasted for around a minute commencing in the three repeats at experiment times of between 1 minute 7 seconds and 1 minute 13 seconds. The reason for this repeatable yet unexpected behaviour is unclear, no other samples spalled in this way and based on the other results it would be expected that the samples in these experiments would not spall. The 250 mm thick samples did not spall at all under the same conditions.

The radiant panels were calibrated just before the experiments were carried out so the thermal exposure should have been accurate. Inspection of the through-thickness temperatures measured during the experimenting does not show anything unusual. The temperatures measured in the three Type 11 experiments are highlighted in red in Figure 6.24 for target depths of (A) 1 mm (B) 5 mm (C) 10 mm (D) 20 mm.

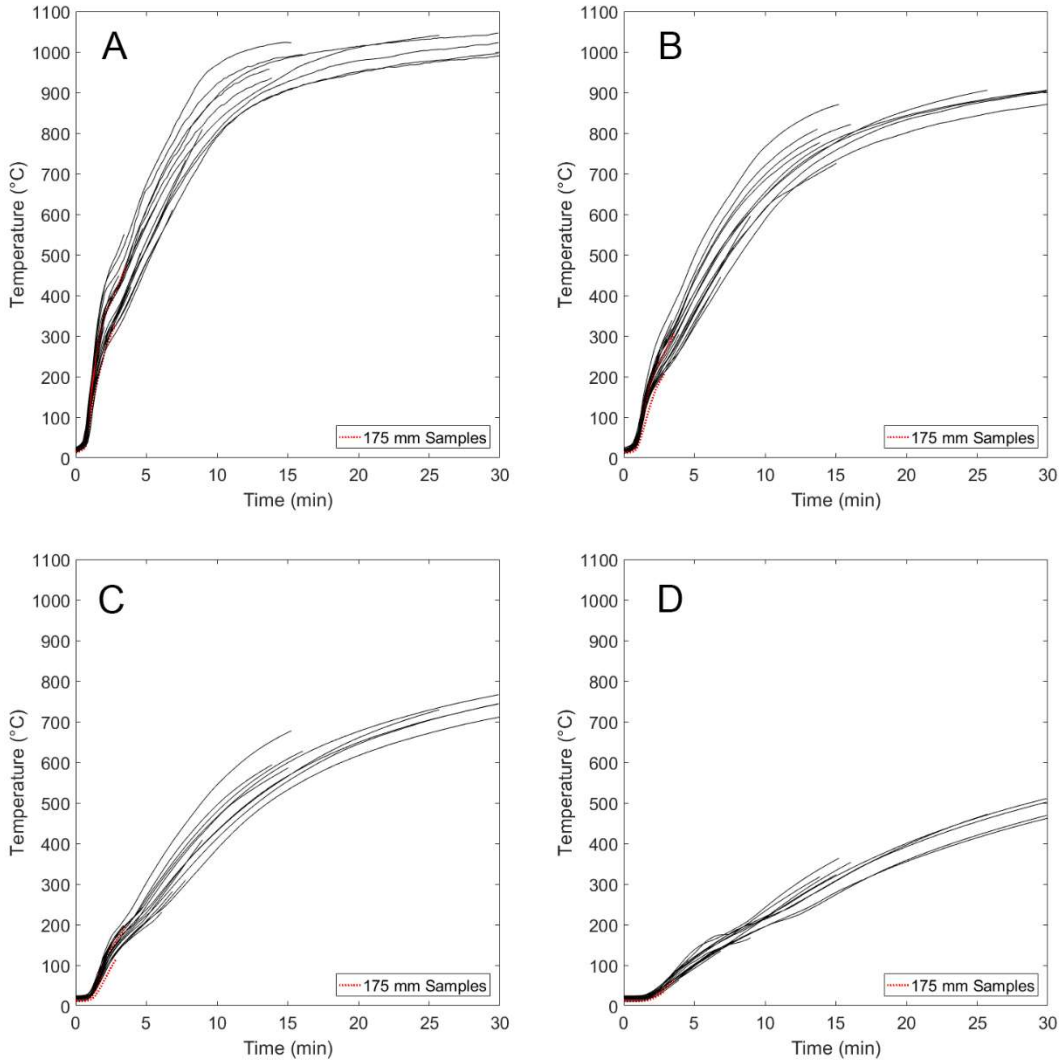

Figure 6.24: Through-thickness temperatures at (A) 1 mm (B) 5 mm (C) 10 mm (D) 20 mm. Data from Type 11 experiments highlighted in red.

From inspection of the surface of the samples before the experiments, there was no noticeable difference between the surface of the 175 mm thick samples and the samples of other thicknesses. The formwork and casting procedure was the same and they were cured in the same way. The age of the samples at time of testing was 1085, 1086 and 1087 days for samples used in experiments a, b and c respectively. It is not thought that the age of the samples could be the critical factor influencing this unusual spalling as other samples were tested both before and after these and no popcorn spalling was observed.

Some theories as to the possible cause of this unexpected behaviour are presented below.

The first theory as to what might have caused this strange result is that the formwork or concrete may have been contaminated in some way. The 175 mm thick samples were all cast in the same formwork, which was a block of six 175 mm thick samples. All of the formwork was stored in The Structures Laboratory at The University of Edinburgh prior to casting. While the formwork was brushed out and coated with form release agent before casting, it is possible that a dust remained in the formwork of the 175 mm samples. However, the author is not aware of any materials being used in The Structure Laboratory that could have left a residue that might cause this effect.

The second theory is that it is possible that the concrete in this form was vibrated excessively. Over 3 m^3 of concrete was cast by hand and the help of the other PhD students had to be enlisted, precise monitoring of concrete vibration was not possible. Excessive vibration would cause the aggregate fines to sink to the bottom of the formwork due to granular convection. The bottom of the formwork is the sample face when heated during experiments.

The third theory proposed is that the first layer of concrete in the formwork for these samples could have been filled with the first concrete to be poured from the ready-mix truck resulting in a slightly different composition. This seems unlikely as the concrete delivery truck mixes the concrete continuously. The first concrete down the chute of the ready mix truck could have picked up some contaminants.

It is not possible to check these proposed theories and to the authors knowledge there is no literature available regarding the influence of over vibration on heat-induced spalling of concrete.

The popcorn spalling introduced a lot of concrete dust and particles into the panels of H-TRIS meaning that they needed to be replaced after these three experiments. As mentioned in Chapter 3 the concrete dust appears to react at the very high temperatures of the radiant panel with the silicon carbide porous media. The panels were working correctly during these three experiments as indicated by the very repeatable times to “popcorn spalling” and the through-thickness temperatures shown in Figure 6.24. The panels were changed after these three experiments as the porous media started to foam.

6.9.5 Low temperatures recorded in Experiment 13B

The through-thickness temperatures measured for this experiment are all noticeably lower than seen in the other ISO equivalent tests. Figure 6.25 shows the temperatures for the different thermocouples in Experiment 13b compared to the rest of the tests. A fresh calibration was carried out immediately prior to Experiment 13b and this calibration was used for other tests that did not show the same low temperatures during experiments. Based on this, it is assumed that the low temperatures at all depths are a result of the thermocouple tree being significantly displaced during casting and that the temperatures were measured at a greater depth from the surface than intended. It is assumed that the thermal exposure experienced by the sample in Experiment 13b was in line with that experienced by other samples tested to the ISO equivalent thermal exposure.

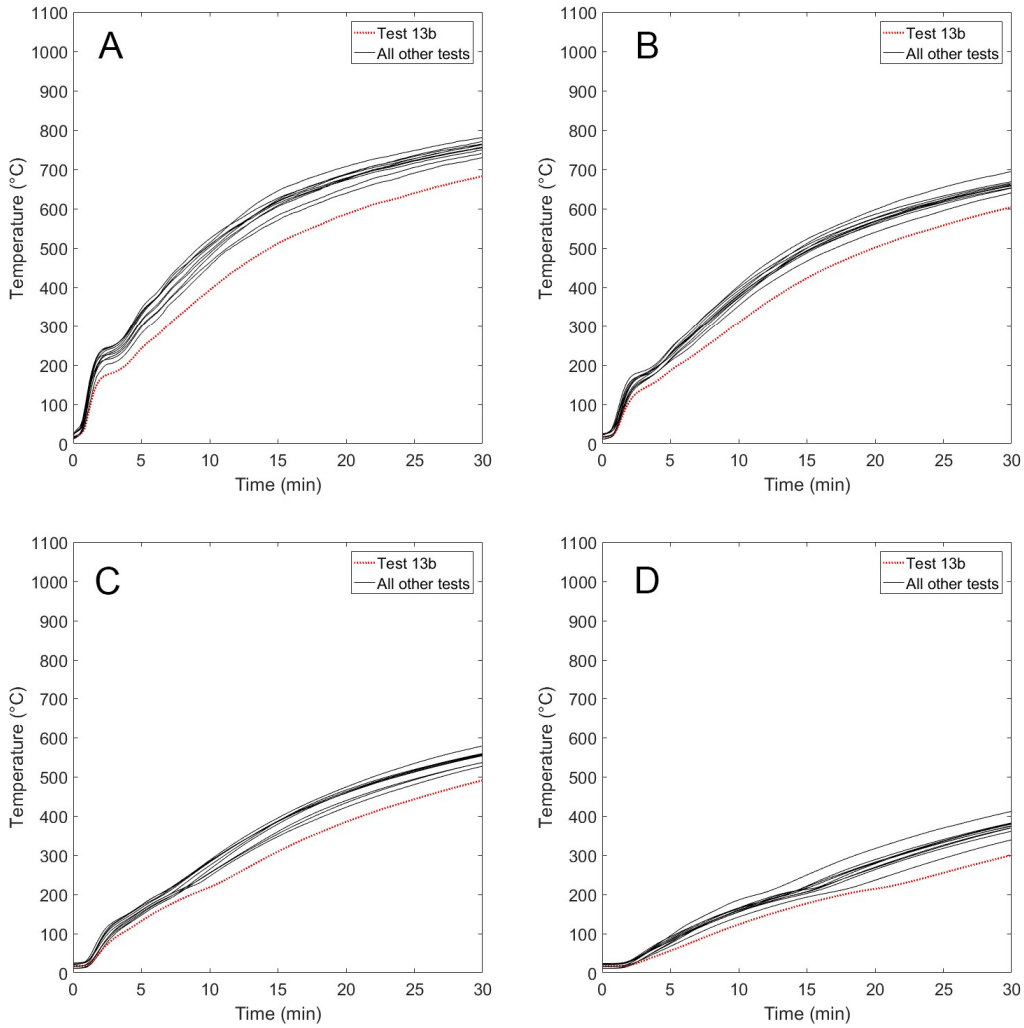

Figure 6.25: Through-thickness temperatures at (A) 1 mm (B) 5 mm (C) 10 mm (D) 20 mm for ISO equivalent experiments. Data from Experiment 13B highlighted in red

6.9.6 Spall volume with spalling time

Comparison of the spalling characteristics further than if spalling occurred or not is challenging. This is due to the experiments being stopped after first spall as discussed in Section 6.5.1. It is not possible to determine whether spalling would continue if heating continued. The clearest metric of spalling severity is the volume of the first spall. This spall volume can be plotted against experiment time as shown in Figure 6.26. While experiment parameters are being varied, including loading, it appears that the volume of the first spall increases with increasing experiment time. Given the limited data, and the data spread, the author would not be prepared to draw conclusions from this plot but it has been included for completeness.

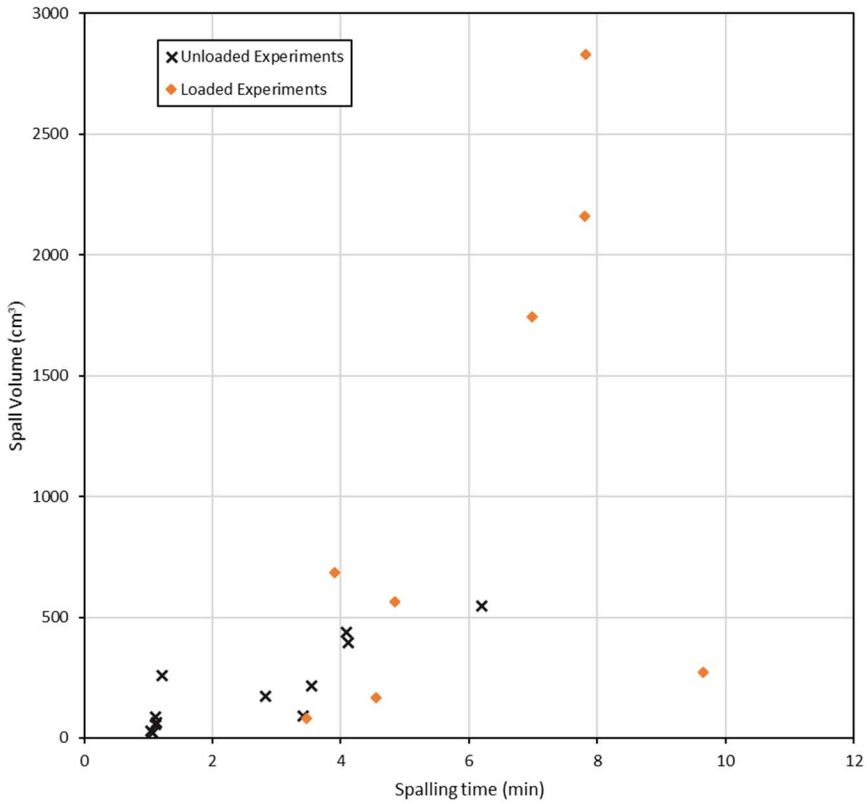

Figure 6.26: Volume of first spall versus time of spalling

6.9.7 Average spall depth with spalling time

The relationship between the spall volume and spall time was assessed above. An alternative metric is to consider the average spall depth (spall volume/spall area) of each spall with spalling time. This is shown in Figure 6.27 and it can be seen that there is a trend of the average spall depth increasing with spalling time.

Again as above, experiment parameters are being varied, including loading. Given the limited data, and the data spread, the author would not be like to draw definitive conclusions from this plot but it does appear that there is a relationship between these two parameters and the plot has been included for completeness. Further experimental work may allow greater confidence in this comparison.

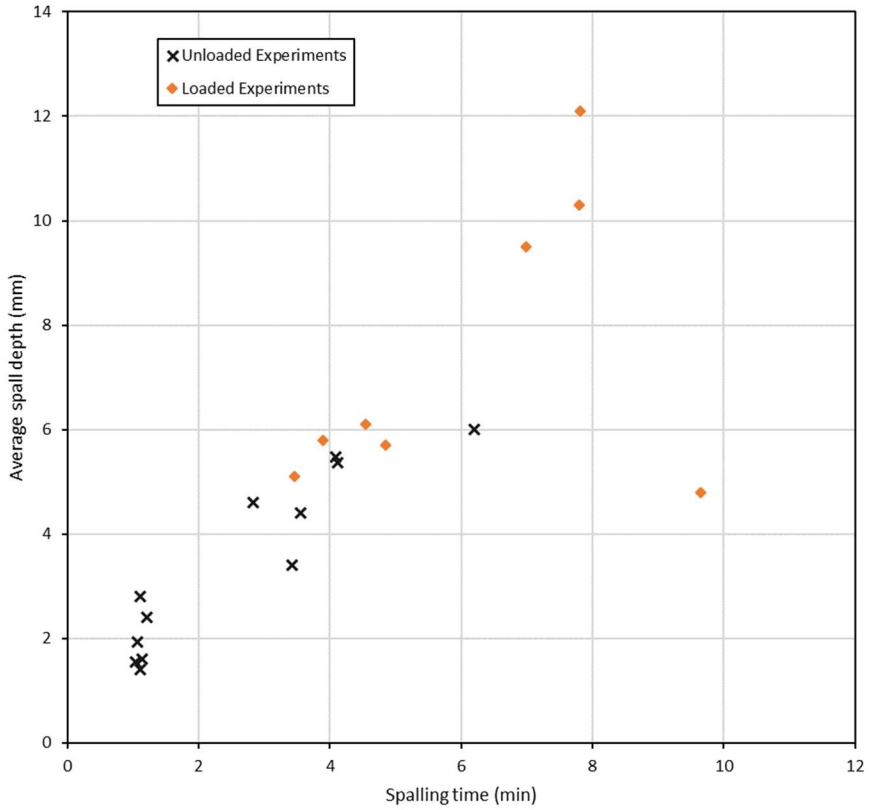

Figure 6.27: Average spall volume with spalling time

6.10 Conclusions

The results for the loaded experiments gave an insight into the influence of load on spalling. It is clear that the application of load has an influence on the spalling behaviour of a concrete. Based on the results of the experiments carried out it is unclear if, beyond a certain level, increased load causes increased or more severe spalling.

It is important when specifying spalling tests that a realistic load representative of the load likely to occur in the end use application is used. The application of external load during spalling approvals tests or in research experiments is currently often overlooked or omitted and this work has shown that load is an important parameter that must be considered. Whilst loaded experiments have been carried out before, this is the first time that it has been possible to load large samples with an externally applied uniaxial load whilst heating using the H-TRIS method.

Drawing conclusions about the influence of the other parameters investigated on the concretes spalling behaviour is more challenging. It is however clear that there is some variation in spalling behaviour between experiments of the same type. This means that multiple repeats of experiments or approvals tests should be carried out to ensure that the behaviour of the concrete is captured properly and is not a misrepresentative result.

In many of the experiment types, if fewer experiments had been carried out there could be a false confidence in the concrete behaviour. Taking the result from one test or experiment to be representative of the behaviour of the concrete could result in a dangerous end use scenario.

The theory from Phase 1 and 2 of the experimental work, that thicker samples are more prone to spalling, seems, based on the results of experiments described in this chapter, not to be valid in all cases. This series of experiments saw both 100 mm and 175 mm samples spall when 250 mm thick samples did not. Caution should be taken when drawing conclusions based on the results of Experiment Type 11 due to the strange unexplained spalling behaviour.

The influence of reduced heating area on spalling is inconclusive. For 100 mm thick unloaded samples the reduced heating area resulted in all three repeats spalling compared to three of nine samples spalling when heated normally. This suggests that

the reduced heating area creates a worse case for spalling. The results of the other experiments using 250 mm thick samples do not support this

Based on observation of all the experiments it can be concluded that no spalling occurs after the samples crack and moisture begins to escape. Samples that spalled did not visibly crack in this manner. The cracking has a combined effect. It both relieves thermal stresses as the heated face is able to expand, and provides a pathway for moisture escape, relieving pore pressure. It is not possible to decouple these two factors.

Based on the results of these experiments it appears that loading can play a critical role in the occurrence of spalling. If the only effect of loading was to prevent the cracking and moisture escape as suggested by some authors (Dougill, 1971) then it would be expected that the samples from Experiment Type 4, where cracking did not visibly occur, would all have spalled rather than just one of three.

The volume and average depth of the first spalling occurrence appears to increase with time to first spall although the author does not believe that establishing a correlation at this stage is appropriate.

While conclusions could not be made about the influence of all parameters investigated, the carefully controlled experiments described in this chapter provided valuable insight into the influence of mechanical load and the potential variability of spalling. Prior to the development of the loading frame and updating of H-TRIS, these experiments would not have been possible.

7 Issues encountered in experimental work

This section provides some general discussion and analysis relating to the thesis as a whole, and the issues encountered with thermocouple placement across all three phases of the experimental work.

The goal of replicating the thermal exposures used in furnace testing was decided at the outset of the project. At this time, even the order of magnitude of the incident heat fluxes that would be required to replicate the more severe thermal exposures in the tunnel specific temperature versus time curves was not known. Section 7.1 and 7.2 provide discussion of the issues faced with thermocouple placement and instrumentation accuracy. Section 7.3 details a heat transfer analysis used to quantify the range of temperatures likely to be recorded within the concrete due to thermocouple placement accuracy.

7.1 Methods of thermocouple placement

The primary issue faced during the project, and the cause of the most uncertainty, was the precision of thermocouple positioning within the concrete, particularly in the samples that were cast at CERIB in France. The author manufactured the instrumentation trees but was not able to be present for the casting and the high number of thermocouples placed meant that some control of the thermocouple positions seems to have been lost.

Typically, in furnace tests there will be limited instrumentation in the samples, and this instrumentation will be located at depths further from the concrete surface than attempted in this project. It is possible that, if more instrumentation was used in other furnace testing, a similar spread of data to that observed in the tests described in Chapter 4 could be seen. The work in this project attempted to link the thermal exposure applied using H-TRIS to the thermal exposures experienced by samples when tested to the ISO 834 (International Organisation for Standardization, 1999) and HCM (Ministère de l'Equipement, 2000) temperature versus time curves in the Prometheus furnace at CERIB.

In order to do this, over 1000 thermocouples were positioned in concrete samples at depths from the sample surface of 1, 5, 10, 20 and 50 mm. The method used to attach thermocouples is shown in Figure 7.1. The thermocouple trees cast into the samples at CERIB in France were the same design as the thermocouples used for the Edinburgh casting. Based on the difficulties experienced positioning the

thermocouples at CERIB, the thermocouple trees used in the Edinburgh casting were stiffened with the use of epoxy at the bend in each thermocouple. While these thermocouple trees are stiff, the pouring and vibrating of concrete can exert forces on the thermocouples if extreme care is not taken. In addition to this, any movement of the reinforcement mesh (if present) can easily knock the thermocouple trees out of alignment. Based on the temperature results obtained and shown in Chapters 4, 5, and 6, the author would not recommend using this method in future research.

Other methods of placing thermocouples for casting, including tensioning the thermocouple wire within the sample formwork, have been used by authors (Connolly, 1995; Hulin *et al.*, 2016), see Figure 7.2. However, scaling of this method to a pour of many large samples was not possible in this project given the time constraints and resources available before the casting had to be carried out.

It is also uncertain if the thermocouple weld would be strong enough to withstand rapid pouring of concrete containing large aggregates, or consolidation by vibrating wands.

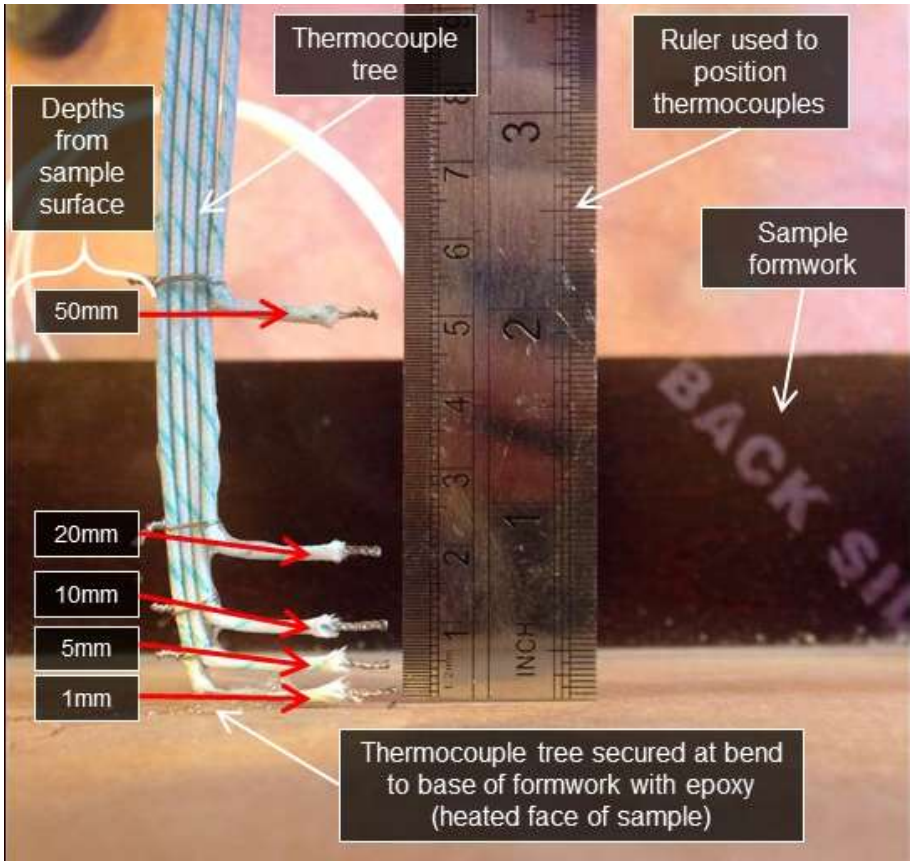

Figure 7.1: Thermocouple tree as used in this thesis project

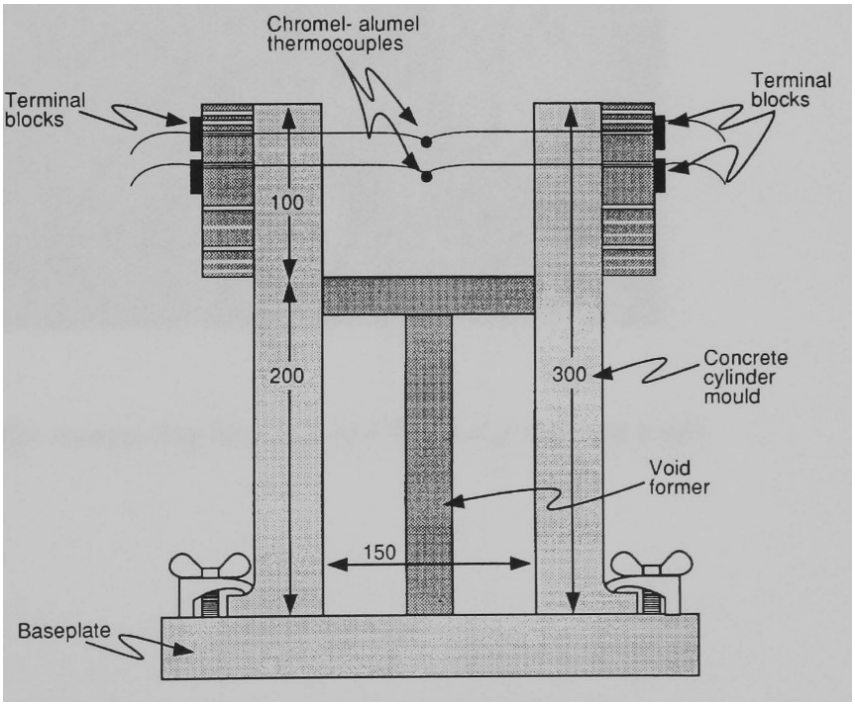

Figure 7.2: Method of positioning thermocouples in cylinders used by Connolly reproduced from(Connolly, 1995)

Placing so much instrumentation into concrete samples being cast in large pours is challenging, and the method used failed to deliver the accuracy of positioning that was desired. Had the thermocouples been positioned perfectly it would be expected that some variation in the through-thickness temperatures would be observed due to slight differences in thermal exposure received by the samples during the early stages of the furnace testing. This has been documented for furnace testing carried out on high performance concrete reinforced with CFRP tendons (Maluk *et al.*, 2015).

7.2 Thermocouple accuracy

Type K (Chromel / Alumel) thermocouples were used in all the experimental work described in this thesis. These thermocouples are the usual choice for experimental work carried out in the fire laboratory at The University of Edinburgh and have been found to perform well when cast inside concrete. These thermocouples were selected based on the knowledge and experience of the research group. K-Type thermocouples are typically considered to have an accuracy of 2.2 °C and function in the temperature range of -200 to 1300 °C (Pico Technology, 2001).

It should be noted that the thermocouples cast within samples were hand welded by the author and as a result, their accuracy has not been certified. However, provided the connection between the two metals is maintained, the accuracy is not expected to vary significantly from the quoted values.

The use of hand welded, fibreglass sheathed, Type K thermocouples is the accepted approach for single use thermocouples cast within concrete samples. The author is confident that the thermocouples perform well, and that any error due to the thermocouple accuracy is not significant when compared to the influence of thermocouple placement. See Section 7.3.

7.3 Theoretical assessment of the influence of thermocouple placement accuracy

The accuracy of the thermocouple placement has been discussed as a contributing factor to the different through-thickness temperatures recorded during the experimental programs described in this thesis. In order to appreciate the impact of thermocouple uncertainty, the predicted temperatures at depths around the target depth can be assessed. It is important to note that the variation in the temperatures recorded is likely to be the result of both a slight variation in furnace thermal exposure combined with errors in thermocouple positioning. Decoupling these two factors is not possible. However, it is possible to assess the credible variation of temperature that would be associated with different thermocouple placement accuracies.

Using an explicit one-dimensional finite difference model (Incropera *et al.*, 2013),the theoretical temperatures within the concrete sample for each thermal exposure can be predicted for different depths around the target thermocouple depth. The finite difference model and stability criteria are provided in Sections 7.3.1 to 7.3.5. Section 7.3.6 explains the input parameters used for the assessment provided. Sections 7.3.7 to 7.3.10 assess the likely range of temperatures associated with misplacement of thermocouples.

7.3.1 Discretisation of geometry and time

A finite difference model requires the sample geometry to be discretised. Figure 7.3 shows the geometrical discretisation with Node 1 being on the heated face and Node M located on the unheated surface.

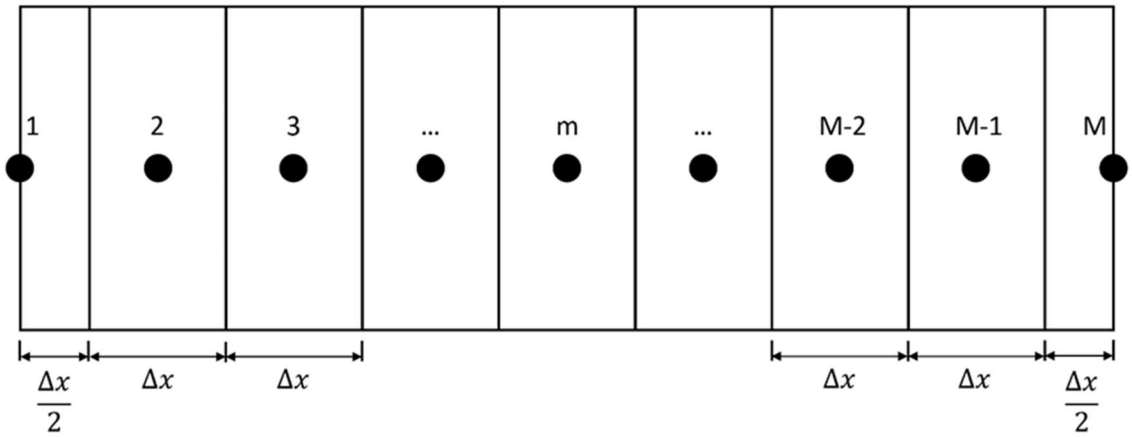

Figure 7.3: Discretisation of geometry

The parameter p has been introduced to discretise the time, t, where:

$$t = p\Delta t$$

The forwards finite difference model calculates the temperatures of elements at the next time step, p+1, based on the thermal properties and temperatures at the current time step, p.

7.3.2 Temperature of first element

The temperature of the first element on the heated side (Node 1) increases with heat from the heat source. This heating may be defined in the form of a gas temperature at the surface, as would be considered in a furnace test or parametric design fire, or by an incident heat flux. In both cases, conventional correlations for convection and radiation are used (Incropera *et al.*, 2013).

In the case of the gas temperature, the net heat flux into the concrete, accounting for energy absorbed and losses at the surface, can be expressed as:

$$\dot{q}''_1 = \sigma\varepsilon\left(T_{gas}^4 - T_1^4\right) + h_c\left(T_{gas} - T_1\right)$$

Where: σ is the Stefan-Boltzmann constant, ε is the emissivity of the surface and h_c is the convective heat transfer coefficient. T_{gas} and T_1 refer to the temperature of the gas and the surface respectively.

Alternatively, the thermal exposure to the surface of the sample can be defined in the form of an incident radiative heat flux. In which case the absorbed heat flux from the incident radiant heat flux can be expressed as:

$$\dot{q}''_{abs} = \varepsilon \dot{q}''_{inc}$$

At the surface of the concrete there is both energy absorbed and energy lost. The net heat flux into the concrete in this case can be expressed as:

$$\dot{q}''_1 = \dot{q}''_{abs} - \sigma\varepsilon T_1^4 + h_c(T_{amb} - T_1)$$

The temperature increase over the time step, ∆t, and the resultant surface temperature of the surface at the next time step, T_1^{p+1}, can be expressed as:

$$T_1^{p+1} = T_1^p + \left(\frac{2\Delta t}{\rho C_p \Delta x}\right) \cdot \left(\dot{q}''_1 - \left(\frac{\lambda_1^p + \lambda_2^p}{2}\right) \cdot \left(\frac{T_1^p - T_2^p}{\Delta x}\right)\right)$$

Where ρ is the concrete density, C_p is the specific heat of the concrete, and λ is the thermal conductivity. The input values used for the heat transfer analysis are provided in Section 7.3.6.

7.3.3 Temperature of intermediate elements

Heat transfer to intermediate elements is through conduction with only the surface elements experiencing convective and radiative heat transfer. The temperature increase with time of an intermediate node, m, can be expressed as:

$$T_m^{p+1} = T_m^p + \frac{2\Delta t}{\rho C_p \Delta x^2} \times \left(\left(\frac{\lambda_{m-1} + \lambda_m}{2} \times (T_{m-1} - T_m)\right) - \left(\frac{\lambda_m + \lambda_{m+1}}{2} \times (T_m - T_{m+1})\right)\right)$$

7.3.4 Temperature of final element on unexposed face

In the case modelled, the final element (Node M) is on the unheated surface and is the location of heat loss to the ambient air. This heat loss $\dot{q}''_{out}$ is the sum of convective and radiative losses, and can be expressed as:

$$\dot{q}''_{out} = \sigma\varepsilon\left(T_M^4 - T_{amb}^4\right) + h_c(T_M - T_{amb})$$

Considering this heat loss, the temperature of the final element can be expressed as:

$$T_M^{p+1} = T_M^p + \frac{2\Delta t}{\rho C_p \Delta x} \cdot \left(\left(\left(\frac{\lambda_{M-1}^p + \lambda_M^p}{2} \right) \cdot \left(\frac{T_{M-1}^p - T_M^p}{\Delta x} \right) \right) - \dot{q}''_{out} \right)$$

7.3.5 Stability of finite difference model

The explicit finite difference method is not unconditionally stable and, if the stability criteria are not met, numerically induced, physically impossible, oscillations can occur. The time step used must be set based on the desired element size, ∆x. The finite difference form of the Fourier number can be expressed as:

$$Fo = \frac{\alpha \Delta t}{(\Delta x)^2} \qquad \text{where: } \alpha = \frac{\lambda}{\rho C_p}$$

The finite difference form of the biot number is:

$$Bi = \frac{h \Delta x}{\lambda}$$

For numerical stability to be maintained the both of the following criteria must be met:

$$Fo \leq \frac{1}{2} \qquad \text{or} \qquad Fo(1 + Bi) \leq \frac{1}{2}$$

7.3.6 Inputs used in theoretical assessment

The thermal properties used in the assessments are from Eurocode 2 with the thermal conductivity taken from the French national annex to Eurocode 2 (AFNOR, 2007). See Figure 7.4. The French thermal conductivity was used initially as part of the collaboration with CERIB and has been used again here for consistency. The specific heat, and density from Eurocode 2 (British Standards Institution, 2005) are shown in Figure 7.5 and Figure 7.6 respectively.

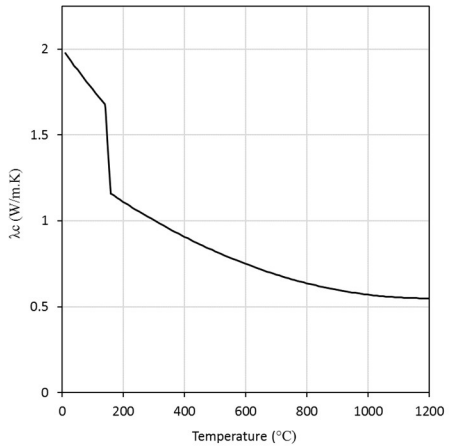

Figure 7.4: Thermal Conductivity (French NA)

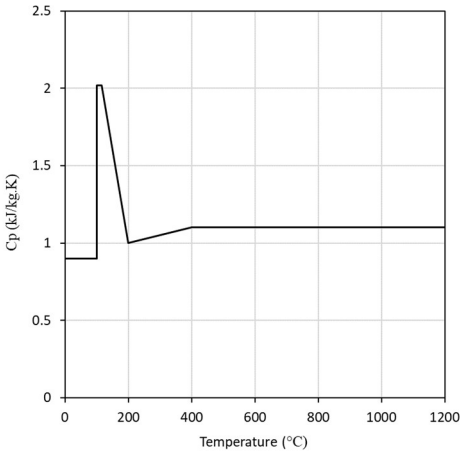

Figure 7.5: Specific heat

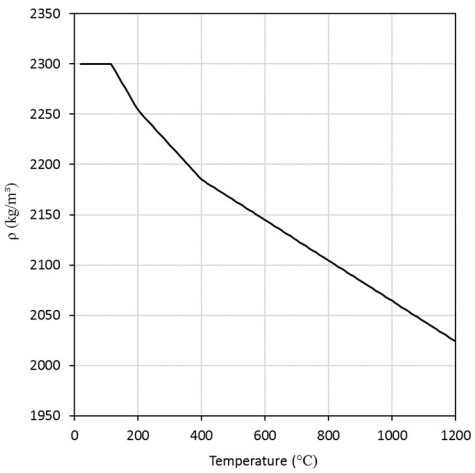

Figure 7.6: Density

An emissivity of the concrete surface, ε, of 0.7 and coefficient of convective heat transfer, h_c, of 25 W/m^{2}K, both as suggested in Eurocode 2 (British Standards Institution, 2005), were adopted for this assessment.

For thermal exposure, either the gas temperature of the ISO 834 or HCM curves were used, referred to as theoretical idealised in the following sections. Alternatively, the incident heat fluxes defined to replicate the thermal exposure received by samples during the furnace tests at CERIB were used. These are referred to as theoretical incident in the following sections.

The sections below present the theoretical through-thickness temperatures with time for different locations. For each target thermocouple depth the dotted lines represent a placement accuracy of ± 0.5 mm and the dashed lines represent an accuracy of ± 1 mm.

7.3.7 ISO 834 – Theoretical idealised exposure

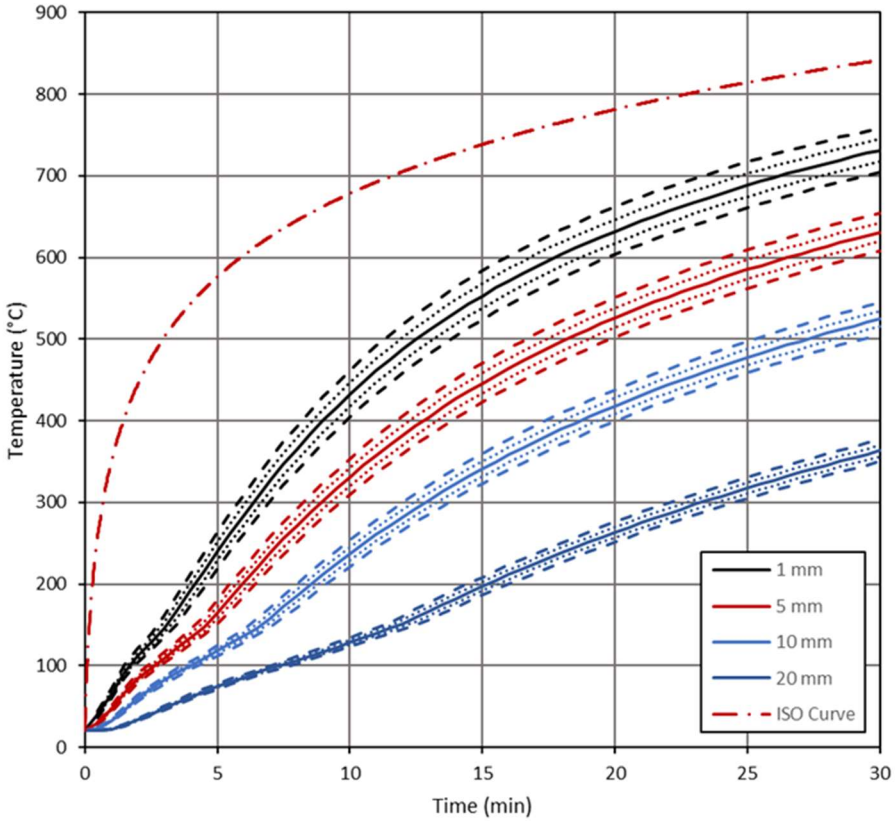

Figure 7.7: Theoretical through-thickness temperatures - Idealised ISO 834 exposure

Table 7.1: Temperature ranges for thermocouple placement accuracies - Idealised ISO 834 exposure

Time (min)	Target thermocouple depth (mm)	Temperature range associated with placement accuracy (°C)		
		± 0.5 mm	± 1 mm	± 1.5 mm
5	1	23.2	46.4	NA
	5	11.2	23.0	35.5
	10	6.5	13.0	19.6
	20	3.2	6.5	9.7
10	1	29.1	58.3	NA
	5	21.6	43.2	65.0
	10	15.7	31.5	47.2
	20	5.3	10.7	16.0
20	1	29.0	58.0	NA
	5	24.1	48.2	72.4
	10	19.2	38.5	57.8
	20	12.3	24.7	37.0
30	1	26.9	53.9	NA
	5	23.3	46.6	69.9
	10	19.3	38.6	58.0
	20	13.4	26.8	40.3

7.3.8 ISO 834 – Theoretical incident heat flux

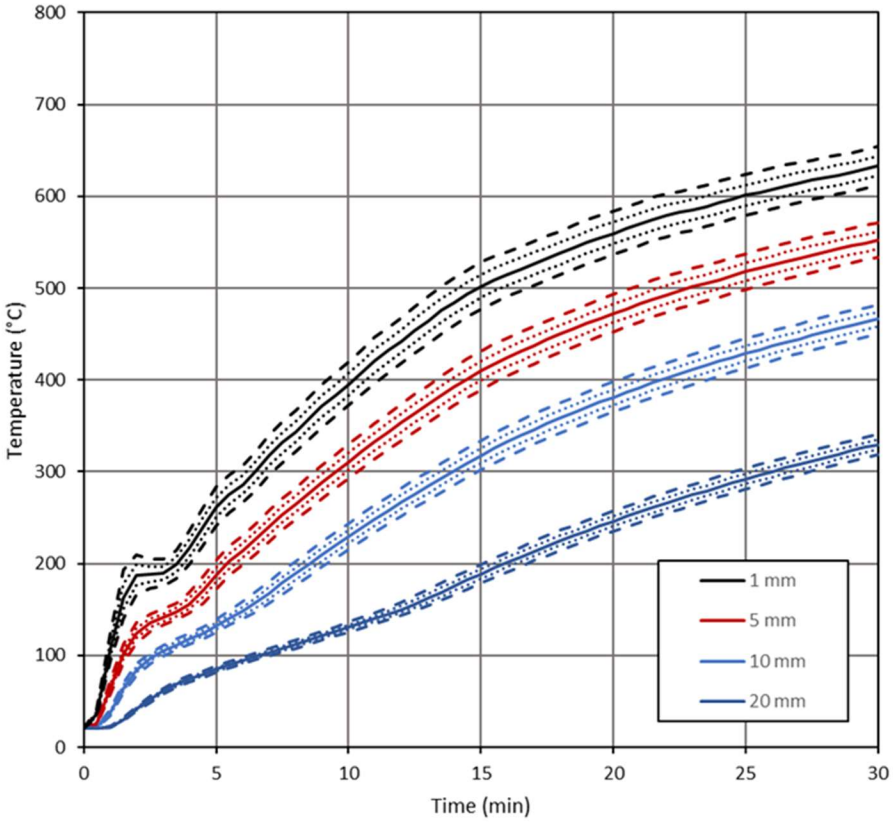

Figure 7.8: Theoretical through-thickness temperatures – ISO 834 incident heat flux

Table 7.2: Temperature ranges for thermocouple placement accuracies - ISO 834 incident heat flux

Time (min)	Target thermocouple depth (mm)	Temperature range associated with placement accuracy (°C)		
		± 0.5 mm	± 1 mm	± 1.5 mm
5	1	20.3	40.5	NA
	5	14.5	28.7	42.5
	10	7.1	14.2	21.4
	20	3.4	6.9	10.3
10	1	24.3	48.7	NA
	5	18.5	37.0	55.5
	10	14.0	27.9	41.9
	20	5.1	10.3	15.4
20	1	23.5	47.1	NA
	5	20.1	40.1	60.2
	10	16.5	32.9	49.4
	20	11.0	22.0	33.1
30	1	21.5	43.1	NA
	5	18.7	37.5	56.3
	10	15.9	31.9	47.8
	20	11.5	23.0	34.5

7.3.9 HCM – Theoretical idealised exposure

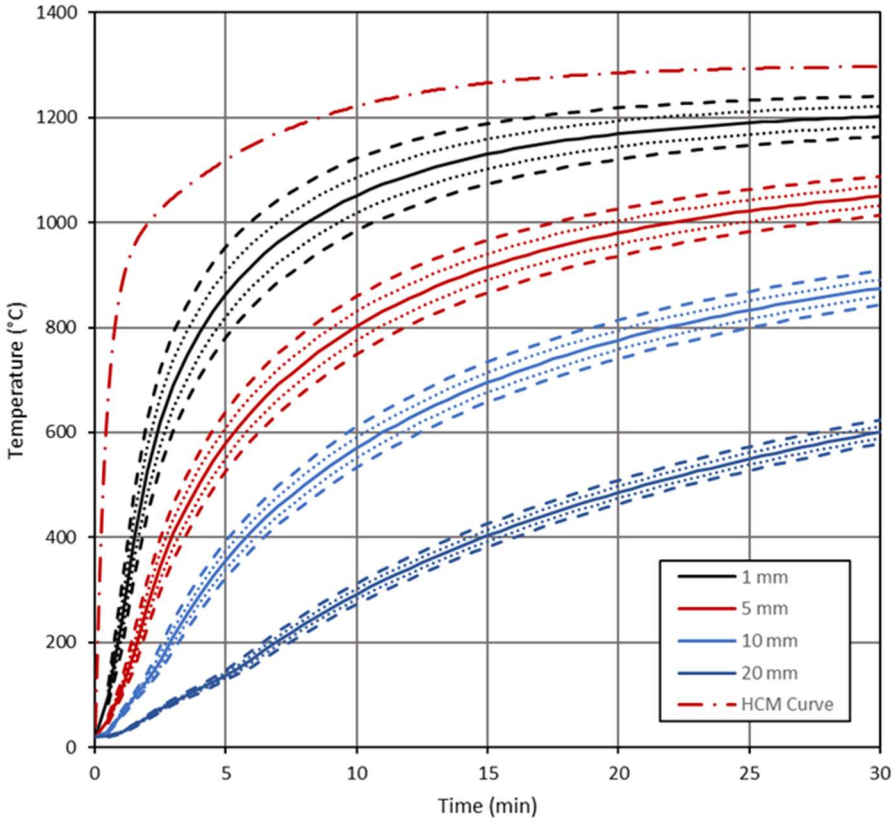

Figure 7.9: Theoretical through-thickness temperatures - Idealised HCM exposure

Table 7.3: Temperature ranges for thermocouple placement accuracies - Idealised HCM exposure

Time (min)	Target thermocouple depth (mm)	Temperature range associated with placement accuracy (°C)		
		± 0.5 mm	± 1 mm	± 1.5 mm
5	1	84.1	168.2	NA
	5	56.6	113.5	170.8
	10	34.6	69.3	104.2
	20	9.3	18.9	29.1
10	1	67.3	134.6	NA
	5	55.5	111.1	166.7
	10	38.4	76.9	115.5
	20	19.3	38.6	58.0
20	1	48.2	96.3	NA
	5	44.5	88.8	133.1
	10	36.7	73.3	110.0
	20	22.6	45.2	67.9
30	1	38.9	77.7	NA
	5	37.0	74.0	111.0
	10	32.7	65.3	98.0
	20	22.6	45.1	67.7

7.3.10 HCM – Theoretical incident heat flux

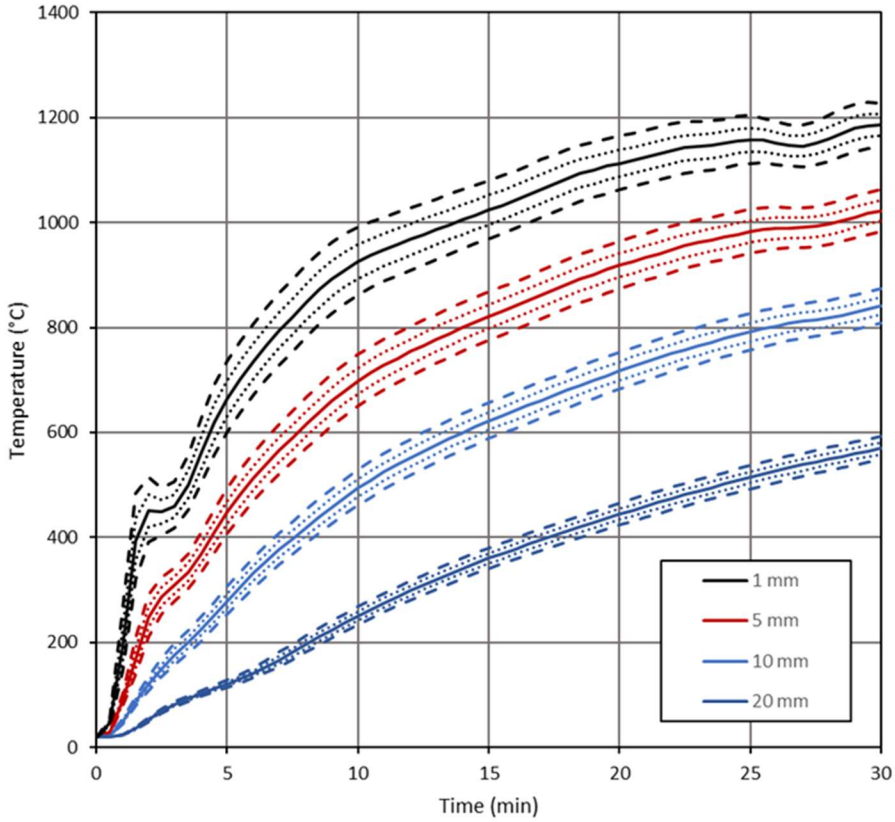

Figure 7.10: Theoretical through-thickness temperatures – HCM incident heat flux

Table 7.4: Temperature ranges for thermocouple placement accuracies - HCM incident heat flux

Time (min)	Target thermocouple depth (mm)	Temperature range associated with placement accuracy (°C)		
		± 0.5 mm	± 1 mm	± 1.5 mm
5	1	67.7	135.5	NA
	5	41.0	82.1	123.5
	10	26.2	52.4	78.8
	20	7.0	14.0	21.1
10	1	62.8	125.6	NA
	5	49.3	98.6	148.0
	10	33.4	66.9	100.5
	20	16.7	33.5	50.3
20	1	50.8	101.6	NA
	5	44.9	89.7	134.6
	10	35.2	70.5	105.8
	20	21.0	42.0	63.1
30	1	41.9	83.7	NA
	5	39.5	78.8	118.1
	10	33.1	66.2	99.3
	20	21.8	43.7	65.6

7.4 Discussion of the influence of thermocouple placement accuracy

The theoretical heat transfer through the concrete samples has been assessed and Table 7.1 to Table 7.4 show the temperature ranges which might be expected for different thermocouple placement accuracies at different times through the heating of the concrete. The placement of many thermocouples, during the casting of many large-scale samples, is particularly challenging and, with hindsight, a consistent placement accuracy of ±0.5 mm is unlikely to be achieved for the method adopted in the experimental work described in this thesis.

A typical placement accuracy of ±1 mm, still ambitious, for a furnace test carried out using the HCM curve could result in a likely temperature range of up to 168°C for a uniform thermal exposure. Factoring in potential variation of thermal exposure across the furnace, the range of temperatures between different thermocouples could be in excess of this without placement accuracy decreasing.

7.4.1 Different thermal exposures

For the HCM exposure, as would be expected, the temperature range associated with thermocouple placement uncertainty is greater than for the same inaccuracy under ISO 834 heating. For example, at a time of 5 minutes and a target thermocouple depth of 1 mm, the range of temperatures associated with a thermocouple placement accuracy of ±0.5 mm under ISO and HCM heating, would be 23.2°C and 84.1°C respectively. This results in the accurate placement of thermocouples being of greater importance when using more severe thermal exposures. This smaller range of temperatures for the ISO 834 exposure compared to the HCM exposure was observed during the experiments carried out in this thesis.

7.4.2 Influence of thermocouple depth

The anticipated temperature range associated with thermocouple placement inaccuracy decreases with increased depth. In typical fire-resistance furnace tests, temperatures within the sample will not be measured as close to sample surface as in the experimental work documented in this thesis. The shallow thermocouples are required in order to gain an understanding of the early test heating which is the critical period for spalling.

7.4.3 Recommendations for future work

The accurate placement of thermocouples is likely to be more achievable on a small scale and for self-consolidating concretes. Large aggregates, reinforcement mesh and vibration used when casting concretes, such as those which may be used for tunnelling applications, all have the potential to dislodge or move thermocouple tips.

Due to the timing of casts and the desire for consistency between the samples cast in France and at The University of Edinburgh, the same method of securing thermocouples was used in both instances. The introduction of any additional support framing or fixings to reinforcement could improve thermocouple placement accuracy but may influence the heat transfer within the concrete and further influence moisture migration. This is an area where further development would be beneficial.

Determination of the thermocouple location forensically is not possible where spalling occurs. However, it is thought that excavation of the thermocouples could be carried out, either using untested samples or samples which did not spall. This would be a labour-intensive approach but could provide confirmation of the thermocouple placement accuracy. Excavation of this sort to assess the accuracy of different approaches could provide a valuable comparison of different fixing systems. The thermocouples were not excavated in the samples tested during the research described in this thesis and the samples are no longer being stored.

7.5 Assumed thermal properties

In the absence of measured thermal properties for a specific concrete mix they must be assumed. This introduces some uncertainty in the heat transfer modelling and some variation if applying the same incident heat flux to a variety of different concretes. For the purpose of demonstrating the influence of assuming thermal conductivity and specific heat, the temperature variation through-thickness can be assessed for different input parameters. This assessment was carried out using the explicit finite difference model described in Section 7.3 and the incident heat flux curves used during the Phase 2 and Phase 3 experimental work. See Chapter 4 and Chapter 5.

7.5.1 Thermal conductivity

The French national annex thermal conductivity (AFNOR, 2007) was used in assessments in this thesis. Eurocode 2 provides an upper and lower thermal conductivity limit (British Standards Institution, 2005) and the French thermal conductivity sits within these. Figure 7.11 shows the French thermal conductivity and the Eurocode 2 upper and lower limits.

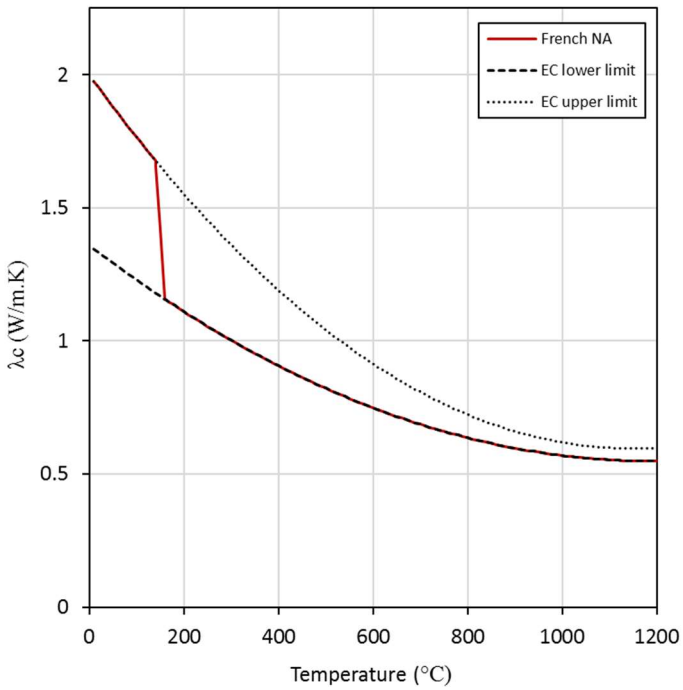

Figure 7.11: Comparison of Eurocode thermal conductivities for concrete

The influence of this thermal conductivity assumption on the through-thickness temperatures can be assessed by comparing theoretical through-thickness

temperatures. Figure 7.12 and Figure 7.13 show the through-thickness temperatures for the concrete as assessed in Section 7.3 but with French thermal conductivity, and the Eurocode upper and lower limit thermal conductivities. As is shown, the influence on the theoretical through-thickness temperatures is limited with the greatest variation occurring at a depth of 20 mm. If using the upper limit thermal conductivity, the temperatures are predicted to be slightly lower close to the surface and higher in depth, see Table 7.5 and Table 7.6.

Table 7.5: Temperature range associated with thermal conductivities used - ISO equivalent exposure

	Temperature range (°C)			
Time (min)	1mm	5mm	10mm	20mm
5	18.2	5.3	9.7	14.9
10	19.6	3.7	12.6	21.8
20	12.4	1.1	11.8	28.3
30	8.2	0.6	10.7	26.8

Table 7.6: Temperature range associated with thermal conductivities used - HCM equivalent exposure

	Temperature range (°C)			
Time (min)	1mm	5mm	10mm	20mm
5	16.7	9.1	29.0	33.3
10	6.1	6.6	24.8	45.8
20	2.0	3.6	13.8	36.5
30	1.1	4.1	10.0	28.4

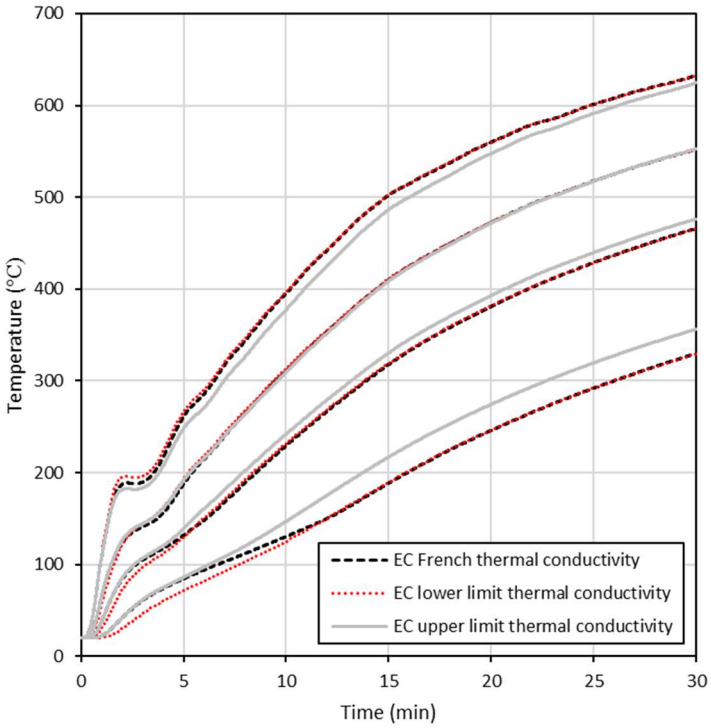

Figure 7.12: Influence of different thermal conductivities on through-thickness temperatures - ISO equivalent incident heat flux

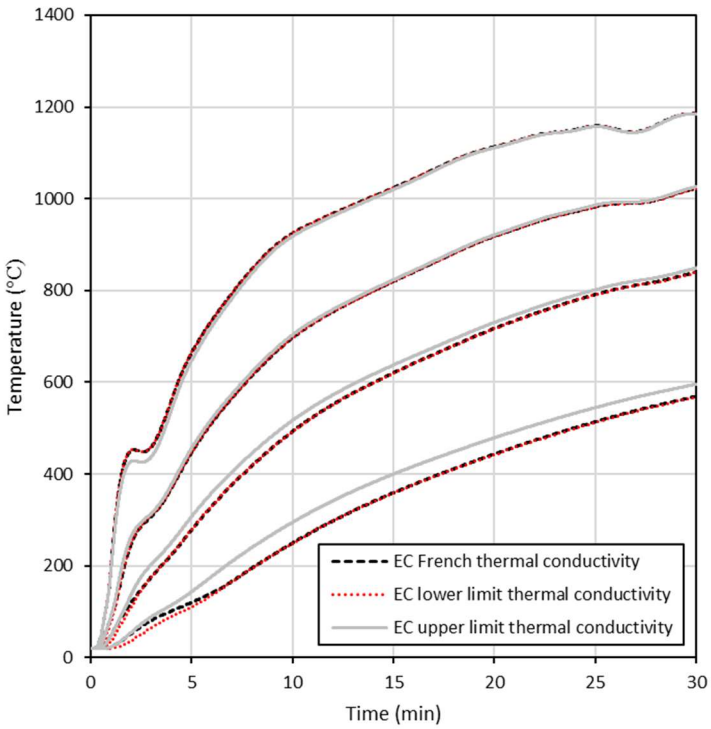

Figure 7.13: Influence of different thermal conductivities on through-thickness temperatures – HCM equivalent incident heat flux

7.5.2 Specific heat

Another assumption of the concrete properties is the specific heat, Cp, of the concrete. This was also based on Eurocode 2 and includes a peak to allow for moisture influence. If different concrete moisture contents are considered, this specific heat peak varies. See Figure 7.14.

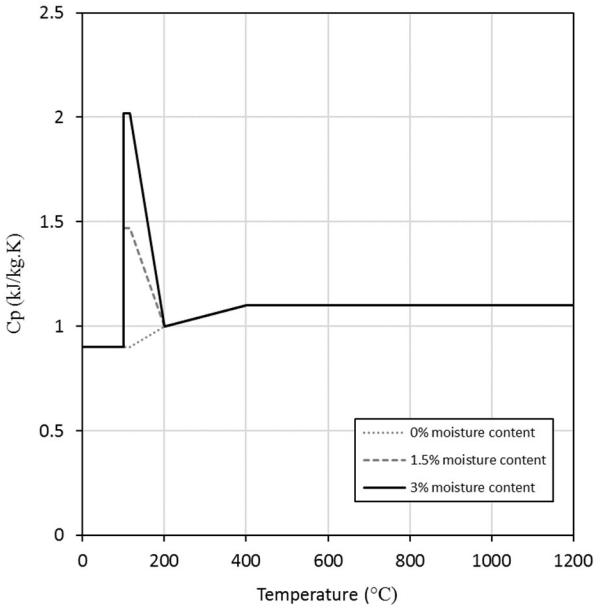

Figure 7.14: Eurocode 2 specific heat, Cp with varying moisture content

The resultant theoretical through-thickness temperatures with different values of specific heat for the incident heat fluxes used in the H-TRIS experiments have been assessed. In this assessment, the French national annex thermal conductivity was used. Figure 7.15 and Figure 7.16 show the influence of using different specific heats/moisture contents on the predicted through-thickness temperatures for the ISO and HCM equivalent exposures. The expected variation would be expected to be less than 40°C, as shown in Table 7.7.

Table 7.7: Comparison of temperature variation predicted for different values of specific heat

Time (min)	Temperature range (°C)							
	ISO Equivalent				HCM Equivalent			
	1mm	5mm	10mm	20mm	1mm	5mm	10mm	20mm
5	30.5	34.3	28.1	15.9	21.0	30.7	37.7	30.7
10	24.3	29.2	34.4	31.1	9.8	20.7	29.1	39.3
20	13.9	19.9	25.9	34.6	5.4	14.6	22.9	32.7
30	9.8	15.4	21.3	30.1	4.1	12.0	20.0	30.0

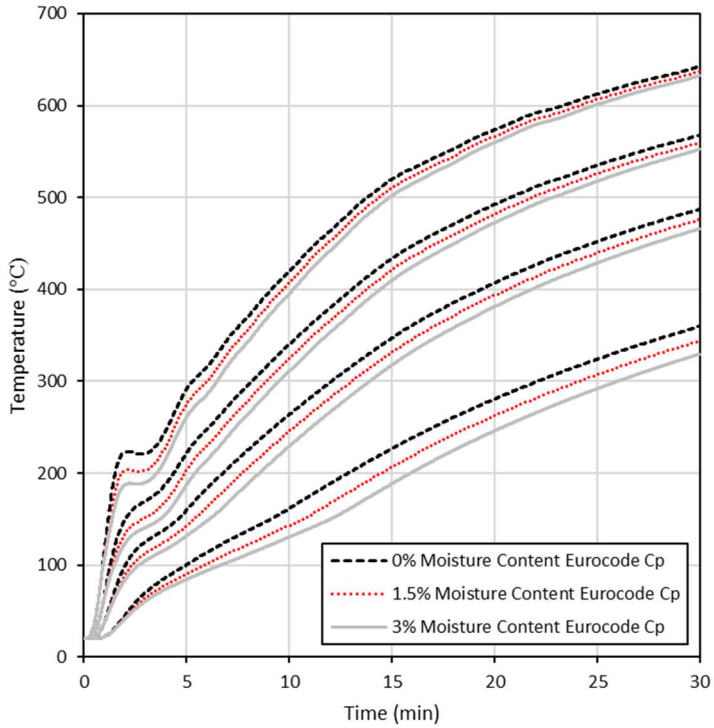

Figure 7.15: Influence of specific heat/moisture content on through-thickness temperatures - ISO equivalent incident heat flux

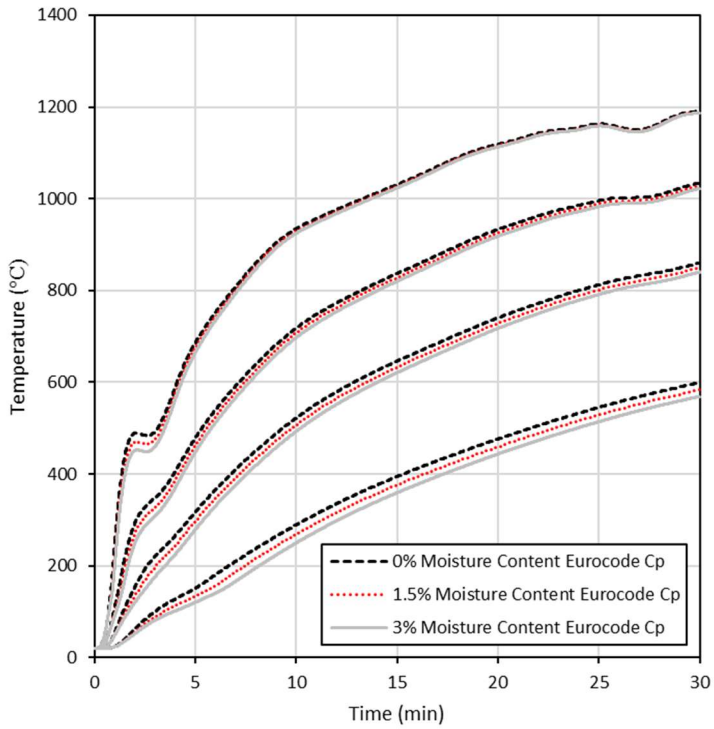

Figure 7.16: Influence of specific heat/moisture content on through-thickness temperatures - HCM equivalent incident heat flux

7.6 Theoretical evaluation of incident heat flux curves

As discussed in Section 5.3 the inverse model (Maluk, 2014) uses a forwards finite difference assessment to evaluate the suitability of the calculated incident heat flux curves. The explicit finite difference model described in Section 7.3 can be also used to evaluate the theoretical through-thickness temperatures that would be expected when a concrete sample is exposed to the incident heat flux curves aiming to reproduce the thermal exposures of the Prometheus furnace. Using the same thermal properties as in Section 7.3.6 the theoretical through-thickness temperatures at thermocouple depths have been calculated. These assessments focus on the first 30 minutes of exposure as this is critical for spalling with all spalling occurring within the first 10 minutes of heating in the experiments reported in this thesis.

Figure 7.17 shows a comparison of theoretical and measured temperatures for the ISO 834 furnace test. The measured data is that of thermocouple tree P2A which was selected in Chapter 4. It can be seen that the theoretical through-thickness temperatures agree well with the temperatures recorded during the furnace test and are within the error margins associated with thermocouple placement accuracies. The maximum variation is 38°C at a time of 30 minutes and depth of 10 mm.

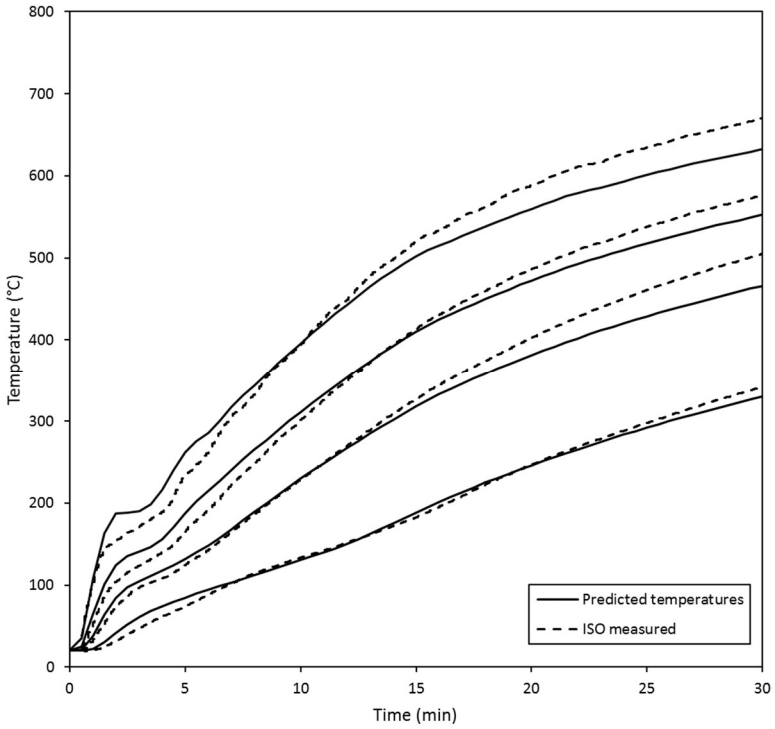

Figure 7.17: Theoretical and measured through-thickness temperatures for ISO 834 equivalent exposure

Figure 7.18 shows the same comparison but for the HCM incident heat flux and thermocouple tree P1E from the Prometheus HCM furnace test as selected in Chapter 4. Again, the theoretical and measured temperatures are in agreement and within the error margins associated with thermocouple placement accuracy. The maximum variation being 90°C at a time of 3 minutes.

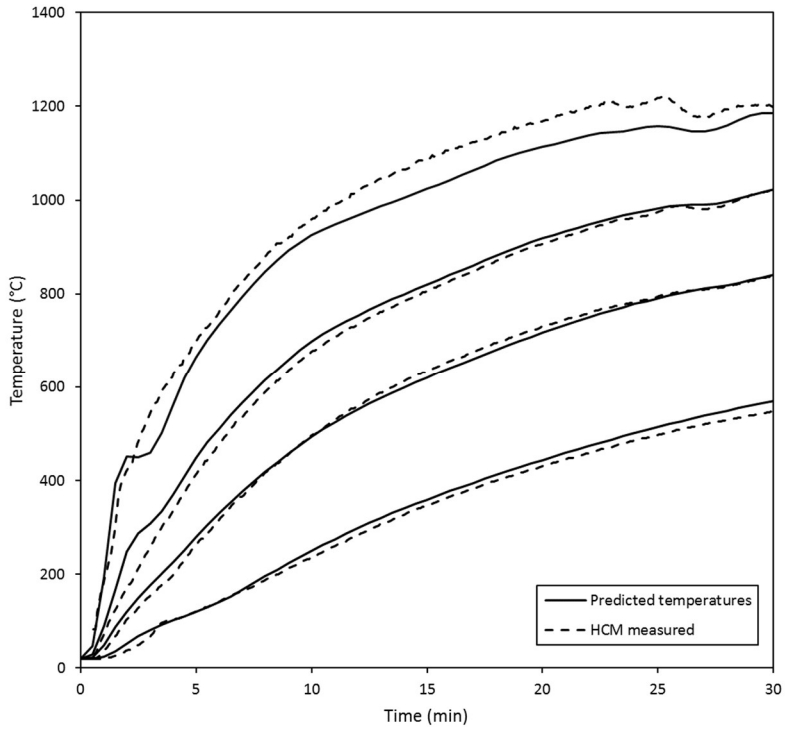

Figure 7.18: Theoretical and measured through-thickness temperatures for HCM equivalent exposure

As reported in Chapters 5 and 6, the through-thickness temperatures recorded in H-TRIS experiments, while repeatable from experiment to experiment, did not align exactly with the target through-thickness temperatures. The ISO equivalent incident heat flux versus time curve appears to produce a more severe thermal exposure than desired. The HCM equivalent incident heat flux versus time curve appears to be a less severe exposure than desired. The analysis above has shown that theoretically this should not be the case.

Figure 7.19 and Figure 7.20 show this visually with a comparison of the theoretical through-thickness temperatures with the average and standard deviations of measured temperatures in the Phase 3 H-TRIS Experiments. As shown, the measured temperatures at a depth of 1mm using the ISO equivalent exposures are consistently 100°C higher that estimated/desired. One obvious explanation is that the incident heat flux curve was input incorrectly into the control software of H-TRIS. The

author has confirmed that the correct inputs were used, and that the experiments were carried out using recent calibrations. This discrepancy was discussed previously and its cause is unclear. Further discussion is provided in Section 7.7. It is worth noting that the temperature data from 23 HCM equivalent experiments is available but only 10 ISO equivalent experiments. Note that deviation towards end of the HCM equivalent thermal exposure comparison in Figure 7.20 is due to the inability of H-TRIS to reproduce heat fluxes much in excess of 300 kW/m^2.

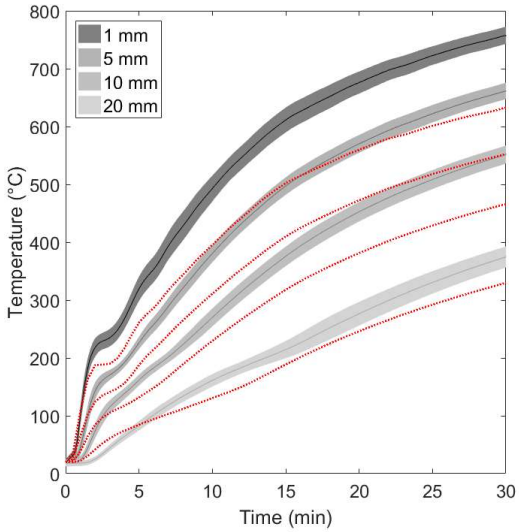

Figure 7.19: Average and standard deviation of ISO equivalent thermal exposure experiments compared to model predictions using the same incident heat flux (red lines)

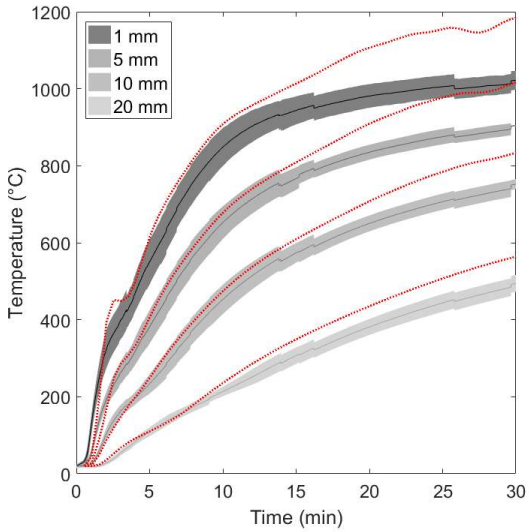

Figure 7.20: Average and standard deviation of HCM equivalent thermal exposure experiments compared to model predictions using the same incident heat flux (red lines)

7.7 Discussion – Sources of error in thermal exposures

In Chapter 4, thermocouple trees were chosen that provided reasonable through-thickness temperatures that related well to the overall distribution of temperatures recorded. The data from these thermocouples was used to determine the equivalent incident heat flux versus time curve to enable an equivalent thermal exposure to be applied using H-TRIS. This thermal exposure was determined using an inverse model developed and validated by Cristian Maluk during his PhD (Maluk, 2014). The thermal properties of the concrete were assumed. In addition, the thermal properties/moisture content are likely to vary between concretes and over time. The influence of using different Eurocode thermal properties was assessed in Section 7.5.

It was shown that, for the thermal exposures used in H-TRIS experimental work, the thermal properties assessed had a limited influence on the through-thickness temperatures. The thermocouple placement accuracy as investigated in Section 7.4 would be expected to have a much greater influence on the recorded through-thickness temperatures and the calculated incident heat flux. The maximum theoretical variation in temperature due to the thermal properties/moisture content was predicted to be 45°C with specific heat corresponding to a concrete with a moisture content of 0%. In comparison, the theoretical variation in temperatures due to a thermocouple placement accuracy of ±1 mm could be up to 135°C. This highlights the importance of thermocouple placement accuracy which is challenging to achieve in large scale casting of samples.

In Chapter 5, the thermal exposure was assessed using further samples cast at CERIB in France. While these had the benefit of being the same concrete mix as the samples tested in the furnace, their age at time of testing was between two and five times the age of the samples when tested in the furnace (concrete age in furnace tests was between 96 and 132 days, and in H-TRIS experiments it was between 249 and 483 days). While there may have been some reduction in moisture content, the discrepancies in the thermal exposures are considered to be primarily due to thermocouple placement accuracies as discussed above. This hypothesis is supported by the HCM equivalent exposure appearing to be slightly less severe than that of the Prometheus furnace in the test carried out, and the ISO equivalent exposure appearing to be more severe. This does not make physical sense in terms of thermal property variation over time, as the concrete used for both HCM and ISO

comparisons was the same and stored in the same conditions, so would be expected to have similar thermal properties.

It was shown in Section 7.6 that theoretically the incident heat flux curves should produce through-thickness temperatures close to those desired to the through-thickness temperatures recorded in the Prometheus tests, which was the desired outcome.

It is unclear why the apparent discrepancies occurred when this incident heat flux was applied to the samples using H-TRIS. The thermal exposure was assessed using the same model and imposed in the same way using the same apparatus in the case of the Phase 3 experimental work. As mentioned in Chapter 6, the heat flux mapping robot was developed between the ISO 834 and HCM experiments, so this may have led to an improved characterisation of the radiant panels. However, the same calibration points were used, so this is thought to be unlikely.

Due to the understood variation from thermocouple placement accuracy, the ability of the H-TRIS apparatus to replicate the furnace was not appreciated until a number of experiments had been carried out. At this stage the decision was taken not to adjust the thermal exposure and instead to prioritise consistency of heating and comparability of H-TRIS results.

The discrepancy observed is thought to be primarily due to issues with thermocouple placement accuracy. However, the full extent of this variation could not be explained with the available data.

While it is desirable to be able to compare results of H-TRIS experiments to those that are obtained in furnaces, upon completion of the experimental work it is the author's view that this was not the correct approach to take. The thermal exposures experienced by samples in standard furnace tests are not likely to be the most suitable thermal exposures for rational and quantified research aiming to improve understanding of the phenomena of heat-induced spalling of concrete.

The perfect recreation of the thermal exposures experienced by samples in the Prometheus furnace is not critical (indeed replication itself may be counter-productive) to the success and value of research being carried out using the H-TRIS apparatus. As discussed in Chapter 2, neither the ISO 834 nor HCM temperature time curves produce thermal exposures in a furnace test based on measured real fire exposures. It is difficult to justify the use of a temperature time curve developed for fire-resistance

testing as the most appropriate thermal exposure for the research of the phenomena of spalling. This concept is discussed further in Section 8.6.2. The important aspect of this work is that the thermal exposure that is applied to samples is quantified and repeatable, and this can assessed with regular calibrations of the apparatus using the heat flux mapping robot that has been developed as part of the work presented herein.

8 Discussion and conclusions – Experimental approach and apparatus

One of the primary aims of the work described in this thesis was to develop a carefully controlled (both thermally and mechanically) and repeatable experimental approach to spalling research, with particular relevance to tunnel lining applications. It was desired that the approach offer improved control of the relevant experimental boundary conditions and allow repeatable experiments to be carried out in order to build a wealth of comparable data on the spalling phenomenon.

In carrying out this work and through time spent immersed in the international spalling research community, the author has both developed an experimental apparatus, and gained an insight into reasons why, in terms of experimental approaches, the understanding of spalling has not progressed significantly.

The following sections cover these points and summarise how the research objectives were met.

8.1 Development of a new experimental approach

In the literature review in Chapter 2, the variety of test methods being used for spalling research was shown, including their deficiencies and the lack of an accepted widely used approach. In order to appreciate why this status quo remains it is worth considering the issues faced when trying to introduce new experimental methods.

Chapter 3 documented the apparatus used in this thesis, the design considerations, and the steps taken to understand and quantify conditions experienced by samples during experiments.

Should an experimental approach such as the one presented in this thesis be widely accepted in the research community, the widespread adoption of the approach/apparatus could allow a wealth of comparable data to be created and result in accelerated development of both the apparatus and methodology. It should be noted that it is not the author's intention to propose that all testing should be carried out using the apparatus described in this thesis but rather that a concerted effort is required to ensure that experimental approaches are fit for purpose, suitably characterised and controlled, and comparable.

An extensive database of results from multiple research laboratories could then be compiled and, while allowing confident comparison of results, it would allow the effectiveness of the experimental method to be demonstrated.

Any new experimental apparatus or experimental approaches face difficulties trying to achieve widespread adoption. As demonstrated in Chapter 2, the spalling research community is well established, and many research laboratories and testing centres use their own, different, experimental setups. The results from which are challenging to compare at best. Some of the current setups used in research laboratories and their deficiencies were covered in the literature review in Chapter 2. It is thought the development of some of these alternative test setups could potentially be motivated by costs, accessibility, or a desire to focus on one particular variable. The motivations and details of the apparatus including quantification of boundary conditions, as presented in this thesis, are not typically available for these other experimental setups.

While the knowledge of the spalling phenomenon is limited, there is likely no perfect experimental apparatus or approach to determine if a concrete is likely to spall. The experimental methods developed in the work described in this thesis show promise as they allow necessary test parameters to be controlled and quantified.

The author believes that the variety of test methods in use and the difficulty in comparing results from them is likely to have slowed the development of an understanding of spalling. It is important that a consensus be reached in the community about the key requirements for a spalling test and the approach to be taken is agreed. This is now a topic of discussion of RILEM Technical Committee 256-SPF of which the author is a member.

It may be possible to use a number of different experimental setups if boundary conditions can be controlled adequately. Difficulties arise when attempting to agree on an approach because, in many cases, researchers or labs have already invested considerable time and funding into equipment. This is a longstanding issue in the research community (Harmathy and Lie, 1970). It is the view of the author that, rather than defining an apparatus and methodology, it may be possible to set a requirement on the level of control of each test parameter and then allow the use of any experimental method as long as the boundary conditions of the experiments could be quantified adequately.

The H-TRIS apparatus consists of a moving radiant panel array and is described in detail Chapter 3. The apparatus was developed with a focus on control of the thermal boundary conditions and addressing issues encountered by other experimental approaches. The latest version allows application of uniaxial compressive load and more severe thermal exposures. The use of this apparatus was demonstrated in Chapters 5 and 6. This approach to spalling experiments shows promise and versions of H-TRIS have now been created internationally with one at the Technical University of Denmark, one at The University of Sheffield, and another at The University of Queensland. Other research laboratories and test centres have also expressed interest in having a similar experimental apparatus, including in China, the USA, and the UK to name just a few.

H-TRIS, or mobile radiant panel arrays, are now being used to test a variety of different materials so the adoption of the apparatus does not mean that spalling research is necessarily being carried out, but it demonstrates that other researchers have confidence in the apparatus and can see a benefit of its use for their own distinct end goals.

8.2 Comparison with standardised fire-resistance tests

The approach within the spalling research community of comparing the experimental methods to standard fire-resistance tests, shown through the description of experimental approaches in Chapter 2, is problematic. The standardisation of testing is an attempt to test different samples in the same way across different test centres and allow comparison between the results of these tests.

The current standard fire-resistance tests carried out by test centres use furnaces to assess the spalling performance of concrete. These furnace tests were discussed in Chapter 2 and, as discussed there, furnaces may not always be the best experimental apparatus to use for spalling tests. Standardisation becomes problematic if the standard tests are in any way unsuitable as, by its very nature, standardisation is inflexible. The current requirement to pass standardised furnace tests to demonstrate spalling performance, either directly for a tunnel construction, or indirectly when assessing fire-resistance of concrete structural members, means that it is challenging to move away from furnace testing completely in an attempt to better understand the spalling phenomenon.

A lot of spalling research is being carried out using alternative experimental setups with attempts to link back to these furnace tests in order to allow some comparison of the results. This linking back is not necessarily the best approach to understanding spalling and restricts the options available. For example, using a suite of thermal exposures to assess the performance of a particular concrete mix under different realistic conditions would not compare easily to furnace testing to a standard temperature versus time curve. It could however provide a greater understanding of the spalling phenomenon and concrete behaviour. Alternatively, credible real thermal exposures used for fire engineering design could be investigated.

In order to link research carried out using the H-TRIS experimental apparatus to the standard approvals furnace tests, the thermal exposures from furnace tests need to be determined by analysing data from furnace tests. This was done during Phase 1 of the experimental work for this project for the Prometheus furnace at CERIB for both the ISO 834 (International Organisation for Standardization, 1999) and French Modified Hydrocarbon (Ministère de l'Equipement, 2000) temperature versus time curves. This work is described in Chapter 4. In order to be able to test to other temperature versus time curves, as used in the control of furnace testing, further furnace tests would be required to obtain the thermal exposure input data. This is costly and demanding of both time and materials.

While not necessarily being the best approach to take for spalling research this approach was taken in order to help to engage with other research that was being carried out internationally and resulted in collaborations with other universities and research institutes (Figueiredo *et al.*, 2017; Jansson McNamee *et al.*, 2017; Richards *et al.*, 2018). Since the use of the H-TRIS test method is not well established, this kind of engagement and easily understandable thermal exposure makes a high-level qualitative comparison of tests straightforward. However, as discussed in the literature review in Chapter 2, there are already issues with the approach to fire-resistance style testing and challenges faced when comparing spalling research.

The temperature versus time curves used for furnace testing do not represent real fires and are somewhat arbitrary (NFPA, 1918), as discussed in Chapter 2. This project, having linked to this way of testing, is in danger of unintentionally further legitimising these thermal exposures as being the correct thermal exposures to use for spalling research. Research to understand spalling could likely achieve better

results if it did not aim to fit into the framework that was designed originally to assign a fire-resistance rating to structural elements.

This project devoted considerable resources to establishing the equivalent thermal exposure to the furnace tests carried out at CERIB. The accuracy of this is debatable and somewhat irrelevant for the purpose of investigating spalling as a phenomenon. Quantifying and controlling the thermal exposure is, in the author's view, more important.

With hindsight, for the purpose of understanding spalling, the time spent attempting to characterise the thermal exposure experienced by samples tested in the Prometheus furnace could have been better focused on testing concrete samples to a range of heat fluxes. It is conceivable that for every concrete mix there will be a range of conditions for which the concrete is unlikely to spall. Performance based design of concrete structures would be possible if researchers were able to achieve this kind of understanding of spalling behaviour rather than positioning around a pass/fail arbitrary heating

A concrete being unable to survive a one-hour test to the ISO curve does not necessarily mean that it would be likely to fail in its end use application. It should be possible to use modern concrete mixes, optimised for properties other than spalling resistance, in areas where it is safe to do so. For example, where the risk of spalling for the credible potential thermal exposure resulting from the fire load and compartment geometry is low.

The practice of testing materials to thermal exposures other than those of the standard fire-resistance tests is not a new concept. Elsewhere in the fire science research community the use of constant and ramping heat fluxes, using apparatus such as the cone calorimeter (British Standards Institution, 2015) or Flame Propagation Apparatus (ASTM, 2013) to understand the material behaviour is commonplace. Just as one would not attempt to understand flammability of a material using a furnace test, it is perhaps not appropriate to attempt to understand spalling in that way.

In conclusion, it is the view of the author that future spalling research should look to define a range of thermal exposures and not focus on linking to the standard furnace tests.

8.3 Experimental apparatus at The University of Edinburgh

The project was successful in developing the H-TRIS experimental apparatus, allowing, for the first time, the replication of the severe thermal exposures experienced in a furnace controlled to a tunnel-specific temperature versus time curve. In addition, a loading frame was developed to allow uniaxial loading, representative of the loading that might be experienced by a tunnel lining, to be imposed on a sample during heating. The apparatus is described in detail in Chapter 3, and through the careful consideration of the boundary conditions during the development of the experimental approach, the research goals relating to the development of an improved apparatus and approach were met.

Extensive use of the apparatus, both for the experiments described in this thesis, and as part of other projects, has allowed diagnosis and troubleshooting of issues to be carried out. Guidance and modifications have been put in place to prevent the same issues occurring in future, or to quickly resolve them if they do occur. Future experiments can now be carried out efficiently with minimal interruption. This is key if an experimental approach is to be adopted by others and used extensively.

The uniformity of the thermal exposure from H-TRIS has been carefully mapped and a bespoke apparatus has been developed at The University of Edinburgh to allow the thermal exposure to be measured and the spatial variation quantified on a repeated basis. This is critical to ensure an accurate calibration of incident radiant heat fluxes and allows experiments to be carried out with confidence in the thermal exposure the sample is receiving. This quantification of thermal exposure is not typically seen in the spalling research community.

While the thermal exposure from H-TRIS is less uniform at higher heat fluxes than at lower heat fluxes (i.e. more variable over the target surface) it was demonstrated that it is both consistent (i.e. repeatable) and quantifiable.

Despite the author now believing it was not the correct approach to take, the aim of linking the thermal exposures to those experienced in standard furnace tests was met. The thermal exposures experienced by concrete samples in the Prometheus furnace at CERIB were quantified using in-depth temperature measurements in concrete samples. These thermal exposures were then ‘reproduced’ using the H-TRIS apparatus (i.e. in terms of the time history of absorbed heat).

A 3 MN loading frame was developed successfully allowing, also for the first time, the testing of large cross section (250 x 500 mm) samples under uniaxial compressive load whilst being exposed to severe, repeatable, thermal exposures. The loading frame was designed by the author and fabricated at The University of Edinburgh, and its functionality was demonstrated via experiments presented within this thesis. The loading frame allows compressive load to be precisely controlled and maintained at the desired levels whilst heating in a precisely controlled manner using H-TRIS Mark 2's radiant panel system.

The H-TRIS experimental setup allows visual and thermal observation of the sample target surface during experiments. The 'open' nature of the experimental setup facilitates the use of novel instrumentation (e.g. image analysis techniques), whilst accurately controlling thermal and structural boundary conditions. The use of ground penetrating radar to investigate moisture migration within samples was demonstrated to be practically feasible and is an area for future work.

The use of optical 3D scanners to measure spalled volumes was demonstrated and allowed a level of precision to be obtained which is not achievable using other conventional methods. However, the high cost of the scanners and the significant data processing times required, combined with the lack of a clear requirement for this data in the context of the current work, mean that at present this should not – in the opinion of the author – be a focus for researchers. It is thought that models will be developed in future which can make use of the precise data characterising spall volume, but such models have yet to materialise and may be some years away.

8.3.1 Measuring concrete moisture content

The free moisture content of the concrete used in the experiments described in this thesis was found by dehydration mass loss, sometimes referred to as a gravimetric test. Standard cylinders, or fragments of test specimens in Phase 2 experiments, were weighed before and after drying in an oven at 105°C to determine the mass loss and free moisture content as a percentage by mass. This method provides the average moisture content but no information on moisture content variation with depth.

While it was not the approach taken in the work described in this thesis, the author believes the split cylinder approach to moisture content assessment to be worthwhile. The split cylinder approach to moisture content determination is shown in Figure 8.1 which is reproduced from literature(Akita, Fujiwara and Ozaka, 1997). The approach, when applied to spalling experiments, involves casting a cylinder corresponding to the sample thickness and sealing all but the ends for the duration of curing. At the time of testing the cylinder is unwrapped and split into discs. The moisture content of each disc is then determined by dehydration mass loss. This allows an approximation of moisture content varying with depth as would be the case in a large concrete sample.

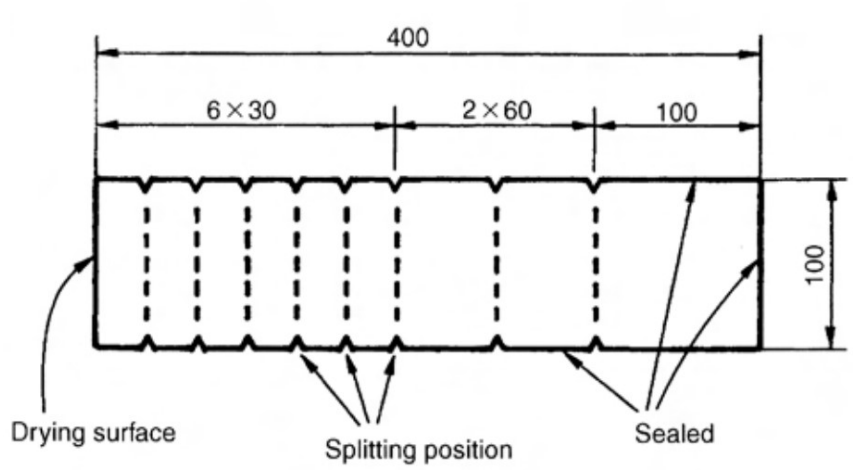

Figure 8.1:Schematic of split cylinder approach to moisture content determination (Akita, Fujiwara and Ozaka, 1997)

An understanding of the through-thickness moisture content may assist in the understanding of spalling and pore pressure development. This approach was used in collaborative project that the author was involved in (Jansson McNamee *et al.*, 2017) and would be recommended for future research.

8.4 Conclusions

One of the objectives of the research described in this thesis was to develop an experimental apparatus and approach suitable for spalling research, with particular relevance to tunnel applications. The approach was to allow repeatable experiments to be carried out in order to build a wealth of comparable data on the spalling phenomenon.

This research goal has been met with the development of the updated H-TRIS apparatus and loading frame that allows repeatable testing of concrete with control of both thermal and mechanical boundary conditions to levels relevant to segmental tunnel lining applications.

The documentation of the apparatus design, both radiant panels and loading frame will assist others in developing a similar experimental setup. This, in combination with the honest documentation of the issues encountered through the experimental work, provides a valuable contribution to the field.

8.5 Further work

The H-TRIS Mark 2 apparatus and loading frame were developed during the course of this project. Now that the behaviour of the components of the experimental setup are understood, there are many opportunities to improve the apparatus; these include:

- Increasing the size of the radiant panel array. This will both improve the uniformity of the thermal exposure and allow higher heat fluxes to be reached at greater distances. Increasing the size of the radiant panel array would also allow larger samples to be tested.
- Further characterisation of the incident heat flux imposed by the H-TRIS panels including investigation into the potential influence of heat feedback from heated samples on the combustion within the radiant panels themselves.
- Development of a serviceable radiant panel to allow easier maintenance
- Developing alternative crossheads for the loading frame developed by the author to allow samples of different thicknesses to be loaded. The comparison of the influence of externally applied load on samples of different thicknesses would be worthwhile.

8.6 Relevance of the H-TRIS experimental apparatus

Moving on from the spalling research described in this thesis there are a number of different applications for the H-TRIS experimental apparatus, and these are discussed in the sections below.

8.6.1 H-TRIS as a screening test

Alignment with fire-resistance style testing allows the H-TRIS test method to be used as a screening test for concrete mixes to understand if they are likely to “pass” the fire-resistance tests in which they must currently demonstrate performance. In this project the screening test capability has allowed engagement with the tunnels community. H-TRIS as a screening test, could provide the industry with a useful tool from the outset.

Discussions with engineers designing real tunnels are underway and will continue in an attempt to carry out some further benchmark testing in order to demonstrate, for a real tunnel concrete, how the performance of a scaled down sample tested using H-TRIS compares to the furnace tests currently used to demonstrate spalling performance.

The repeatability furnace testing is a variable that will affect the use of H-TRIS as a screening test. H-TRIS needs to be producing a comparable thermal exposure to the furnace tests that a candidate concrete will be assessed in. This work has only evaluated the thermal exposures experienced by samples in one test to the ISO 834 temperature versus time curve and one test to the HCM temperature versus time curve. Further work would be required to characterise the thermal exposures experienced by samples in different furnaces and using different standard temperature versus time curves.

While this type of work allows H-TRIS to be used for screening, it is the view of the author that this is not likely to be the best approach to spalling research. See Section 8.2.

8.6.2 H-TRIS as a tool to understand spalling

H-TRIS has the potential to apply virtually any incident heat flux versus time history up to the peak heat flux that can be achieved by the apparatus. This allows for experiments designed with a focus on understanding the influence of different, well-quantified thermal exposures on the spalling behaviour to be carried out. For example, testing to heat flux ramps to investigate the influence of heating rate on spalling

propensity in a quantifiable manner. Carrying out experiments in this way would reduce the ability of the results to provide insight into the behaviour of a concrete in a fire-resistance test carried out for approvals purposes, but the data obtained from testing in this way would improve the understanding of the spalling phenomena.

8.6.3 H-TRIS as modern spalling approval test

In the future, there is potential for approvals testing to no longer be restricted to the use of furnaces. It is thought that with further development and validation, a test method based on the H-TRIS experimental approach could be used. This may be facilitated in part by the lack of guidance for tunnels approvals testing. Currently in many countries, the approvals tests to be carried out, in terms of which fire curve to use and the appropriate sample to test, are decided on a project-by-project basis.

If a precast concrete company and/or tunnel designer were happy with the H-TRIS test method they may have some flexibility to move away from furnace testing. With time, it may be possible for methods other than furnace tests to be deemed satisfactory for approvals testing.

9 Discussion and conclusions – Spalling experiment results

9.1 Summary

The project set out to improve the knowledge and understanding of heat-induced concrete spalling through the development of a new experimental apparatus and extensive, well controlled, comparable testing. The discussion and conclusions relating to the experimental approach are provided in Chapter 8.

One of the research objectives was to gain further insight into the spalling phenomenon by carrying out extensive repeatable spalling experiments under conditions relating to those that may be experienced by concrete in a tunnel lining.

This research objective was met by successfully testing 36 samples across four standard fire-resistance furnace tests, followed by 78 separate spalling experiments that were carried out while developing a repeatable and quantifiable experimental method to investigate heat-induced spalling. The use of only three distinct concrete mixes across the 114 samples allowed simplified comparisons of the influences of different parameters on heat-induced explosive concrete spalling.

Comparable data from experiments on this number of samples represents a significant contribution to the available data, which often consists of data from small, challenging to compare, test series with few repeat experiments.

Carrying out multiple repeat experiments under carefully controlled conditions allowed insight into the inherent variability or randomness of spalling to be gained. This is an aspect of spalling behaviour which, to the author's knowledge, has not been captured before and may provide explanation for unexpected results when no repeat experiments have been carried out.

After establishing this apparent variability caution is required when attempting to draw conclusions from the experimental results. While trends can be observed, further repeat experiments may have provided further clarity on the influence of different parameters. The experiments carried out provided new insight into the spalling phenomenon, particularly variability, and the research objectives have been met.

It is apparent from the work described in this thesis that carrying out experimental spalling research with few or no repeat experiments is not likely to be appropriate in most cases.

9.2 Variability

The extensive experimental programme, including many repeat experiments, gave insight into the influence of different parameters on spalling but most critically demonstrated the potential variability of results that can be obtained; both within one furnace test and between carefully controlled identical experiments. This is an important finding and it is critical that this is observed. Many experiments carried out for spalling research or assessment carry out very few, or no repeats, and the results of the experimental work described in this thesis have shown that this is not an appropriate approach to testing.

To the author's knowledge, this is the first time such a large experimental campaign has been undertaken with such carefully controlled experiments, on simplified samples, and with so many repeats. When nine repeats of an experiment type were carried out as part of the Phase 3 experimental work, despite careful control of the boundary conditions, three samples spalled and six did not.

It is likely that if sufficient experiments could be carried out the probability of the concrete spalling under certain conditions could be assessed. While there is potential inherent variability in the results, the author believes this to be the case only under certain conditions and that for some experimental conditions, spalling would never occur, and likewise would likely occur every time in other experiments.

This increased understanding of an inherent variability is a significant contribution to spalling knowledge. Variability is something which, to the author's knowledge, has not been documented before and many modern experimental programmes do not carry out repeat experiments and neglect to consider the potential for an inherent variability in performance.

An inherent variability is logical due to the non-homogeneous nature of concrete and, if not captured, may account for some of the conflicting results seen in literature or the lack of progression of knowledge in the field.

9.3 Other observations

In addition to the key findings on the apparent variability or randomness of spalling the results of the 114 samples tested allow further insight into the spalling phenomenon. The large set of data from carefully controlled experiments represents a significant contribution to spalling knowledge and the author is not aware of such an extensive research program of this kind being attempted before.

It is worth noting that if the results of the three experimental phases were reviewed in isolation, conclusions could be drawn which do not apply when considering all the experimental results. It is unclear why this is the case, however the observed potential variability could be contributing to apparent conflicting results. Further repeats may provide an improved understanding. The conclusions that could be drawn from each phase of experimental work are reviewed in the following sections. The highlighted potential for variability should be considered when reviewing these sections.

9.3.1 Phase 1 experimental work

The conclusions that were drawn from the phase one experimental work in isolation are summarised below. It is important to note that multiple samples were tested within the same furnace test, which, in terms of fire-resistance furnace testing, could be expected to provide the most consistent conditions for comparison of results. See Chapter 4 for a full description of the experimental work.

- The more severe HCM curve was a worse case for spalling than the ISO 834 curve for the tests carried out in the Prometheus furnace.
- The 250 mm thick samples are more prone to spalling than the thinner 100 mm thick samples, likely due to differential thermal stresses developed upon one-sided heating.
- The addition of 2 kg/m^3 of PP fibres can reduce spalling but is not necessarily enough to prevent spalling when testing to the HCM curve.
- Reinforcement had a positive influence on spalling with samples identical, apart from the presence of reinforcement, spalling when no reinforcement was present and not spalling when reinforced.
- It is unclear whether increased moisture content provides a worse case for spalling; the results of the samples that could be compared were inconclusive. Three sets of samples suggested that the increased moisture content

increased spalling. The other three comparisons suggested the opposite was true.

- The need to carry out repeat testing and be cautious when analysing spalling results was demonstrated by the variation in spalling performance with moisture content.
- There did not appear to be a worst case sample size (plan dimensions rather than thickness)

9.3.2 Phase 2 experimental work

The second phase of experimental work consisted of H-TRIS experiments on unloaded concrete samples of the same concrete as used in Phase 1. Chapter 5 documents this work. The conclusions from this chapter with respect to spalling behaviour can be summarised as:

- The more severe HCM equivalent thermal exposure provides a worse case for spalling than the ISO 834 equivalent.
- Maintaining sealed conditions through the curing process increased the spalling propensity.
- The addition of 2 kg/m^3 of polypropylene fibres reduced the chance of spalling occurring in tests at both thermal exposures.
- The presence of the thermocouple trees does not appear to influence the spalling behaviour of this concrete mix in H-TRIS experiments despite allowing the escape of moisture.
- The 250 mm thick samples appear more prone to spalling than the 100 mm thick samples, although insufficient spalling occurred to allow multiple comparisons of the influence of thickness.
- The results suggest that the smaller 350 x 350 mm samples are more prone to spalling than the larger 750 x 450 mm samples. The reason for this is unclear.

9.3.3 Phase 3 experimental work

The third and final phase of experimental work included investigation of the influence of uniaxial compression on the spalling behaviour of concrete when tested using H-

TRIS. This work is described in Chapter 6. The primary conclusions relating to the spalling behaviour can be summarised as:

- The application of load has an influence on the spalling behaviour of a concrete. Although it remains unclear if, beyond a compressive stress of 10 MPa, increased load causes increased or more severe spalling.
- There can be variation in spalling behaviour between repeat experiments of the same type. This means that multiple repeats of experiments or approvals tests should be carried out to ensure that the behaviour of the concrete is captured properly and is not a misrepresentative result. Three out of nine repeats were observed to spall in one case.
- In many of the experiment types if fewer experiments had been carried out there could be a false confidence in the concrete behaviour. Taking the result from one test or experiment to be representative of the behaviour of the concrete could result in a potentially dangerous end use scenario.
- For the comparisons possible, an increase in sample thickness does not appear to lead to increased spalling. This series of experiments saw both 100 mm and 175 mm samples spall when 250 mm thick samples did not. This contradicts results from Phase 1 and Phase 2 of this project. The reasons for this are not clear.
- The influence of reduced heating area on spalling is inconclusive.
- No spalling occurs after the samples cracked and moisture begins to escape. Samples that spalled did not visually crack in this manner prior to spalling.

The volume and average depth of the first spalling occurrence appears to increase with time to first spall although the author does not believe that attempting to establish a correlation at this stage is appropriate.

9.3.4 Comparison of individual experimental phase conclusions

Comparison of the conclusions from each phase of experiments highlight areas where the conclusions conflict or there is uncertainty. In phases one and two, thicker samples appeared to be more prone to spalling. However, this was not the case in the experiments carried out in Phase 3.

Increased concrete moisture content, achieved by sealing samples during curing, did not appear to contribute to spalling propensity in the Phase 1 experiments. However

the sealed samples were observed to spall when the unsealed samples did not in Phase 2.

It is thought that the variability which has been observed through carrying out multiple repeats may be a contributing factor in ascertaining the influence of these parameters and further repeats and experimental work may provide clarity.

The qualitative nature of the results and the increased understanding of the potential variability of results mean that, if assessing spalling risk for a specific application, the recommendation remains that concrete should be tested in conditions as representative of the in service conditions as is possible and that multiple repeats must be carried out.

9.4 Conclusions

In each chapter of this thesis, conclusions have been given based on the work described in that chapter. This section summarises the most important of those conclusions and draws general conclusions based on the project as a whole.

One of the research objectives was to improve the understanding of the spalling phenomenon by carrying out extensive, well controlled, repeatable experiments. While providing general insights, the research described in this thesis has served to demonstrate and highlight the apparent variability and complexity of explosive concrete spalling behaviour that can be observed when multiple repeat tests are carried out under essentially identical experimental conditions. This variability was observed both within individual standard furnace tests, and in the large experimental programme carried out using the H-TRIS apparatus. As discussed, this variability is often neglected in the research community and the work presented in this thesis demonstrates the importance of carrying out repeat experiments and the dangers of drawing conclusions from limited data.

The conclusions that can be drawn based on the results of the testing carried out and presented within this thesis can be summarised as:

- The more severe thermal exposure of the HCM temperature versus time curve (Ministère de l'Equipement, 2000) was demonstrated to increase both the likelihood of spalling occurring and the severity of spalling when it does occur, as compared against the ISO 834 temperature versus time curve (International Organisation for Standardization, 1999).
- The presence of a 5 MPa uniaxial compressive stress on samples was demonstrated to be sufficient to cause severe spalling in samples that did not spall when tested unloaded. This highlights the need to apply representative compressive loads during testing in order to confidently assess propensity for heat-induced explosive concrete spalling.
- When considering loaded concrete samples, based on initial observations, the increase in load beyond a certain "critical" load level may not increase the spalling propensity further. For the samples tested, an increase in compressive stress beyond 10 MPa did not lead to more severe spalling.
- The addition of 2 kg/m^3 of polypropylene fibres to the concrete mix was found to reduce or prevent the occurrence of spalling in the tests carried out. The specific mechanism by which the addition of fibres mitigates heat-induced

explosive concrete spalling remains unknown, despite a number of theories being available within the research literature (Zeiml *et al.*, 2006; Khoury, 2008).

- Carrying out multiple repeat spalling experiments under controlled conditions demonstrated that there is variability in spalling behaviour that may not be captured if fewer repeat tests are carried out. This highlights the importance of multiple identical repeat tests in order to properly assess spalling risk associated with a given concrete mix under given heating and loading conditions and at different scales.
- Contradictory results can be observed even within one fire-resistance furnace test, with samples used for comparison being identical with the exception of one parameter being varied. This was seen with the samples cured under different conditions: one comparison of samples was inconclusive; three suggested that a 'sealed' curing condition created a worse case for spalling, and the other three suggested the opposite result.
- The influence of sample size (i.e. plan dimension) was not established on the basis of the work undertaken and presented herein. Based on the results of the furnace testing, it appears that all but the smallest sample size tested exhibited similar behaviour. In the corresponding H-TRIS experiments this was less certain as the smaller samples were observed to spall when larger ones did not. The potential shadowing of small samples in the furnace tests is thought to have influenced their behaviour in this case.

While the work presented in this thesis has been successful in producing a wealth of comparable data, the increased understanding of the potential variability of spalling limits the confidence with which conclusions can be reported. Increased understand of the potential variability under controlled conditions, as something which is not considered in the spalling research community, is in the opinion of the author the key finding of this experimental research project and should be considered in all future experimental work to investigate spalling.

9.5 Further work

Now that the H-TRIS apparatus and test method have been developed, carrying out further experiments should be comparatively straightforward. Given that other research institutes are beginning to show interest in the use H-TRIS, it would be beneficial to ensure that any results obtained internationally are as comparable as possible. This could be achieved by working with other researchers to agree on detailed guidance for spalling experiments using H-TRIS. Suggestions for future H-TRIS experimental work include:

- Exhaustive testing using a range of concrete mixes. This would lead to the development of a wealth of knowledge on the spalling performance of concrete. This easily comparable data could be used to create probabilistic models for spalling.
- Research and testing to define a suite of thermal exposures that will allow the behaviour of a specific concrete to be quantified with confidence. The result being that, for a particular concrete mix, the conditions for which spalling can be expected and the conditions under which spalling will not occur can be identified. Separate to the work described in this thesis the author has recently, via his post-graduate employment, begun work in this area with a focus on performance based design of buildings (Rickard *et al.*, 2019)
- Testing in parallel with real tunnel projects going through the approvals process. This would allow further benchmarking of the H-TRIS methodology and increase its applicability as a spalling screening test.

10 Recommendations for structural and fire engineers

Reinforced concrete has a good record of performance in real fires, and the information presented in this thesis should not be construed as a criticism of concrete as compared with other candidate construction materials. All construction materials present risks in fire; how the engineering community manages these risks will differ between materials and must necessarily change as construction materials continue to evolve, presenting new and different fire risks.

This thesis has demonstrated the levels of uncertainty that exist in spalling research and guidance. While spalling is not currently directly considered for all types of construction, the available research suggests that modern high performance concretes are more prone to spalling than has historically been the case (Maluk *et al.*, 2015; Hulin *et al.*, 2016). As a result, it is recommended structural and fire engineers consider whether spalling is likely to occur for a given credible design fire scenario and evaluate the potential impact this may have on the structure's ability to meet the agreed functional performance objectives in fire. Mitigating actions, which will depend on the particular circumstances of a given application, should be taken if necessary.

The available guidance (British Standards Institution, 2005) on concrete spalling in fire is based in research but is not fully supported by the available experimental evidence, posing a challenge for designers who must ensure that potential for spalling is not overlooked. Care should also be taken when consulting research papers as conflicting theories and results are often presented with an inappropriate level of certainty. Currently the only available method to quantify the spalling risk is to carry out testing. However as demonstrated in this thesis, the design and specification of appropriate testing should be carried out with care. The influence of different parameters are not well understood for all concretes and so the testing should be carried out in as close to realistic conditions as is practical. It is the author's view that particular emphasis should be placed on the specification and control of the thermal exposure and mechanical load/ restraint, and that the testing of unloaded samples is inappropriate and unlikely to display a representative spalling behaviour. Multiple repeats of any tests should also be carried out, as there is a certain amount of variation to be expected in the results as demonstrated in the experimental work described in this thesis.

11 References

AFNOR (2007) *NF EN 1992-1-2 / NA Eurocode 2 : Calcul des structures en béton — Partie 1-2 : Règles générales — Calcul du comportement au feu - Annexe Nationale a la NF EN 1992-1-2:2005 - Calcul du comportement au feu*.

Akita, H., Fujiwara, T. and Ozaka, Y. (1997) 'A practical procedure for the analysis of moisture transfer within concrete due to drying', *Magazine of Concrete Research*, 48(6), pp. 129–137. doi: 10.1680/macr.1997.49.179.129.

Ali, F. (2002) 'Is high strength concrete more susceptible to explosive spalling than normal strength concrete in fire?', *Fire and Materials*. Wiley Online Library, 26(3), pp. 127–130. doi: 10.1002/fam.791.

Almand, K. H. (2012) *NIST GCR 12-958 - Structural Fire Resistance Experimental Research – Priority Needs of U.S. Industry*. Gaithersburg, MD. Available at: http://ws680.nist.gov/publication/get_pdf.cfm?pub_id=910971 (Accessed: 6 December 2017).

Anderberg, Y. (1997) 'Spalling phenomena of HPC and OC', *Proceedings of the International Workshop on Fire Performance of High-Strength Concrete, NIST, Gaithersburg, Maryland*, pp. 69–73. Available at: papers2://publication/uuid/63700DE6-2604-48F5-8F26-59894506F038.

ASTM (2013) 'E2058 Standard Test Methods for Measurement of Material Flammability Using a Fire Propagation Apparatus (FPA)'. West Conshohocken: ASTM International, p. 31.

ASTM International (2018) *ASTM E119-18 Standard Test Methods for Fire Tests of Building Construction and Materials*. West Conshohocken. doi: 10.1520/E0119-18.

Baharudin, E. *et al.* (2017) 'Modelling Reinforced Concrete Slabs in Furnace Tests: Validation and Sensitivity to Input Parameters.', in Nigro, E. and Bilotta, A. (eds) *Proceedings of 2nd International Fire Safety Symposium*. Naples, Italy: Doppiavoce, Italy, pp. 695–702.

Bailey, C. and Khoury, G. A. (2011) *Performance of Concrete Structures in Fire*. Surrey: MPA - The Concrete Centre.

Beard, A. and Carvel, R. O. (2012) *Handbook of Tunnel Fire Safety*. Second Edi. Edited by A. Beard and R. O. Carvel. London201: ICE Publishing.

Bisby, L., Gales, J. and Maluk, C. (2013) 'A contemporary review of large-scale non-standard structural fire testing', *Fire Science Reviews*, 2(1), pp. 1–27. doi: 10.1186/2193-0414-2-1.

Bisby, L., Mostafaei, H. and Pimienta, P. (2014) *White paper on fire resistance of concrete structures*. Gaithersburg, MD. doi: 10.6028/NIST.GCR.15-983.

Bodnarova, L., Valek, J. and Novosad, P. (2015) 'Testing of Action of Direct Flame on Concrete', *The Scientific World Journal*, 2015, p. 8. doi: http://dx.doi.org/10.1155/2015/371913.

Bosnjak, J. (2014) *Explosive spalling and permeability of high performance concrete under fire – numerical and experimental investigations*. Stuttgart.

Boström, L. and Jansson, R. (2011) ‘The age effect on fire spalling of concrete’, in Koenders, E. A. . and Dehn, F. (eds) *Concrete Spalling due to Fire Exposure: Proceedings of the 2nd International Workshop*. Delft, The Netherlands: RILEM Publications S.A.R.L., pp. 33–41.

Boström, L. and Larsen, C. K. (2006) ‘Concrete for tunnel linings exposed to severe fire exposure’, *Fire Technology*, 42(4), pp. 351–362. doi: 10.1007/s10694-006-0006-0.

Boström, L., Wickström, U. and Adl-Zarrabi, B. (2007) ‘Effect of specimen size and loading conditions on spalling of concrete’, *Fire and Materials*. John Wiley & Sons, Ltd., 31(3), pp. 173–186. doi: 10.1002/fam.931.

Breunese, A. J., Both, C. and Wolsink, G. M. (2008) ‘Efectis- R0695 : Fire testing procedure for concrete tunnel linings’, p. 25.

British Standards Institute (2017) ‘BS EN ISO / IEC 17025 : 2017 BSI Standards Publication General requirements for the competence of testing and calibration laboratories’, (March), p. 9.

British Standards Institution (2004a) *BS EN 1992-1-1:2004 Eurocode 2 — Design of concrete structures — Part 1-1: General rules and rules for buildings*. London.

British Standards Institution (2004b) *UK National Annex to Eurocode 2 : Design of concrete structures - Part 1-2: General rules - Structural fire design*. London.

British Standards Institution (2005) *BS EN 1992-1-2 : 2004 Eurocode 2 : Design of concrete structures*. London: BSI.

British Standards Institution (2014) ‘BS ISO 14934-4:2014 Fire tests - Calibration and use of heat flux meters - Part 4 : Guidance on the use of heat flux meters in fire tests’. BSI, p. 32.

British Standards Institution (2015) ‘BS ISO 5660-1:2015. Reaction-to-fire tests — Heat release , smoke production and mass loss rate. Part 1 : Heat release rate (cone calorimeter method) and smoke production rate (dynamic measurement)’. London: BSI, p. 66pp.

BSI (1999) ‘BS EN 1363-2:1999 - Fire resistance tests - Part 2: Alternative and additional procedures’. London: BSI Standards Limited, p. 20.

Callister, W. D. and Rethwisch, D. G. (2010) *Materials Science and Engineering - An Introduction*. Eighth Edi. Hoboken, NJ: John Wiley & Sons, Inc.

CETU (2017) ‘Systemes de protection passive contre l’incendie’. Bron, France: Centre d’Études des Tunnels, p. 28.

Chandra, S., Berntsson, L. and Anderberg, Y. (1980) ‘Some effects of polymer addition on the fire resistance of concrete’, *Cement and Concrete Research*, 10(3), pp. 367–375. doi: 10.1016/0008-8846(80)90112-X.

Clayton, N. and Lennon, T. (2000) *Effect of polypropylene fibres on performance in fire of high grade concrete*. Available at: http://www.ihsti.com/tempimg/1319F71-CIS888614800250673.pdf.

Connolly, R. J. (1995) *The spalling of concrete in fires*. The University of Aston in Birmingham. Available at: http://eprints.aston.ac.uk/14310/.

Copier, W. J. (1983) 'The Spalling of Normal Weight and Lightweight Concrete Exposed to Fire', *American Concrete Institute (ACI) Special Publication SP80-7*, 80, p. 18. doi: 10.14359/6591.

Crossrail Ltd (2020) *Railway Tunnels - Lining the tunnels*, *Webpage*. Available at: http://www.crossrail.co.uk/construction/tunnelling/railway-tunnels/ (Accessed: 9 January 2020).

Debicki, G., Haniche, R. and Delhomme, F. (2011) 'An experimental method to investigate concrete spalling in temperature', in Koenders, E. A. . and Dehn, F. (eds) *Concrete Spalling due to Fire Exposure: Proceedings of the 2nd International Workshop*. Delft, The Netherlands: RILEM Publications S.A.R.L., pp. 189–195.

Debicki, G., Haniche, R. and Delhomme, F. (2012) 'An experimental method for assessing the spalling sensitivity of concrete mixture submitted to high temperature', *Cement and Concrete Composites*, 34(8), pp. 958–963. doi: http://dx.doi.org/10.1016/j.cemconcomp.2012.04.002.

Deeny, S. *et al.* (2014) 'A Novel Design', *World Tunneling*, May, pp. 9–12.

Dehn, F. (ed.) (2015) 'Proceedings from the 4th International Workshop on Concrete Spalling due to Fire Exposure', in. Leipzig: MFPA Leipzig GmbH, p. 440.

Dougill, J. W. (1971) *The Effects of High Temperature on the Strength of Concrete with reference to thermal spalling*. The University of London.

Dougill, J. W. (1972) 'Modes of failure of concrete panels exposed to high temperatures', *Magazine of Concrete Research*, 24(79), pp. 71–76. doi: 10.1680/macr.1972.24.79.71.

Du, Y. and Qi, H. (2019) 'Prevent high strength concrete from spalling subject to ISO834 fire', in Huang, S.-S. and Burgess, I. (eds) *Proceedings from the 6th International Workshop on Concrete Spalling*. Sheffield: The University of Sheffield, pp. 132–137.

Dwaikat, M. B. and Kodur, V. K. R. (2009) 'Fire Induced Spalling in High Strength Concrete Beams', *Fire Technology*, 46(1), p. 251. doi: 10.1007/s10694-009-0088-6.

Efectis Group (2012) *The mobile furnace by Efectis: MobiFiRe*, *Technical Note*. Available at: https://www.efectis.com/upload/documents/MobiFireEssaisEcaillageBeton.pdf.

Ernst and Young LLP (2016) *Economic footprint of the Channel Tunnel fixed link*. London. Available at: http://www.eurotunnelgroup.com/uploadedFiles/assets-uk/the-channel-tunnel/EY-Channel-Tunnel-UK.pdf.

Felicetti, R. and Lo Monte, F. (2013) 'Concrete spalling: Interaction between tensile behaviour and pore pressure during heating', in P. Pimienta, F. M. (ed.) *Concrete Spalling due to Fire Exposure – Proceedings of the 3rd International Workshop*. Paris: Edp Sciences , pp. 160–169. doi: 10.1051/matecconf/20130603001.

Felicetti, R., Lo Monte, F. and Pimienta, P. (2017) 'A new test method to study the influence of pore pressure on fracture behaviour of concrete during heating', *Cement and Concrete Research*, 94, pp. 13–23. doi: 10.1016/j.cemconres.2017.01.002.

FibreTech (2018) *Burner Media and System*. Available at: https://lthns123.wixsite.com/fibertech/1-c24t5 (Accessed: 25 September 2018).

Figueiredo, F. *et al.* (2017) 'Recycled tyre polymer fibres to mitigate heat-induced spalling of concrete', in Jansson McNamee, R. and Boström, L. (eds) *Proceedings from the 5th International Workshop on Concrete Spalling*. Boras, Sweden: RISE Research Institutes of Sweden, pp. 359–364.

Gawin, D., Pesavento, F. and Schrefler, B. A. (2011) 'What physical phenomena can be neglected when modelling concrete at high temperature? A comparative study. Part 1: Physical phenomena and mathematical model'. doi: 10.1016/j.ijsolstr.2011.03.004.

Gerasimov, N. (2020) *The behaviour of intumescent coatings under non-standard heating conditions*. The University of Edinburgh.

GoGaS Goch GmbH & Co (2018) 'Process Heat and Drying Technology'. Dortmund: GoGas, p. 16. Available at: https://www.gogas.com/sites/default/files/gogas_ceramic_burner.pdf.

Guerrieri, M. *et al.* (2019) 'Australian large scale structural fire test facility for concrete tunnel linings', in Huang, S.-S. and Burgess, I. (eds) *Proceedings from the 6th International Workshop on Concrete Spalling*. Sheffield: The University of Sheffield, pp. 122–131.

Guerrieri, M. and Fragomeni, S. (2016) 'Mechanisms of Spalling of Concrete Panels of Different Geometry in Hydrocarbon Fire', *Journal of Materials in Civil Engineering*, 28(12), p. 04016164. doi: 10.1061/(ASCE)MT.1943-5533.0001680.

Guglielmetti, V. *et al.* (eds) (2007) *Mechanized Tunneling in Urban Areas - Design methodology and construction control*. Leiden: Taylor& Francis.

Gulik, T. G. van der W. van *et al.* (2016) 'Design, assessment and application of passive fire protection in the Port of Miami tunnel according to NFPA 502', in Lonnermark, A. and Ingason, H. (eds) *Seventh International Symposium on Tunnel Safety and Security*. Montreal: SP Technical Research Institute of Sweden, pp. 147–157.

Haack, A. (1998) 'Fire protection in traffic tunnels: General aspects and results of the EUREKA project', *Tunnelling and Underground Space Technology*, 13(4), pp. 377–381. doi: 10.1016/S0886-7798(98)00080-7.

Halstead, P. E. (1969) 'The significance of concrete cube tests', *Magazine of Concrete Research*, 21(69), pp. 187–194. doi: 10.1680/macr.1969.21.69.187.

Al Hamd, R. K. S. *et al.* (2018) 'The effect of load-induced thermal strain on flat slab behaviour at elevated temperatures'. doi: 10.1016/j.firesaf.2018.02.004.

Hannant, D. J. (1978) *Fibre Cements and Fibre Concretes*. Chichester: John Wiley & Sons, Ltd.

Harmathy, T. Z. (1965) *Effect of moisture on the fire endurance of building elements*, *ASTM STP385*. Philadelphia, Pa. doi: 10.1520/STP48429S.

Harmathy, T. Z. and Lie, T. T. (1970) 'Fire Test Standard in the Light of Fire Research', *Fire Test Performance*, pp. 85–97. doi: 10.1520/STP44713S.

Heo, Y.-S. *et al.* (2011) 'Critical parameters of nylon and other fibres for spalling protection of high strength concrete in fire', *Materials and Structures*, 44(3), pp. 599–610. doi: 10.1617/s11527-010-9651-3.

Heo, Y. S. *et al.* (2012) 'Relationship between inter-aggregate spacing and the optimum fiber length for spalling protection of concrete in fire', *Cement and Concrete Research*. Elsevier Ltd, 42(3), pp. 549–557. doi: 10.1016/j.cemconres.2011.12.002.

Hertz, K. (1984) *Institute of Building Design Report No. 166 : Heat-induced Explosion of Dense Concretes*. Lyngby. Available at: http://scholar.google.com/scholar?hl=en&btnG=Search&q=intitle:Heat+induced+explosion+of+dense+concretes#0 (Accessed: 28 March 2013).

Hertz, K. D. and Sørensen, L. S. (2005) 'Test method for spalling of fire exposed concrete', *Fire Safety Journal*, 40(5), pp. 466–476. doi: 10.1016/j.firesaf.2005.04.001.

Høj, N. P., Tait, C. and Macdonald, M. (1999) 'Great Belt Tunnel Repairs and Refurbishmanet Following a Fire', *Tunnel Management International*, pp. 16–22. Available at: http://trid.trb.org/view.aspx?id=492171.

Huang, S.-S. *et al.* (2015) 'REUSED TYRE POLYMER FIBRE FOR FIRE-SPALLING MITIGATION', in *Applications of Structural Fire Engineering*. Dubrovnik. doi: http://dx.doi.org/10.14311/asfe.2015.056.

Huang, S.-S. and Burgess, I. (eds) (2019) *Proceedings of the 6th International Workshop on Concrete Spalling due to Fire Exposure*. Sheffield: The University of Sheffield.

Hulin, T. *et al.* (2016) 'Experimental Studies on the Fire Behaviour of High Performance Concrete Thin Plates', *Fire Technology*, 52(3), pp. 683–705. doi: 10.1007/s10694-015-0486-x.

Hull, W. A. (1918) 'Fire Tests of Concrete Columns', in *American Concrete Institute - Proceedings of the Fourteenth Annual Convention*. Atlantic City, N.J.: American Concrete Institute, pp. 138–164.

Hull, W. A. (1919) *A Comparison of the Heat Insulating Properties of some of the Materials used in Fire-Resistive Construction*. Washington, DC.

Hull, W. A. (1920) 'Fire Tests of Concrete Columns', in *Proceedings of the 16th annual Convention of the American Concrete Institute*. Chicago: ACI, pp. 20–45.

Hyatt, T. (1877) 'An account of some experiments with Portland-cement-concrete combined with iron, as a building material, with reference to economy of metal in construction, and for security against fire in the making of roofs, floors, and walking surfaces.' London: Printed for private circulation, at the Chiswick Press, p. 28 p. Available at: file://catalog.hathitrust.org/Record/012311327.

Incropera, F. *et al.* (2013) *Principles of Heat and Mass Transfer*. 7th Editio. John Wiley & Sons.

International Organisation for Standardization (1999) 'ISO 834-1 Fire-resistance tests - Elements of building construction - -Part 1: General Requirements'. International Organisation for standardization.

Jansson McNamee, R. *et al.* (2017) 'Screening test methods for determination of fire spalling of concrete - an international comparison', in Jansson McNamee, R. and Boström, L. (eds) *Proceedings from the 5th International Workshop on Concrete Spalling*. Boras, Sweden: RISE Research Institutes of Sweden, pp. 301–315.

Jansson McNamee, R. and Boström, L. (eds) (2017) 'Proceedings from the 5th International Workshop on Concrete Spalling', in *Proceedings from the 5th*

International Workshop on Concrete Spalling. Boras, Sweden: RISE Research Institutes of Sweden, p. 389. Available at: https://3-files.conferencemanager.dk/medialibrary/95B20059-9A60-444D-8AB2-6F7B3F8C58E9/images/Web-version.pdf.

Jansson, R. (2013) *Fire Spalling of Concrete : Theoretical and Experimental Studies*. KTH Royal Institute of Technology. Available at: http://www.diva-portal.org/smash/record.jsf?pid=diva2:647411.

Jansson, R. and Boström, L. (2010) 'The Influence of Pressure in the Pore System on Fire Spalling of Concrete', *Fire Technology*. Springer US, 46(1), pp. 217–230. doi: 10.1007/s10694-009-0093-9.

Jansson, R. and Boström, L. (2013) 'Factors influencing fire spalling of self compacting concrete', *Materials and Structures*, 46(10), pp. 1683–1694. doi: 10.1617/s11527-012-0007-z.

Johnson, W. H. and Parsons, W. H. (1944) 'Thermal expansion of concrete aggregate materials', *Journal of Research of the National Bureau of Standards*, 32(3), p. 101. doi: 10.6028/jres.032.002.

Kalifa, P., Menneteau, F.-D. and Quenard, D. (2000) 'Spalling and pore pressure in HPC at high temperatures', *Cement and Concrete Research*, 30(12), pp. 1915–1927. doi: 10.1016/S0008-8846(00)00384-7.

Kelly, F. and Purkiss, J. (2008) 'Reinforced concrete structures in fire: a review of current rules', *The Structural Engineer*, 86(19), pp. 33–39.

Khoury, G. a. (2008) 'Polypropylene fibres in heated concrete. Part 2: Pressure relief mechanisms and modelling criteria', *Magazine of Concrete Research*, 60(3), pp. 189–204. doi: 10.1680/macr.2007.00042.

Khoury, G. A. (2000) 'Effect of fire on concrete and concrete structures', *Progress in Structural Engineering and Materials*, 2(4), pp. 429–447. doi: 10.1061/41016(314)299.

Kirnbauer, J. (2019) 'Spalling behaviour of UHPC with modified microstructure due to fire load', in Huang, S.-S. and Burgess, I. (eds) *Proceedings from the 6th International Workshop on Concrete Spalling*. Sheffield: The University of Sheffield, pp. 110–121.

Kirnbauer, J. and Schneider, U. (2011) 'Influence of cement type and aggregate shape on explosive concrete spalling', in Koenders, E. A. . and Dehn, F. (eds) *Concrete Spalling due to Fire Exposure: Proceedings of the 2nd International Workshop*. Delft, The Netherlands: RILEM Publications S.A.R.L., pp. 411–417.

Klimek, A., Hothan, S. and Rogge, A. (2019) 'Investigation of size effects in concrete spalling', in Huang, S.-S. and Burgess, I. (eds) *Proceedings from the 6th International Workshop on Concrete Spalling*. Sheffield: The University of Sheffield, pp. 61–70.

Ko, J., Ryu, D. and Noguchi, T. (2011) 'The spalling mechanism of high-strength concrete under fire', *Magazine of Concrete Research*, 63(5), pp. 357–370. doi: 10.1680/macr.10.00002.

Kodur, V. K. R. (2000) 'Spalling in High Strength Concrete Exposed to Fire: Concerns, Causes, Critical Parameters and Cures', in *Advanced Technology in Structural Engineering*. Reston, VA: American Society of Civil Engineers, pp. 1–9. doi: 10.1061/40492(2000)180.

Koenders, E. A. . and Dehn, F. (eds) (2011) ‘Concrete Spalling due to Fire Exposure: Proceedings of the 2nd International Workshop’, in. Delft, The Netherlands: RILEM Publications S.A.R.L.

Kuhn, T. S. and Hacking, I. (2012) *The structure of scientific revolutions*. 4th edn. University of Chicago Press.

Lee, G. *et al.* (2012) ‘Combining polypropylene and nylon fibers to optimize fiber addition for spalling protection of high-strength concrete’, *Construction and Building Materials*. Elsevier Ltd, 34, pp. 313–320. doi: 10.1016/j.conbuildmat.2012.02.015.

Lenglet, C. (2011) ‘Evolution of spalling with time and age’, in Koenders, E. A. . and Dehn, F. (eds) *Concrete Spalling due to Fire Exposure: Proceedings of the 2nd International Workshop*. Delft, The Netherlands: RILEM Publications S.A.R.L., pp. 19–25.

Li, Y. *et al.* (2019) ‘Mitigation of fire-induced spalling of concrete using recycled tyre polywmer fibre’, in Huang, S.-S. and Burgess, I. (eds) *Proceedings from the 6th International Workshop on Concrete Spalling*. Sheffield: The University of Sheffield, pp. 42–51.

Liu, J.-C., Tan, K. H. and Yao, Y. (2018) ‘A new perspective on nature of fire-induced spalling in concrete’, *Construction and Building Materials*, 184, pp. 581–590. doi: https://doi.org/10.1016/j.conbuildmat.2018.06.204.

Liu, L., Xiao, J. and Liu, X. (2019) ‘Experimental study on mechanical behaviours of cementitious grouts after elevated temperatures’, in Huang, S.-S. and Burgess, I. (eds) *Proceedings from the 6th International Workshop on Concrete Spalling*. Sheffield: The University of Sheffield, pp. 138–147.

Lucio-Martin, T., Puentes, J. and Alonso, M. C. (2019) ‘Effect of geometry in concrete spalling risk subjected to high temperatures for thermal inertia studies’, in Huang, S.-S. and Burgess, I. (eds) *Proceedings from the 6th International Workshop on Concrete Spalling*. Sheffield: The University of Sheffield, pp. 71–80.

Malhotra, H. L. (1984) *CIRIA Technical Note 118 - Spalling of concrete in fires*. London: Construction Industry Research and Information Association.

Maluk, C. (2014) *Development and Application of a Novel Test Method for Studying The Fire Behaviour of CFRP Prestressed Concrete Structural Elements*. University of Edinburgh. Available at: http://hdl.handle.net/1842/16157.

Maluk, C. *et al.* (2015) ‘Fire resistance tests on thin CFRP prestressed concrete slabs’, *Construction and Building Materials*, 101, pp. 558–571. doi: 10.1016/j.conbuildmat.2015.10.031.

Maluk, C. *et al.* (2016) ‘A Heat-Transfer Rate Inducing System (H-TRIS) Test Method’, *Fire Safety Journal*. Elsevier, pp. 1–13. doi: 10.1016/j.firesaf.2016.05.001.

Maluk, C. (2017) ‘Motivation, drivers and barriers for a knowledge-based test environment in structural fire safety engineering science’, *Fire Safety Journal*. Elsevier, 91, pp. 103–111. doi: 10.1016/J.FIRESAF.2017.05.009.

Maluk, C., Bisby, L. and Terrasi, G. P. (2014) ‘Experimental parametric study on the effectiveness of polypropylene fibres at mitigating heat-induced concrete spalling’, *Concrete In Australia*, 40(3), p. 32.

Maluk, C., Bisby, L. and Terrasi, G. P. (2017) ‘Effects of polypropylene fibre type and

dose on the propensity for heat-induced concrete spalling', *Engineering Structures*, 141, pp. 584–595. doi: 10.1016/j.engstruct.2017.03.058.

Matesová, D. and Keršner, Z. (2006) 'Effect of Porosity and Fracture Toughness on Explosive Spalling of Concrete', *Brittle Matrix Composites 8*, pp. 581–588. doi: 10.1533/9780857093080.581.

McGrattan, K. *et al.* (2013) *Fire Dynamics Simulator, User's Guide*, *National Institute of Standards and Technology Special Publication 1019*. Available at: http://www.thunderheadeng.com/wp-content/uploads/2013/08/FDS_User_Guide.pdf.

Miah, M. J. *et al.* (2016) 'Effect of Biaxial Mechanical Loading and Cement Type on the Fire Spalling of Concrete', in Garlock, M. and Kodur, V. (eds) *Structures in Fire - Proceedings of the Ninth International Conference*. Princeton: DEStech Publications, Inc., pp. 233–239.

Miah, M. J. *et al.* (2017) 'The Effect of Loading on the Residual Gas Permeability of Concrete', in Jansson McNamee, R. and Boström, L. (eds) *Proceedings from the 5th International Workshop on Concrete Spalling*. Boras, Sweden: RISE Research Institutes of Sweden, pp. 259–268.

Mindeguia, J. *et al.* (2015) 'Experimental discussion on the mechanisms behind the fire spalling of concrete', *Fire and Materials*, 39(7), pp. 619–635. doi: 10.1002/fam.2254.

Mindeguia, J. C. *et al.* (2010) 'Temperature, pore pressure and mass variation of concrete subjected to high temperature - Experimental and numerical discussion on spalling risk', *Cement and Concrete Research*. Elsevier Ltd, 40(3), pp. 477–487. doi: 10.1016/j.cemconres.2009.10.011.

Ministère de l'Equipement (2000) *Circulaire interministérielle no 2000-63 du 25 Aout 2000 relative à la sécurité dans les tunnels du réseau routier français*. Paris, France.

Lo Monte, F. and Felicetti, R. (2017) 'Heated slabs under biaxial compressive loading: a test set-up for the assessment of concrete sensitivity to spalling', *Materials and Structures*, 50(4), p. 192. doi: 10.1617/s11527-017-1055-1.

NFPA (1917) 'Report of Committee on Fire-Resistive Construction', in NFPA (ed.) *Proceedings of the 21st National Fire Protection Association Annual Meeting*. Washington, DC, pp. 391–413. Available at: https://hdl.handle.net/2027/hvd.hb17v0.

NFPA (1918) 'Report of Committee on Fire-Resistive Construction', in *Proceedings of the 22nd National Fire Protection Association Annual Meeting*. Boston, pp. 170–221. Available at: https://hdl.handle.net/2027/iau.31858051348674.

NFPA (2008) *NFPA 502: Standard for Road Tunnels, Bridges, and Other Limited Access Highways*. 2008 Editi. NFPA.

NFPA (2011) *NFPA 502, Standard for Road Tunnels, Bridges, and Other Limited Access Highways*. 2011 Editi. Quincy, MA: NFPA.

NFPA (2017) *NFPA 502: Standard for Road Tunnels, Bridges, and Other Limited Access Highways*. 2017 Editi. NFPA. Available at: http://www.nfpa.org/.

Ngan Vu, M., Broere, W. and Bosch, J. W. (2017) 'Structural Analysis for Shallow Tunnels in Soft Soils', *International Journal of Geomechanics*. American Society of Civil Engineers, 17(8), pp. 1–12. doi: 10.1061/(ASCE)GM.1943-5622.0000866.

Nuruddin, M. F., Azmee, N. M. and Yung, C. K. (2014) 'Effect of fire flame exposure on ductile self-compacting concrete (DSCC) blended with MIRHA and fly ash', *Construction and Building Materials*. Elsevier Ltd, 50, pp. 388–393. doi: 10.1016/j.conbuildmat.2013.09.038.

Ozawa, M. and Morimoto, H. (2014) 'Effects of various fibres on high-temperature spalling in high-performance concrete', *Construction and Building Materials*. Elsevier Ltd, 71, pp. 83–92. doi: 10.1016/j.conbuildmat.2014.07.068.

Ozawa, M., Sukekawa, M. and Akasaka, H. (2019) 'Investigation of the preventive effect on fire spalling of natural jute fibre in high performance concrete through ring-restrained specimen tests', in Huang, S.-S. and Burgess, I. (eds) *Proceedings from the 6th International Workshop on Concrete Spalling*. Sheffield: The University of Sheffield, pp. 91–100.

Pardon, D. *et al.* (2019) 'In situ concrete spalling risk assessment in tunnel by means of a mobile oil-fired furnace', in Huang, S.-S. and Burgess, I. (eds) *Proceedings from the 6th International Workshop on Concrete Spalling*. Sheffield: The University of Sheffield, pp. 81–90.

Peng, G.-F. *et al.* (2018) 'Combined curing as a novel approach to improve resistance of ultra-high performance concrete to explosive spalling under high temperature and its mechanical properties', *Cement and Concrete Research*, 109, pp. 147–158. doi: https://doi.org/10.1016/j.cemconres.2018.04.011.

Phan, L. (1996) 'Fire Performance of High-Strength Concrete: A Report of the State-of-the-Art', *Fire Research*, p. 118. Available at: http://scholar.google.com/scholar?hl=en&btnG=Search&q=intitle:Fire+Performance+of+High-Strength+Concrete+:+A+Report+of+the+State-of-the-Art#0.

Pico Technology (2001) 'Improving the accuracy of temeprature measurements', *Sensor Review, The international journal of sensing for industry*. Available at: https://www.picotech.com/library/application-note/improving-the-accuracy-of-temperature-measurements#thermocouples.

Pimienta, P. and Meftah, F. (eds) (2013) 'Concrete Spalling due to Fire Exposure – 3rd International Workshop', in. Paris: Edp Sciences.

Rahim, A. *et al.* (2013) 'Effect of load on thermal spalling of reinforced concrete containing various mineral admixtures', in *Concrete Spalling due to Fire Exposure: Proceedings of the 3rd International Workshop*. Paris. doi: 10.1051/matecconf/20130601006.

Richards, O. *et al.* (2018) 'Response of concrete cast in permeable moulds to severe heating', *Construction and Building Materials*. Elsevier, 160, pp. 526–538. doi: 10.1016/J.CONBUILDMAT.2017.11.097.

Rickard, I. *et al.* (2015) 'Predictive Testing for Heat-Induced Spalling of Concrete', in Brühwiler, E. (ed.) *IABSE Conference Geneva, Structural Engineering: Providing Solutions to Global Challenges*. Geneva: IABSE, pp. 929–936.

Rickard, I. *et al.* (2016) 'Predictive Testing for Heat Induced Spalling of Concrete Tunnels - The Influence of Mechanical Loading', in Garlock, M. and Kodur, V. K. R. (eds) *Structures in Fire - Proceedings of the Ninth International Conference*. Princeton: DEStech Publications, Inc., pp. 217–224.

Rickard, I. *et al.* (2017) 'Predictive testing for heat induced spalling of concrete tunnel

linings - The potential influence of sustained mechanical loading', in Bostrom, L. and Jansson McNamee, R. (eds) *Proceedings from the 5th International Workshop on Concrete Spalling*. Boras, Sweden: RISE Research Institutes of Sweden, pp. 337–344. Available at: http://3-files.conferencemanager.dk/medialibrary/95B20059-9A60-444D-8AB2-6F7B3F8C58E9/images/Web-version.pdf.

Rickard, I. *et al.* (2019) 'Assessing spalling risk in buildings: Considering spalling in probabilistic fire safety design', in Huang, S.-S. and Burgess, I. (eds) *Proceedings from the 6th International Workshop on Concrete Spalling*. Sheffield: The University of Sheffield, pp. 258–267.

Robert, F. *et al.* (2017) 'Eurocode 1992-1-2: Do we need to change the requirements on spalling?', in Jansson McNamee, R. and Boström, L. (eds) *Proceedings from the 5th International Workshop on Concrete Spalling*. Boras, Sweden: RISE Research Institutes of Sweden, pp. 21–27. Available at: https://3-files.conferencemanager.dk/medialibrary/95B20059-9A60-444D-8AB2-6F7B3F8C58E9/images/Web-version.pdf.

Robert, F. and Colina, H. (2009) 'The influence of aggregates on the mechanical characteristics of concrete exposed to fire', *Magazine of Concrete Research*, 61(5), pp. 311–321. doi: 10.1680/macr.2007.00121.

Robert, F., Collignon, C. and Scalliet, M. (2013) 'Large scale fire test on tunnel segment : Real boundary conditions in order to evaluate spalling sensitivity and fire', in *Concrete Spalling due to Fire Exposure: Proceedings of the 3rd International Workshop*. Paris, France: EDP Sciences. doi: http://dx.doi.org/10.1051/matecconf/20130604001.

Rossino, C. *et al.* (2013) 'Concrete spalling sensitivity versus microstructure: Preliminary results on the effect of polypropylene fibers', in P. Pimienta, F. M. (ed.) *Concrete Spalling due to Fire Exposure – Proceedings of the 3rd International Workshop*. Paris: Edp sciences, pp. 110–119. doi: 10.1051/matecconf/20130602002.

Sachs, E. O. (1903) 'Suggested Standards of Fire Resistance', in Woolson, I. H. (ed.) *Report of Proceedings of the International Fire Prevention Congress*. London: Martin Brown Press, New York, pp. 243–248.

Saito, H. (1965) *Explosive Spalling of Prestressed Concrete in Fire*. Tokyo, Japan.

Sanchayan, S. and Foster, S. J. (2016) 'High temperature behaviour of hybrid steel--PVA fibre reinforced reactive powder concrete', *Materials and Structures*, 49(3), pp. 769–782. doi: 10.1617/s11527-015-0537-2.

Schneider, M. and Sajina, A. (2019) 'Experimental study of the spalling behaviour of ultra-high performance fibre reinforced concrete during fire', in Huang, S.-S. and Burgess, I. (eds) *Proceedings from the 6th International Workshop on Concrete Spalling*. Sheffield: The University of Sheffield, pp. 52–60.

Schrefler, B. A., Pesavento, F. and Gawin, D. (2014) 'Multiphase Porous Media, High Temperature', in Hetnarski, R. B. (ed.) *Encyclopedia of Thermal Stresses*. Dordrecht: Springer Netherlands, pp. 3251–3262. doi: 10.1007/978-94-007-2739-7_672.

Serrano, R. *et al.* (2016) 'Analysis of fire resistance of concrete with polypropylene or steel fibers', *Construction and Building Materials*, 122, pp. 302–309. doi: 10.1016/j.conbuildmat.2016.06.055.

Sugino, Y., Ozawa, M. and Tanibe, T. (2019) 'Fire-related spalling evaluation of ring-

restrained polymer cement mortar and normal cement mortar', in Huang, S.-S. and Burgess, I. (eds) *Proceedings from the 6th International Workshop on Concrete Spalling*. Sheffield: The University of Sheffield, pp. 101–109.

Tanibe, T. *et al.* (2011) 'Explosive spalling behaviour of restrained concrete in the event of fire', in Koenders, E. A. . and Dehn, F. (eds) *Concrete Spalling due to Fire Exposure: Proceedings of the 2nd International Workshop*. Delft, The Netherlands: RILEM Publications S.A.R.L., pp. 319–326.

Tanibe, T. *et al.* (2013) 'Thermal stress estimation in relation to spalling of HSC restrained with steel rings at high temperatures', in *MATEC Web of Conferences - Concrete Spalling due to Fire Exposure: Proceedings of the 3rd International Workshop*, p. 1004. doi: 10.1051/matecconf/20130601004.

Torelli, G. *et al.* (2016) 'Concrete strains under transient thermal conditions: A state-of-the-art review'. doi: 10.1016/j.engstruct.2016.08.021.

Torero, J. L., Law, A. and Maluk, C. (2017) 'Defining the thermal boundary condition for protective structures in fire', *Engineering Structures*, 149, pp. 104–112. doi: https://doi.org/10.1016/j.engstruct.2016.11.015.

Toropovs, N. *et al.* (2015) 'Real-time measurements of temperature, pressure and moisture profiles in High-Performance Concrete exposed to high temperatures during neutron radiography imaging', *Cement and Concrete Research*. Elsevier Ltd, 68, pp. 166–173. doi: 10.1016/j.cemconres.2014.11.003.

Walton, P. L. and Majumdar, A. J. (1978) 'Properties of cement composites reinforced with Kevlar fibres', *Journal of Materials Science*, 13(5), pp. 1075–1083. doi: 10.1007/BF00544703.

Werner, S. and Rogge, A. (2014) 'The effect of various fire-exposed surface dimensions on the spalling of concrete specimens', *Fire and Materials*. doi: 10.1002/fam.2256.

Wickström, U. (1994) 'The plate thermometer - a simple instrument for reaching harmonized fire resistance tests', *Fire Technology*. Kluwer Academic Publishers, 30(2), pp. 195–208. doi: 10.1007/BF01040002.

Wolfenden, A. *et al.* (1987) 'Comparison of Severity of Exposure in ASTM E 119 and ISO 834 Fire Resistance Tests', *Journal of Testing and Evaluation*, 15(January), pp. 371–375. doi: 10.1520/JTE11036J.

Woolson, I. H. (1918) *'Red books' of the British Fire Prevention Committee - No. 214 : Fire in a Reinforced Concrete Warehouse at Far Rockaway, New York, USA*.

Xing, Z. *et al.* (2011) 'Influence of the nature of aggregates on the behaviour of concrete subjected to elevated temperature', *Cement and Concrete Research*, 41(4), pp. 392–402. doi: 10.1016/j.cemconres.2011.01.005.

Yermak, N. *et al.* (2017) 'Influence of steel and/or polypropylene fibres on the behaviour of concrete at high temperature: Spalling, transfer and mechanical properties', *Construction and Building Materials*, 132, pp. 240–250. doi: https://doi.org/10.1016/j.conbuildmat.2016.11.120.

Zeiml, M. *et al.* (2006) 'How do polypropylene fibers improve the spalling behavior of in-situ concrete?', *Cement and Concrete Research*, 36(5), pp. 929–942. doi: 10.1016/j.cemconres.2005.12.018.

Zeiml, M. (2008) *Concrete Subjected to Fire Loading - From Experimental Investigation of Spalling and Mass-Transport Properties to Structural Safety Assessment of Tunel Linings Under Fire*. Vienna University of Technology.

Zeiml, M., Lackner, R. and Mang, H. a. (2008) 'Experimental insight into spalling behavior of concrete tunnel linings under fire loading', *Acta Geotechnica*, 3(4), pp. 295–308. doi: 10.1007/s11440-008-0069-9.

Zhang, H. L. and Davie, C. T. (2013) 'A numerical investigation of the influence of pore pressures and thermally induced stresses for spalling of concrete exposed to elevated temperatures', *Fire Safety Journal*. Elsevier, 59, pp. 102–110. doi: 10.1016/j.firesaf.2013.03.019.

Zhao, R. and Sanjayan, J. G. (2009) 'Test method for concrete spalling using small electric furnace', *Fire and Materials*. John Wiley & Sons, Ltd., 34(4), pp. 189–201. doi: 10.1002/fam.1020.